SHRP-P-393

Sensitivity Analyses for Selected Pavement Distresses

Ms. Amy L. Simpson
Dr. J. Brent Rauhut
Dr. Peter R. Jordahl
Brent Rauhut Engineering Inc.
8240 North Mopac, #220
Austin, Texas 78759

Dr. Emmanuel Owusu-Antwi
Dr. Michael I. Darter
Mr. Riaz Ahmad
ERES Consultants, Inc.
8 Dunlap Court
Savoy, Illinois 61874

Dr. Olga J. Pendleton
Texas Transportation Institute
Texas A&M University
College Station, Texas 77843-3135

Dr. Ying-Haur Lee
University of Illinois
Urbana-Champaign, Illinois 61801-2352

Strategic Highway Research Program
National Research Council
Washington, D.C. 1994

SHRP-P-393
Contract P-020
ISBN 0-309-05771-X
Product No. 5000

Program Manager: *Neil F. Hawks*
Project Manager: *A. Robert Raab*
Program Area Secretaries: *Cynthia Baker, Francine A. Burgess*
Production Editor: *Katharyn L. Bine*

key words:
data analysis
distress prediction equations
pavement performance models
sensitivity analyses

April 1994

Strategic Highway Research Program
National Research Council
2101 Constitution Avenue N.W.
Washington, DC 20418

(202) 334-3774

1.5M/NAP/494

Acknowledgments

The research described herein was supported by the Strategic Highway Research Program (SHRP). SHRP is a unit of the National Research Council which was authorized by Section 128 of the Surface Transportation and Uniform Relocation Assistance Act of 1987.

We wish to acknowledge the valuable review, discussion, and suggestions by the Expert Task Group on Experimental Design and Analysis, the Pavement Performance Advisory Committee, SHRP staff, and SHRP Contract P-001 staff. The many technical memoranda developed by Contract P-001 staff were also especially valuable.

Contents

List of Figures

List of Tables

Abstract

One of the Long-Term Pavement Performance (LTPP) objectives is "to determine the effects of (a) loading, (b) environment, (c) material properties and variability, (d) construction quality, and (e) maintenance levels on pavement distress and performance."[1] This volume reports the results of early sensitivity analyses on the National Information Management System to determine the effects of loading, pavement structure, environment, and material properties on pavement performance. In order to conduct the sensitivity analyses, it was first necessary to develop statistically linear regression equations to predict the occurrence of distresses. Once a predictive equation was available, the effects of variations in significant independent variables were quantified by calculating the change in the predicted distress as each significant variable was varied from one standard deviation above its mean to one standard deviation below its mean, with all other variables held at their mean values. The sensitivities of the distress predictions to the individual variations in the significant variables were then plotted to display the relative significance of the independent variables in the equation to the prediction of the distress. The primary products of these studies are increased understanding of the relative effects of these parameters on the occurrence of distress and the predictive equations themselves. While it is believed that these products will prove useful in the interim, the reliability of the results are limited at this point in time. The products are expected to be greatly improved through later analyses when more time sequence data are available.

Executive Summary

The original planners for the Long-Term Pavement Performance (LTPP) studies established six objectives. The fourth objective follows:

> 4. Determine the effects of (a) loading, (b) environment, (c) material properties and variability, (d) construction quality, and (e) maintenance levels on pavement distress and performance.

The research, described in this report concerned the effects of loading, the environment, pavement structure, and material properties on pavement distress and performance. Data were not available for a meaningful study of the effects of material variability, construction quality, or maintenance levels on pavement distress and performance. In addition, these studies served as pilot studies for developing procedures for conducting the sensitivity analyses, gaining insight into the nature of the database, gaining experience with conducting such studies with this database, and developing recommendations for use by future analysts when the database is enhanced by time sequence data.

It was fully recognized by those planning and those conducting this research that the analyses at this point in forming the database would be limited. However, it was expected that the products of the research would have considerable interim value, and that the trailblazing aspects of this effort would prove valuable to future analysts. It was also expected that deficiencies in the data would be discovered, so that these deficiencies could be repaired before the next major analytical effort is undertaken.

This project began with the development of a tentative analysis plan, in coordination with a Strategic Highway Research Program (SHRP) Expert Task Group on Experimental Design and Analysis and with input from the highway community at large during a SHRP data analysis workshop. The work effort was then unfortunately delayed 1 1/2 years because of delays in data availability. Some important data, such as layer elastic moduli, were still not available in time for use in the studies. However, the research staff was able to maximize the value of the results, considering the time constraint and the quality of the data available.

"Sensitivity analysis" is not a common descriptor for either research engineers or statisticians, but it has come to have a specific meaning to some individuals from both disciplines. The definition as applied to this research follows:

> Sensitivity analyses are statistical studies to determine the sensitivity of a dependent variable to variations in independent variables (sometimes called explanatory variables) over reasonable ranges.

An example could be a study of the sensitivity of rutting in hot-mix asphalt concrete (HMAC) pavements to variations in layer thicknesses, traffic, material properties, or other variables significant to the occurrence of rutting. Such studies are generally conducted by first developing predictive equations for the distresses of interest and then studying the effects of varying individual explanatory variables across reasonable ranges. The development of suitable predictive equations for use in the sensitivity analyses required thousands of multiple regressions before the best equations suitable for sensitivity analyses were produced. Because of the nature of sensitivity analyses, the regression equations had to be statistically linear, which means that the coefficients must be linear and that nonlinear regression techniques could not be used.

Some limitations of the database that constrained the sensitivity analyses are as follows:

- The values of cumulative equivalent single axle loads (ESALs) were simply estimates from the state highway agencies and are not believed to be very reliable.

- Initial roughness in terms of International Roughness Index (IRI) had to be estimated.

- There generally was only one measurement of distress for each test section, plus an estimated or assumed initial value (e.g., rutting, faulting, and such were assumed to be zero when the pavement was opened to traffic). Two values are generally not enough to explain the curvature in a relationship, but the ages of the pavements were distributed reasonably well over 20 years, so that the curvatures were partially explained.

- A number of test sections were missing data which precluded their use in these early analyses.

- There was relatively little distress in the test sections at this early point in the 20 year studies. Many test sections with adequate data had to be omitted because they had not experienced distress.

Because there were over 100 data elements in each of the databases for flexible and rigid pavements, it was necessary to materially reduce the number of data elements to be considered in the analyses. It was also important to avoid strong correlations between independent variables that were included in the studies. The approach taken to eliminating less significant data elements was to obtain relative significance rankings from experts in

pavement performance modeling. This approach offered a means for bringing expert knowledge into the analysis at an early stage, as well as offering insight in the selection of variables considered in the analyses. These selections required balancing relative significance, data availability, and correlations with other variables.

Because the selection instructions for the General Pavement Studies (GPS)-1 and GPS-2 experiments allowed considerable overlap in pavement structure for test sections, it was decided to view these two data sets as resources and then to recombine them into more specific data sets such as HMAC on granular base, full-depth HMAC, HMAC over portland cement-treated base, and so on. These latter databases were those finally used in the analyses, and the data sometimes had to be combined to get enough test sections with distress for analysis.

The data sets for the GPS-3 and GPS-4 experiments were also combined for a number of rigid pavement studies (e.g., studies of joint spalling and faulting), where the presence of or lack of reinforcement was not believed to be important.

The development of the procedures for producing the required predictive equations and for conducting the sensitivity analyses after the equations were available were highly interactive and time consuming. These are discussed in detail in Chapters 5 and 6 of this report.

It became apparent early in the analyses of HMAC pavements that predictive models developed from the entire database, whose inference space included all of the United States and parts of Canada, would generally not result in reliable models. Consequently, databases were formed for each of the four environmental zones and separate predictive models were developed. These models have values of the adjusted coefficient of determination R^2 ranging from 0.65 to 0.93. For example, the model developed for prediction of rutting in the wet-freeze environmental zone appears as Table 1. The form of the equation appears at the top of the table, with the explanatory variables or interactions appearing in the table, along with the coefficients that provide the details of the equation. The exponents B and C are calculated by multiplying the explanatory variables or interactions in the left column by the regression coefficients b_i and c_i and adding the results.

The results of the sensitivity analyses conducted with this predictive equation appear as Figure 1a. This figure shows that the strongest impact on the occurrence of rutting in the wet-freeze zone may be expected to be the cumulative number of KESALs (1000 ESALs). The dashed lines and arrow pointing to the left indicate that reductions in KESALs decrease rutting, but the standard deviation for KESALs is greater than the mean, and negative KESALs are not possible. Freeze index is the next most important, followed by the percentage of the HMAC aggregate passing a #4 sieve, air voids, and so on. It can also be seen from the directions of the arrows that increasing KESALs and freeze index may be expected to increase rut depths, while increasing amounts of aggregate passing the #4 sieve, air voids, and asphalt thickness may be expected to decrease rutting. It should be remembered that the relative sensitivities depend on the model form selected for the predictive equation, so some differences would be expected if a different equation was used for the sensitivity analyses.

Table 1. Coefficients for Regression Equations Developed to Predict Rutting in HMAC Over Granular Base for the Wet-Freeze Data Set

Rut Depth (In.) $= N^B 10^C$ Where

N = Number of Cumulative KESALs

$B = b_1 + b_2 x_1 + b_3 x_2 + ... + b_n x_{n-1}$

$C = c_1 + c_2 x_1 + c_3 x_2 + ... + c_n x_{n-1}$

Explanatory Variable or Interaction (x_i)	Units	Coefficients for Terms In	
		b_i	c_i
Constant Term	--	0.183	0.0289
Log (Air Voids in HMAC)	% by Volume	0	-0.189
Log (HMAC Thickness)	Inches	0	-0.181
Log (HMAC Aggregate #4 Sieve)	% by Weight	0	-0.592
Asphalt Viscosity at 140°F (60°C)	Poise	0	1.80×10^{-5}
Log (Base Thickness)	Inches	0	-0.0436
(Annual Precipitation *	Inches	0	
Freeze Index)	Degree-Days	0	3.23×10^{-6}

$R^2 = 0.73$ Adjusted $R^2 = 0.68$ RMSE in Log_{10} (Rut Depth) = 0.19

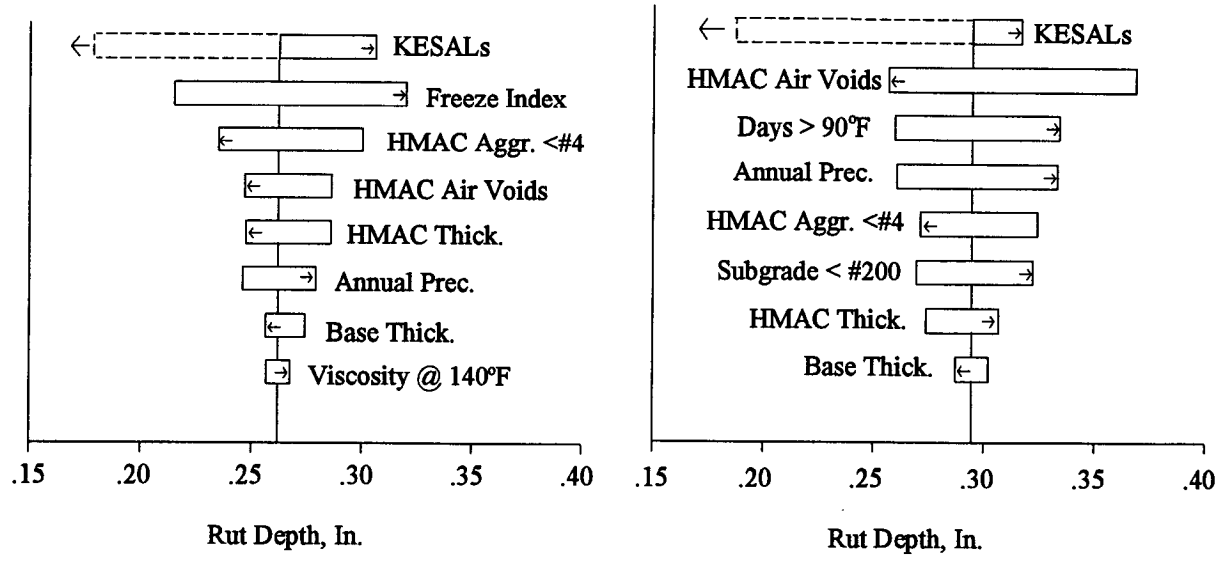

a. Wet-Freeze Data Set **b. Dry-No Freeze Data Set**

Figure 1. Results From Sensitivity Analysis for Rutting in HMAC Over Granular Base

To illustrate how different the sensitivities may be from one environmental zone to another, the sensitivity analysis results for the dry-no freeze environmental zone are included as Figure 1b. Most of the variables are the same as for the wet-freeze zone, but there are some differences and the relative levels of sensitivities vary between environmental zones.

Unfortunately, the number of test sections for specific combinations of distress type and pavement type was not sufficient for the portland cement concrete (PCC) pavement studies to allow development of regional models. Consequently, the reliabilities of these equations are generally somewhat lower than those for the HMAC regional equations.

While the sensitivity analyses offer useful insight, it must be remembered that most of these pavements are in very good shape, so the interactive effects of water seeping through cracks and expediting deterioration in lower layers really is not represented here.

The twelve most significant variables from the sensitivity analyses for HMAC pavements are listed below by distress type in order of relative ranking, with the most significant variable at the top and the least at the bottom:

Rutting	**Change in Roughness**	**Transverse Cracking**
KESALs	KESALs	Age
Air Voids in HMAC	Asphalt Viscosity	Annual Precipitation
HMAC Thickness	Days With Temp. > 90°F (32°C)	HMAC Thickness
Base Thickness	HMAC Thickness	Base Thickness
Subgrade < #200 Sieve	Base Thickness	Asphalt Viscosity
Days With Temp. > 90°F (32°C)	Freeze Index	Base Compaction
HMAC Aggregate < #4 Sieve	Subgrade < #200 Sieve	Freeze Index
Asphalt Viscosity	Air Voids in HMAC	Days With Temp. > 90°F (32°C)
Annual Precipitation	Base Compaction	Subgrade < #200 Sieve
Freeze Index	Annual Precipitation	Annual KESALs
Base Compaction	Daily Temp. Range	Annual Freeze-Thaw Cycles
Average Annual Min. Temp.	Annual Freeze-Thaw Cycles	HMAC Aggregate < #4 Sieve

The assignment of rankings for PCC pavements is more complex because of the strong impacts of dowels and reinforcement on performance. The general significance rankings for all ten PCC models combined follow:

1. Age
2. CESALs
3. Slab Thickness
4. Static k-Value
5. Precipitation
6. Joint Spacing
7. Percentage of Steel
8. Tied Shoulders
9. Annual Freeze-Thaw Cycles
10. Type of Subgrade
11. PCC Flexural Strength
12. Monthly Temperature Range

Other useful results follow:

- For joint faulting of jointed concrete pavements (JCP) and roughness in jointed plain concrete pavements, the analyses indicate that environment becomes important only if the joints are not doweled. Therefore, the use of dowels is especially important in wet or cold climates and for high traffic.

- Joint spalling is generally dependent on age and the environment.

- The use of shorter slabs for JCP tends to reduce joint faulting and transverse cracking, which results in less roughness.

- The use of a widened traffic lane appears to reduce roughness in continuously reinforced concrete pavement.

- It is important not to overcompact HMAC, because this will reduce the air flow through the mix. In mixes of moderately high air voids (5 to 9%), early hardening occurs, which stiffens the mix and substantially reduces the rate of compaction under traffic. (It is also important to get sufficient compaction so that the early compaction under traffic is not excessive.)

- The HMAC aggregate passing a #4 sieve was selected to represent the effects of gradation. Within its inference spaces in the separate data sets, increasing amounts of aggregate passing a #4 sieve appeared beneficial in reducing rutting.

1

Introduction

Because of the diversity of the research activities and the bulk of the text required to describe them, this report has been produced in five reports, which include an Executive Summary. The overall title is Early Analyses of LTPP General Pavement Studies Data, but each separate report has an additional title as follows:

- SHRP-P-392, Executive Summary
- SHRP-P-684, Data Processing and Evaluation
- SHRP-P-393, Sensitivity Analyses for Selected Pavement Distresses
- SHRP-P-394, Evaluation of the AASHTO Design Equations and Recommended Improvements
- SHRP-P-680, Lessons Learned and Recommendations for Future Analyses of LTPP Data

Each report is written as a stand-alone document, but it may be useful to refer to other reports for additional detail.

This is a report on the results from data evaluations and sensitivity analyses for Strategic Highway Research Program (SHRP) Contract P-020, "Data Analysis," which served as the primary vehicle for harvesting the results from the first 5 years of the SHRP Long-Term Pavement Performance (LTPP) studies and transforming this new information into implementable products supporting the LTPP goal and objectives. The research was conducted by Brent Rauhut Engineering Inc. and ERES Consultants, Inc.

The goal for the LTPP studies, as stated in the Strategic Highway Research Program Research Plans, (1986)[1], is

> To increase pavement life by investigation of various designs of pavement structures and rehabilitated pavement structures, using different materials and under different loads, environments, subgrade soil, and maintenance practices.

LTPP Objectives and Expected Products

The following six objectives were established by the SHRP Pavement Performance Advisory Committee in 1985 to accomplish the overall goal:

- evaluate existing design methods;
- develop improved design methods and strategies for pavement rehabilitation;
- develop improved design equations for new and reconstructed pavements;
- determine the effects of (1) loading, (2) environment, (3) material properties and variability, (4) construction quality, and (5) maintenance levels on pavement distress and performance;
- determine the effects of specific design features on pavement performance; and
- establish a national long-term pavement data base to support other SHRP objectives and future needs.

This research was the first to use the National Pavement Data Base (later renamed the National Information Management System [NIMS]) to pursue these objectives. The early products that were expected from this data analysis are listed below and related to project tasks (to be described later):

- A better understanding of the effects of a broad range of loading, design, environmental, materials, construction, and maintenance variables on pavement performance (Task 2);
- Evaluation of and improvements to the models included in the 1986 American Association of State Highway and Transportation Officials (AASHTO) Pavement Design Guide (Tasks 3 and 4);
- Evaluation and improvement of AASHTO overlay design procedures using data from the General Pavement Studies (GPS) (Task 5); and

- Data analysis plans for future analyses as GPS time sequence data and Specific Pavement Studies (SPS) data enter the NIMS and the LTPP Traffic Data Base and offer opportunities for further insight and design improvements (Task 6).

This project began with development of tentative analysis plans for this initial analytical effort. These plans were presented July 31, 1990, to the SHRP Expert Task Group on Experimental Design and Analysis and on August 2, 1990, to the highway community in a SHRP data analysis workshop. A detailed work plan was developed from the initial plans, and from the comments and guidance received from these and subsequent meetings. Guidance was furnished to the contractors throughout the research by a Data Analysis Working Group (composed of SHRP staff and SHRP contractors), the Expert Task Group on Experimental Design and Analysis, and the Pavement Performance Advisory Committee.

Research Tasks

The specified tasks for SHRP Contract P-020a were

- Task 1— Develop data evaluation procedure and hold workshop,
- Task 1A— Process and evaluate data,
- Task 2— Perform sensitivity analysis of explanatory variables in the National Pavement Performance Data Base,
- Task 3— Evaluate the AASHTO design equations,
- Task 4— Improve the AASHTO design equations,
- Task 5— Evaluate and improve AASHTO overlay procedures using GPS data, and
- Task 6— Develop future LTPP data analysis plans.

The relationships between the tasks and the general flow of the research appear in Figure 1.1. This report documents Task 2. As can be seen, this task provided the data and information needed for Tasks 3, 4, 5, and 6.

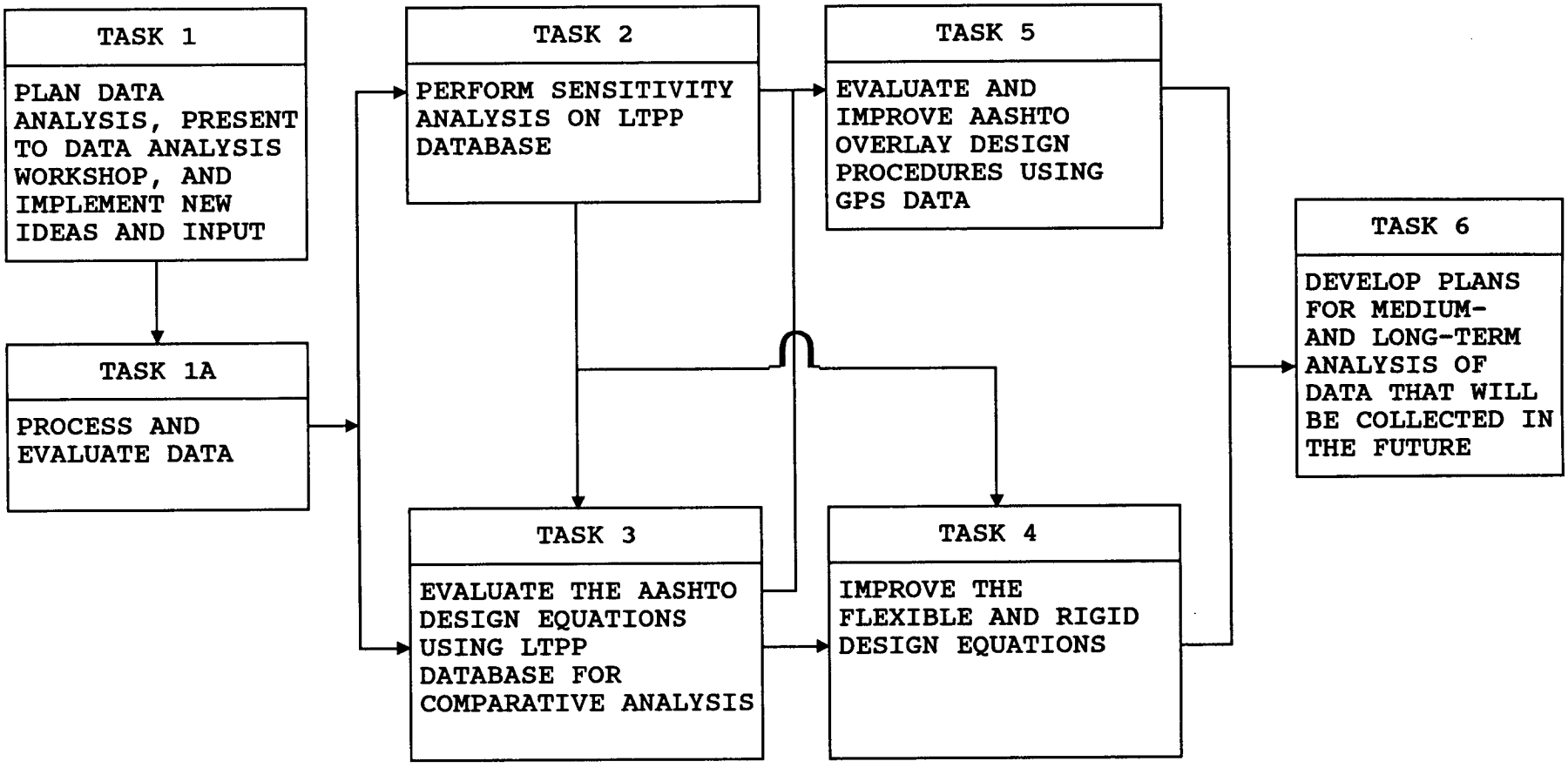

Figure 1.1. General Task Flow Diagram

Data Bases Used in the Analyses

The NIMS will eventually include data for both the GPS and SPS, but only the GPS data were even marginally adequate for these early analyses. In May 1993, the SPS data were only beginning to be entered into the NIMS for projects recently constructed, and many of the projects are not yet constructed. It should be noted that all data collected for LTPP studies are for test sections 500 feet (152.4 meters) in length and include only the outside traffic lane.

The GPS experiments are identified and briefly described in Table 1.1. The sensitivity analyses were conducted only for the five data sets for pavements that had not yet been rehabilitated, i.e., were in their first service period before being overlaid or otherwise rehabilitated (GPS-1 through GPS-5). The limited data bases available for the pavements with overlays were used for Task 5, Evaluate and Improve AASHTO Overlay Procedures Using GPS Data (see Volume 4 of this report). There were not sufficient test sections in GPS-6, GPS-7, and GPS-9, for which condition prior to overlay was known, to support development of reasonable predictive models for conducting sensitivity analyses.

Table 1.1. Listing of SHRP LTPP General Pavement Studies Experiments

GPS Experiment Number	Brief Description	No. of Projects in the Database
1	Asphalt Concrete Pavement on Granular Base	253
2	Asphalt Concrete Pavement on Bound Base	133
3	Jointed Plain Concrete Pavement (JPCP)	126
4	Jointed Reinforced Concrete Pavement (JRCP)	71
5	Continuously Reinforced Concrete Pavement (CRCP)	85
6A	AC Overlay of AC Pavement (Prior Condition Unknown)	61
6B	AC Overlay of AC Pavement (Prior Condition Known)	31
7A	AC Overlay of Concrete Pavement (Prior Condition Unknown)	34
7B	AC Overlay of Concrete Pavement (Prior Condition Known)	15
9	Unbonded PCC Overlays of Concrete Pavement	28

Some statisticians prefer to call the GPS experimental factorials "sampling templates" rather than experimental factorials, because existing in-service pavements were used instead of test sections that were constructed to satisfy rigorous experimental designs. In fact, the factorials were established to encourage reasonable distributions of the parameters expected to be significant, and test sections were sought to meet the factorial requirements. The SPS will follow the requirements of designed experiments.

The environmental factors considered in the sampling templates were freeze, no freeze, wet, and dry. These broad factors were applied to encourage selection of test sections with distributions of environmental variables. The four environmental zones (or regions) considered for the selection of test sections appear in Figure 1.2. Where feasible, data sets for the individual distress types were further divided into four separate data bases by environmental zones, and separate analyses were conducted on each.

Definition of Sensitivity Analysis

"Sensitivity analysis" is not a common descriptor for either research engineers or statisticians, but it has come to have a specific meaning to some individuals from both disciplines. The definition as applied to this research follows:

> Sensitivity analyses are statistical studies to determine the sensitivity of a dependent variable to variations in independent variables (sometimes called explanatory variables) over reasonable ranges.

An example is the study of the sensitivity of rutting in hot mix asphalt concrete (HMAC) pavements to variations in layer thicknesses, traffic, material properties, or other variables significant to the occurrence of rutting. Such studies are generally conducted by first developing predictive equations for the distresses of interest and then studying the effects of varying individual explanatory variables across reasonable ranges.

There is no single method of conducting sensitivity analyses. Some involve standardizing the values of the independent variables so that the coefficients in the equations indicate directly the relative sensitivity of the distress of interest to the explanatory variable the coefficient multiplies. The procedure used for the studies reported involved setting all explanatory variables in a predictive equation at their means and then varying each one independently from one standard deviation below the mean to one standard deviation above the mean. The relative sensitivity of the distress prediction for that variable is the change in the predicted distress across the range of two standard deviations, compared to the changes when other explanatory variables were varied in the same manner. Because the relative sensitivities depend on the predictive equations selected, they would be expected to change somewhat if other equations were used.

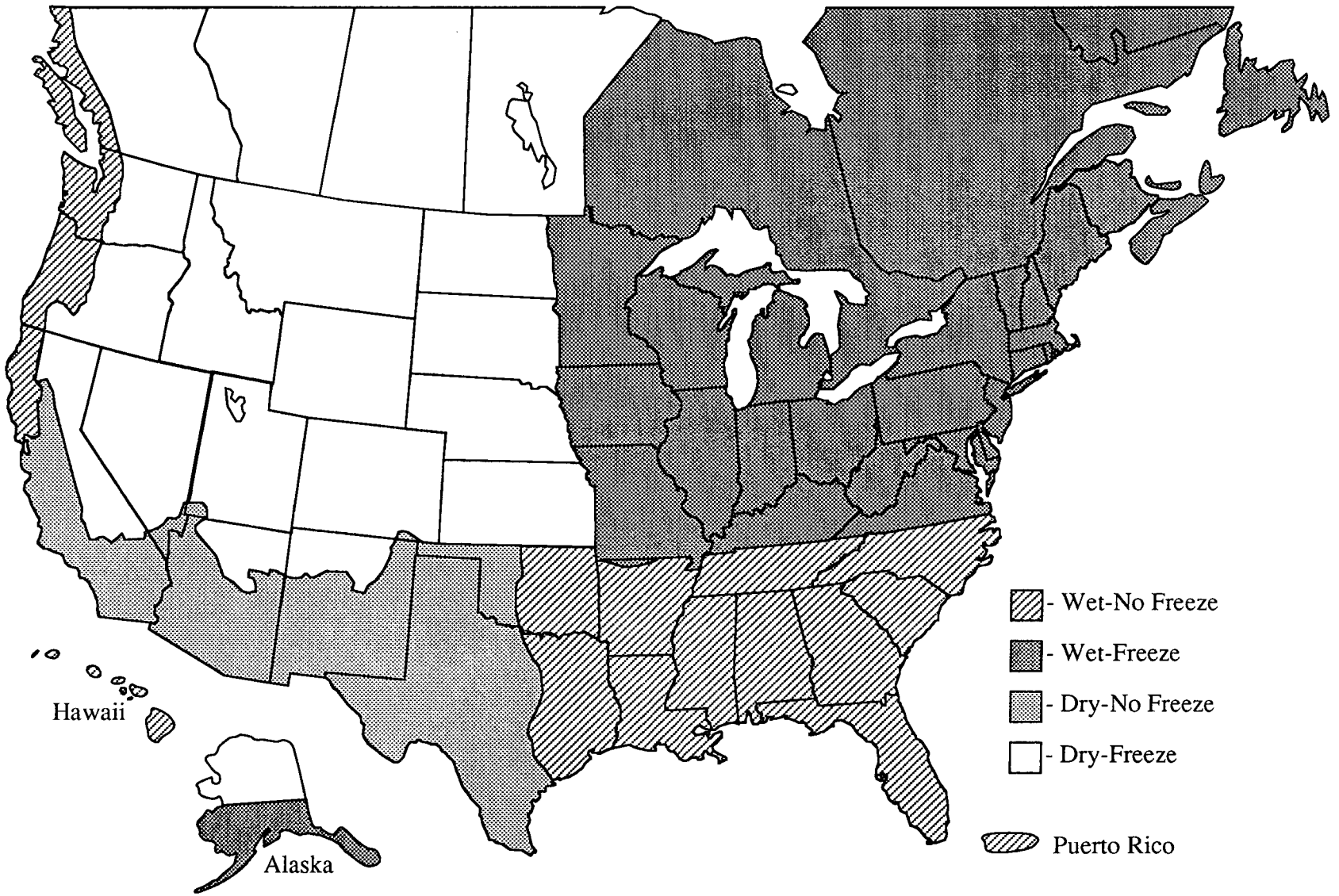

Figure 1.2. Environmental Zones for SHRP LTPP Studies

No matter what procedure is used to establish the sensitivities, most of the work is spent on statistical evaluations of the data that identify the independent variables significant to the occurrence of the pavement distress of interest and the development of suitable predictive equations by using the significant independent variables that were identified.

Analytical Limitations Resulting From Data Shortcomings

This project involves the analysis of data gleaned from in-service pavements, and none of the early results may be expected to exceed in quality the adequacy of the database from which they are developed. Therefore, it is important to discuss the data resources available to the research team. There are certain limitations to the studies that are an unavoidable consequence of the timing of the early data analyses. For instance, excellent traffic data will be available to future data analysts from the recently installed monitoring equipment but this early data analysis must rely on estimates of past equivalent single axle loads (ESALs) of limited accuracy. While years of time sequence monitoring data will be available later, these studies have distress measurements for only one or at most two points in time. For most distresses, an additional data point may be inferred for conditions just after construction; e.g., rutting, cracking, faulting of joints, and so on were generally determined as zero initially. Analyses for roughness increases depend for most test sections on educated estimates for initial roughness (derived from State Highway Agencies [SHAs] estimates of initial Pavement Serviceability Index [PSI]).

The distribution in ages of the test sections offered some assistance in overcoming the lack of time sequence data. As an example, Figure 1.2 shows the distribution of pavement age for the GPS-1 experiment, Asphalt Concrete Over Granular Base. A number of test sections are represented in all time intervals through 20 years of age.

Another shortcoming of the databases that influenced the results were missing items of inventory data, collected from SHAs that concern the design and construction of the pavements. Inventory data include such elements as date of construction, pavement structure, and mix design. Some data elements were available for all the test sections, while others such as asphalt viscosity were not known for some test sections and could not be found. Unfortunately, it will generally not be possible to obtain these missing inventory data so they will be missing for future analyses as well.

The plans developed for these analyses were well accepted, but during the processing and evaluation of the data, it became apparent that all the plans could not be carried out. Reflecting a tendency for SHAs to offer only pavements in reasonable condition, many test sections had not experienced distresses as yet, and those that had generally had only one or two distress types. The only type of distress that was generally available for all test sections was roughness, and it was necessary to estimate the initial roughness to study increases in roughness. For flexible pavements, rutting information was also available for all these test sections. It was not possible to study alligator cracking in flexible pavements, because only eighteen test sections were reported to have any of this

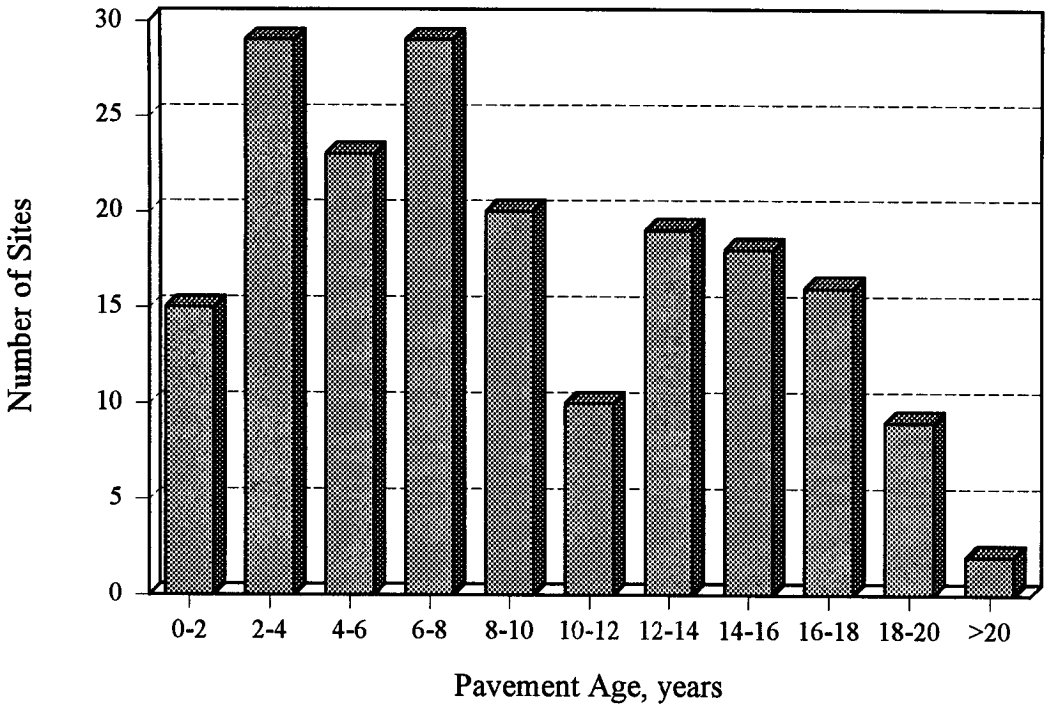

Figure 1.3. Distribution of Pavement Age, Experiment GPS-1, AC Over Granular Base

cracking. Similarly, raveling and weathering could not be studied because only three test sections had experienced this distress. The only three distress types for flexible pavements for which sufficient data were available to support the studies were rutting, change in roughness (measured as International Roughness Index [IRI]), and transverse (or thermal) cracking.

Friction loss was also eliminated from the studies because there were only three data elements in addition to ESALs, to use for independent variables and none of them would be expected to relate closely to the polishing of aggregates. Also, initial friction values were not available and would have to be estimated to study friction loss.

The study of overlaid pavements was to have been of high priority, but it was generally agreed that pavement condition prior to overlay was an important variable and this information was not available for pavements that were overlaid prior to entering the GPS. It was decided early in the implementation of the LTPP studies that test sections would be sought for pavements for which overlays were imminent, so that the condition prior to overlay would be available. A number of such test sections have been implemented, but none of these are old enough to have appreciable distress. The total number of overlaid pavements was limited, and for the reasons discussed above only a few had sufficient information for successful analyses. Consequently, analyses for the overlaid pavements have been limited to the studies in Task 5, i.e., used only to evaluate the AASHTO overlay design equations.

It should be noted that the roughness reported for a test section is an average for that test section. Software called PROQUAL[2] was applied to the profile data to check it for anomalies. Values of IRI were calculated for each of the five 100 foot intervals in a test section. In some cases, there were significant differences in roughness among the 100 foot intervals, which may contribute to the unexplained error in the equations developed to predict roughness or change in roughness.

It was also proposed that current knowledge be integrated into the analyses by use of mechanistic clusters of variables in the regression equations to predict distresses, which would then be used to conduct the sensitivity analyses. This plan to use mechanistic clusters of variables, based on theory, was thwarted by a lack of layer stiffness data, which only started to become available in fall 1992, and were still not all available as this report was being written. Because the mechanistic theory required layer moduli of elasticity, use of mechanistic clusters was limited to providing guidance for organizing interaction terms to try in the multiple regressions used to develop the predictive equations for distresses.

As with any data analysis, the analysis staff had to be concerned about potential biases in the databases. Several areas of concern identified by Paul Benson, a member of the Expert Task Group for Experimental Design and Analysis, were (1) imbalances in the number of sections provided by different states, leading to possible undue influence from one state's design, construction, and maintenance practices; (2) the possibility of systematic differences in the interpretation of SHRP guidelines for test section selection by the states and the four SHRP regional offices and their engineers; (3) uneven distribution of test sections in experimental factorials; (4) the possibility that the older non overlaid pavements selected represent survivors, which are not typical of pavements in general; and (5) in a similar vein, the possibility that by basing much of our analysis on older pavements we may not be reflecting changes already made in modern construction and design practices. The following recommendations by Mr. Benson were followed in the analyses:

- Limit the inference space of a model where the data are limited or grossly unbalanced, and consider regional models where the data do not warrant a national model.

- Combine experiments (where distress mechanisms may be similar) to achieve a better balance (specifically GPS experiments 1 and 2).

- Examine the distributions of independent and dependent variables for non normality, bi-modulism, and extreme values; where such are found, attempt to determine their source.

- Conduct a thorough residual examination as soon as preliminary models are available, comparing residuals to project age, state, season tested, and other variables to determine possible sources of bias.

Sets of distress types to be studied were separately selected for pavements with asphalt concrete (AC) and portland cement concrete (PCC) surfaces, in coordination with the Expert Task Group on Experimental Design and Analysis, SHRP staff, and other interested parties. Once these distress types were selected, separate tables for flexible and rigid pavements, with the distress types as columns and all the data elements as rows, were furnished to a set of experts. These experts were asked to indicate on a scale of 1 to 3 how significant they believed a particular data element would be to the occurrence of each of the distresses. The results from these surveys were then combined, and studies were conducted to consider the expected availability of the individual data elements and possibility of substituting other correlated data elements when important data elements were not available. These studies identified data sets for the sensitivity studies to be used for the combinations of distress types and pavement types, and are described in more detail in Chapter 2.

2

Preliminary Selection of Data Elements for Sensitivity Analyses

The National Information Management System (NIMS) has "bins" for 117 data elements for pavements with asphalt concrete surfaces, 128 data elements for jointed concrete pavements (JCP), and 120 data elements for continuously reinforced concrete pavements (CRCP). Because it clearly would not be practical to attempt to model pavement performance with so many independent variables and literally hundreds of potential interactions, it was necessary to considerably reduce the number of variables (data elements) to develop meaningful performance prediction equations and reasonable estimates of the relative significance of the independent variables to the occurrence of specific distresses (dependent variables).

Relative Significance Studies

The approach adopted for preliminary elimination of less significant variables was to obtain relative significance rankings from experts in pavement performance modeling. This offered a means for bringing expert knowledge into the analysis at an early stage, as well as offering insight for selecting the variables to be considered in the analyses. These selections require balancing relative significance, data availability, and correlations with other variables. Tables were developed for the three pavement types that listed the data elements as rows and the significant distresses selected for study as columns. These significance tables were distributed to various experts who had agreed to participate.

Three levels of significance were considered. The assignment of a "1"indicated that the rater considered the data element to be clearly significant in predicting the distress of interest. Assignment of a "2"indicated moderate significance, and a "3"indicated little or no significance. Space was also included in the tables for listing other data elements that were believed to be correlated with the one identified on that line.

When the significance rating forms were returned, the entries for each block were averaged. If the average score for a data element and distress combination was less than 2, that data element was considered to be significant for prediction of that distress. If the average score was exactly 2, it was retained in the significance studies in some cases but not in others on the basis of the research team's judgment. Data elements with scores greater than 2 were not considered further.

Criteria for Selection of Data Elements

Upon completion of the relative significance studies discussed above, sets of independent variables had been developed that individually were believed to be significant to the prediction of specific distresses. However, significant independent variables to be included in the studies needed also to be available in the database. Therefore, the percentage of data expected to be available had to be considered in selection of the data elements to be included in the sensitivity analyses.

It was soon apparent that many of the data elements considered to be individually significant would not be available in sufficient numbers to support the analyses. However, a great many of these variables were correlated to various degrees with other independent variables that were represented in greater percentages of the test sections involved. These correlations were considered, and it became apparent that the "explanation" of variations in the distresses (dependent variables) could for the most part be offered by other data elements with which they were correlated. That is, by omitting many of the variables the growth in the error pool would be manageable because of the inclusion of other correlated variables.

It was possible through consideration of correlations as discussed above to replace most of the significant explanatory variables. However, a few of the significant data elements remained that were not replaceable with other correlated data elements. The level of the effect on the results was evaluated, as well as the probability of finding values for them, which resulted in a very small group of data elements for which the Strategic Highway Research Program (SHRP) regional offices were asked to seek values. As an example, the database includes bins for grade, penetration, and viscosity of the original asphalt cement for flexible pavements. Because these data cannot be obtained by testing the hardened asphalt taken from the in-service pavements, there was no source other than the inventory data from the files of the State and Provincial Highway Agencies. It was concluded that approximate values of the other two could be obtained if any one of the three was known. Therefore, values were sought in the few cases where none of the three values were furnished.

Appendix A provides a document developed in March 1991 to record the results from the studies described briefly above for pavements with AC surfaces. The general procedure applied is illustrated in Figure 2.1.

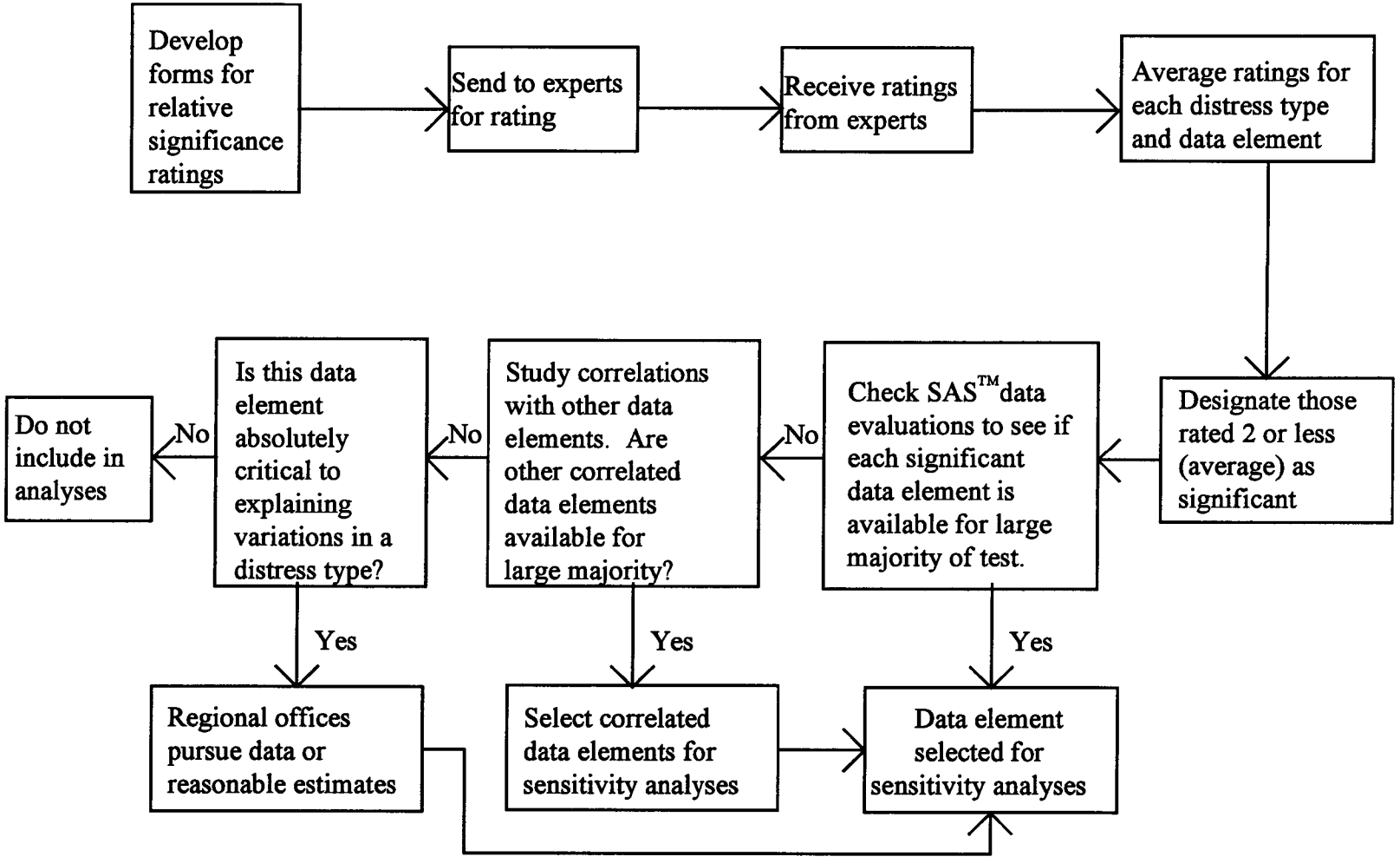

Figure 2.1. Procedures for Selecting Data Elements for the Sensitivity Analyses

In summary, the criteria for selecting the data elements to be included in the sensitivity analyses were (1) the data element must have been rated by the experts as significant, (2) the data must be available for a sufficient number of the test sections, and (3) the data element should not be highly correlated to other data elements considered to be more significant or to have data for more test sections.

Data Elements Selected for Sensitivity Analyses

The data elements that survived the preliminary selection process described above are listed in Tables 2.1 and 2.2. For Table 2.1, an "X" in a box representing a specific data element and specific distress indicates that the data element would be included in the development of predictive equations for the specific distress, and would be further considered in the sensitivity analyses if the statistical studies support the opinions of the experts as to its importance. As discussed previously, data elements with average significance rating scores greater than 2 were not considered further. However, those that were considered very significant by at least one rater have been identified by a "#" in Table 2.1 and may be considered further in future analyses when more data and time are available.

Table 2.2 provides combined information for both JCP and CRCP. An "X" indicates selection for a JCP distress, whereas an "O" indicates selection for the CRCP studies. As an example, portland cement concrete (PCC) surface thickness is considered significant for transverse cracking, longitudinal cracking, pumping, roughness, and joint faulting for JCP, but is only considered significant for localized failures, pumping, and roughness for CRCP. As for flexible pavements, data elements that one rater considered to be very significant have been identified in Table 2.2 by a "#" symbol for JCP and a "+" symbol for CRCP.

It can be readily seen that a number of data elements are available for some distress types, while there are only a few for others.

There are no surprises in the data elements selected as significant. Thicknesses and stiffnesses of layers control strains in the pavement structure, while other data elements reflecting material properties (e.g., asphalt viscosity, percentage of air voids, gradations of aggregates and base materials, and strengths) affect layer stiffnesses and durability under the impacts of loads and the environment. Plasticity indices of the subgrades affect roughness through differential volume change by interacting with moisture content. Drainage can affect moisture content in base, subbase, and subgrade, which in turn affects layer stiffnesses and loss of fines. Performance of JCP depends heavily on joint efficiency from deflection measurements, which indicate movements in joints under loads.

Table 2.1. Significant Data Elements for Predicting Distresses in Pavements With Asphalt Concrete Surfaces

Significant Data Elements	Distress Types					
	Alligator Cracking	Transverse Cracking	Rutting	Roughness	Friction Loss	Raveling/ Weathering
Surface Thickness	X	X	X	X		
Base/Subbase Thickness	X		X	X		
Surface Stiffness	X	X	X			
Unbound Base/Subbase Stiffness	X		X			
Bound Base/Subbase Stiffness	X	#	X			
Subgrade Stiffness	X		X	X		
Age of Pavement	X	X	X	X	X	X
Cumulative ESALs	X	X	X	X	X	X
Asphalt Viscosity	X	X	X	#		
Asphalt Content	X	X	X		#	X
Percentage of Air Voids	X	X	X		#	X
HMAC Aggregate Gradation	X		X		#	#
Percentage of Compaction of Base/Subbase	X		X			
Subgrade Soil Classification	#		X	#		
In Situ Moisture Content of Subgrade	#		X			
Subsurface Drainage Yes/No	#		X	X		
Geological Classification of Course Aggregate in HMAC					X	
% of Subgrade Soil Passing #200 Sieve			#	X		

Table 2.1(continued). Significant Data Elements for Predicting Distresses in Pavements With Asphalt Concrete Surfaces

Significant Data Elements	Distress Types					
	Alligator Cracking	Transverse Cracking	Rutting	Roughness	Friction Loss	Raveling/ Weathering
Plasticity Index of Subgrade Soil	#		#	X		
Liquid Limit	#		#	#		
Percent of Subgrade Soil Finer Than 0.02 mm			#	X		
Type of Environment	#	#	X	X	X	X
Average Maximum Daily Temperature by Month	#	#	X	#		#
Average Minimum Daily Temperature by Month	#	#	#	#		X
Thornthwaite Index	#		#	X		
Freeze Index	#	X	#	X		
No. of Days Minimum Temperature < 32°F (0°C)	X	X	#			X
No. of Days Maximum Temperature > 90°F (32°C)	X	#	X	X	#	
Number of Air Freeze-Thaw Cycles	X	X	#	X		X
Annual Precipitation	X	X	X	X		X

Notes: X = data element was selected for analyses.
# = average score greater than 2, but considered very significant by at least one rater.
ESALS = equivalent single axle loads; HMAC = hot mix asphalt concrete.

Table 2.2. Significant Data Elements for Predicting Distresses in Pavements With Portland Cement Concrete Surfaces

Significant Data Elements	Distress Types						
	Transverse Cracking	Longitudinal Cracking (JCP)/ Localized Failures (CRCP)	Pumping	Roughness	Friction Loss	Joint Faulting	Joint/ Crack Spalling
PCC Surface Thickness	X	X O	X O	X O		X	# +
Base Thickness	#	# O	X O	X O		X	+
PCC Surface Stiffness	X	X O	X O	# +		#	# O
Base Stiffness	X	X O	X O	X O		X	
Subgrade Stiffness	X	X O	X O	X O		X	+
Age of Pavement	X	X O	X +	X O	X O		X O
Cumulative 18 kip ESAL	X	X O	X O	X O	X O	X	X O
Type of Coarse Aggr. for PCC	X	X O		X +	X O	#	X O
Gradation of Coarse Aggr. for PCC	#	# O	#	# +	# +	X	X O
PCC Compressive Strength	X	X O		X O			X O
AASHTO Soil Class Base/Subbase		O	X O	X O		X	# 0
% Compact. of Base/Subbase	#	# O	x O	X		X	
Coarse Aggregate Gradation of Base/Subbase	#	O	X O	#		X	#

Table 2.2(continued). Significant Data Elements for Predicting Distresses in Pavements With Portland Cement Concrete Surfaces

Significant Data Elements	Distress Types						
	Transverse Cracking	Longitudinal Cracking (JCP)/ Localized Failures (CRCP)	Pumping	Roughness	Friction Loss	Joint Faulting	Joint/ Crack Spalling
Fine Aggr. Gradation of Base/Subbase	#	# +	X O	#			
AASHTO Soil Classification of Subgrade	X	X O	X O	X O			
Subgrade % Passing #200 Sieve		+	X O	# +			
Moisture Content of Subgrade	#	# +	X	#			
Joint Efficiency		#	X	X		X	X
Thornthwaite Index	#	# O	X O	X O	#	X	#
Annual Precipitation	X	O	X O	# O		X	X
Precipitation Days by Year		O	X O	# O		X	
Shoulder Type	X	# O	# O	# O		#	+
Subsurface Drainage Type	X	# O	# O	# O		X	X O
Avg. Max. Daily Temperature by Month	X	X O	X O	X O		X	X O

Table 2.2(continued). Significant Data Elements for Predicting Distresses in Pavements With Portland Cement Concrete Surfaces

Significant Data Elements	Distress Types						
	Transverse Cracking	Longitudinal Cracking (JCP)/ Localized Failures (CRCP)	Pumping	Roughness	Friction Loss	Joint Faulting	Joint/ Crack Spalling
Avg. Min. Daily Temp. by Month	X	X O	X O	X O		X	X O
No. of Days Min. Temp. < 32°F (0°C)	X	X O	O	O			O
No. of Days Max. Temp. > 90°F (32°C)		O	X			X	X
Air Freeze-Thaw Cycles	X	X	X	X		X	X

Notes:
- X = data element was selected for JCP studies
- O = data element was selected for CRCP studies
- # = average score greater than 2, but considered very significant by at least one rater.
- PCC = portland cement concrete
- ESAL = equivalent single axle load
- AASHTO = American Association of State Highway and Transportation Officials
- JCP = jointed concrete pavement
- CRCP = continuously reinforced concrete pavement

Large sets of deflection measurements are available for each test section, but these were not included in the sensitivity analyses. Although it is logical to include deflections in a predictive equation to be used for overlay design or other purposes, it is not appropriate to include them in models built for sensitivity analyses, because the responses to load are already explained by other data elements that represent the pavement structure. Including the deflection responses would account twice for the same effects.

From the significance ratings and studies described above the data elements (or independent variables) were selected that were included in the sensitivity analyses for each distress type. Separate analyses are planned for each of the distress types that appear in Tables 2.1 and 2.2 and for each of the applicable GPS experiments. Data limitations and logic led to combinations of data into studies that were not strictly along the GPS experiment lines. These revised data sets (or studies) are described in the next chapter.

3

Restructuring of Sensitivity Analysis Plans

In the original experimental design for the General Pavement Studies (GPS) each experiment was to be analyzed separately. However, subsequent changes in the experimental designs (possibly more reasonably called sampling plans as the test sections were acquired from in-service highways rather than being test sections rigidly controlled as to construction details) and other database limitations led to logical groupings of the data sets to obtain as many test sections with a distress type of interest as possible. This led to combining data sets from GPS-1 and GPS-2 that really fit either experiment, and in combining data sets from GPS-3 and GPS-4, where the presence or lack of reinforcement would have a limited effect on the occurrence of distress. The restructuring of the data sets is discussed separately below for pavements with asphalt concrete surfaces and those with portland cement concrete (PCC) surfaces.

Pavements With Asphalt Concrete Surfaces

Studies were conducted on the combined GPS-1 and GPS-2 data in early 1991 with only the inventory data available at that time. Twelve different categories of pavement structures were identified (Column 1 of Table 3.1), and the number of test sections for each were determined (Column 2 of Table 3.1). It can be seen that an ample database appeared to be available for hot-mix asphalt concrete (HMAC) on granular base, and that reasonable numbers were available for full-depth HMAC without stabilized subgrade and for HMAC on a cement aggregate mixture base. In general, there were not enough test sections of the other types for meaningful individual analysis. Therefore, a study was conducted to identify potential analysis combinations, which appear in Table 3.2.

Table 3.2 indicates pavements with bases that are not subject to vertical shrinkage cracks and those with bases that are subject to vertical shrinkage cracks. This differentiation was made because of its anticipated importance to the modeling of transverse cracking.

Table 3.1. Categories of Pavement Structures in GPS-1/GPS-2 Data Pool and Number of Test Sections for Which Data Are Available

(1) Category of Pavement Structure	(2) Total Test Sections Based on Inventory Data	(3) Total Test Sections Based on Available Data	Test Sections With Data for		
			(4) Rutting	(5) Roughness	(6) Transverse Cracking
1. HMAC on Granular Base	218	202	152	108	85
2. HMAC on Asphalt-Treated Base (ATB) and Granular Base	11	2	2	2	2
3. Full-Depth HMAC With Unstabilized Subgrade	52	50	46	33	22
4. Full-Depth HMAC With Lime-Stabilized Subgrade	7	14	14	12	6
5. Full-Depth HMAC With Cement-Stabilized Subgrade	3	1	1	1	0
6. HMAC Over ATB With Unstabilized Subgrade	18	27	17	21	8
7. HMAC Over ATB With Lime-Stabilized Subgrade	3	3	3	2	0
8. HMAC Over ATB With Cement-Stabilized Subgrade	1	0	0	0	0
9. HMAC with Soil Cement Base	20	16	11	5	8
10. HMAC with Lean Concrete Base	4	6	5	5	4
11. HMAC with Cement Aggregate Mixture Base	40	38	31	26	23
12. HMAC with Pozzolanic Aggregate Mixture Base	2	1	1	0	0
TOTALS	379	360	283	215	158

Table 3.2. Potential Analysis Combinations, GPS-1/GPS-2 Data Pool

Category Combinations	Test Sections	Includes
1	218	All HMAC on Granular Base
1, 2, 3, & 6	299	All Pavements with Bases Not Subject to Vertical Shrinkage Cracks
4, 5, 7, 8, 9, 10, 11, & 12	80	All Pavements with Bases Subject to Vertical Shrinkage Cracks
3, 4, & 5	62	All Full-Depth HMAC
3	52	All Full-Depth HMAC with Unstabilized Subgrade
4 & 5	10	All Full-Depth HMAC with Lime or Cement-Stabilized Subgrade
9	20	All HMAC with Soil Cement Base
9, 10, 11, & 12	66	All HMAC with Soil Cement, Lean Concrete, Cement Aggregate Mixture, or Pozzolanic Aggregate Base

NOTE: The selection of a combination will depend on type of distress and type of structure, as well as reflect experience from other analyses.

HMAC = hot mix asphalt concrete

Study of the data that appeared to be available (Column 2, Table 3.1) and the potential analysis combinations (Table 3.2) led to the proposed steps in the analyses for the distresses indicated in Tables 3.3 and 3.4. The general objective was to start with large data sets and learn as much as possible about suitable equation forms and variable clusters. This experience would then be brought to bear as other combinations were studied and comparisons carried out.

All test sections were assumed to be included in the analyses; however, when only a few test sections were available for a structure type, these test sections would only be used for trials of equations that had been developed from larger databases to see if they might be adequate for somewhat different pavement structures as well. As discussed previously, these plans were developed from inventory data and prior to the availability of data from actual monitoring and material testing. Although friction loss and raveling/weathering were not studied, Table 3.5 has been included because of its potential use to future analysts.

The research team studied the data to see what test sections had experienced the distresses of interest and had the data required for use in the analyses. Table 3.1 also indicates results from these later studies as follows: (1) the numbers of test sections by pavement structure category that generally had sufficient data available for use in analyses (Column 3) and (2) the number of these test sections that had experienced each of the three types of distresses to be studied (Columns 4, 5, and 6). The actual numbers of test sections that could be used in analyses for a particular distress were generally much smaller than originally expected. It became apparent that data limitations would considerably reduce the opportunities for analysis, and some test sections were moved to other categories when materials data from sampling and testing became available. As discussed previously, the only distress types for which the data would support the planned analyses were rutting, roughness, and transverse cracking. There were only eighteen test sections for which fatigue cracking data were available. Future analyses may possibly include those test sections that have not as yet experienced the distresses of interest. These techniques are identified for future consideration in SHRP-P-680, Early Analyses of LTPP General Pavement Studies Data, Lessons Learned and Recommendations for Future Analyses of LTPP Data.

Pavements With Portland Cement Concrete Surfaces

The categories of PCC pavements that were available for the analyses were the jointed plain concrete pavements (JPCP) of GPS-3, the jointed reinforced concrete pavements (JRCP) of GPS-4, and the continuously reinforced concrete pavements (CRCP) of GPS-5. As for the HMAC pavements, there was an investigation to determine whether it would be possible to combine the data available into more logical data sets that would be amenable to the development of the required predictive models.

Unlike HMAC pavements, however, most types of distress that occur on PCC pavements are directly related to the surface type (JCPC, JRCP, or CRCP). In fact, the

mechanisms of distress for PCC pavements almost always relate to the surface type. For example, the distress mechanisms for CRCP are generally different from those for jointed concrete pavements (JCP), and different models are often required for JPCP and JRCP to adequately predict the same type of distress.

Consequently, it was not feasible to combine data sets, other than to combine JPCP and JRCP for faulting and roughness. Even then, because of the strong effects of dowels on the occurrence of joint-related distresses, it was necessary to separate the data sets into one for test sections with dowels and one for those without dowels.

Table 3.3. Proposed Steps in Separate Analyses for Alligator Cracking, Rutting, and Roughness in Pavements With Asphalt Concrete Surfaces

1.	Develop regression equations by using the Statistical Analysis System (SAS®)[3] PROC REG procedure and the data for HMAC over granular base (218 test sections).
2.	If the data elements found to be significant are available for the 11 HMAC/ATB/granular base sections, use their data to see if their performance varies appreciably from that of sections with HMAC on granular base. (Do equations from Step 1 provide reasonable predictions for the 11 HMAC/ATB/granular base sections?)
	Note: If the equations from Step 1 are adequate for the 11 HMAC/ATB/granular base sections, the resultant predictive equations may be recommended for such pavements that include ATB.
3.	Apply experience from Step 1 on equation forms and clusters in the development of regression equations with data for the 52 full-depth HMAC sections without stabilized subgrade. If Step 2 indicates that pavements that include an ATB layer do not perform significantly different from sections whose bituminous layers are all HMAC, then include the 18 HMAC over ATB without stabilized subgrade for a total of 70.
4.	If the 18 HMAC over ATB sections are not included in Step 3, use the equations from Step 3 and the data from the 18 HMAC over ATB sections to see if their performance varies appreciably from that of sections with full-depth HMAC.
5.	Apply experience from previous steps on equation forms and clusters in the development of regression equations with data for the 60 test sections with HMAC over soil cement base (20) or cement-aggregate mixture base (40).
6.	Use the equations from Step 5 and data for the 4 sections with lean concrete base and the 2 sections with pozzolanic-aggregate mixture base to determine whether the equations developed in Step 5 provide reasonable predictions for these types of nonbituminous base.
7.	Review the results from the previous steps to see if better equations could be developed by revising clusters or equation forms. If significant improvements appear possible, pursue the improved equations.
8.	Conduct sensitivity analyses on the predictive equations developed.
9.	Develop graphs and/or other means of presenting the results of the sensitivity analyses.

Table 3.4. Proposed Steps in Sensitivity Analyses for Transverse Cracking in Pavements With Asphalt Concrete Surfaces

1. Develop regression equations using SAS® PROC REG and the data for all HMAC sections without nonbituminous bound base or stabilized subgrade. These will include 218 HMAC over granular base, 11 HMAC over ATB over granular base, 52 full-depth HMAC without stabilized subgrade, and 18 full-depth HMAC over ATB without stabilized subgrade.

2. From the experience from Step 1 concerning equation forms and clusters, develop regression equations for all full-depth HMAC sections with stabilized subgrade (10), HMAC over ATB with stabilized subgrade (4), and HMAC with nonbituminous bound base (66). These includes the following:

    a. 10 test sections with full-depth HMAC (or HMAC/ATB) over lime-stabilized subgrade.

    b. 4 test sections with full-depth HMAC (or HMAC/ATB) over lime- or cement-stabilized subgrade.

    c. 20 test sections with HMAC over soil-cement base.

    d. 4 HMAC test sections over lean concrete base.

    e. 40 HMAC test sections with cement-aggregate mixture base.

    f. 2 HMAC test sections with pozzolanic-aggregate mixture base.

3. Compare the two resulting equations from Steps 1 and 2 by applying the equation from Step 1 to the data used in Step 2, and vice versa. Study residuals in each case to learn what can be done about the effects of differences in base materials on the prediction of transverse cracking.

4. If there do not appear to be serious differences attributable to whether base materials were subject to initial vertical fractures because of shrinkage cracking, regress again, with all data. Study the residuals from each of the equations developed and decide which is to be used for the sensitivity analyses.

5. Conduct sensitivity analyses on the predictive equations developed.

6. Develop graphs and/or other means of presenting the results of the sensitivity analyses.

Table 3.5. Proposed Steps in Separate Analyses for Friction Loss and Raveling/Weathering in Pavements With Asphalt Concrete Surfaces

It appears reasonable to assume that the effects from characteristics of layers below the surface layer will be minor, especially in view of the limited data available that are considered significant to the occurrence of these distresses. Consequently, data from all 379 test sections will be used in the analyses when these data are available. Friction measurements and initial estimates will not be available for all test sections.

It is obvious that the presence of a seal coat, friction course, and such surface treatments will affect the occurrences of these distresses, so identification of the type of surface treatment (if any) and its characteristics (when available) will also be considered in the analysis. However, no testing of thin non-HMAC layers is conducted in the SHRP laboratories, other than measurements of thickness and designation as a seal coat, porous friction course, or surface treatment. The other possibilities for data are from the inventory data or maintenance data. The inventory data only include a code that identifies what type of seal it is (chip, slurry, fog, sand, or chip with modified binder) and the layer thickness. There are virtually no maintenance data currently in the database, but future maintenance activities will be recorded in great detail for future analyses.

The only three available data elements considered to be significant for predicting friction loss are (1) age of pavement, (2) cumulative ESALs, and (3) geological classification of course aggregate. As the latter data element will only be available for HMAC surfaces, there is really no hope for developing equations to predict friction loss for pavements with thin layers of seal coat, porous friction course, or other surface treatments. Consequently, test sections with such surface layers will be omitted from the analyses. Similarly, materials information will also not be available for raveling/weathering of such thin surface layers, so these test sections will be omitted from studies of this distress as well.

The proposed steps follow:

1. Develop regression equations using SAS® PROC REG[3] and data for all 379 test sections, except those with a thin surface layer other than HMAC and those for which distress data are not available.

2. Conduct sensitivity analyses on the predictive equations developed.

3. Develop graphs and/or other means of presenting the results of the sensitivity analyses.

4

Theoretical Variable Clusters and Constraints Imposed by Late and Missing Data

The research staff had hoped to use theoretical clusters of variables to impose current knowledge into the predictive models and to decrease the number of variables to be regressed. The intent was to apply partial differentiation to segregate the relative sensitivities for the individual explanatory variables. In support of this intention, Dr. Robert L. Lytton, consultant to the project, applied mechanistic theory to develop such clusters of variables for use in the studies of pavements with asphalt concrete surfaces. This technical memorandum appears as Appendix B.

Similarly, Drs. Michael I. Darter and Emmanuel Owusu-Antwi developed clusters of variables for use in the studies of pavements with portland cement concrete surfaces. This technical memorandum appears as Appendix C.

Because the use of these theoretical clusters of variables depends on knowing the elastic modulus of the various layers, it was not possible to use these as intended in the regressions. Resilient modulus testing in the laboratories to gain the elastic moduli of the layers did not reach the production testing stage until mid-1992, because of problems in resolving issues in testing protocols and procedures and conducting the round robin tests between laboratories to ensure uniformity. Results from laboratory testing were still not available at the time writing began on this report. Similarly, the capabilities for conducting backcalculations on deflection data were delayed while software was developed to interface with the Regional Information Management Systems, and this software was not available until the analyses were in an advanced stage. As a result, the research staff could use the technical developments only as guidelines in structuring interactive terms within the regression equations.

The technical memoranda discussed above are included in this report; they will have direct applicability for future analyses when the necessary data are available.

5

General Procedures Followed in Developing Predictive Equations for the Sensitivity Analyses

To conduct successful sensitivity analyses of the type considered here, it is necessary to develop equations that are both statistically linear and contain a minimum of collinearity between the independent variables to predict the distresses of interest. Predictive equations linear in the coefficients are required for sensitivity analyses for the following reasons:

- The magnitudes of the effects from varying the individual independent variables would not be directly comparable, otherwise.
- Nonlinear regression techniques are deficient in the diagnostics needed to identify collinearity and influential observations. Because collinearity must be minimized if the relative sensitivities are to be meaningful, use of nonlinear regressions could seriously limit confidence in the results.
- The research staff, including Dr. Olga J. Pendleton, the statistical consultant, are not aware of any existing procedures for conducting sensitivity analyses on nonlinear models; therefore, it would have been necessary to develop a complex computer program which would have been far out of the scope and funding for these studies.

Because it became obvious early in the contract period that there would be delays in delivery of the required data, it was decided to develop a practice data base that Dr. Pendleton could use to demonstrate the appropriate statistical procedures. A practice database was developed for the General Pavement Studies (GPS)-1 experiment by the research staff, who used a combination of data from a variety of sources, some of which were necessarily estimated on the basis of engineering judgment, and by using other available data. These data and sources are indicated below:

- Inventory data that describe the pavement structure, its materials, and some construction information.
- Distress data from early visual surveys during initial acceptance visits to the test sections.
- Equivalent singl axle loads (ESALs) per year from early State Highway Agencies (SHAs) estimates during candidate test section recruitment.
- Environmental data from climatic isobar maps.
- Stiffness data for asphalt concrete (AC) and base, estimated through consideration of materials types, classification data from state records, and other inventory data.
- Subgrade stiffness calculated from Sensor 6 deflections.
- AC layers combined and base and subbase combined to restrict data to three-layer structures.

This practice database was used to study the nature of the data and develop the procedures to be used. Because the Statistical Analysis Systems (SAS®) software[3] was selected for conducting the studies, the procedures developed were based on that software and identification of subroutines all refer to the SAS® software.

A tutorial was conducted for the research staff from both Brent Rauhut Engineering Inc. (BRE) and ERES Consultants, Inc. (ERES) at Texas A&M University. The technical manager for the Strategic Highway Research Program (SHRP), Dr. Robert Raab, also attended. Amy Simpson, BRE's staff engineer, who was later trained, conducted the sensitivity analyses. A detailed technical memorandum was written to explain these procedures in detail and gives examples. This technical memorandum appears in Appendix D. While this chapter will provide a brief discussion of these procedures, the technical memorandum provides additional detail.

General Procedures

A flow chart for the general procedures to be applied appears in Figure 5.1. The selections of independent variables to be included in the studies are described in Chapter 2, and the development of theoretical clusters of variables was discussed briefly in Chapter 4. The selections of transformations of the variable (e.g., in logarithmic form rather than arithmetic) and interactions were primarily carried out as part of the multiple regressions themselves, which were part of the multivariate analyses indicated in Figure 5.1.

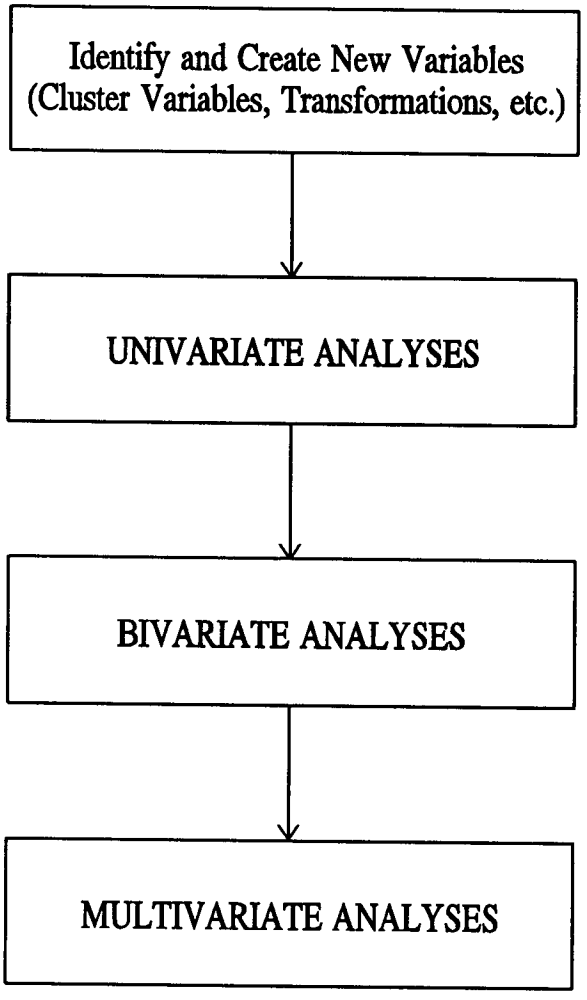

Figure 5.1. Flow Chart for Data Studies and Development of Equations to Predict Significant Distresses

The univariate analyses examine the data to determine potential distributional problems and anomalies. (Results from similar studies appear in SHRP-P-684, Early Analyses of LTPP General Pavement Studies Data, Data Processing and Evaluation for each GPS experiment.) The purposes were to examine marginal distributions, identify gaps in the data, identify any unusual observations, and identify functional forms. The procedures included studies of continuous data descriptive statistics and frequency distributions by using PROC UNIVARIATE, and partitioning continuous variables by categorical ones, by using PROC UNIVARIATE with BY option.

The bivariate analyses were used to study pairs of data elements, which may turn out to be unusual although each variable by itself is not unusual. The specific expectations from the bivariate analyses are to identify two-variable relationships, bivariate unusual points, bivariate collinearities, data gaps, functional forms, and data clusters. The procedures are as follows:

- Study two-variable scatter plots produced from PROC PLOT.
- Study correlations produced by PROC CORR.
- Study categorical data contingency tables obtained by PROC FREQ.
- Study partitioned correlations or plots by categorical data levels, produced by PROC CORR and PROC PLOT with BY option.

The final step in the development of the predictive equations is collectively termed "multivariate analyses." These analyses included studies to identify multivariate collinearities and the development of the pavement distress models. The procedures planned included the following:

- Discriminant analysis to identify distressed and nondistressed pavements, using PROC REG with transformed variables.
- Development of regression analysis models for distressed pavements, using PROC REG.
- Analysis of variance, comparing the means of independent variables for distressed and nondistressed pavements, using PROC GLM.

The procedures described above were carried out as indicated, but it became apparent during the analyses that revisions and additions would be required. These are discussed in the next section of this chapter.

Principal component analysis was used to detect collinearity and influential observations. This method uses plots of eigenvector pairs to identify collinearities that may be masked by outliers.[4]

In addition to the use of the univariate and principal component analysis procedures to detect outliers and influential observations, a procedure was used that is very similar to the principal component analysis. Once the model had been completely developed, the observations were examined in n-dimensional space to determine which were the farthest from the center of the data set. The center was found by determining the average of each data element. The five observations found to be the farthest from the center of the data set were deleted from each regression. It was not determined whether these five observations were significant influential observations. In the future, contours can be drawn around the data sets at specific significance levels. Any points lying outside the 95% contour should be considered significant influential observations.

It should be noted that the measured distresses for the in-service pavements do not include the period just after the lane was opened to traffic. Consequently, early compaction from traffic is not directly represented. As a boundary condition, the log of cumulative KESALs (1,000 ESALs) was included in each equation as a separate term to enforce zero rutting with zero ESALs. Mathematically, the equations are undefined at zero ESALs; however, for practical purposes it is assumed that zero to some power is zero. The same boundary condition was enforced to ensure zero change in International Roughness Index (IRI) with zero cumulative ESALs, and age was used to enforce zero transverse cracking at the time of construction. Consequently, the predicted progression of distresses very early in a pavement's life is not reliable (and not especially important either as will be seen later).

Problems Encountered and Modifications to Procedures

Once the procedures were developed, work began with the complete database. The first distress type considered was rutting of hot mix asphalt concrete (HMAC) pavements over granular base. As problems were encountered, this data set was used as a "test bed" for identifying problems and working out solutions before continuing with data sets for other distresses and pavement types.

As required for the sensitivity analyses, modeling was conducted using the least squares linear regression technique which minimizes random error. This technique also assumes that the dependent variable is normally distributed about the regression line and that the independent variables are fixed and without error. It is believed that the distresses have approximately log-normal distributions about the regression line; therefore, the regressions were conducted to predict the common logarithm of the distress.

The first step was to analyze the individual independent variables with the SAS® all possible subset selection procedure. This procedure allows the user to offer a list of independent variables, and the system will select which of these variables, singly and in combination, best predict the dependent variable. This procedure was not expected to give the final model; however, it was expected to aid in determining which variables were the most influential to prediction of the dependent variable.

The second step was similar to the first, except that all possible two- and three-way interactions were tried in the regressions. The interactive terms were selected through consideration of the theoretical variable clusters discussed in Chapter 4, terms appearing in prior distress equations, and engineering experience and judgment. When the sensitivity analyses were conducted on the resulting model, it became apparent that each independent variable needed to be in either log form or nonlog form, but not in both. This model did not meet that criterion. For example, asphalt thickness was present both as asphalt thickness and log asphalt thickness. Although both an independent variable and its logarithm might be found to contribute to the explanation of the variance in the dependent variable, only one or the other was considered for subsequent models.

The third step was to raise variables within the model to some power. The power was determined through an iterative process that found the models with the best root mean square error (RMSE), coefficient of determination (R^2), and *P* value on the individual variable. The *P* value is used to determine whether the independent variable is significant to the prediction of the dependent variable. However, the sensitivity analysis on the resulting equation did not produce logical or believable results. These results led to serious discussions and experimentation, which then led to the conclusion that three-way interactions (containing three independent variables in a single term) and the powers of the variables were confounding the sensitivity analyses. It was decided to limit the models to main effects (single independent variables) and two-way interactions. While the fit of the resultant models was slightly (though not significantly) worse, the sensitivity results appeared much more logical.

As an additional trial, it was decided to try producing a predictive model for rutting by using only test sections with two rutting measurements taken at different points in time. Two measurements (other than the zero at construction) were available for 121 sections, and those sections with only one measurement were deleted *for this trial only*. The analyses were rerun, but the model statistics were no better than before. The two points were no more (and generally less) than 2 years apart; it is likely that more time series data will be required to improve the fit.

To determine the stability of the model, regression analyses were completed on five different sets of 80% of the complete data set (a different 20% deleted each time), by using the same equation form. The coefficients for each independent variable for each run were compared and found to be quite variable. If the equation had been stable, the coefficients would have been very similar.

Correlation among independent variables can lead to estimates of model coefficients that are illogical in sign. For example, when the variables "average monthly maximum temperature" and "annual number of days greater than 90°F (32°C)" were used in the equation for rutting, they had opposite signs. Although these nonintuitive model estimates do not generally mar the model's predictive ability, they are somewhat disconcerting to the practitioner and are difficult to explain. At this point it was decided to try the technique of ridge regression,[5] a statistical method that adjusts for collinearity (correlated independent variables) and produces more stable and logical model estimates. One may visualize the procedure as adding *m* dummy equations of condition to the *n* real equations of condition, where *m* is the number of independent variables in the regression, and *n* is the number of observations. (An equation of condition is an equation in the form of the desired regression between the dependent variable for a given observation and the independent variables for that same observation.) The parameter estimates in many cases change dramatically when the ridge regression procedure is used. At some point during the iterative model developments the change in the parameter estimates becomes much smaller, and this equation is the final one that is used.

The terms in the equations previously checked by using five different sets of 80% of the data set had been primarily interactions between the independent variables. Thus, some of the main effects (individual independent variables) were added to the equation form, and the regressions were repeated, with a different 80% of the data set for each model. The comparisons of the five sets of coefficients proved to be much more consistent, which indicated that the revised equation form fit the data better.

The model was found to contain certain highly correlated variables such as age and KESALs and subgrade moisture and annual precipitation. These pairs were identified and the variables in each pair with relatively low sensitivities were replaced by the variables with which they were correlated. The sensitivity analysis results for this equation were much more reasonable. The equation was then changed so that the other half of the pair was used in the interactions. The model created by using the variables with higher sensitivities produced much more logical results.

All the models produced to this point and their resulting statistics were established from a data set that involved the entire data set. In an effort to improve model statistics, the data were separated according to the four environmental zones used in the sampling templates, and each data set was regressed using the equation form that contained the better half of the pair. The results from some of the sensitivity analyses were not always reasonable. To try to remedy the problems encountered in the sensitivity analyses, models were (as described above) found using main effects alone. The R^2s decreased and RMSEs increased somewhat; however, the results from the sensitivity analyses were more reasonable. Next, interactions that had previously been found to work well (including some of the three-way interactions) were added to the equations with just main effects. Values of R^2 and RMSE were improved, but the results from the sensitivity analyses were not all reasonable. The above interactions were dropped from the equations, and only two-way interactions were added. The values of R^2 and RMSE were not as good as those that included the three-way interactions but were better than the equations with just main effects. The results from the sensitivity analyses were more logical but still problematic, particularly for the wet-no freeze and dry-no freeze zones.

For the wet-no freeze and dry-no freeze zones, log(KESALs) was replaced with age in the equations. Problems still existed for the sensitivity analyses for these zones. Age was then replaced by log(KESALs) in these two equations, and new two-way interactions were introduced. Sensitivity analysis results for the dry-freeze zone were somewhat improved.

Coordination with the statistical consultant indicated that sufficient collinearity had not been expelled from the equation, so eigenanalysis (see Appendix D) was used to identify additional variables to delete from the models. The ridge regressions mentioned previously were then used to develop new models. In each of the models, KESALs and structural thicknesses were forced into the equations. That is, the variables were placed in the models even if they did not improve the statistics.

It was concluded, at this point, that the five models — one for the entire data set and one each for each of the four environmental zones — were as good as could reasonably be expected within the constraints imposed by the requirements for sensitivity analyses and by limitations in the data sets available (primarily lack of adequate time sequence data for these early analyses). The techniques finally used for the rutting model were then adopted for other distresses and pavement types.

Procedures Adopted for Developing Distress Models for Sensitivity Analyses

The procedure, arrived at by the experimentation described above for developing distress models to be used for sensitivity analyses, is described in the next chapter. The modeling and sensitivity analyses are best combined as one process, so judgment can be applied to iterate toward the optimum models for use. The analyst must carefully reach a balance between (1) expectations and knowledge from past research and (2) maintaining opportunity for the data to communicate new knowledge.

This procedure does not offer the best models for predicting pavement distress. It is likely that nonlinear regression techniques would result in better models. However, these models would not have been practical for the sensitivity analyses, because sensitivity analyses for nonlinear models are much more complex, and there are no computer programs (such as SAS® for linear models) to use in conducting them. However, this does not preclude common transformations, such as the use of logarithms or powers of the independent variables, as long as the equations are linear in the coefficients.

Alternative Procedures Used for Developing Models for PCC Pavement Distresses

The procedures used by ERES research staff for developing the portland cement concrete (PCC) pavement models were essentially those discussed above, except that the staff decided to take advantage of some graphical capabilities in the S-Plus statistical software while the studies were in progress[6]. This allowed them to easily view scatter plots and three-dimensional plots of the data, which indicated relationships between all the dependent and independent variables being considered. From observations of the two- and three-dimensional plots, the explanatory variables that were not linearly related to the dependent variables were noted. Such variables were linearized by determining the best exponents for these variables, which was done by use of the Alternating Conditional Expectations (ACE) algorithm introduced by Breiman and Friedman, along with the Box-Cox transformation. Detailed descriptions of these techniques are provided in "Design of Joints in Concrete Pavements" by R.D. Bradbury[7].

These procedures were used to develop the final models used in the sensitivity analyses. In several cases, this general procedure had to be modified to meet the specific demands for the model to be developed.

6

General Procedures for Establishing Sensitivities of Predicted Distresses to Variations in Significant Independent Variables

The original intent was to standardize all independent variables in a distress model so that the coefficients on each term would represent the impact of that term. This step would be done by subtracting each observation from the mean for that variable (to calculate deviation from the mean) and dividing by the standard deviation. The model would then be regressed again with these standardized observations and using the same equation form. The sensitivity of the distress to an independent variable would then be determined by varying each variable in the standardized equation individually from one standard deviation above its mean to one standard deviation below its mean. The resulting change in predicted distress would then represent the relative sensitivity of the distress type to that independent variable.

Depending on the types of independent variables, short-cut mathematical transformations can at times be used to facilitate computations. In the days of hand calculations, independent variables that were evenly spaced could be recoded with an orthogonal coding scheme to make such hand calculations easier. This is not an issue in today's world of computers and is mentioned here only to relate to previous sensitivity analyses that were able to take advantage of this simplification. In reality, x-variables are seldom, if ever equally spaced, especially with observational, noncontrolled experimental situations. All that is necessary is to subtract the mean and divide by the standard deviation of each x-variable (standardization). In analyses where a single x-variable is actually a cluster of more than one independent variable, and the sensitivity of the individual components of the cluster is of interest, this standardization is slightly modified. The cluster is standardized in the usual fashion. To determine the sensitivity of a given component of the cluster, all other components in the cluster are set to their mean and the component of interest is varied.

General Procedures for Establishing Sensitivities of Predicted Distresses for HMAC Pavements

All the previously discussed trials were run on the data set for rutting in hot mix asphalt concrete (HMAC) pavements on granular base. These procedures led to an algorithm that has been consistently used to determine all the models. The algorithm appears in Figure 6.1 as a flow chart and is also described below:

1. Starting with log traffic, each single variable of the set of variables considered and its transformations are tried in the model. If a variable is found to improve the coefficient of determination (R^2), adjusted R^2, and root mean square error (RMSE) without adding collinearity, it is allowed to stay. After all the individual independent variables have been tried once, any that are not in the model at that point are tried again. For consistency's sake the first set of variables tried after log traffic are those dealing with the HMAC layers. Next, the variables identifying the base layers are tried, followed by the subgrade variables, and finally the environmental variables.

2. Once an equation with the main effects (variables identified as significant) has been established, other equations are tried that include two-way interactions of the main effects. If a trial interaction improves the R^2, the adjusted R^2, and the RMSE, but does not add collinearity, it is allowed to stay in the model. This process is repeated until all possible two-way interactions have been tried. Although techniques previously described were used to identify outliers, the analyst should be alert for other outliers that may be revealed as the analysis continues. It should be noted that the main effects in some cases were replaced by interactions.

3. The ridge regression technique is then applied to stabilize the model, using the main effects and interactions that survived Step 2.

4. The sensitivity analysis on the final model is conducted as discussed above.

It should be understood that the calculated sensitivities that are assigned for the individual independent variables very much depend on the predictive equation itself. The values will vary, depending on the form of the equation and the set of independent variables included. As will be seen in the next chapter, models for different environmental zones can vary considerably in form and in variables that are significant to the prediction of a distress. Therefore, the relative sensitivities of the independent variables should be considered indicative of their relative significance, rather than as absolute measures of the relative importance of the variables in terms of magnitude. As obvious examples, it can be concluded that traffic, HMAC thickness, and precipitation merit consideration in design and pavement management, but one may not be exactly twice as important or a half as important than another.

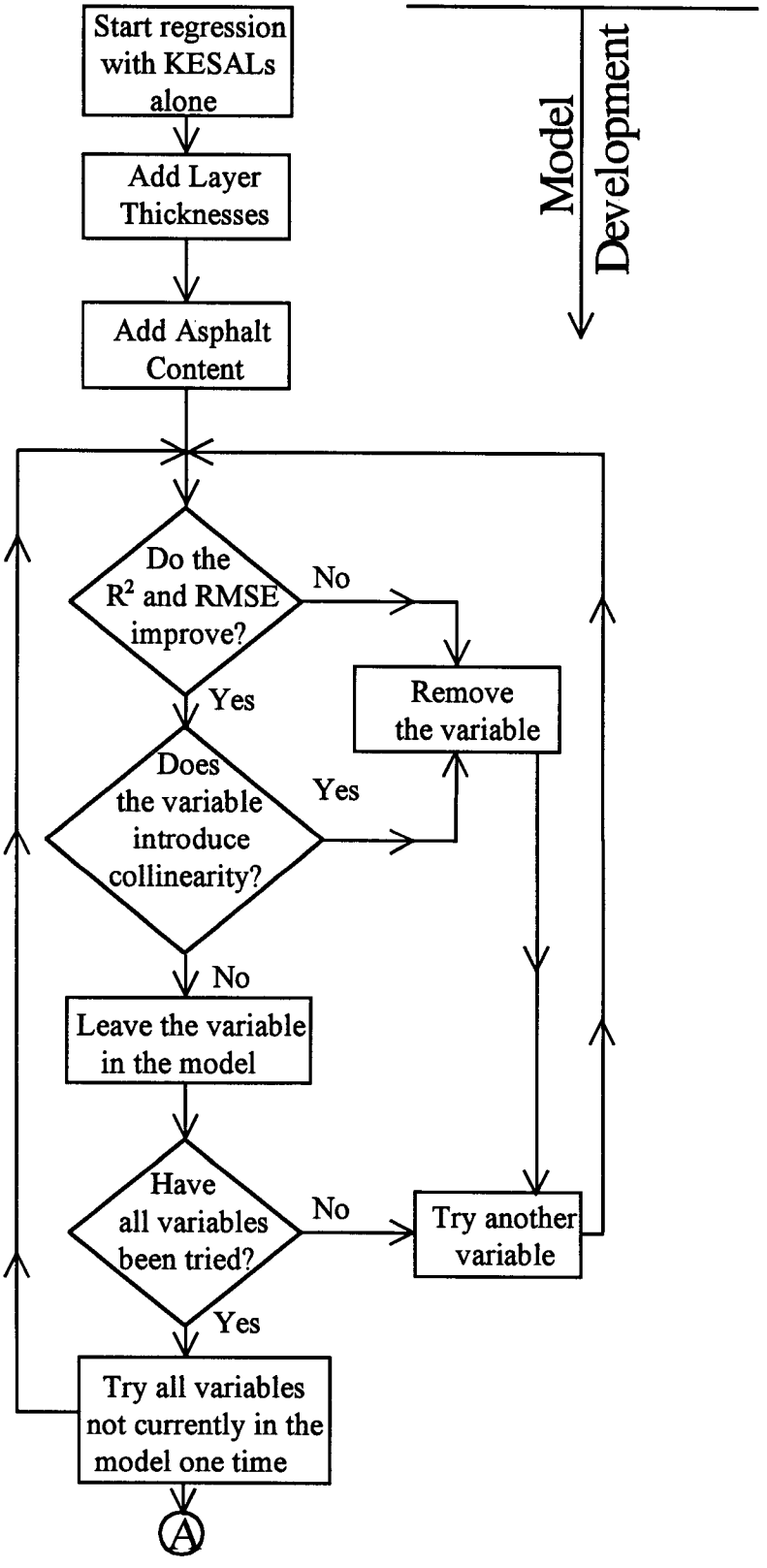

Figure 6.1. Flow Chart for Developing Distress Models and Conducting Sensitivity Analyses

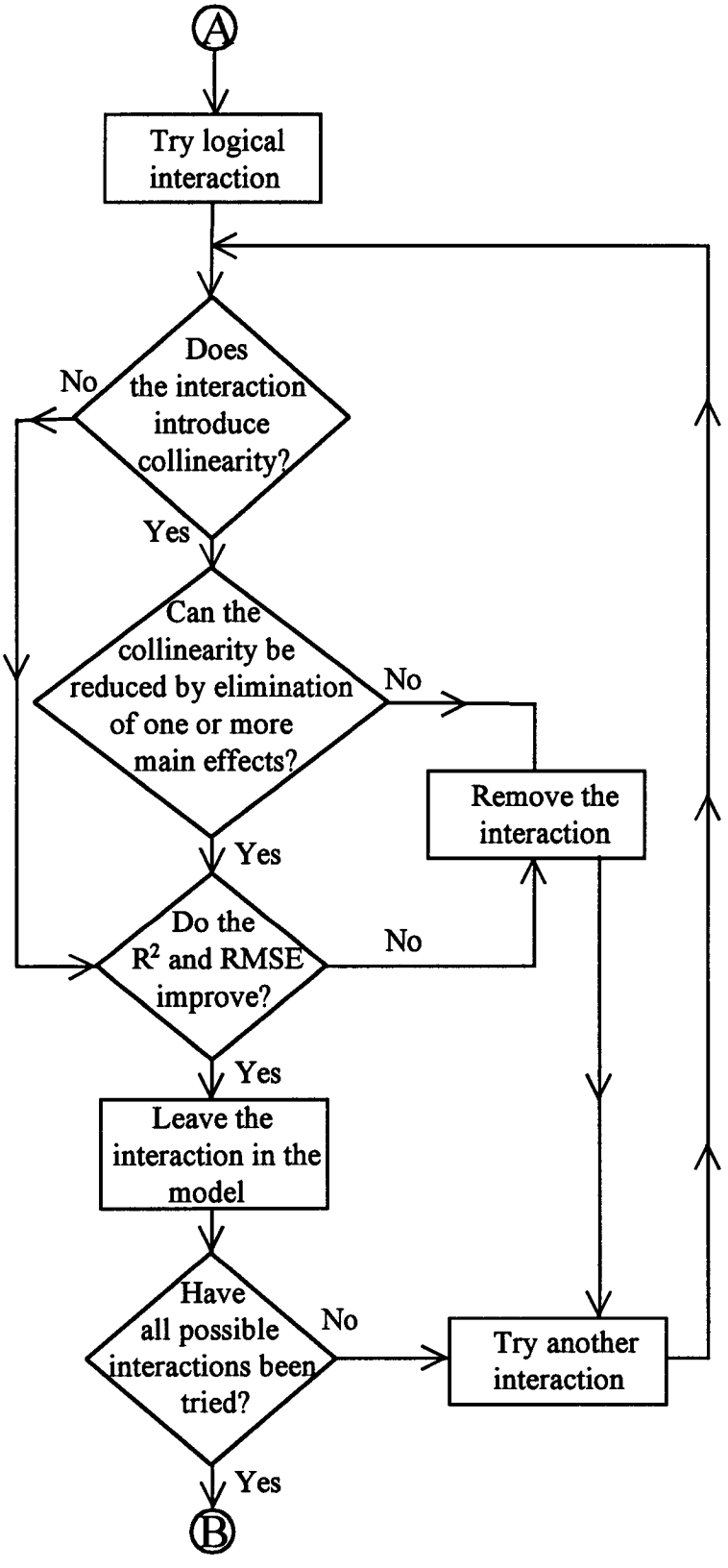

Figure 6.1(continued). Flow Chart for Developing Distress Models and Conducting Sensitivity Analyses

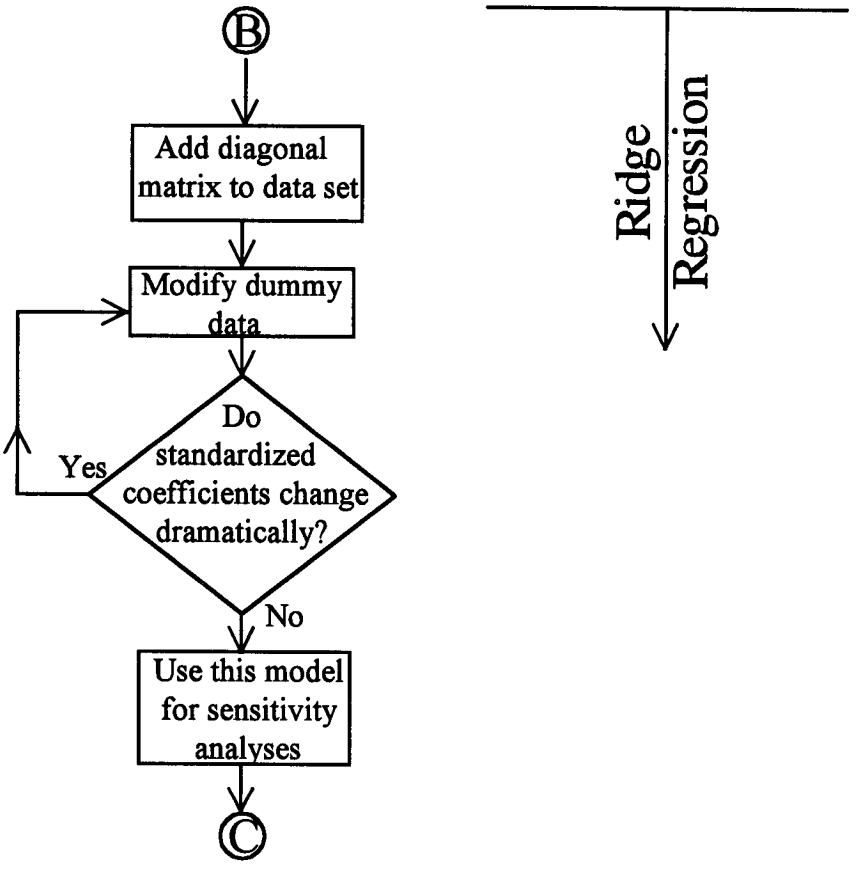

Figure 6.1(continued). Flow Chart for Developing Distress Models and Conducting Sensitivity Analyses

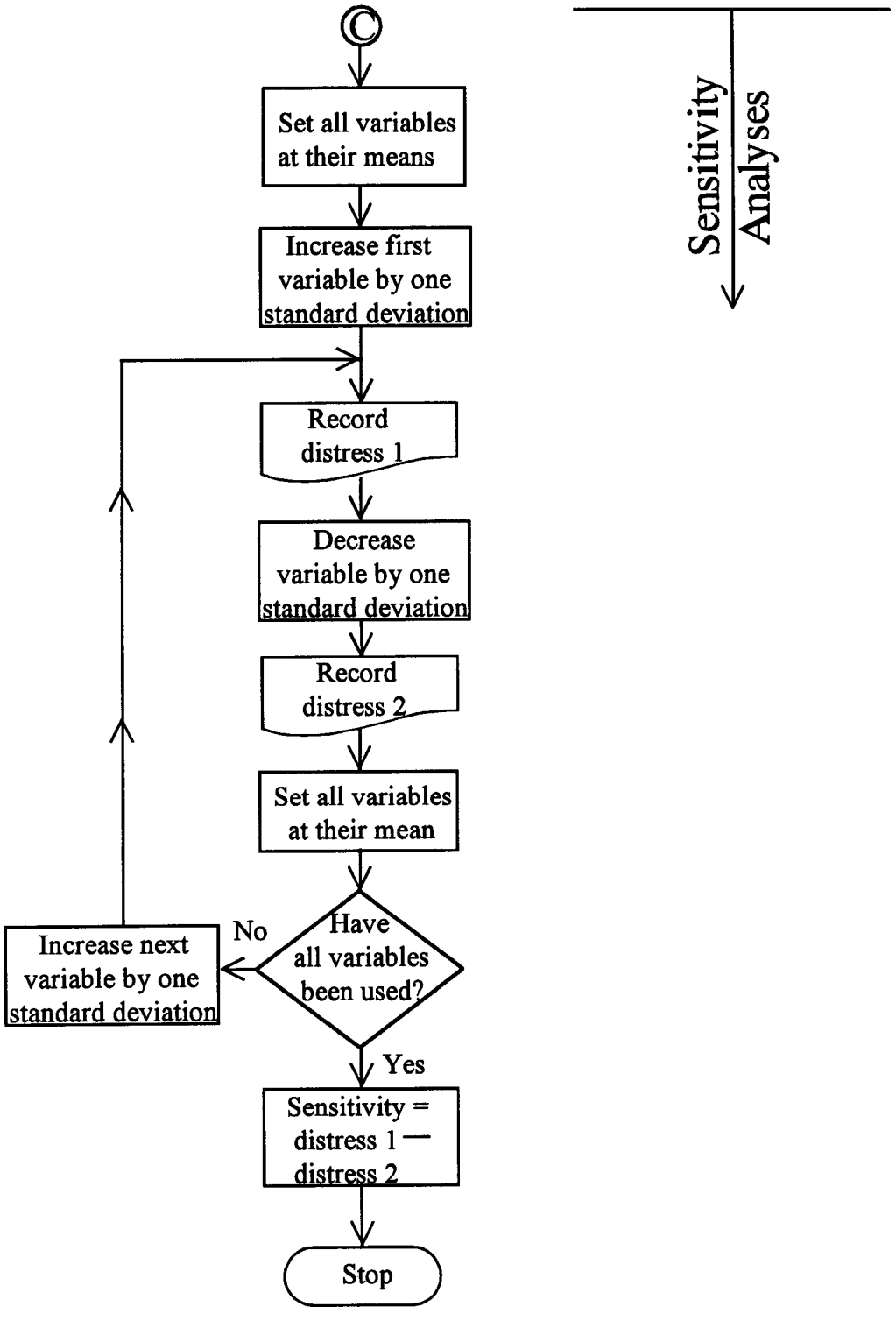

Figure 6.1(continued). Flow Chart for Developing Distress Models and Conducting Sensitivity Analyses

While future predictive equations may be more precise and consequently offer higher confidence in the relative importance of individual variables, it is likely that truly precise evaluations may never be reached. However, the present equations should suffice if the significant variables here continue to be found significant in future analyses and are found to have more or less the same relative importance in relation to each other.

General Procedures for Establishing Sensitivities of Predicted Distresses for PCC Pavements

The only differences between the procedures used for the sensitivity analyses for HMAC and portland cement concrete (PCC) pavements were in the modeling process, as discussed in Chapter 5. The use by the ERES staff of the S-Plus™ plotting capabilities and their linearization of the independent variables replaced the use of ridge regression and some of the iterations in the HMAC procedures discussed above. Figure 6.2 shows the procedures that were used to develop distress/International Roughness Index (IRI) models for PCC pavements.

Once modeling had been completed, the ERES research staff used the same procedures to determine the sensitivities of the dependent variable to variations in the independent variables as were used for the HMAC data. These procedures are also shown in Figure 6.2.

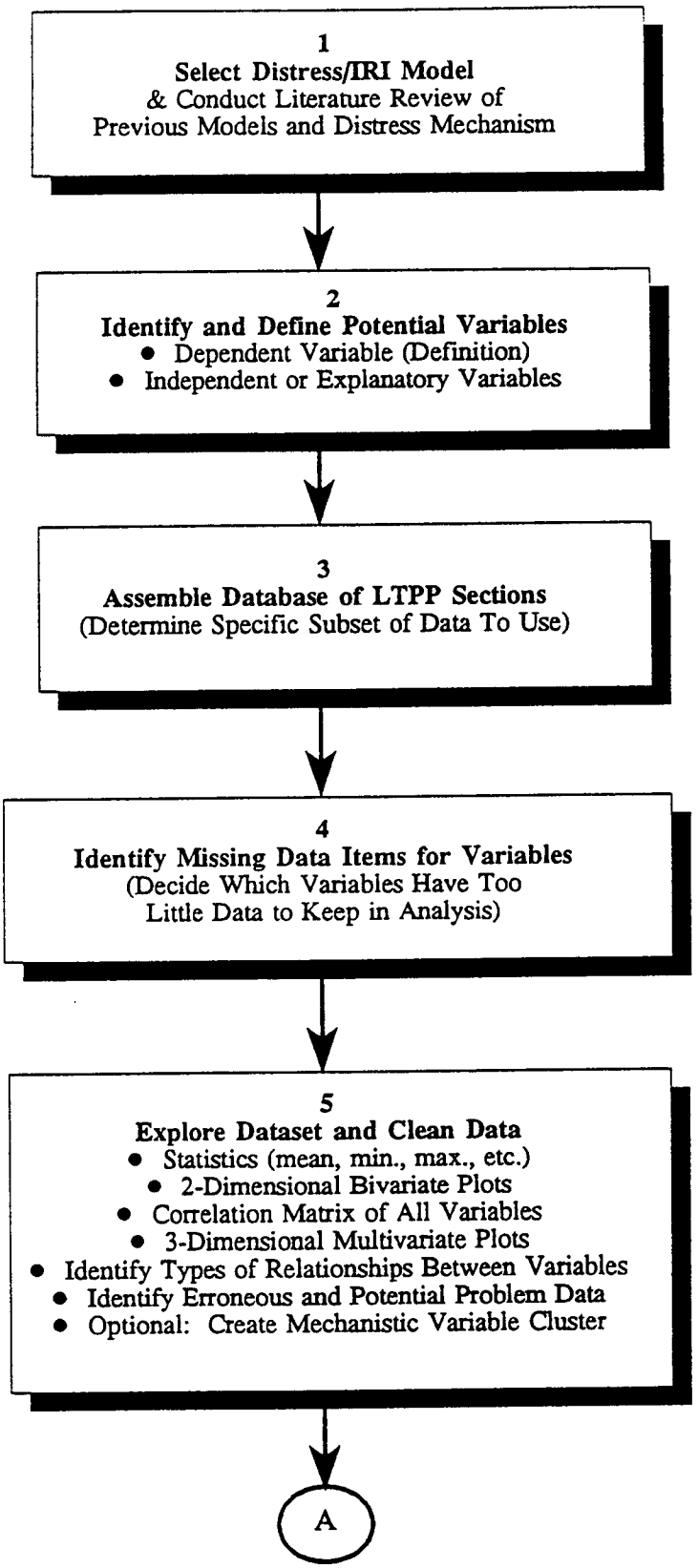

Figure 6.2. Flow Chart for Developing Distress Models for Rigid Pavements

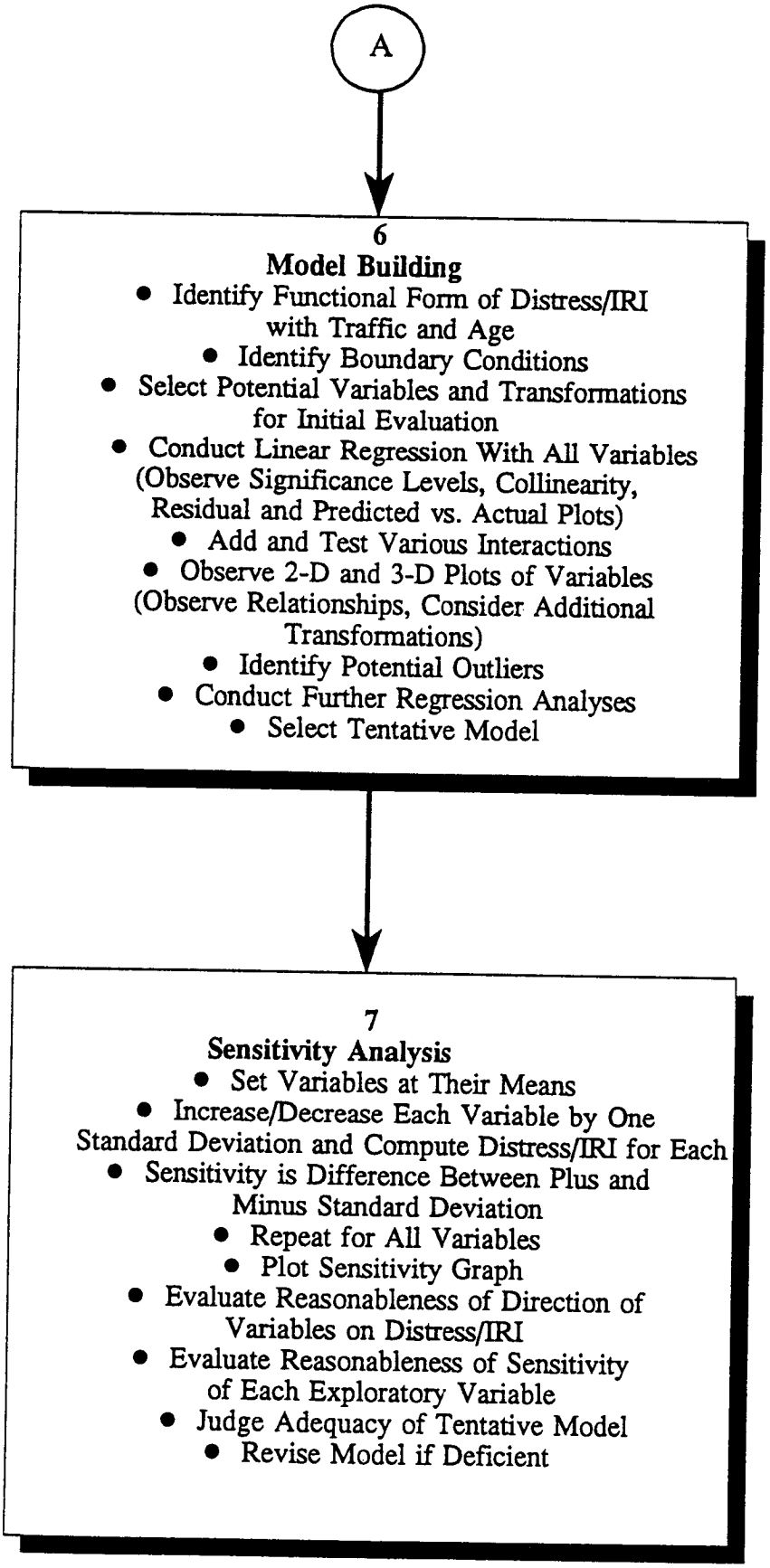

Figure 6.2(continued). Flow Chart for Developing Distress Models for Rigid Pavements

7

Predictive Equations for Distress Types and Results of Sensitivity Analyses for Asphalt Concrete Pavements

Previous chapters have dealt with the methodology applied to select significant data elements that impact the occurrence of pavement distresses, to sort the data into data sets for analysis, to develop predictive distress models, and to conduct sensitivity analyses. This chapter presents the results in terms of predictive equations and relative sensitivity analysis results for hot mix asphalt concrete (HMAC) pavements. The results for the various combinations of distress and pavement types are discussed separately below.

Data Review and Evaluation

Detailed statistical evaluations of the data were conducted for each specific combination of distress and pavement types as described in Chapter 5. Products from these evaluations that were used in the development of predictive equations included the following:

- Two-variable scatter plots
- Variable frequency distributions for the entire database and by enviromental zones
- Correlation matrices for the separate data sets individually
- Complete eigenanalysis for each data set individually
- Residual plots for trial equations
- Plots of predicted versus actual distresses

Traffic data were also reviewed for individual test sections as to their reasonability while they were being processed into each data set.

These products are far too voluminous to include in this report. The Statistical Analysis System[3] (SAS®) correlation analyses alone filled a stack of paper 3/4-in. (19 mm) thick. Most of these data appear in SHRP-P-684, Early Analyses of LTPP General Pavement Studies Data, Data Processing and Evaluation, except they are recorded by General Pavement Studies (GPS) experiment rather than by the databases used in these analyses. Some examples are included in this section, and plots of predicted versus actual distresses and residuals versus predicted distresses appear in subsequent sections for the equations selected.

Figures 7.1, 7.2, and 7.3 show scatter plots for rut depth, change in roughness, and transverse cracking versus cumulative KESALs (1,0000 equivalent single axle loads), cumulative KESALs, and age, respectively, for the HMAC over granular base data set. While the scatter when plotting a single variable versus another single variable is always broad, these plots do provide some insight as to what type of function would fit the data.

Figure 7.4 shows the frequency distribution of cumulative KESALs by environmental zone for the HMAC over granular base data set for change in roughness. Because these distributions appear to be more log normal than normal, this fact influenced the research staff to conduct the regressions on log(KESALs). The general equation forms selected also provided for zero distress when KESALs were zero.

Figures 7.5, 7.6, and 7.7 show distributions of rut depth, change in International Roughness Index (IRI), and transverse crack spacing, respectively, for the HMAC over granular base data sets. It should be remembered that the test sections represented by each data set are not the same for the different distresses. The tendency toward log normal distributions illustrated in these figures contributed to the research staff's decision to develop the regression equations for the logarithm of distress as the dependent variable in each case.

Table 7.1 shows the correlation matrix (as it is printed out with the SAS® software) for change in roughness (DIRI) of HMAC over granular base. The top line for a variable identified in the left-hand column reports the correlation between that variable and a specific variable of those identified along the top row. The bottom line reports the probability that the variables identified in a column and row are *not* correlated. If the probability indicated in the bottom line is less than 0.05, significant correlation may be assumed. As can be seen, the first two pages in the table are required to include all variables identified in the rows, and the third and fourth pages add additional columns. This was necessary to include all twenty-two variables in the analysis. Items found to have significant correlation have been shaded.

Although some of the variables in the correlation matrix can be easily identified, others cannot, and so they are identified below:

DIRI	=	change in roughness measured as IRI
BOTHIRI	=	measured IRI
INITIRI3	=	estimated initial IRI
A_THICK	=	thickness of HMAC layers combined

ASPHALT	=	asphalt content
AIR_VOID	=	air voids in HMAC layer in place
NO_FOUR	=	percentage of HMAC aggregate passing a #4 sieve
VISC_140	=	viscosity of asphalt at 140°F (60°C)
B_THICK	=	thickness of granular base and subbase layers combined
COMPACTI	=	base compaction
PI	=	Plasticity Index of subgrade soil
#200	=	percentage of subgrade soil passing a #200 sieve
YEARS	=	age of pavement
KESALs	=	cumulative equivalent single axle loads in thousands
TOTPREC_	=	total precipitation
AVG90	=	average days per year when air temperature exceeds 90°F (32°C)
AVGFRZTH	=	average number of air freeze-thaw cycles per year
AVGMAX	=	average of maximum daily temperatures for each month
AVGMIN	=	average of minimum daily temperatures for each month
TEMPDIF	=	average daily temperature range
MAXTEMP	=	average maximum temperature for June, July, and August
MINTEMP	=	average minimum temperature for December, January, and February

It can be seen from Table 7.1 that DIRI is apparently only directly correlated with asphalt viscosity. The correlation matrix was used primarily to identify independent variables that were correlated with other independent variables. If two variables were highly correlated, only one would be included in a trial equation. In some cases where the correlations were more limited, the two variables were sometimes combined in an interaction and were included in a trial equation.

It can also be seen from Table 7.1 that most of the climatic variables are highly correlated, so one variable could often explain the effects of several others.

The eigenanalysis is described in Appendix D.

Rutting of HMAC Pavements on Granular Base

The predictive equations for the entire data set and those for the four environmental zones appear in Table 7.2. As discussed previously, the actual regressions were conducted to predict $\log_{10}$(rut depth), which led to the equation form indicated at the top of the table, which applies for all five predictive equations. The statistics for the equations also appear below each equation box, as well as the number (n) of

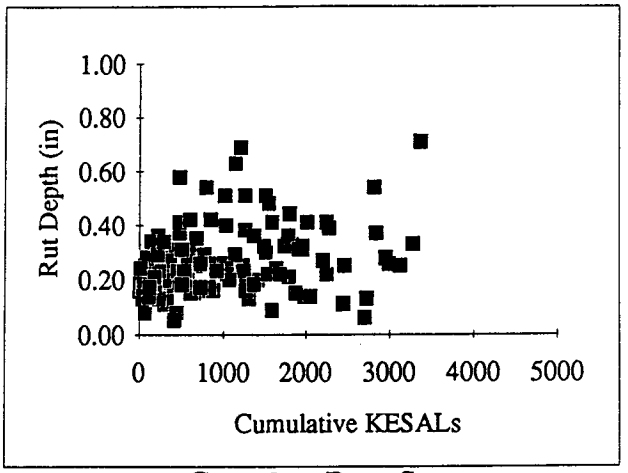

a. Complete Data Set

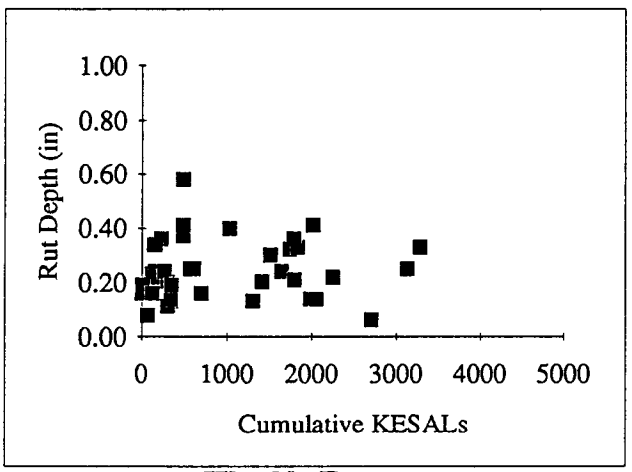

b. Wet-No Freeze

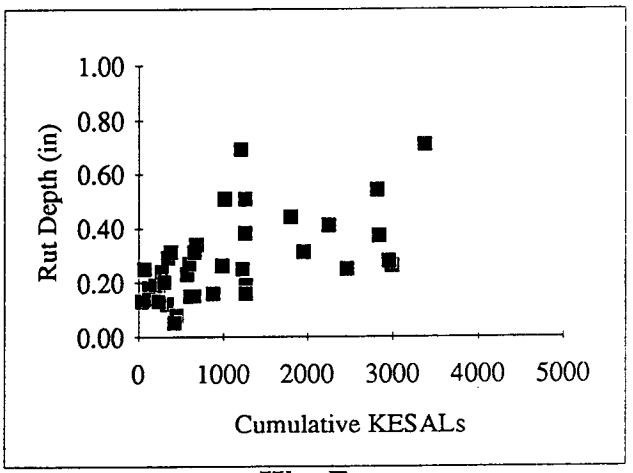

c. Wet-Freeze

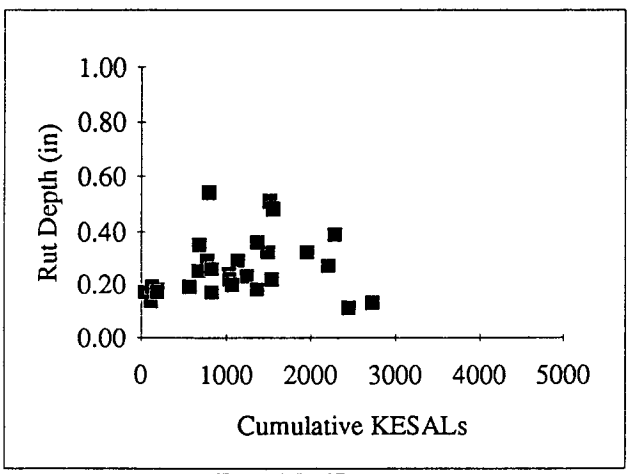

d. Dry-No Freeze

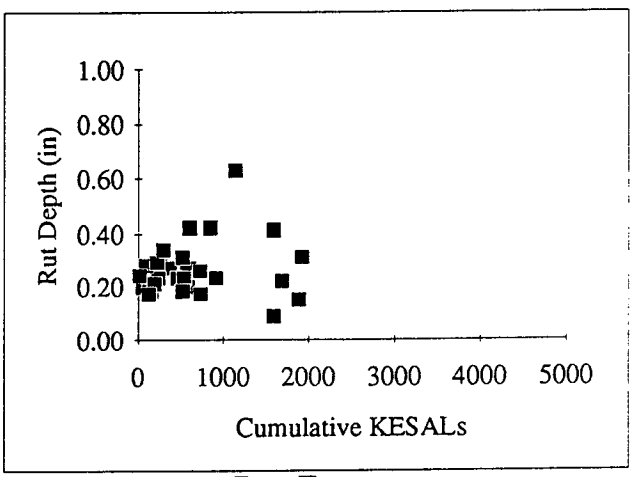

e. Dry-Freeze

Figure 7.1. Scatter Plots of Rut Depth vs. Cumulative KESALs for Complete and Regional Data Sets, HMAC Over Granular Base

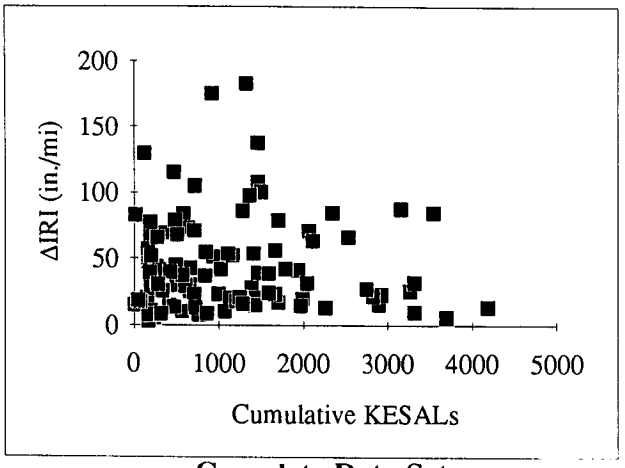

a. Complete Data Set

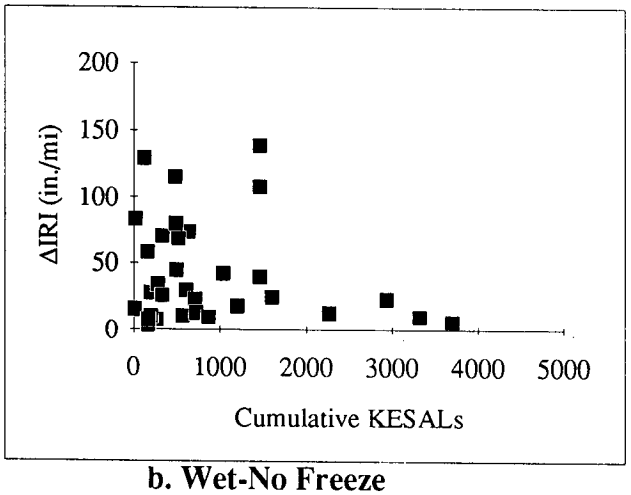

b. Wet-No Freeze

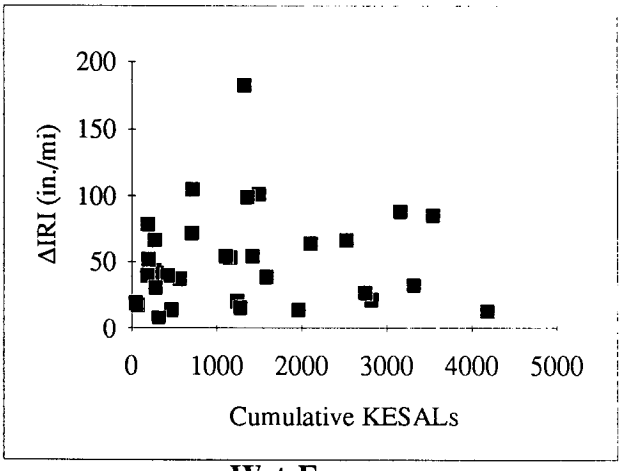

c. Wet-Freeze

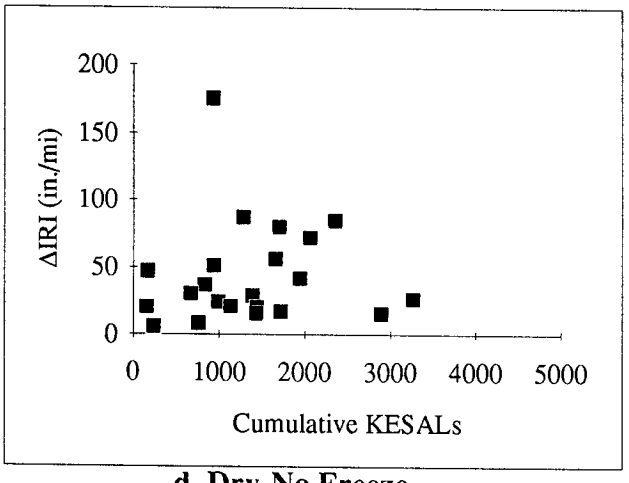

d. Dry-No Freeze

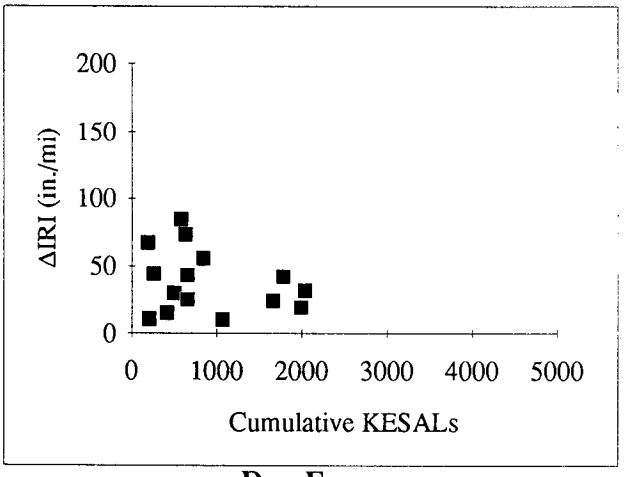

e. Dry-Freeze

Figure 7.2. Scatter Plots of Change in Roughness vs. Cumulative KESALs for Complete and Regional Data Sets, HMAC on Granular Base

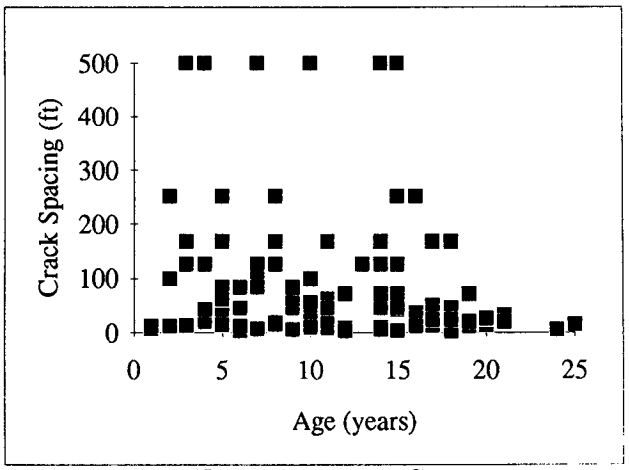

a. Complete Data Set

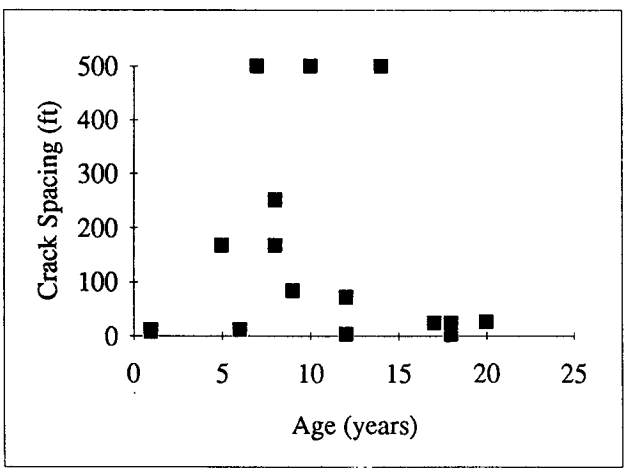

b. Wet-No Freeze

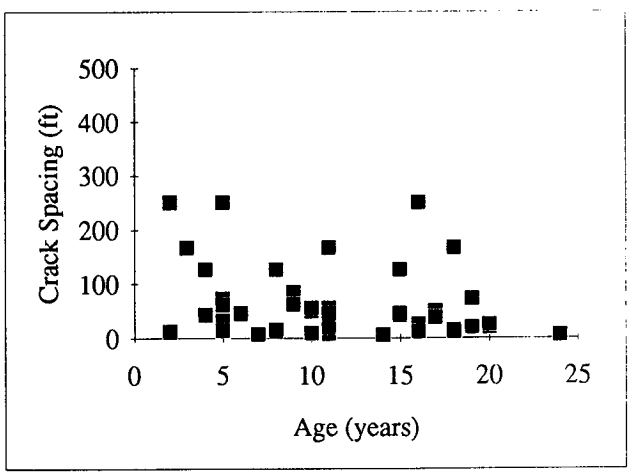

c. Wet-Freeze

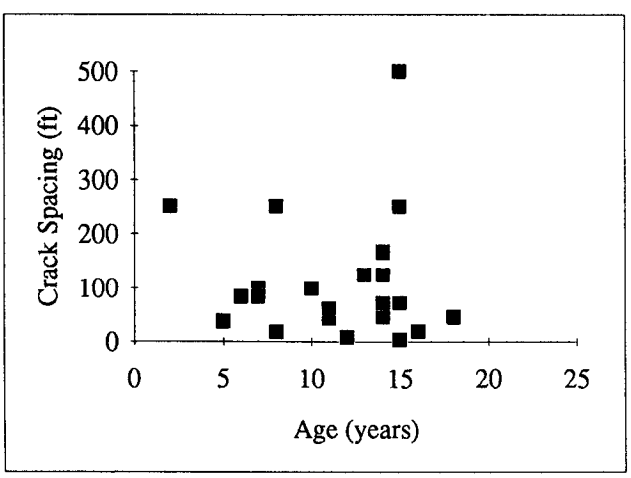

d. Dry-No Freeze

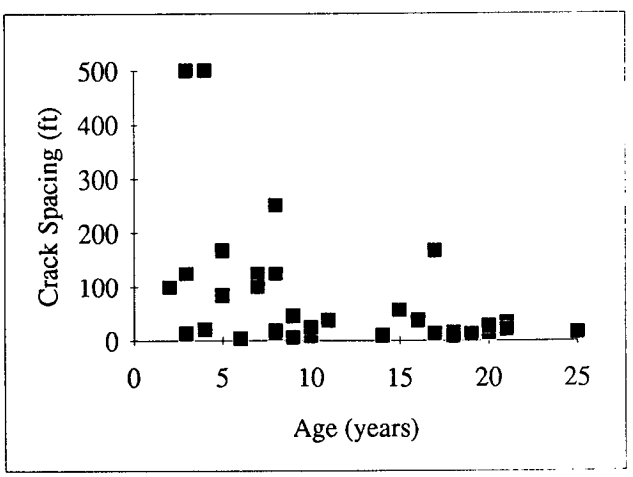

e. Dry-Freeze

Figure 7.3. Scatter Plots of Transverse Crack Spacing vs. Pavement Age for Complete and Regional Data Sets, HMAC Over Granular Base

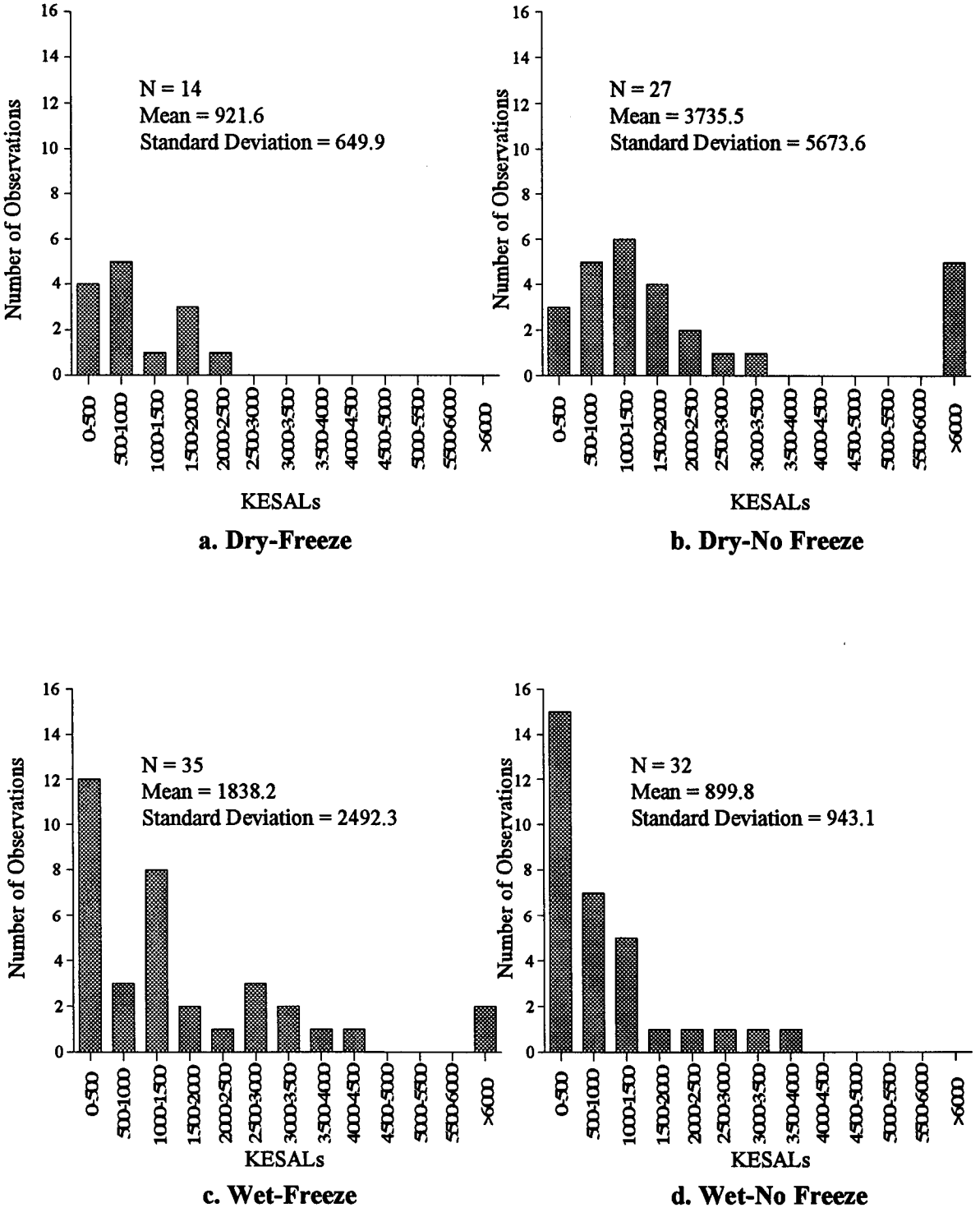

Figure 7.4. Distributions of KESALs by Environmental Zones for HMAC Over Granular Base, IRI Data Set

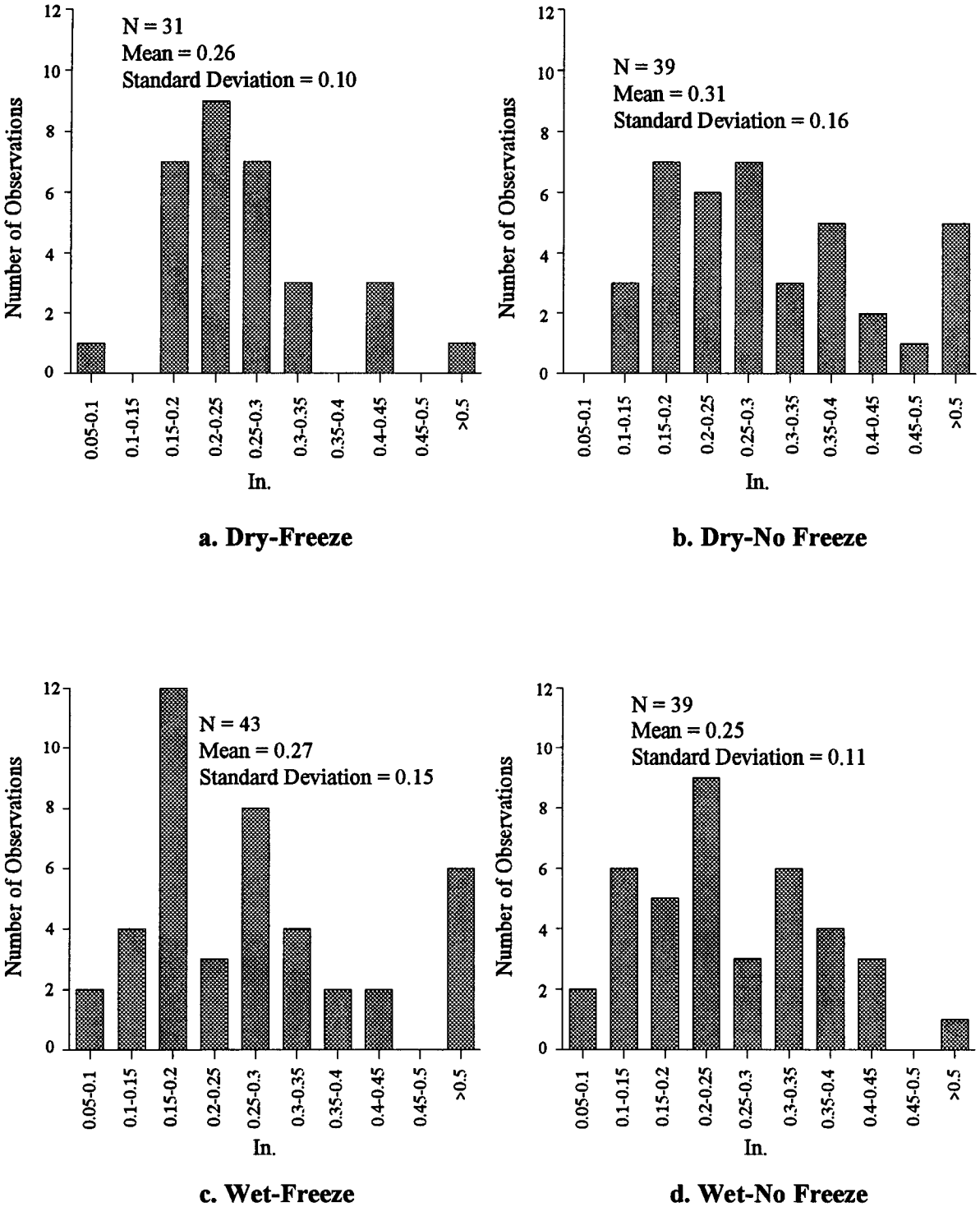

Figure 7.5. Distributions of Rut Depth by Environmental Zones for HMAC Over Granular Base Data Set

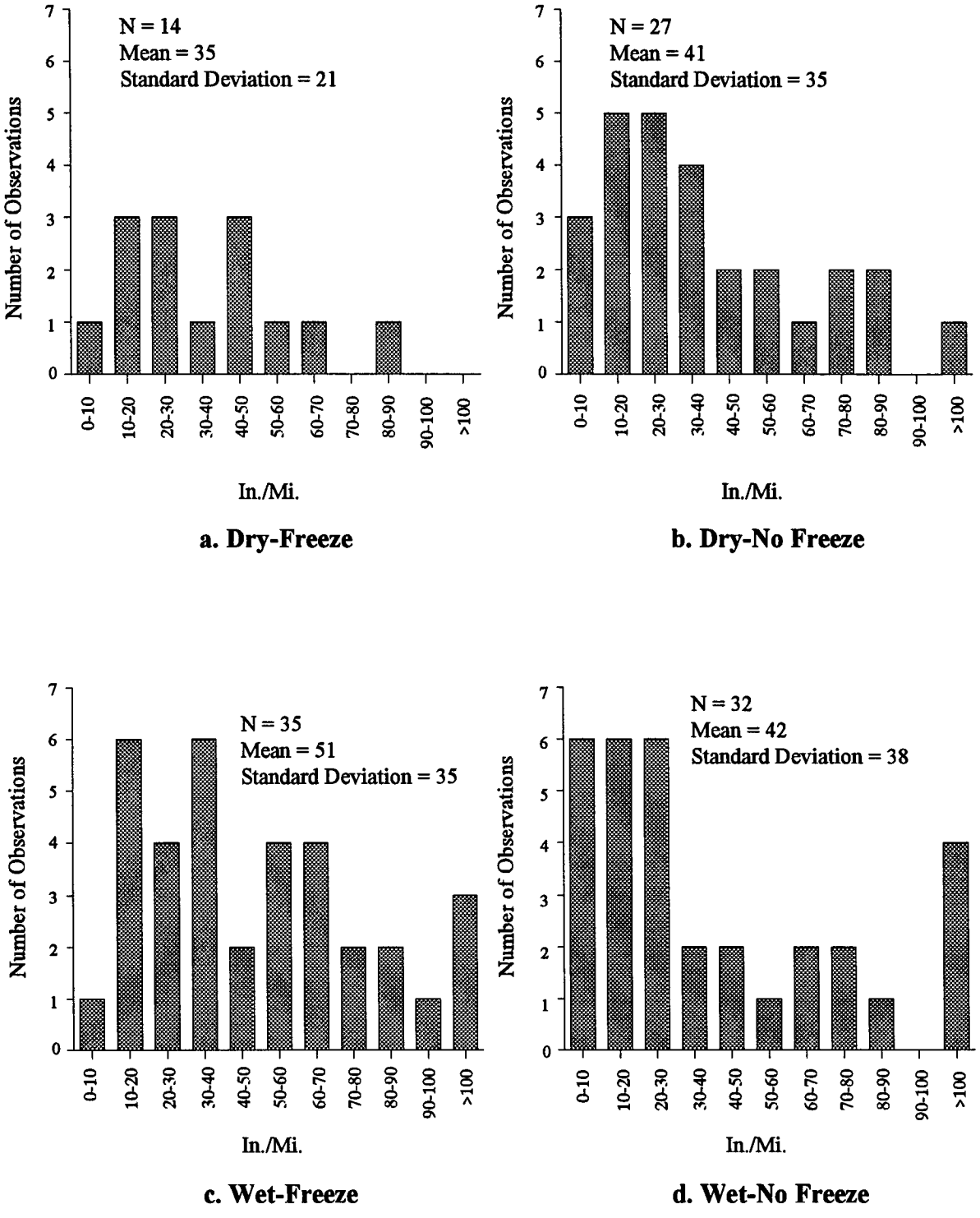

Figure 7.6. Distributions of Change in IRI by Environmental Zones for HMAC Over Granular Base Data Set

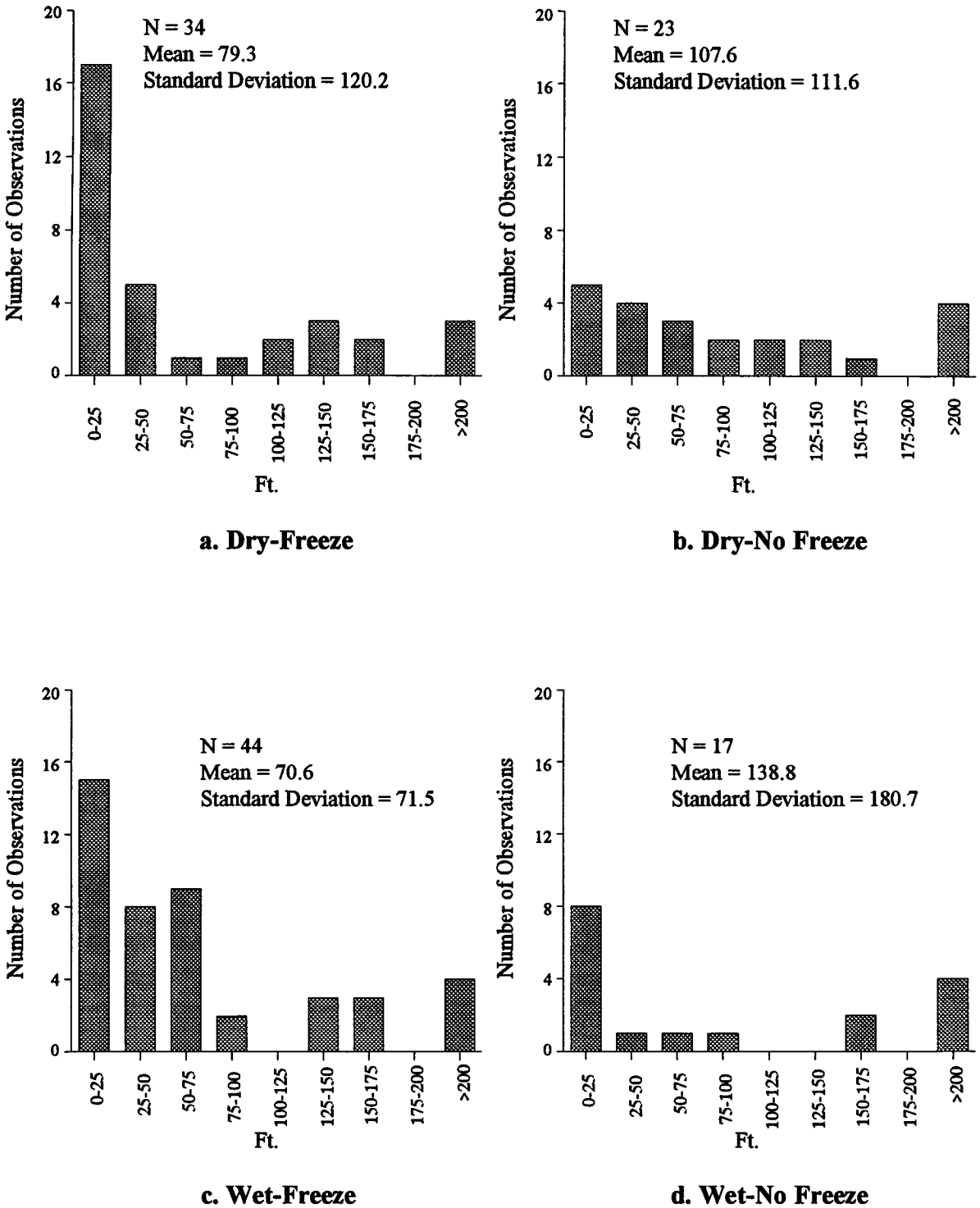

Figure 7.7. Distributions of Average Crack Spacing by Environmental Zones for HMAC Over Granular Base Data Set

Table 7.1. Correlation Matrix for Change in Roughness, HMAC Over Granular Base Data Set

Pearson Correlation Coefficients / Prob > |R| under Ho: Rho=0 / N = 108

	DIRI	BOTHIRI	INITIRI3	A_THICK	ASPHALT	AIR_VOID	NO_FOUR	VISC_140	B_THICK	COMPACTI	PI	#200
DIRI	1.00000 0.0	0.88143 0.0001	-0.17099 0.0768	-0.12691 0.1906	-0.00707 0.9421	0.06997 0.4718	0.02287 0.8143	0.23778 0.0132	0.10633 0.2734	0.09125 0.3476	0.01271 0.8961	-0.02079 0.8309
BOTHIRI	0.88143 0.0001	1.00000 0.0	0.31466 0.0009	-0.15473 0.1098	0.09117 0.3481	0.10859 0.2633	0.05846 0.5479	0.10084 0.2991	0.07918 0.4153	0.05307 0.5854	0.07275 0.4543	0.06294 0.5176
INITIRI3	-0.17099 0.0768	0.31466 0.0009	1.00000 0.0	-0.06773 0.4861	0.20437 0.0339	0.08589 0.3768	0.07598 0.4345	-0.26751 0.0051	-0.04852 0.6180	-0.07267 0.4548	0.12621 0.1931	0.17307 0.0733
A_THICK	-0.12691 0.1906	-0.15473 0.1098	-0.06773 0.4861	1.00000 0.0	-0.14417 0.1366	0.03075 0.7520	-0.42021 0.0001	-0.02556 0.7929	-0.15076 0.1194	-0.24537 0.0105	-0.00011 0.9991	0.11704 0.2277
ASPHALT	-0.00707 0.9421	0.09117 0.3481	0.20437 0.0339	-0.14417 0.1366	1.00000 0.0	-0.00673 0.9449	0.29286 0.0021	-0.02425 0.8032	0.04925 0.6128	-0.16311 0.0917	0.06108 0.5300	-0.02333 0.8106
AIR_VOID	0.06997 0.4718	0.10859 0.2633	0.08589 0.3768	0.03075 0.7520	-0.00673 0.9449	1.00000 0.0	0.00615 0.9496	0.01327 0.8915	-0.22606 0.0186	-0.07205 0.4587	0.25431 0.0079	0.13204 0.1731
NO_FOUR	0.02287 0.8143	0.05846 0.5479	0.07598 0.4345	-0.42021 0.0001	0.29286 0.0021	0.00615 0.9496	1.00000 0.0	-0.02016 0.8360	-0.01747 0.8576	0.01653 0.8652	0.05208 0.5924	0.00447 0.9634
VISC_140	0.23778 0.0132	0.10084 0.2991	-0.26751 0.0051	-0.02556 0.7929	-0.02425 0.8032	0.01327 0.8915	-0.02016 0.8360	1.00000 0.0	0.00455 0.9627	-0.08200 0.3989	0.02187 0.8222	-0.00992 0.9188
B_THICK	0.10633 0.2734	0.07918 0.4153	-0.04852 0.6180	-0.15076 0.1194	0.04925 0.6128	-0.22606 0.0186	-0.01747 0.8576	0.00455 0.9627	1.00000 0.0	0.02149 0.8253	-0.08744 0.3682	-0.08300 0.3931
COMPACTI	0.09125 0.3476	0.05307 0.5854	-0.07267 0.4548	-0.24537 0.0105	-0.16311 0.0917	-0.07205 0.4587	0.01653 0.8652	-0.08200 0.3989	0.02149 0.8253	1.00000 0.0	-0.14149 0.1441	0.06529 0.5020
PI	0.01271 0.8961	0.07275 0.4543	0.12621 0.1931	-0.00011 0.9991	0.06108 0.5300	0.25431 0.0079	0.05208 0.5924	0.02187 0.8222	-0.08744 0.3682	-0.14149 0.1441	1.00000 0.0	0.67760 0.0001
#200	-0.02079 0.8309	0.06294 0.5176	0.17307 0.0733	0.11704 0.2277	-0.02333 0.8106	0.13204 0.1731	0.00447 0.9634	-0.00992 0.9188	-0.08300 0.3931	0.06529 0.5020	0.67760 0.0001	1.00000 0.0
YEARS	0.12576 0.1947	0.12485 0.1979	0.00770 0.9369	0.07936 0.4143	0.03888 0.6895	0.02990 0.7587	-0.22338 0.0201	-0.20628 0.0322	-0.13731 0.1565	-0.10496 0.2797	0.04603 0.6362	-0.07589 0.4350

Table 7.1(continued). Correlation Matrix for Change in Roughness, HMAC Over Granular Base Data Set

Pearson Correlation Coefficients / Prob > |R| under Ho: Rho=0 / N = 108

	DIRI	BOTHIRI	INITIRI3	A_THICK	ASPHALT	AIR_VOID	NO_FOUR	VISC_140	B_THICK	COMPAC	PI	#200
KESALS	-0.11516	-0.12573	-0.03084	0.23864	-0.01649	-0.20252	-0.17381	-0.01869	-0.09752	-0.13282	0.02818	-0.07018
	0.2353	0.1948	0.7514	0.0129	0.8655	0.0356	0.0720	0.8478	0.3153	0.1706	0.7722	0.4704
TOTPREC_	0.05260	-0.07162	-0.25511	0.11943	-0.27849	0.10620	-0.21061	0.12514	0.06981	0.11496	-0.19360	-0.21890
	0.5887	0.4614	0.0077	0.2183	0.0035	0.2740	0.0282	0.1969	0.4728	0.2361	0.0447	0.0228
AVG90	-0.11766	-0.01663	0.20176	-0.27298	0.05639	0.01791	0.06111	-0.04020	-0.22241	-0.02503	0.25609	0.10154
	0.2252	0.8644	0.0363	0.0043	0.5622	0.8541	0.5298	0.6795	0.0207	0.7971	0.0075	0.2957
AVGFRZTH	-0.05688	-0.03449	0.04235	0.39033	-0.07553	-0.16665	-0.10392	-0.37441	0.01923	0.02268	-0.16446	0.10770
	0.5588	0.7231	0.6634	0.0001	0.4372	0.0847	0.2845	0.0001	0.8434	0.8157	0.0890	0.2672
AVGMAX	-0.00782	-0.00145	0.01270	-0.29055	0.05046	0.13023	0.02320	0.36393	-0.22995	-0.02792	0.29232	0.11073
	0.9360	0.9882	0.8962	0.0023	0.6040	0.1791	0.8116	0.0001	0.0167	0.7742	0.0021	0.2539
AVGMIN	0.05247	0.02414	-0.05508	-0.31438	0.04656	0.19245	0.03753	0.47569	-0.11259	-0.01558	0.22970	0.03253
	0.5897	0.8041	0.5713	0.0009	0.6323	0.0460	0.6998	0.0001	0.2460	0.8728	0.0166	0.7382
TEMPDIF	-0.17565	-0.07471	0.19716	0.04303	0.01766	-0.16738	-0.03865	-0.29303	-0.36039	-0.04136	0.20846	0.23913
	0.0690	0.4422	0.0408	0.6584	0.8561	0.0834	0.6913	0.0021	0.0001	0.6708	0.0304	0.0127
MAXTEMP	-0.12943	-0.07028	0.11349	-0.23229	-0.02815	0.03610	0.00696	0.10890	-0.31561	0.00870	0.25207	0.15661
	0.1819	0.4698	0.2422	0.0156	0.7724	0.7107	0.9430	0.2619	0.0009	0.9288	0.0085	0.1055
MINTEMP	0.08081	0.03011	-0.09958	-0.28311	0.09456	0.16270	0.05903	0.54865	-0.09562	-0.03861	0.23188	0.03162
	0.4058	0.7570	0.3052	0.0030	0.3303	0.0925	0.5440	0.0001	0.3249	0.6916	0.0157	0.7453

Table 7.1(continued). Correlation Matrix for Change in Roughness, HMAC Over Granular Base Data Set

Pearson Correlation Coefficients / Prob > |R| under Ho: Rho=0 / N = 108

	YEARS	KESALS	TOTPREC_	AVG90	AVGFRZTH	AVGMAX	AVGMIN	TEMPDIF	MAXTEMP	MINTEMP
DIRI	0.12576	-0.11516	0.05260	-0.11766	-0.05688	-0.00782	0.05247	-0.17565	-0.12943	0.08081
	0.1947	0.2353	0.5887	0.2252	0.5588	0.9360	0.5897	0.0690	0.1819	0.4058
BOTHIRI	0.12485	-0.12573	-0.07162	-0.01663	-0.03449	-0.00145	0.02414	-0.07471	-0.07028	0.03011
	0.1979	0.1948	0.4614	0.8644	0.7231	0.9882	0.8041	0.4422	0.4698	0.7570
INITIRI3	0.00770	-0.03084	-0.25511	0.20176	0.04235	0.01270	-0.05508	0.19716	0.11349	-0.09958
	0.9369	0.7514	0.0077	0.0363	0.6634	0.8962	0.5713	0.0408	0.2422	0.3052
A_THICK	0.07936	0.23864	0.11943	-0.27298	0.39033	-0.29055	-0.31438	0.04303	-0.23229	-0.28311
	0.4143	0.0129	0.2183	0.0043	0.0001	0.0023	0.0009	0.6584	0.0156	0.0030
ASPHALT	0.03888	-0.01649	-0.27849	0.05639	-0.07553	0.05046	0.04656	0.01766	-0.02815	0.09456
	0.6895	0.8655	0.0033	0.5622	0.4372	0.6040	0.6323	0.8561	0.7724	0.3303
AIR_VOID	0.02990	-0.20252	0.10620	0.01791	-0.16665	0.13023	0.19245	-0.16738	0.03610	0.16270
	0.7587	0.0356	0.2740	0.8541	0.0847	0.1791	0.0460	0.0834	0.7107	0.0925
NO_FOUR	-0.22338	-0.17381	-0.21061	0.06111	-0.10392	0.02320	0.03753	-0.03865	0.00696	0.05903
	0.0201	0.0720	0.0287	0.5298	0.2845	0.8116	0.6998	0.6913	0.9430	0.5440
VISC_140	-0.20628	-0.01869	0.12514	-0.04020	-0.37441	0.36393	0.47569	-0.29303	0.10890	0.54865
	0.0322	0.8478	0.1969	0.6795	0.0001	0.0001	0.0001	0.0021	0.2619	0.0001
B_THICK	-0.13731	-0.09752	0.06981	-0.22241	0.01923	-0.22995	-0.11259	-0.36039	-0.31561	-0.09562
	0.1565	0.3153	0.4728	0.0207	0.8434	0.0167	0.2460	0.0001	0.0009	0.3249
COMPACTI	-0.10496	-0.13282	0.11496	-0.02503	0.02268	-0.02792	-0.01558	-0.04136	0.00870	-0.03861
	0.2797	0.1706	0.2361	0.7971	0.8157	0.7742	0.8728	0.6708	0.9288	0.6916
PI	0.04603	0.02818	-0.19360	0.25609	-0.16446	0.29232	0.22970	0.20846	0.25207	0.23188
	0.6362	0.7722	0.0447	0.0075	0.0890	0.0021	0.0168	0.0304	0.0085	0.0157
#200	-0.07589	-0.07018	-0.21890	0.10154	0.10770	0.11073	0.03253	0.23913	0.15661	0.03162
	0.4350	0.4704	0.0228	0.2957	0.2672	0.2539	0.7382	0.0127	0.1055	0.7453
YEARS	1.00000	0.18467	-0.12147	-0.03530	0.18787	-0.04280	-0.12622	0.23922	0.00942	-0.11580
	0.0	0.0557	0.2105	0.7168	0.0515	0.6601	0.1930	0.0127	0.9229	0.2327

Table 7.1(continued). Correlation Matrix for Change in Roughness, HMAC Over Granular Base Data Set

Pearson Correlation Coefficients / Prob > |R| under Ho: Rho=0 / N = 108

	YEARS	KESALS	TOTPREC_	AVG90	AVGFRZTH	AVGMAX	AVGMIN	TEMPDIF	MAXTEMP	MINTEMP
KESALS	0.18467 0.0557	1.00000 0.0	-0.17853 0.0645	0.34734 0.0002	-0.13264 0.1712	0.22466 0.0194	0.10222 0.2925	0.37627 0.0001	0.34116 0.0003	0.08073 0.4062
TOTPREC_	-0.12147 0.2105	-0.17853 0.0645	1.00000 0.0	-0.24481 0.0107	-0.05586 0.5658	-0.03056 0.7535	0.11291 0.2446	-0.42048 0.0001	-0.20238 0.0357	0.11456 0.2378
AVG90	-0.03530 0.7168	0.34734 0.0002	-0.24481 0.0107	1.00000 0.0	-0.61900 0.0001	0.79802 0.0001	0.67049 0.0001	0.44159 0.0001	0.92603 0.0001	0.55817 0.0001
AVGFRZTH	0.18787 0.0515	-0.13264 0.1712	-0.05586 0.5658	-0.61900 0.0001	1.00000 0.0	-0.78168 0.0001	-0.88533 0.0001	0.23124 0.0160	-0.55399 0.0001	-0.84834 0.0001
AVGMAX	-0.04280 0.6601	0.22466 0.0194	-0.03056 0.7535	0.79802 0.0001	-0.78168 0.0001	1.00000 0.0	0.94309 0.0001	0.25401 0.0080	0.87040 0.0001	0.91084 0.0001
AVGMIN	-0.12622 0.1930	0.10222 0.2925	0.11291 0.2446	0.67049 0.0001	-0.88533 0.0001	0.94309 0.0001	1.00000 0.0	-0.08202 0.3988	0.72164 0.0001	0.96875 0.0001
TEMPDIF	0.23922 0.0127	0.37627 0.0001	-0.42048 0.0001	0.44159 0.0001	0.23124 0.0160	0.25401 0.0080	-0.08202 0.3988	1.00000 0.0	0.50964 0.0001	-0.08781 0.3661
MAXTEMP	0.00942 0.9229	0.34116 0.0003	-0.20238 0.0357	0.92603 0.0001	-0.55399 0.0001	0.87040 0.0001	0.72164 0.0001	0.50964 0.0001	1.00000 0.0	0.61956 0.0001
MINTEMP	-0.11580 0.2327	0.08073 0.4062	0.11456 0.2378	0.55817 0.0001	-0.84834 0.0001	0.91084 0.0001	0.96875 0.0001	-0.08781 0.3661	0.61956 0.0001	1.00000 0.0

Table 7.2. Coefficients for Regression Equations Developed to Predict Rutting in HMAC Pavements Over Granular Base

Rut Depth (In.) $= N^B 10^C$ Where N = Number of Cumulative KESALs

$B = b_0 + b_1 x_1 + b_2 x_2 + \ldots + b_n x_n$

$C = c_0 + c_1 x_1 + c_2 x_2 + \ldots + c_n x_n$

a. Entire Data Set

Explanatory Variable or Interaction (x_i)	Units	Coefficients for Terms In	
		b_i	c_i
Constant Term	-	0.151	-0.00475
Log (HMAC Aggregate < #4 Sieve)	% by Weight	0	-0.596
Log (Air Voids in HMAC)	% by Volume	-0.0726	0
Log (Base Thickness)	Inches	0	0.190
Subgrade < #200 Sieve	% by Weight	0	0.00582
Freeze Index	Degree-Days	8.49×10^{-6}	0
(Log (HMAC Thickness) * Log (Base Thickness))	Inches Inches	0	-0.161

$n = 152$ $R^2 = 0.45$ Adjusted $R^2 = 0.41$ RMSE in Log_{10}(Rut Depth) = 0.18

b. Wet-No Freeze Data Set

Explanatory Variable or Interaction (x_i)	Units	Coefficients for Terms In	
		b_i	c_i
Constant Term	-	0.0739	0.00998
Log (HMAC Aggregate < #4 Sieve)	% by Weight	0	-0.373
Log (Air Voids in HMAC)	% by Volume	0	-0.215
Subgrade < #200 Sieve	% by Weight	-0.00056	0
Annual Number of Days > 90°F	Number	0	-0.00022
Log (Annual Freeze-Thaw Cycles +1)	Number	0	0.0337
(Log (HMAC Thickness) * Log (Base Thickness))	Inches Inches	0	-0.135

$n = 41$ $R^2 = 0.72$ Adjusted $R^2 = 0.66$ RMSE in Log_{10}(Rut Depth) = 0.18

Table 7.2(continued). Coefficients for Regression Equations Developed to Predict Rutting in HMAC Pavements Over Granular Base

Rut Depth (In.) $= N^B 10^C$ Where N = Number of Cumulative KESALs

$B = b_0 + b_1 x_1 + b_2 x_2 + \ldots + b_n x_n$

$C = c_0 + c_1 x_1 + c_2 x_2 + \ldots + c_n x_n$

c. Wet-Freeze Data Set

Explanatory Variable or Interaction (x_i)	Units	Coefficients for Terms In	
		b_i	c_i
Constant Term	-	0.183	0.0289
Log (Air Voids in HMAC)	% by Volume	0	-0.189
Log (HMAC Thickness)	Inches	0	-0.181
Log (HMAC Aggregate < #4 Sieve)	% by Weight	0	-0.592
Asphalt Viscosity at 140°F	Poise	0	1.80×10^{-5}
Log (Base Thickness)	Inches	0	-0.0436
(Annual Precipitation * Freeze Index)	Inches Degree-Days	0	3.23×10^{-6}

$n = 41$ $R^2 = 0.73$ Adjusted $R^2 = 0.68$ RMSE in Log_{10} (Rut Depth) = 0.19

d. Dry-No Freeze Data Set

Explanatory Variable or Interaction (x_i)	Units	Coefficients for Terms In	
		b_i	c_i
Constant Term	-	0.156	-0.00163
Log (HMAC Aggregate < #4 Sieve)	% by Weight	0	-0.628
Log (HMAC Thickness)	Inches	0	0.0918
Log (Air Voids in HMAC)	% by Volume	-0.0988	0
Base Thickness	Inches	0	0.00257
Subgrade < #200 Sieve	% by Weight	0	0.00153
(Annual Precipitation * Annual Number of Days > 90°F)	Inches Numbers	0	6.588×10^{-5}

$n = 36$ $R^2 = 0.75$ Adjusted $R^2 = 0.70$ RMSE in Log_{10} (Rut Depth) = 0.16

Table 7.2(continued). Coefficients for Regression Equations Developed to Predict Rutting in HMAC Pavements Over Granular Base

Rut Depth (In.) = $N^B 10^C$ Where N = Number of Cumulative KESALs

$B = b_0 + b_1 x_1 + b_2 x_2 + ... + b_n x_n$

$C = c_0 + c_1 x_1 + c_2 x_2 + ... + c_n x_n$

e. Dry-Freeze Data Set

Explanatory Variable or Interaction (x_i)	Units	Coefficients for Terms n	
		b_i	c_i
Constant Term	-	0.0394	0.00451
Log (HMAC Thickness)	Inches	0	0.0600
Mod. AASHTO Base Compaction	% of Max. Density	0	-0.00849
(Base Thickness * Log (HMAC Thickness))	Inches Inches	0	0.00875
(Log (Subgrade < #200 Sieve) * Log (Freeze Index +1))	% by Weight Degree-Days	0	0.0107
(Log (Subgrade < #200 Sieve) * Log (Air Voids in HMAC))	% by Weight % by Volume	0	-0.00567

n = 34 R^2 = 0.85 Adjusted R^2 = 0.81 RMSE in Log_{10} (Rut Depth) = 0.11

observations (test sections) upon which the equation was based. It can be seen that only 152 of the 218 available test sections survived the data evaluations.

It should be noted that the quoted root mean square error (RMSE) is in $\log_{10}$ of rut depth. The meaning of a standard error of regression, or RMSE on a logarithmic variable, in terms of the effect on the variable itself, can be explained as follows, by using arbitrary yet convenient values for an example. Assume that the RMSE of fit for a regression on log y is 0.3. This means that 68% of the values of log y for a specific set of x_i lie between w - 0.3 and w + 0.3, where w is the value of log y predicted by the regression. Assume w is 1.0 (i.e., y = 10), then 68% of the values of log y lie between 0.7 and 1.3. This means that 68% of the values of y lie between 5 and 20, or stated another way, they lie within a factor of approximately 2 (antilog 0.30 = 1.995) of 10.

Thus, we see that an RMSE of ϵ in log y may be expressed as precision of prediction to within a factor of (antilog ϵ) in the value of y itself.

Some typical values of ϵ and the corresponding factor (antilog ϵ) are

ϵ	Antilog ϵ
0.05	1.122
0.10	1.259
0.15	1.412

0.20	1.585
0.25	1.778
0.30	1.995

The values of adjusted R^2 look quite reasonable for the data available as of May 1993, *but the RMSEs indicate that the equations are of limited reliability*. As an example, the equation for predicting rutting in the wet-freeze environmental zone appears in Table 7.2.c. For simplicity, assume that all values of independent variables are at their means so we can use the plots in Figure 7.10. A rut depth of approximately 0.16 in. (4 mm) is predicted for 100 KESALs and about 0.21 in. (5 mm) for 500 KESALs. The RMSE for this case in log(rut depth) is 0.19 and the antilog is 1.55. If this is applied as a factor value, then

KESALs	Predicted Rut Depth (In.)	(Predicted Rut Depth) ÷ 1.55 (In.)	(Predicted Rut Depth) x 1.55 (In.)
100	0.16	0.10	0.25
500	0.21	0.14	0.33

At a 68% confidence level in the log of rut depth, the upper and lower confidence levels for rut depth after 100 KESALs have been applied are 0.25 and 0.10 in. (6 and 3 mm), respectively. Those for 500 KESALs are 0.33 and 0.14 in. (8 and 4 mm), respectively. Thus, the precisions for these equations are poor, even though the values of R^2 look quite good.

Figure 7.8 shows plots of predicted versus actual rut depths for the four environmental zones, each with its own predictive equation. Figure 7.9 shows plots of the residuals versus predicted rut depths.

Figure 7.10 shows the predicted rut depths versus KESALs for each environmental zone when the independent variables appearing in the five separate predictive equations are held at their means for their respective data sets. From these graphs the following may be determined:

- A substantial portion of rutting may be expected to occur very early in the life of a pavement.
- After the rapid densification early in a pavement's life, the rate of rutting decreases rapidly, approaching a much reduced rate for the rest of the pavement's life. While the rate appears to be constant in the plots, it does continue to decrease slightly but might be expected to increase again when cracking starts and moisture increases occur in the base/subbase and subgrade (However, pavements are generally repaired well before rapid acceleration of rutting begins.)

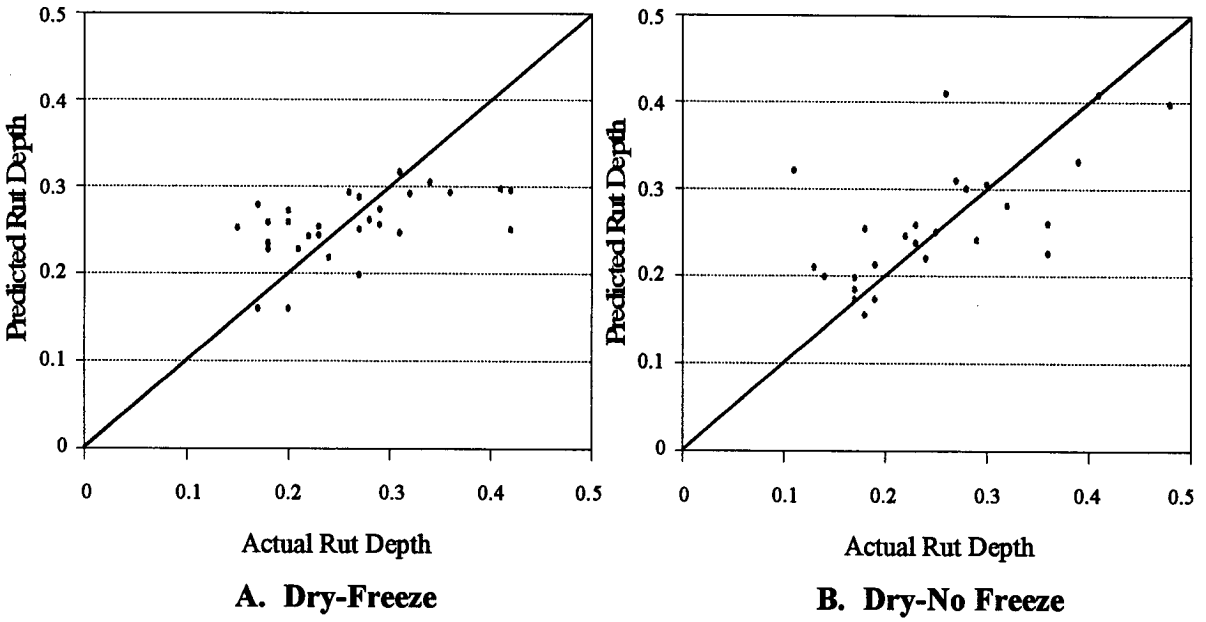

A. Dry-Freeze

B. Dry-No Freeze

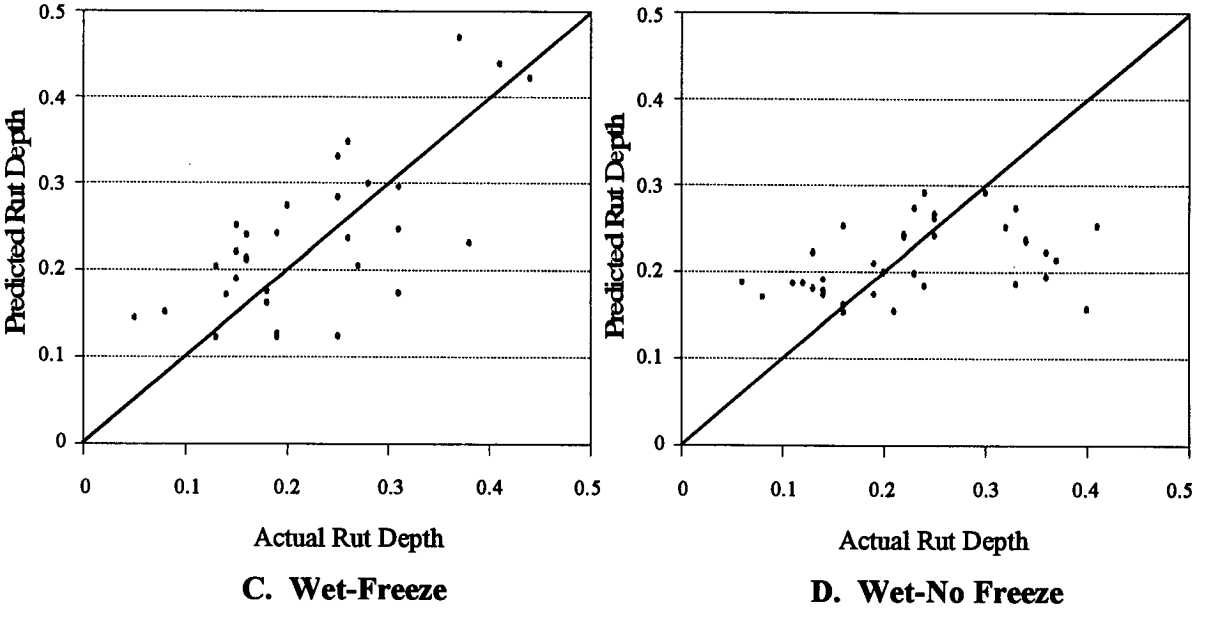

C. Wet-Freeze

D. Wet-No Freeze

Figure 7.8. Plots of Predicted vs. Actual Rut Depth for HMAC Over Granular Base Data Sets

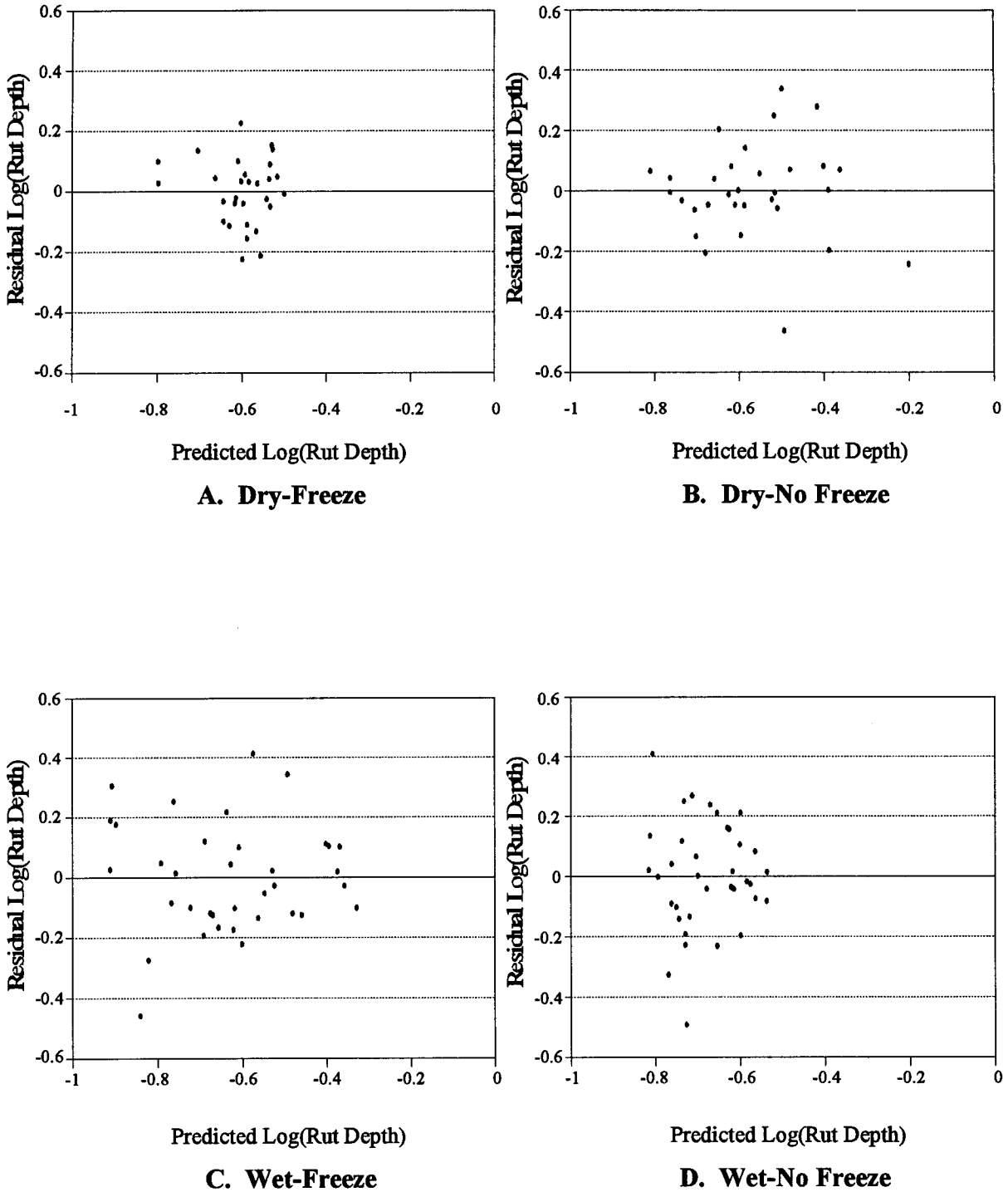

Figure 7.9. Plots of Residuals vs. Predicted Log(Rut Depth) for HMAC Over Granular Base Data Sets

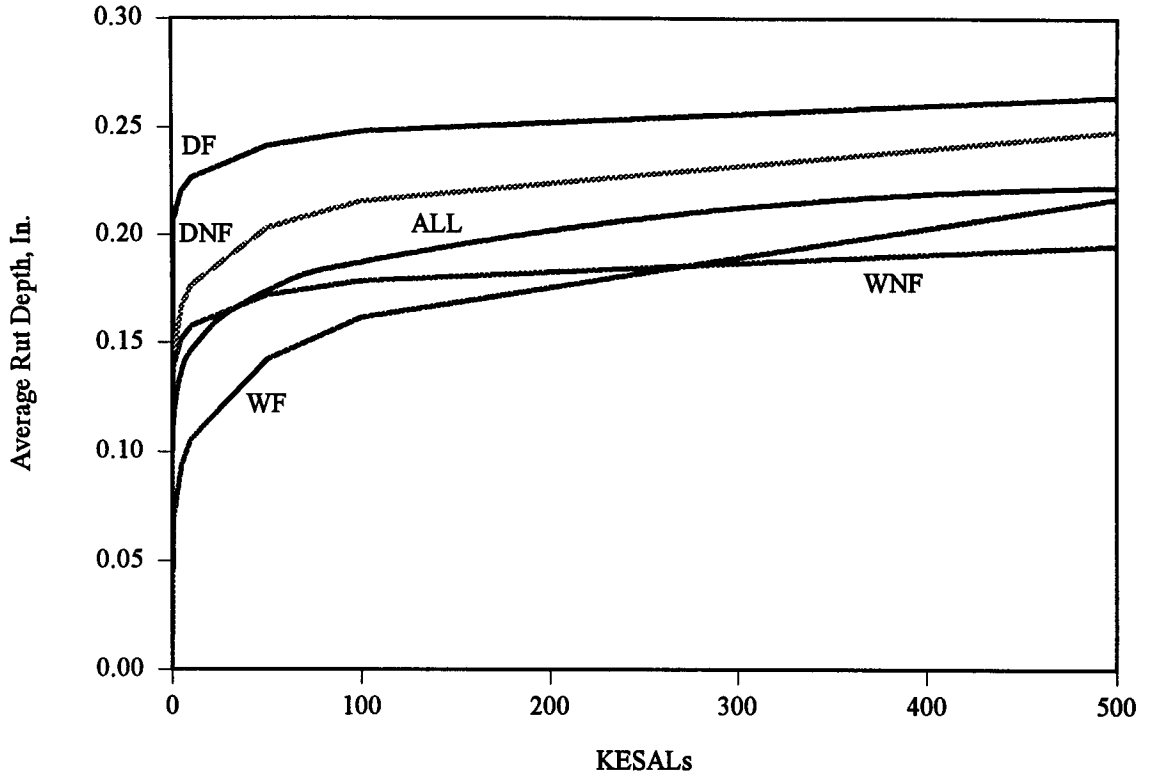

Figure 7.10. Predicted Rutting vs. KESALs With All Other Independent Variables at Their Mean Values, HMAC Pavements on Granular Base

- On a cursory basis, it might be decided that typical pavements in the dry zones rut more than those in wet zones; however, this finding could be a consequence of the particular test sections selected. It should be noted that the mean values for rutting in all the zones are relatively low, which probably indicates a bias resulting from the better highways being offered by State Highway Agencies (SHAs).

- The graph for the wet-no freeze zone appears to indicate virtually no increase in rutting after a very few KESALs. It is probable that this result is from a bias caused by the presence of some older highways, with very high traffic but very little rutting, in that particular data set.

It is critical to remember that plots of predicted distress in terms of one independent variable are useful but can be very misleading. Figures 7.1, 7.2, and 7.3 and the scatter plots in SHRP-P-684, Early Analyses of LTPP General Pavement Studies Data, Data Processing and Evaluation, illustrate the actual variances when the independent variables are not held at their mean values.

There are several causes of rutting, including densification of the HMAC mixtures, horizontal displacement of the HMAC mixture, densification and/or horizontal displacement of unbound materials, combinations of these, and probably others. The mechanisms for rutting are not considered directly in the predictive equations, but may

be partially explained implicitly through such independent variables as air voids, layer thicknesses, asphalt viscosity, climatic variables, and the interactions between variables.

The results from the sensitivity analyses conducted on the equations appearing in Table 7.2 appear in Figures 7.11 and 7.12. The vertical lines through the boxes are located at the predicted mean values of rut depth for each data set. For Figure 7.11, this mean is between 0.25 and 0.26 in. (6 and 7 mm). The boxes begin and end at the rut depths calculated when that independent variable is varied from one standard deviation above to one standard deviation below the mean value, with all other independent variables at their mean values. The arrows within the boxes indicate whether an increase in that variable increases or decreases predicted rut depth. As an example, increasing KESALs in Figure 7.11 increases rut depth and increasing HMAC thickness decreases rut depth.

The dashed boxes with arrows pointing to the left that appear to the left of the mean rut depths for KESALs in Figures 7.11, 7.12b, and 7.12c, simply indicate that the standard deviations for KESALs in these cases exceeded the mean, and that negative values of KESALs have no physical meaning. This phenomenon was caused by a number of test sections that had very high levels of KESALs.

The relative sensitivities for specific independent variables are indicated by the horizontal widths of the boxes in the figures, and the relative sensitivity levels decrease from top to bottom. For example, the occurrence of rut depth for the entire data set represented in Figure 7.11 is most sensitive to KESALs and least sensitive to the percentage of the subgrade soils passing a #200 sieve. For each of these two variables, increases in the independent variables result in increases in predicted rut depth.

By comparing the sensitivity plots (Figure 7.12) for the four environmental zones, it can be seen that predicted rut depths for three zones are most sensitive to KESALs, while predicted rut depths for the dry-freeze zone are more sensitive to four other variables than to KESALs. In the latter case, rut depth appears to be most sensitive to base compaction. Although we can theorize about the relative sensitivities and their causes, the causes are not always obvious. One might speculate that, in general for the test sections in the dry-freeze data set, compaction was not quite adequate and that much of the densification was in the base. This theory is supported by the fact that base thickness is the next variable in level of sensitivity.

Also, air voids in the HMAC appear to be significant for all four zones, and higher air voids (within the ranges in the data sets) tend to decrease rutting. At first glance, this scenario appears questionable but has been found to be the case by other researchers. The hypothesis for this phenomenon is that increased air flow through the HMAC results in earlier aging and stiffness, which in turn decreases rutting.

The independent variables found to be significant to rut depth predictions are not always the same between zones, and the relative significance of specific variables also varies between zones. As an example, base thickness is not very important in three zones and increases in it tend to decrease rutting, while it is quite significant in the dry-freeze zone and tends to increase rutting as it increases. This finding seems to be consistent with the

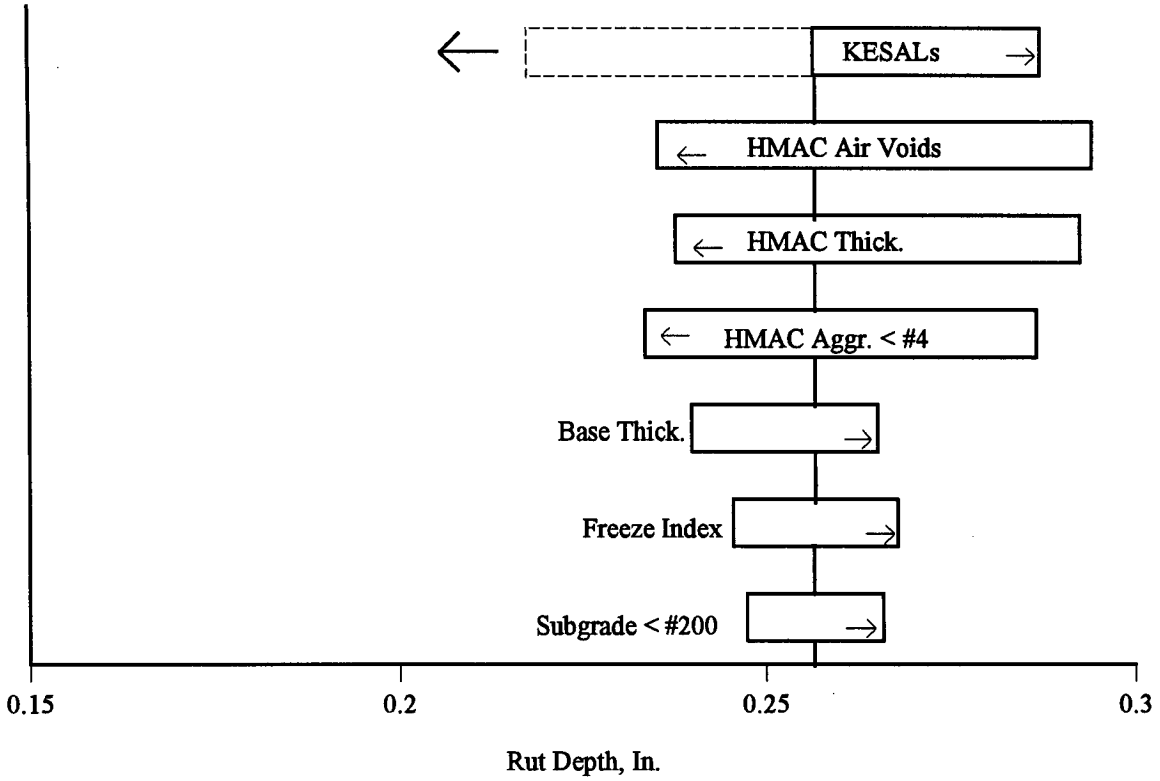

Figure 7.11. Results From Sensitivity Analyses for Rutting in HMAC Pavements on Granular Base

hypothesis offered above that base compaction is generally not adequate and that substantial densification occurs in the base.

It can also be seen that the percentage of the HMAC aggregate passing a #4 sieve appears to be moderately significant for three of the four zones, and that rutting tends to decrease in mixes with more material passing a #4 sieve (within the ranges existing in the data sets).

Different environmental variables were found to be significant for the different environmental zones. This is not surprising, but it should be remembered that many (if not most) of the environmental variables are correlated. One would expect correlations among freeze index, annual air freeze-thaw cycles, and number of days per year experiencing temperatures greater than 90°F (32°C). Consequently, one data element may represent one or more other data elements in the predictive equations.

As the graphs in Figure 7.10 represent predicted rut depths when all variables are at their mean values in the separate data sets, they do not represent directly the poor pavements that will experience considerable rutting or the good pavements that will experience very little. To provide some insight, fourteen cases were examined for the wet-no freeze environmental zone, as indicated in Table 7.3, by using three levels for each variable. Because it would have required 6561 case studies to consider the entire

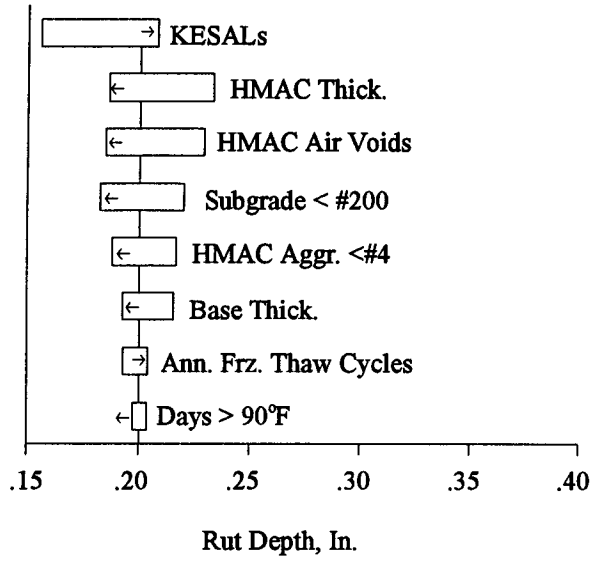

a. Wet-No Freeze Data Set

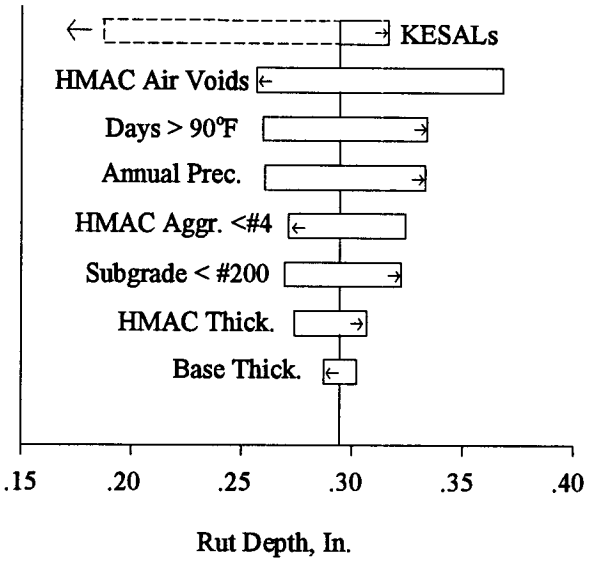

b. Dry-No Freeze Data Set

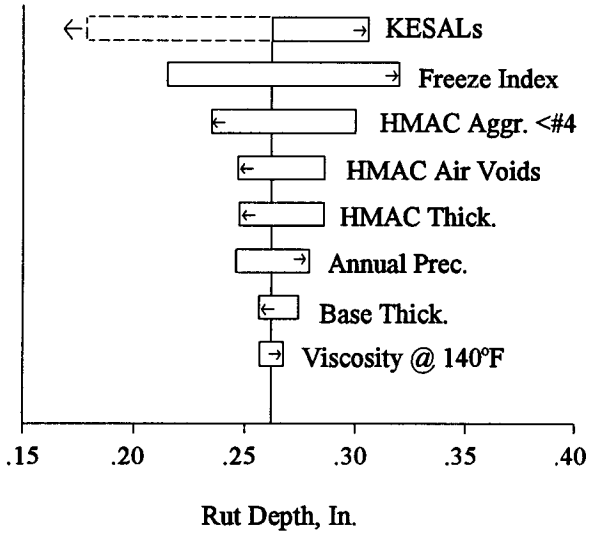

c. Wet-Freeze Data Set

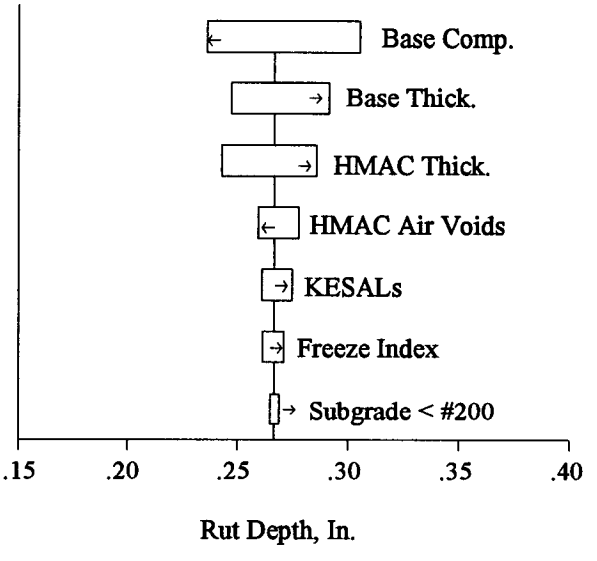

d. Dry-Freeze Data Set

Figure 7.12 Results From Sensitivity Analyses for Rutting in HMAC Pavements on Granular Base, by Environmental Zone

Table 7.3. Calculated Rut Depths for Various Combinations of Independent Variable Magnitudes, Wet-No Freeze Equation

Independent Variable	Case Numbers													
	1	2	3	4	5	6	7	8	9	10	11	12	13	14
KESALs	100	5000	20,000	5000	5000	5000	5000	5000	5000	5000	5000	20,000	5000	5000
HMAC Thickness	6	6	6	2	2	10	6	6	6	6	6	10	6	10
HMAC Air Voids	5	5	5	3	5	5	3	8	5	5	5	5	3	5
Subgrade <#200	60	60	60	20	60	20	20	20	100	100	100	100	60	20
HMAC Aggr. < #4	50	50	50	30	50	50	50	50	50	30	50	70	30	50
Base Thickness	12	12	12	4	12	12	12	12	12	12	20	20	12	4
Days > 90°F	60	60	60	0	60	60	60	60	60	60	60	60	60	60
Ann. Freeze-Thaw Cycles	30	30	30	60	30	30	30	30	30	30	30	0	30	30
Calculated Rut Depth	0.17	0.20	0.21	0.42	0.23	0.22	0.27	0.22	0.16	0.20	0.16	0.11	0.27	0.26

factorial at three levels, the 14 were selected to include the worst case (Case 4) and to illustrate the effects of variations in the most significant independent variables.

Cases 1, 2, and 3 show the effects of KESALs. Note that the majority of the rutting is expected early in the life of a pavement, with the rest occurring at a rate decreasing with cumulative ESALs. The other cases represent various combinations of variable magnitudes. Case 12 represents a pavement with a heavy structure, heavy traffic, and a mix with 70% of its aggregate passing a #4 sieve and compacted to 5% air voids. The predicted rut depth was 0.11 in. (3 mm), whereas the prediction for Case 3 (same traffic but less structure) was 0.21 in. (5 mm).

Because the predicted rut depths for full-depth HMAC pavements and those with portland cement treated-base would be expected to vary similarly with variations in their independent variables, similar examples have subsequently not been provided for those types of pavements.

The discussion of the meaning of RMSE in terms of a dependent variable when RMSE is expressed in the log of that dependent variable applies to all the other results reported in this chapter, so this discussion will not be repeated.

Rutting of Full-Depth HMAC Pavements

Only forty-two of the fifty-two full-depth HMAC pavements with unstabilized subgrade survived the data evaluations. Because the number of test sections was quite small, models were developed for the entire data set, a data set of the two dry zones, a data set of the two wet zones, a data set of the two no freeze zones, and a data set of the two freeze zones. The predictive equation for the entire data set appears in Table 7.4, the prediction equations for the wet and dry data sets in Table 7.5, and the equations for the no freeze and freeze data sets in Table 7.6. As with the HMAC over granular base, the multiple regressions were conducted to predict log(rut depth), which led to the same equation form appearing at the top of each table. The statistics for the equations for full-depth HMAC are essentially comparable to those developed for HMAC over granular base, even though the numbers of observations were much lower.

Figure 7.13 shows plots of predicted versus actual rut depths for the four full-depth HMAC models for the different environmental zones, and Figure 7.14 shows plots of the residuals versus predicted log(rut depth).

Figure 7.15 shows the predicted rut depths versus KESALs when the other independent variables in the five separate predictive equations are held at their means for their respective data sets. It can be seen that the forms of the equations are similar to those for HMAC on granular base.

Table 7.4. Coefficients for Regression Equations Developed to Predict Rutting in Full-Depth HMAC Pavements, Entire Data Set

Rut Depth (In.) $= N^B 10^C$ Where N = Number of Cumulative KESALs

$B = b_0 + b_1 x_1 + b_2 x_2 + ... + b_n x_n$

$C = c_0 + c_1 x_1 + c_2 x_2 + ... + c_n x_n$

Explanatory Variable or Interaction (x_i)	Units	Coefficients for Terms In	
		b_i	c_i
Constant Term	-	0.0280	-0.0149
Log (HMAC Thickness)	Inches	0.0184	0
Log (Subgrade < #200)	% by Weight	0.0810	0
Log (Daily Temperature Range)	°F	0	-0.715
(Log (Air Voids in HMAC) * Log (Subgrade < #200))	% by Volume % by Weight	0	-0.129
(Annual Precipitation * Log (Daily Temperature Range))	Inches °F	0	0.00094

n = 42 R^2 = 0.60 Adjusted R^2 = 0.54 RMSE in Log_{10} (Rut Depth) = 0.20

Also, the magnitudes of the predicted rut depths for the equation from the dry data set are much higher than those for the equation from the wet data set. The actual mean rut depths are 0.38 and 0.28 in. (10 and 7 mm), respectively. The broad implication is that more rutting may be expected in the dry areas of western North America than in the wet areas of eastern North America. However, this theory is far too simplistic. Traffic rates are generally higher in the wet zones, so the pavement structures should generally be more substantial. However, the thirteen test sections for the dry zones included five test sections in Arizona that had experienced an estimated 4000 to 23,000 KESALs (mean of 12,000 KESALs), which had resulted in rutting from 0.16 to 0.99 in. (4 to 25 mm), with a mean of 0.43 in. (11 mm). One must be very careful about generalizing on the basis of predictions from these equations when distress is plotted against one or even two independent variables. The scatter plots in Figure 7.1 and those in SHRP-P-684, Early Analyses of LTPP General Pavement Studies Data, Data Processing and Evaluation, clearly indicate the variance that actually occurs when the distresses are considered as functions of only one independent variable. The difference in rutting between the no freeze and freeze zones, based on these predictions, appear to be rather minor.

The results from the sensitivity analysis on the equation appearing in Table 7.4 appear in Figure 7.16. As for the HMAC on granular base, number of KESALs was the most significant independent variable. However, as the amount of fines in the subgrade soil took on more significance, HMAC thickness dropped in relative importance, and daily temperature range and annual precipitation replaced freeze index in representing the environment. In assessing the importance of these comparisons, it should be

Table 7.5. Coefficients for Regression Equations Developed to Predict Rutting in Full-Depth HMAC Pavements, Wet and Dry Data Sets

Rut Depth (In.) $= N^B 10^C$ Where N = Number of Cumulative KESALs

$B = b_0 + b_1 x_1 + b_2 x_2 + \ldots + b_n x_n$

$C = c_0 + c_1 x_1 + c_2 x_2 + \ldots + c_n x_n$

a. Wet Data Set

Explanatory Variable or Interaction (x_i)	Units	Coefficients for Terms n	
		b_i	c_i
Constant Term	-	0.242	-0.0160
Log (HMAC Thickness)	Inches	0	-0.615
Log (Air Voids in HMAC)	% by Volume	-0.0740	0
Log (Annual No. of Days > 90°F)	Number	0	-0.363
(Log (Subgrade < #200)) * (Asphalt Viscosity at 140°F)	% by Weight Poise	0	0.000119
(Log (Viscosity at 140°F) * Log (HMAC Aggregate < #4 Sieve))	Poise % by Weight	0	-8.60×10^{-5}

$n = 27$ $R^2 = 0.79$ Adjusted $R^2 = 0.73$ RMSE in Log_{10} (Rut Depth) = 0.17

b. Dry Data Set

Explanatory Variable or Interaction (x_i)	Units	Coefficients for Terms n	
		b_i	c_i
Constant Term	-	0.0111	0.558
HMAC Thickness	Inches	0.00222	0
Average Annual Minimum Temperature	°F	0	-0.0412
(Log (Subgrade < #200) * Annual Number of Days > 90°F)	% by Weight °F	0	0.00650

$n = 13$ $R^2 = 0.87$ Adjusted $R^2 = 0.79$ RMSE in Log_{10} (Rut Depth) = 0.10

Table 7.6. Coefficients for Regression Equations Developed to Predict Rutting in Full-Depth HMAC Pavements, No Freeze and Freeze Data Sets

Rut Depth (In.) $= N^B 10^C$ Where N = Number of Cumulative KESALs

$B = b_0 + b_1 x_1 + b_2 x_2 + \ldots + b_n x_n$

$C = c_0 + c_1 x_1 + c_2 x_2 + \ldots + c_n x_n$

a. No Freeze Data Set

Explanatory Variable or Interaction (x_i)	Units	Coefficients for Terms n	
		b_i	c_i
Constant Term	-	-0.0717	-1.053
Log (HMAC Thickness)	Inches	-0.0458	0
Log (Subgrade < #200)	% by Weight	0.0446	0
Log (Annual Precipitation)	Inches	0	0.00532
Annual Number of Days > 90°F	Number	0.00168	0
(Log (HMAC Thickness) * Daily Temperature Range)	Inches °F	0	0.0128
(Annual Number of Days > 90°F * Asphalt Viscosity at 140°F)	Number Poise	0	-1.618×10^{-6}

$n = 22$ $R^2 = 0.70$ Adjusted $R^2 = 0.55$ RMSE in Log_{10} (Rut Depth) = 0.14

b. Freeze Data Set

Explanatory Variable or Interaction (x_i)	Units	Coefficients for Terms n	
		b_i	c_i
Constant Term	-	0.149	-0.0159
Asphalt Content	% by Weight	0	-0.116
HMAC Thickness	Inches	-0.00443	0
Log (Air Voids in HMAC)	% by Volume	-0.121	0
Log (Subgrade < #200 Sieve)	% by Weight	0.0687	0
Annual Number of Days > 90°F	Number	0	-0.292

$n = 18$ $R^2 = 0.84$ Adjusted $R^2 = 0.78$ RMSE in Log_{10} (Rut Depth) = 0.15

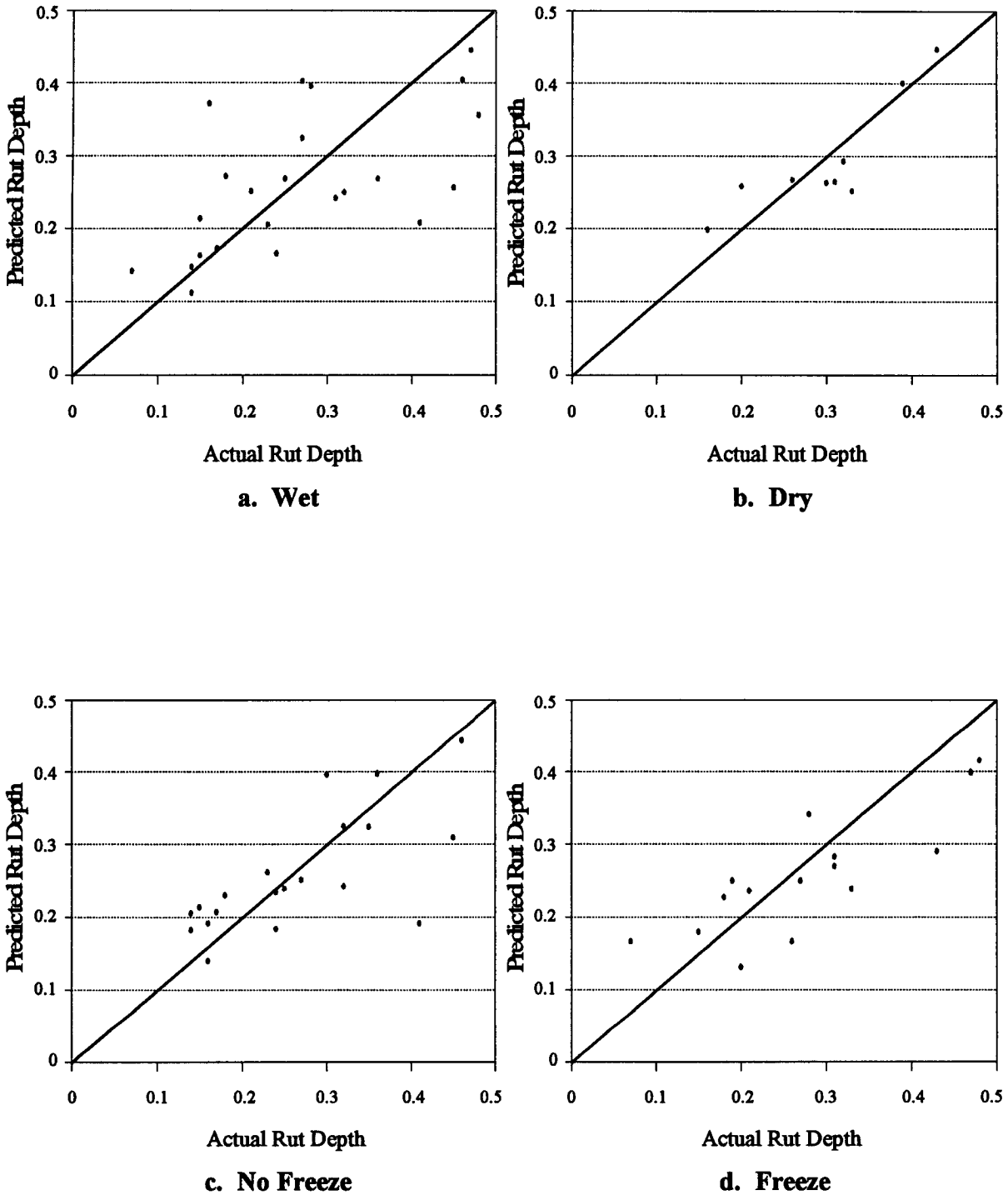

Figure 7.13. Plots of Predicted vs. Actual Rut Depth for Full-Depth HMAC Pavement Data Sets

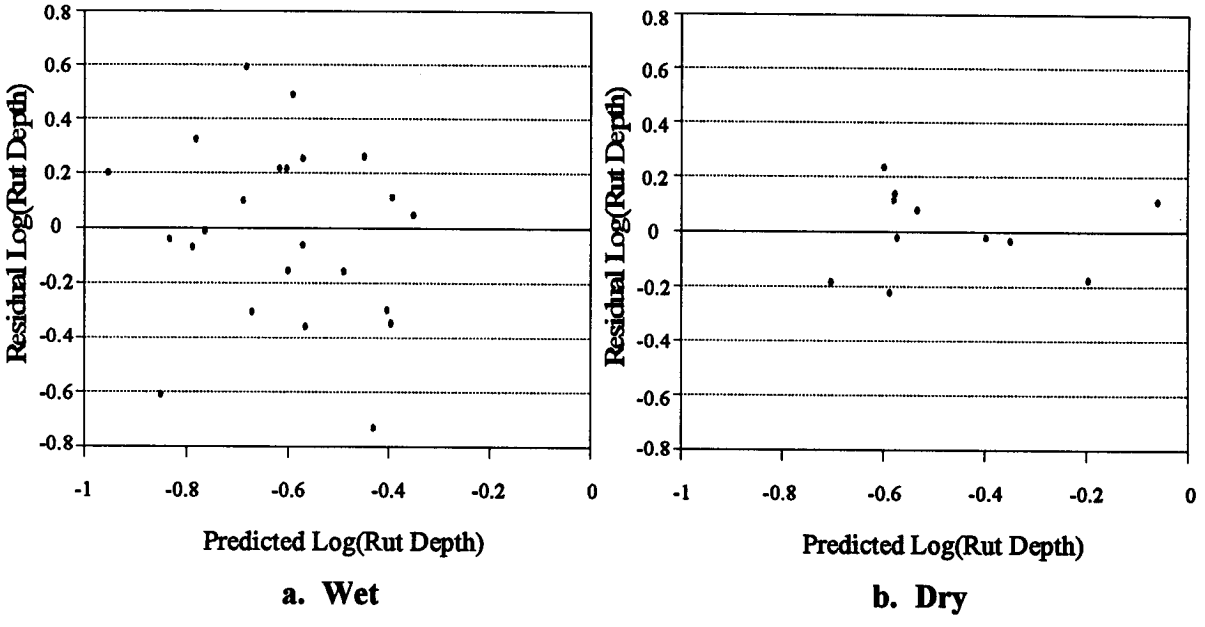

a. Wet

b. Dry

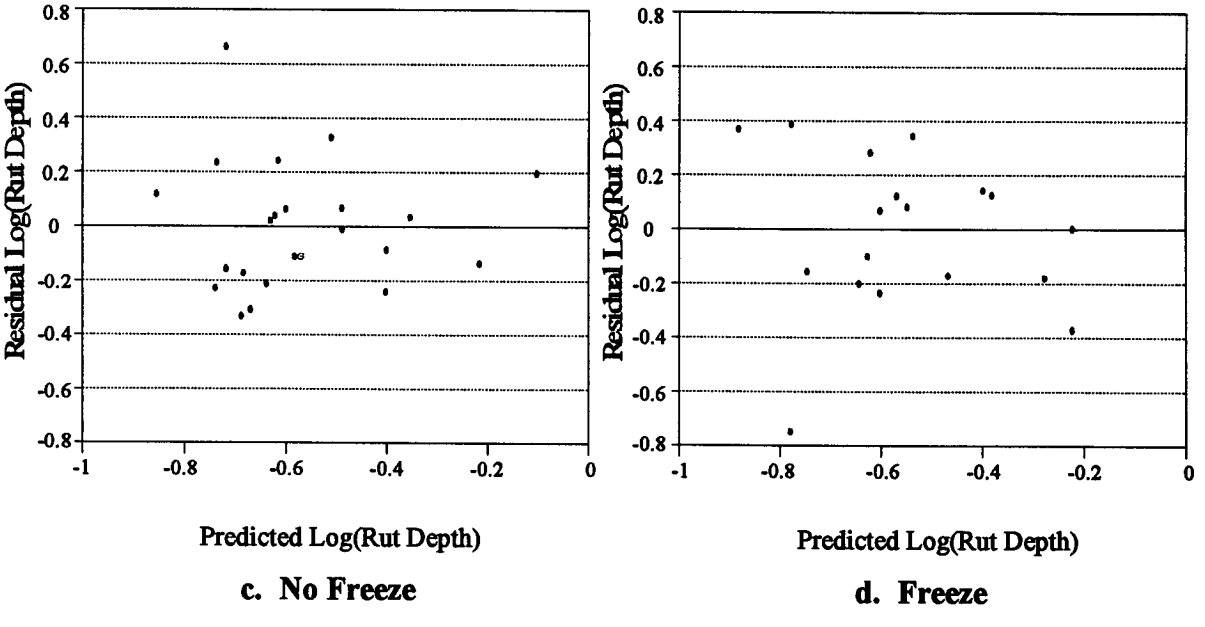

c. No Freeze

d. Freeze

Figure 7.14. Plots of Residuals vs. Predicted Log(Rut Depth) for Full-Depth HMAC Pavement Data Sets

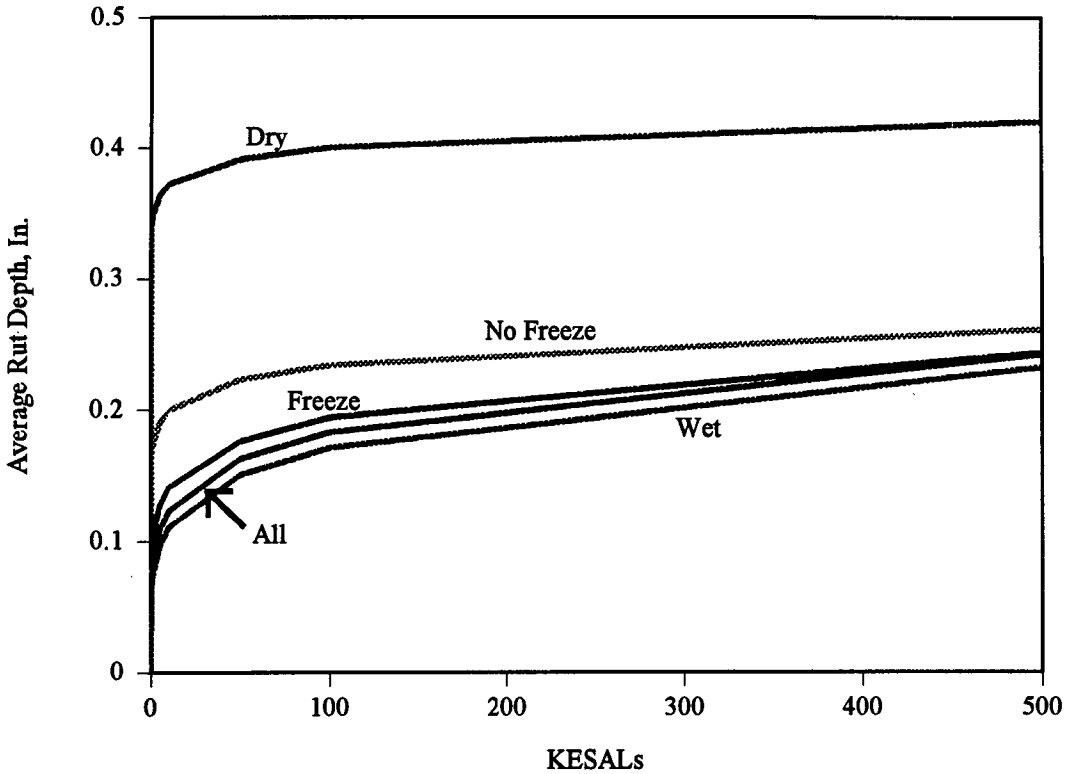

Figure 7.15. Predicted Rutting vs. KESALs With All Other Independent Variables at Their Mean Values, Full-Depth HMAC Pavements

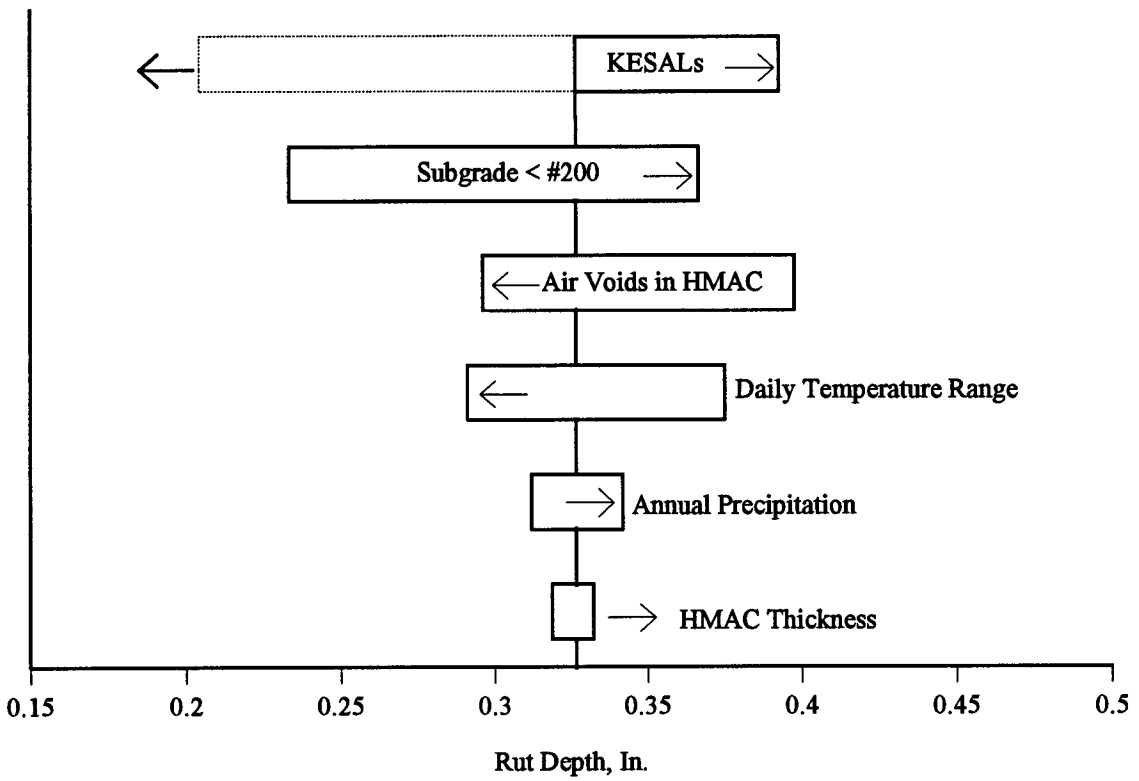

Figure 7.16. Results From Sensitivity Analyses for Rutting in Full-Depth HMAC Pavements, Entire Data Set

remembered that neither the equation for the HMAC on granular base or full-depth HMAC was considered very acceptable, which was the reason for developing models for different environmental zones.

The sensitivities developed from the four environmental models appear in Figure 7.17. It can be seen that KESALs were found to be most significant for the data sets from the wet, no freeze, and freeze zones. The environmental variables appear to be more significant for the data set from the dry zones. The HMAC thickness was retained in each equation, even though it was found to be marginally significant for most of them. The amount of fines in the subgrade soil also appeared in all four equations. Number of days per year experiencing temperatures greater than 90°F (32°C) also appeared in all four equations and was found to be quite significant.

Rutting of HMAC Pavements on Portland Cement-Treated Base

This data set is identified as Combinations 9, 10, 11, and 12 in Table 3.2, and the specific types of base materials and numbers of each appear in Table 3.1. Of the sixty-six test sections, only forty-nine survived the data evaluations for use in the analyses. These test sections were distributed as follows by environmental zones:

- Wet-no freeze — 22
- Wet freeze — 8
- Dry-no freeze — 11
- Dry freeze — 8

Because only one environmental zone had sufficient test sections for modeling, the entire data set had to be used to develop predictive equations. The resulting equation appears in Table 7.7. It can be seen from the statistics that the equation should not be considered very reliable.

Figure 7.18 shows plots of predicted versus actual rut depths for HMAC over Portland cement-treated base, and Figure 7.19 shows plots of the residuals versus predicted log(rut depth).

A plot of rut depths, predicted by the equation in Table 7.7, versus KESALs appears in Figure 7.20. The primary thing to be noted is that the equation appears to predict that most of the rutting will occur very early in the pavement's life (at least with other independent variables at their means).

The results from the sensitivity analysis appear in Figure 7.21. It may be noted that these results are similar to those obtained for HMAC pavements over granular base and full-depth HMAC pavements.

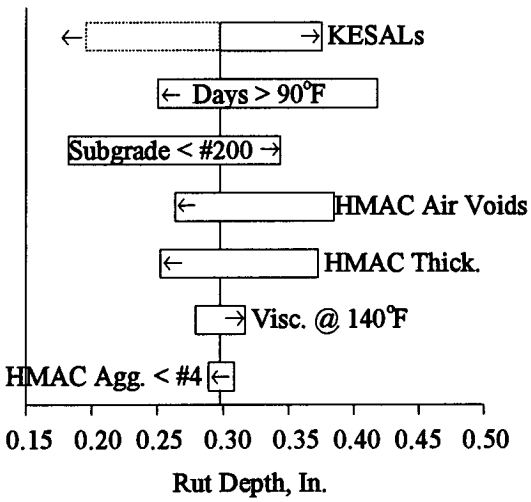

a. Wet

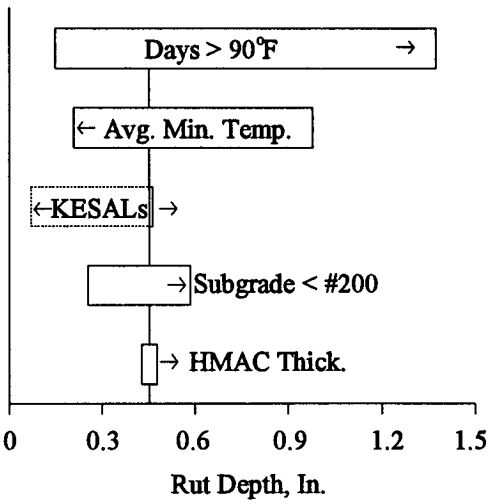

b. Dry

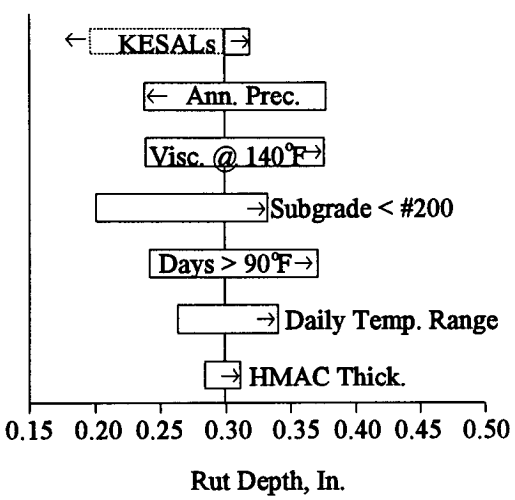

c. No Freeze

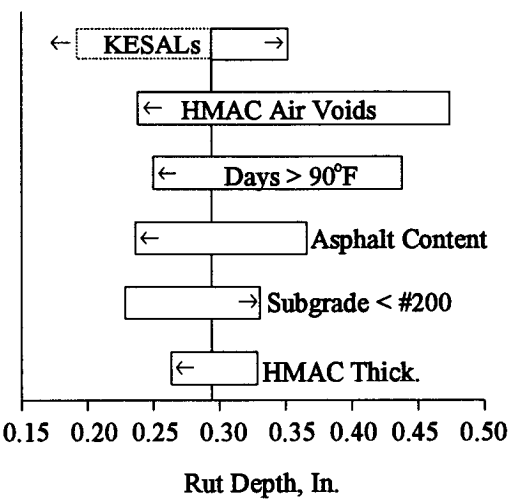

d. Freeze

Figure 7.17. Results From Sensitivity Analyses for Rutting in Full-Depth HMAC Pavements, by Environmental Zones

Table 7.7. Coefficients for Regression Equations Developed to Predict Rutting in HMAC Pavements on Portland Cement-Treated Base

Rut Depth (In.) = $N^B 10^C$ Where N = Number of Cumulative KESALs

$B = b_0 + b_1 x_1 + b_2 x_2 + ... + b_n x_n$

$C = c_0 + c_1 x_1 + c_2 x_2 + ... + c_n x_n$

Explanatory Variable or Interaction (x_i)	Units	Coefficients for Terms In	
		b_i	c_i
Constant Term	-	-0.218	-0.126
HMAC Aggregate < #4 Sieve	% by Weight	0.00412	0
Log (Base Thickness)	Inches	0	-0.474
(Log (HMAC Thickness) * Log (Air Voids in HMAC))	Inches % by Volume	0	-0.401
(Log (HMAC Thickness) * (Asphalt Viscosity at 140°F))	Inches Poise	0	0.000104
(HMAC Aggregate < #4 Sieve * Log (Annual Minimum Temperature))	% by Weight °F	0	-0.00198

n = 49 R^2 = 0.57 Adjusted R^2 = 0.51 RMSE in Log_{10} (Rut Depth) = 0.21

Summary of Sensitivity Analyses for Rutting in HMAC Pavements

The data base limitations for developing predictive models for HMAC have been previously discussed and will be discussed again later. In general, these restrictions apply to individual models, but some statistical advantage should be gained by comparing results from the eleven models and their sensitivity analyses.

Table 7.8 lists the rankings for the individual independent variables, in terms of relative sensitivities, for each of the eleven separate models and sensitivity analyses. One column indicates the number of models for which a specific independent variable was found to be significant. The far right column gives average rankings, with a ranking of 10 arbitrarily assigned for cases when the variable was not found to be significant and is not included in the model. The numbers of independent variables varied from 5 to 8 per model, with a mean of 6.7, so the assigned priority when not significant had to be greater than 8. Because there could be other nonsignificant variables having more sensitivity, the value of 10 appeared logical.

The independent variables are listed below in order of combined rankings. One list is based on average rankings and one is based on the number of models in which the

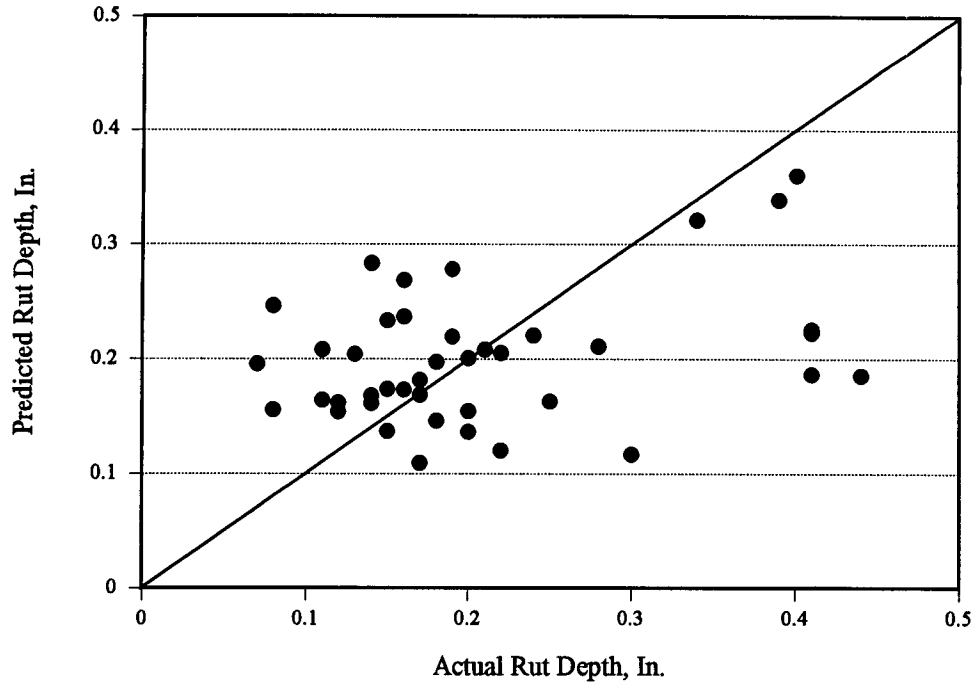

Figure 7.18. Plots of Predicted vs. Actual Rut Depth for HMAC Over Portland Cement-Treated Base Data Set

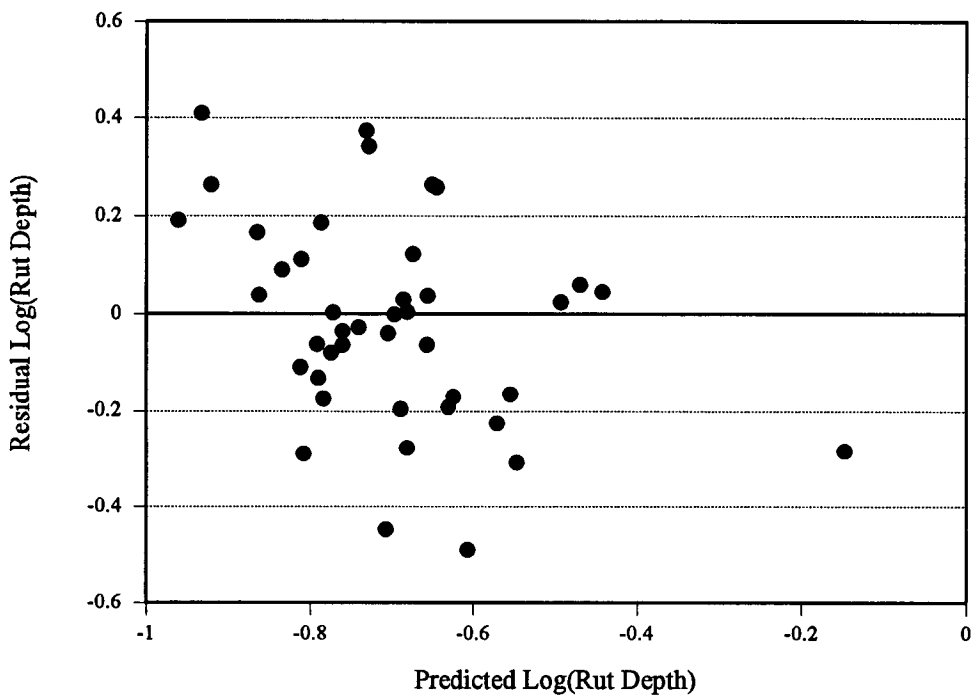

Figure 7.19. Plots of Residuals vs. Predicted Log(Rut Depth) for HMAC Over Portland Cement-Treated Base Data Set

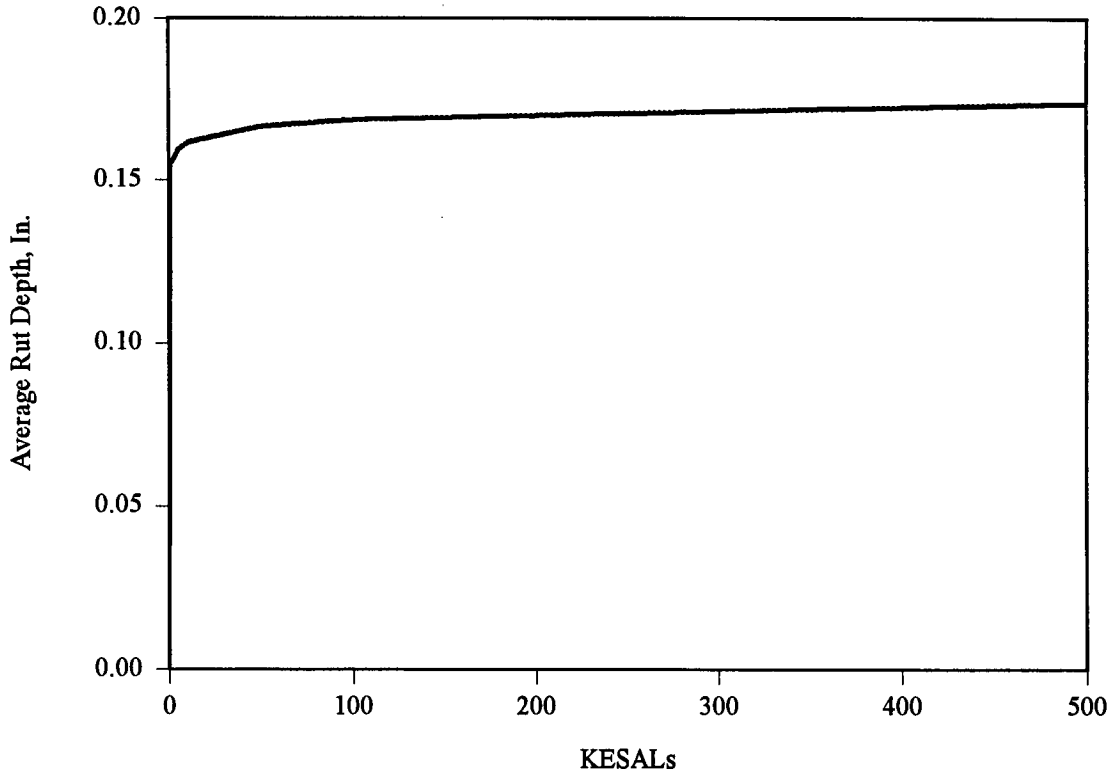

Figure 7.20. Predicted Rutting vs. KESALs, With All Other Independent Variables at Their Mean Values, HMAC Over Portland Cement-Treated Base

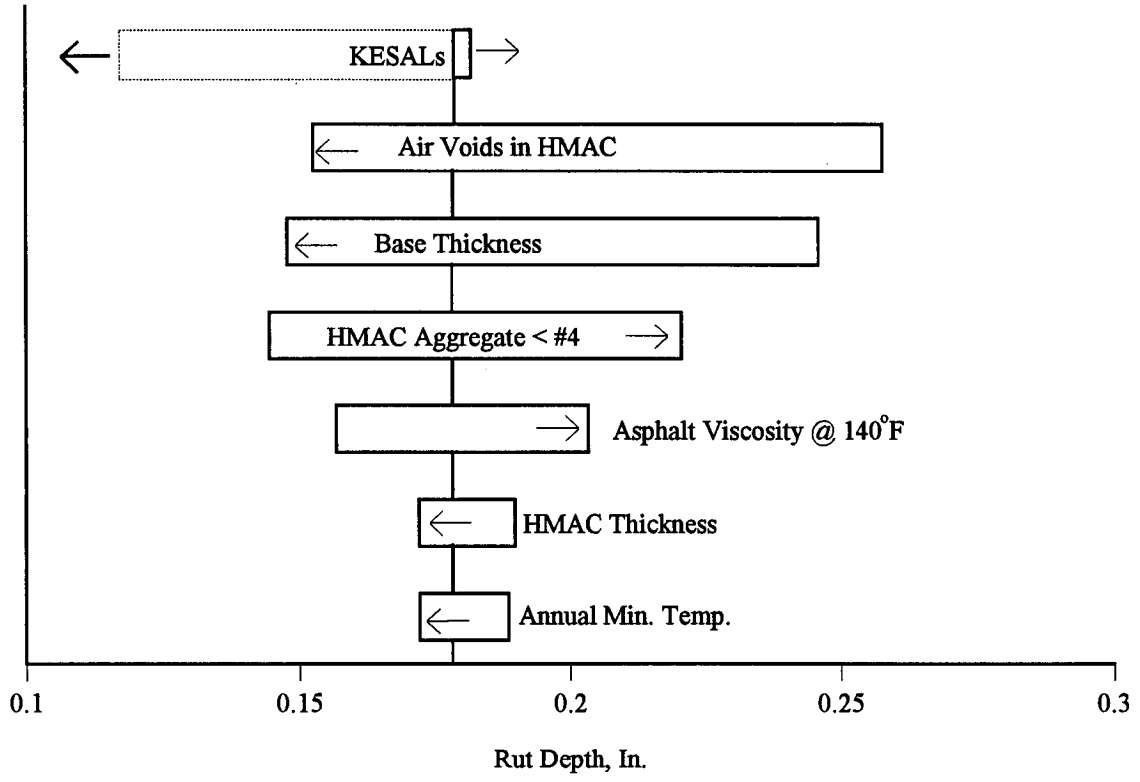

Figure 7.21. Results From Sensitivity Analyses for Rutting in HMAC Over Portland Cement-Treated Base

variable was included (in the case of a "tie", the other ranking basis was used to order the two variables):

Ranking by Averages	Ranking by Number of Models Found Significant
KESALs	KESALs
Air Voids in HMAC	HMAC Thickness
HMAC Thickness	Base Thickness
Base Thickness	Air Voids in HMAC
Subgrade < #200 Sieve	Subgrade < #200 Sieve
Days With Temp. > 90°F	Days With Temp. > 90°F
HMAC Aggregate < #4 Sieve	HMAC Aggregate < #4 Sieve
Asphalt Viscosity	Asphalt Viscosity
Annual Precipitation	Annual Precipitation
Freeze Index	Freeze Index
Base Compaction	Average Annual Minimum Temp.
Average Annual Minimum Temp.	Daily Temp. Range
Daily Temp. Range	Base Compaction
Asphalt Content	Asphalt Content
Annual Freeze-Thaw Cycles	Annual Freeze-Thaw Cycles

It can be seen that nine of the fifteen independent variables have the same rankings for both bases, and the others never vary more than two positions. The rankings generally appear to be logical.

Change in Roughness in HMAC Pavements on Granular Base

The IRI was used to study changes in roughness. The values of IRI were available from profile monitoring data, while estimates of initial IRI were obtained from State Highway Agencies (SHAs) estimates of initial Present Serviceability Index (PSI) by using the following equation[8]:

$$\text{Initial IRI} = 347 \ln (5/\text{Initial PSI})$$

The change in IRI was taken to be the difference between the monitored value and the estimated initial value.

The multiple regressions were conducted with $\log_{10}$ (ΔIRI) as the dependent variable, and the same equation forms used for rut depth predictions apply. The resulting equations for the entire data set and the four environmental zones appear in Table 7.9.

Table 7.8. Orders of Significance for Independent Variables, All Models for Rutting of HMAC Pavements

Independent Variables	HMAC on Granular Base					Full-Depth HMAC					HMAC on Portland Cement-Treated Base	No. of Models Found Significant	Average Rankings
	All Zones	WNF Zones	WF Zones	DNF Zones	DF Zones	All Zones	W Zones	D Zones	NF Zones	F Zones			
KESALs	1	1	1	1	5	1	1	3	1	1	1	All	1.5
HMAC Air Voids	2	3	4	2	4	3	4	-	-	2	2	9	4.2
HMAC Thickness	3	2	5	7	3	5	5	5	7	6	6	All	4.9
HMAC Aggr.< #4	4	5	3	5	-	-	-	-	-	-	4	5	7.4
Asphalt Viscosity	-	-	8	-	-	-	6	-	3	-	5	4	8.4
Asphalt Content	-	-	-	-	-	-	-	-	-	4	-	1	9.5
Base Thickness	5	6	7	8	2	N/A	N/A	N/A	N/A	N/A	3	All	5.2
Base Compaction	-	-	-	-	1	N/A	N/A	N/A	N/A	N/A	-	1	8.5
Subgrade <#200	7	4	-	6	7	2	3	4	4	5	-	9	5.6
Days > 90°F	-	8	-	3	-	-	2	1	5	3	-	6	6.5
Annual Precipitation	-	-	6	4	-	-	-	-	2	-	-	3	8.4
Freeze Index	6	-	2	-	6	-	-	-	-	-	-	3	8.5
Annual Freeze-Thaw Cycles	-	7	-	-	-	-	-	-	-	-	-	1	9.7
Daily Temp. Range	-	-	-	-	-	4	-	-	6	-	-	2	9.1
Avg. Annual Min. Temp.	-	-	-	-	-	-	-	2	-	-	7	2	9.0

Note: N/A = Variable not in equation

Figure 7.22 shows plots of predicted versus actual changes in roughness for HMAC over granular base models for the four environmental zones, and Figure 7.23 shows plots of the residuals versus predicted changes in roughness.

Figure 7.24 shows the predicted changes in roughness versus KESALs for the entire data set and for each environmental zone, when the independent variables appearing in the five separate predictive equations are held at their means for the respective data sets. It appears from these graphs that the change in IRI was much greater in the freeze zones than in the no freeze zones, and the rate of change in IRI was also much greater for the freeze zones than for the no freeze zones.

The results from the sensitivity analyses conducted on the equations in Table 7.9 appear in Figures 7.25 and 7.26. KESALs were found to be the most significant independent variable for the wet freeze and dry-no freeze data sets, while other variables were found to be more significant for the wet-no freeze and dry freeze data sets. HMAC thickness was found to be significant in each of the equations, as it had been for rutting, but generally significance was only moderate. Somewhat surprisingly, the amount of the subgrade passing the #200 sieve was only found to be significant for the dry-no freeze data set, and there it was ranked sixth, although the variations and relative significance in this case were fairly minor. This result may have come from a bias toward coarse-grained subgrades in the data set.

As the lines in Figure 7.24 represent predicted changes in IRI when all variables are at their mean values in the separate data sets, fourteen case studies were conducted for the wet-freeze zone to provide some insight as to the effects of variations of these variables from their means. As occurred in the similar rutting studies, three levels of most variables were used in various combinations of variable magnitudes. The magnitudes of variables for each case study and the resulting calculated changes in IRI appear in Table 7.10.

Cases 1, 2, and 3 show the effects of KESALs. Unlike rutting, the predicted changes in roughness do not so much indicate the distress early in the life of a pavement, but that the rate of roughness decreases over the pavement's life.

Case 12 represents a substantial pavement structure with heavy traffic and a freeze index typical for parts of the northern United States. Its moderately high increase in roughness likely reflects the unexpected finding that roughness in this zone increases with increasing HMAC thickness (see Figure 7.26.c). Because this effect is the opposite that indicated for the other three zones and does not appear to be logical, it may have been a consequence of a bias in the data set.

The highest predicted change in IRI in this set of cases was found for Case 4, which was conducted as a worst case scenario. Case 8 resulted in the next highest prediction, reflecting the relatively high positive sensitivity to increases in HMAC air voids. It can be seen from Figure 7.26 that there are differences in sense (positive or negative sensitivities) among zones for several of the independent variables.

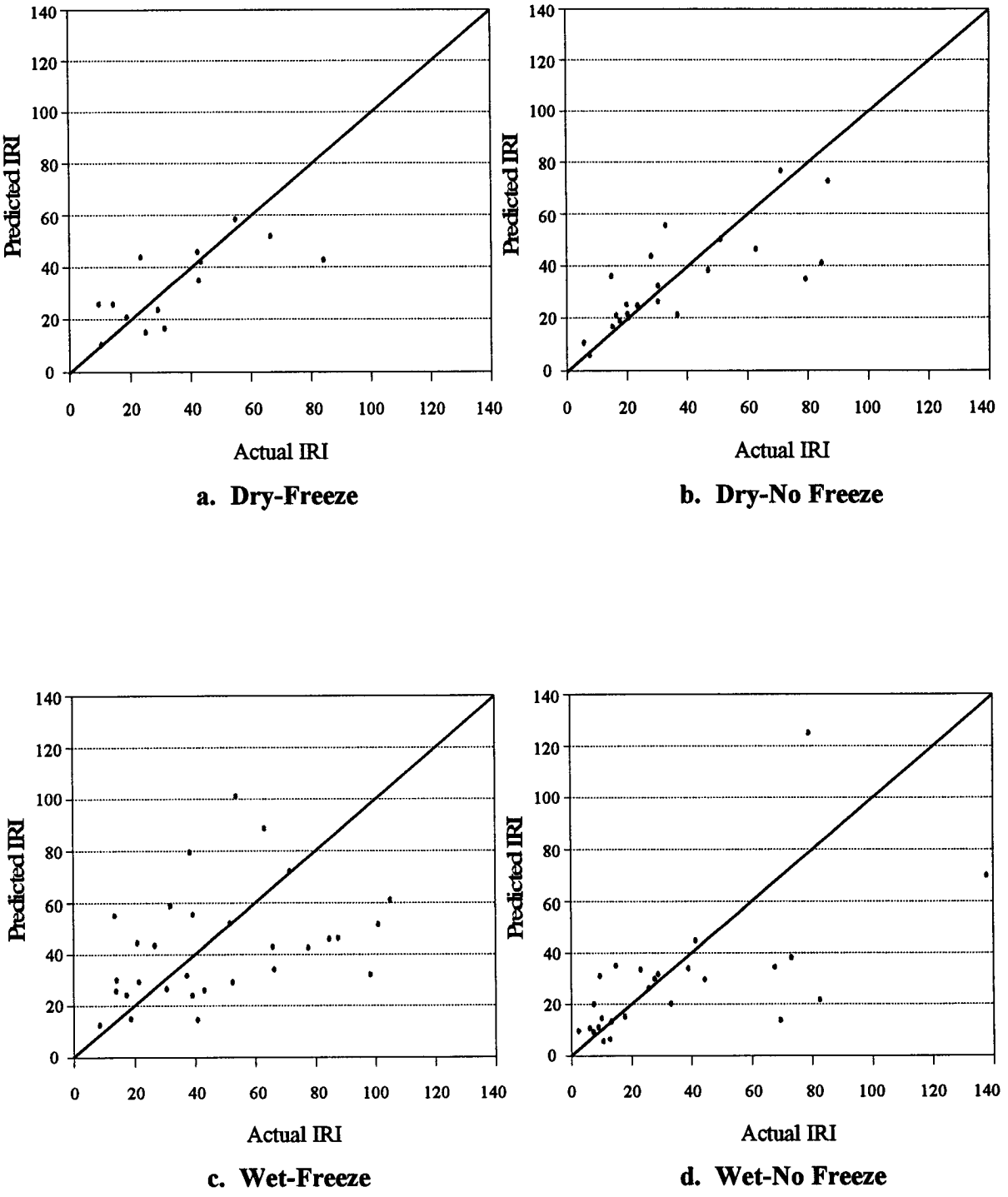

Figure 7.22. Plots of Predicted vs. Actual Change in IRI for HMAC Over Granular Base Data Set

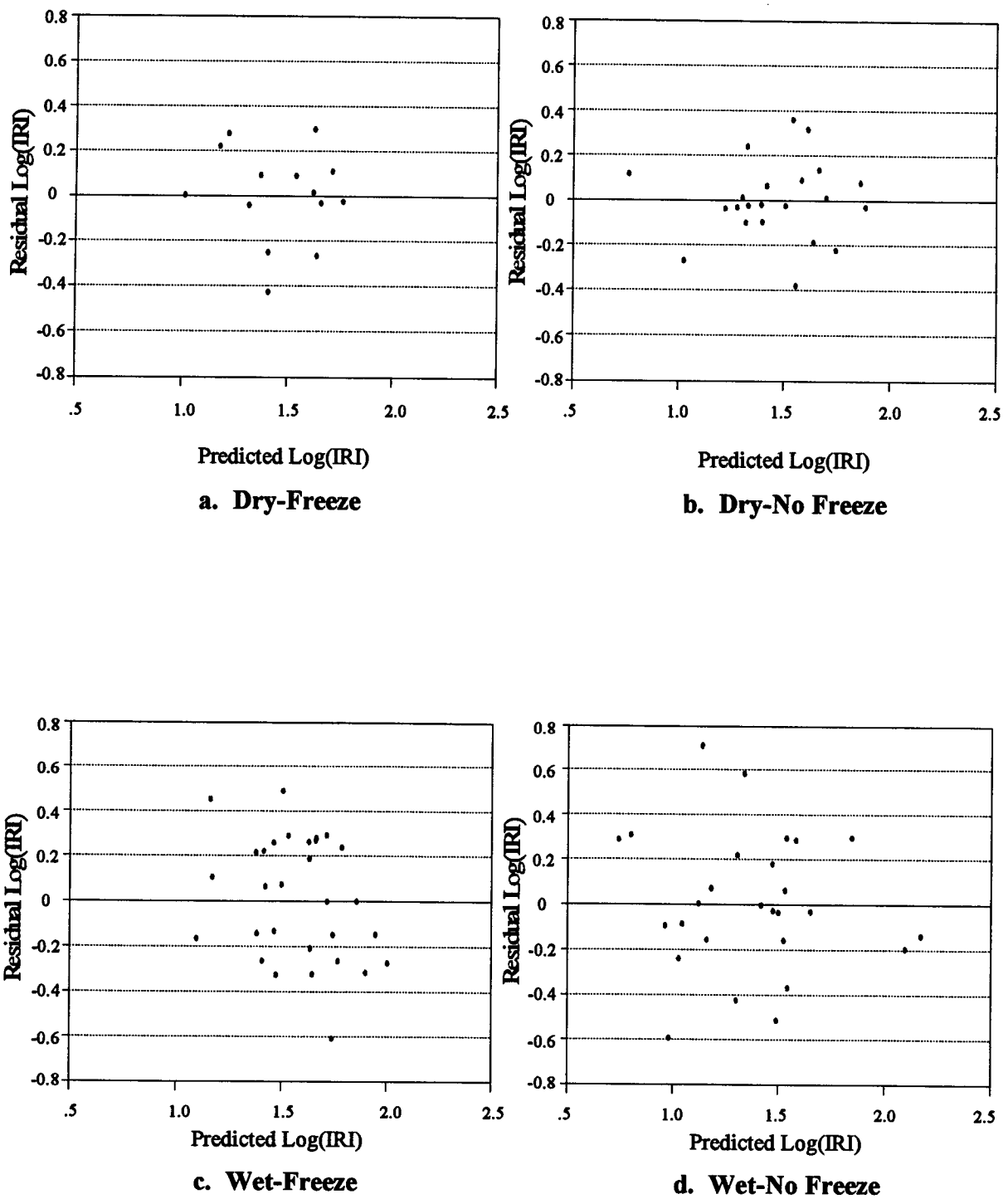

Figure 7.23. Plots of Residuals vs. Predicted Log(IRI) for HMAC Over Granular Base Data Set

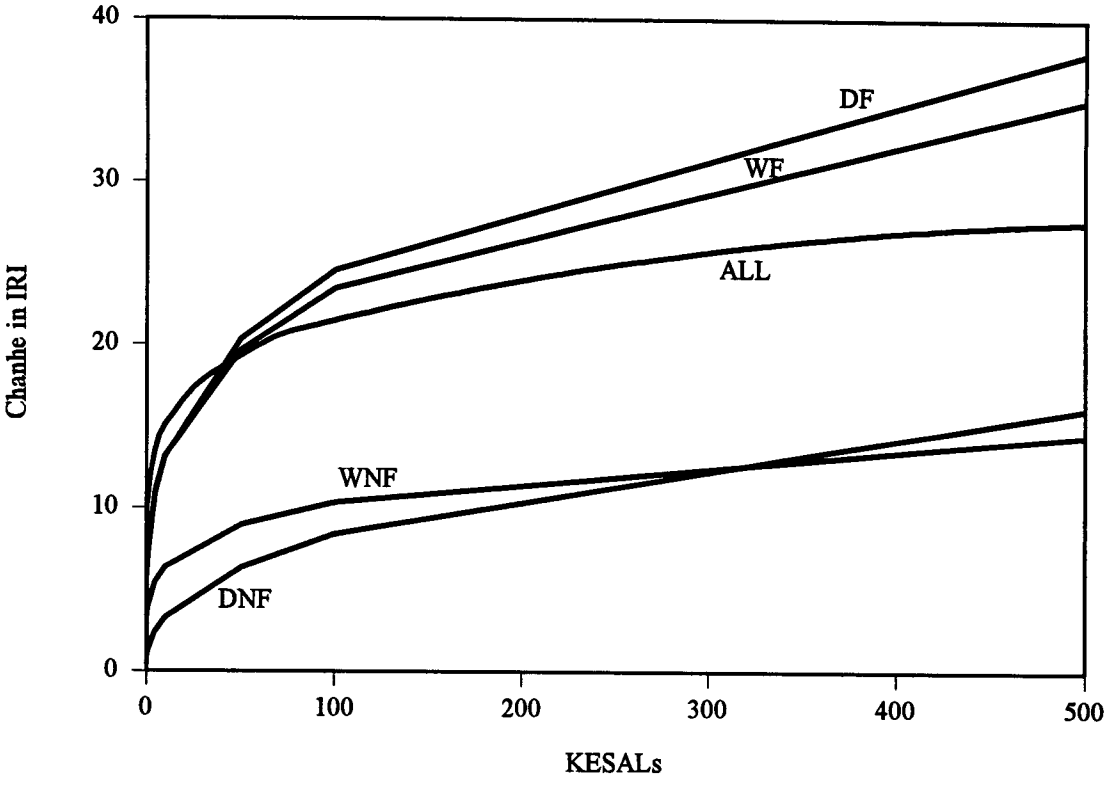

Figure 7.24. Predicted Change in IRI vs. KESALS, With All Other Independent Variables at Their Mean Values, HMAC on Granular Base

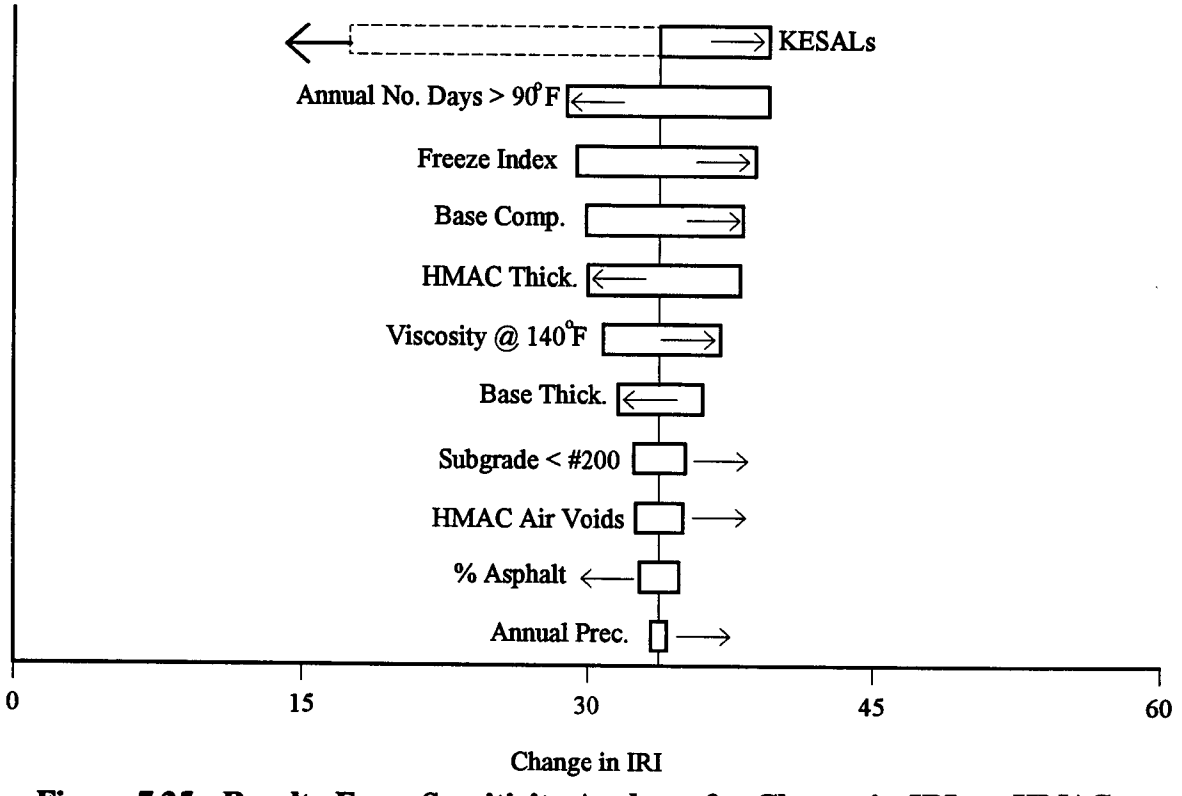

Figure 7.25. Results From Sensitivity Analyses for Change in IRI on HMAC on Granular Base

Table 7.9. Coefficients for Regression Equations Developed to Predict Change in Roughness in HMAC on Granular Base

$\Delta IRI = N^B 10^C$ (In./Mile)

Where N = Number of Cumulative KESALs

$B = b_0 + b_1 x_1 + b_2 x_2 + ... + b_n x_n$

$C = c_0 + c_1 x_1 + c_2 x_2 + ... + c_n x_n$

a. Entire Data Set

Explanatory Variable or Interaction (x_i)	Units	Coefficients for Terms In	
		b_i	c_i
Constant Term	-	0.153	-0.000543
Asphalt Content	% by Weight	0	-0.0160
Annual Precipitation	Inches	0	0.000359
Asphalt Viscosity at 140°F	Poise	0	3.634×10^{-5}
Base Thickness	Inches	0	-0.00335
Base Compaction (Mod. AASHTO)	% of Max. Density	0	0.0113
Subgrade < #200 Sieve	% by Weight	0	0.00062
Freeze Index	Degree-Days	0	8.107×10^{-5}
(Annual Number of Days > 90°F * HMAC Thickness)	Number Inches	0	-0.000437
(Annual Number of Days > 90°F * Air Voids in HMAC)	No. % by Volume	0	0.000178

n = 108 R^2 = 0.65 Adjusted R^2 = 0.62 RMSE in Log_{10} (ΔIRI) = 0.34

Change in Roughness for Full-Depth HMAC Pavements

This data set is identified in Table 3.1 as having fifty-two total test sections, but only thirty-three were suitable for the studies on change in roughness (fifteen of thirty-three were from the wet-freeze environmental zone). Because the data set was so limited, only one equation was developed for the entire data set, and this equation appears as Table 7.11. The test sections not included were omitted because no profile monitoring data were available at the time of these early analyses. However, that data should be available for future analyses.

Table 7.9(continued). Coefficients for Regression Equations Developed to Predict Change in Roughness in HMAC on Granular Base

$\Delta IRI = N^B 10^C$ (In./Mile)

Where: N = Number of Cumulative KESALs

$B = b_0 + b_1 x_1 + b_2 x_2 + \ldots + b_n x_n$

$C = c_0 + c_1 x_1 + c_2 x_2 + \ldots + c_n x_n$

b. Wet-No Freeze Data Set

Explanatory Variable or Interaction (x_i)	Units	Coefficients for Terms In	
		b_i	c_i
Constant Term	-	0.210	0.0233
Base Thickness	Inches	0	-0.0372
Annual Number of Days > 90°F	Number	0	0.00249
Annual Precipitation	Inches	0	0.0214
(HMAC Thickness * Base Compaction (Mod AASHTO))	Inches % of Max. Density	0	-0.000761
(Log (Air Voids in HMAC) * Daily Temperature Range)	% by Volume °F	0	0.0322
(Asphalt Viscosity at 140°F * Log (Annual Freeze-Thaw Cycles +1))	Poise Number	0	-0.000299
(Asphalt Viscosity at 140°F * Daily Temperature Range)	Poise °F	0	1.702×10^{-5}

$n = 32$ $R^2 = 0.85$ Adjusted $R^2 = 0.81$ RMSE in Log_{10} (ΔIRI) = 0.31

c. Wet-Freeze Data Set

Explanatory Variable or Interaction (x_i)	Units	Coefficients for Terms In	
		b_i	c_i
Constant Term	-	0.250	0.0403
Asphalt Viscosity at 140°F	Poise	0	0.00014
Air Voids in HMAC	% by Volume	0	0.0704
Log (HMAC Thickness)	Inches	0	0.314
Base Thickness	Inches	0	-0.00162
Annual Number of Days > 90°F	Number	0	-0.00165
(Freeze Index * Air Voids in HMAC)	Degree-Days % by Volume	0	1.628×10^{-5}

$n = 35$ $R^2 = 0.87$ Adjusted $R^2 = 0.84$ RMSE in Log_{10} (ΔIRI) = 0.27

Table 7.9(continued). Coefficients for Regression Equations Developed to Predict Change in Roughness in HMAC Pavements on Granular Base

$\Delta IRI = N^B 10^C$ (In./Mile)

Where: N = Number of Cumulative KESALs

$B = b_0 + b_1 x_1 + b_2 x_2 + \ldots + b_n x_n$

$C = c_0 + c_1 x_1 + c_2 x_2 + \ldots + c_n x_n$

d. Dry-No Freeze Data Set

Explanatory Variable or Interaction (x_i)	Units	Coefficients for Terms In	
		b_i	c_i
Constant Term	-	0.406	-0.00994
HMAC Thickness	Inches	0	0.0255
Asphalt Viscosity at 140°F	Poise	0	0.00024
Base Thickness	Inches	0	-0.0329
Annual Precipitation	Inches	0	0.0124
(Annual Number of Days > 90°F * HMAC Thickness)	Number Inches	0	-0.00114
(Subgrade < #200 Sieve * Annual Precipitation)	% by Weight Inches	0	0.000268

$n = 27$ $R^2 = 0.95$ Adjusted $R^2 = 0.93$ RMSE in Log_{10} (ΔIRI) = 0.18

e. Dry-Freeze Data Set

Explanatory Variable or Interaction (x_i)	Units	Coefficients for Terms In	
		b_i	c_i
Constant Term	-	0.271	0.00393
Asphalt Viscosity at 140°F	Poise	0	0.000317
Base Thickness	Inches	0	0.0240
Annual Number of Days > 90°F	Number	0	-0.0125
(Log (Air Voids in HMAC) * HMAC Thickness)	% by Volume Inches	0	-0.00197
(Freeze Index * Annual Number of Days > 90°F)	Degree-Days Number	0	1.451×10^{-5}

$n = 14$ $R^2 = 0.94$ Adjusted $R^2 = 0.92$ RMSE in Log_{10} (ΔIRI) = 0.21

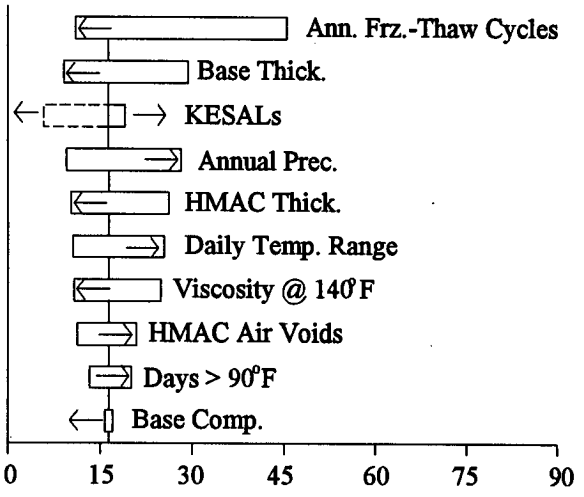

a. **Wet-No Freeze Data Set**

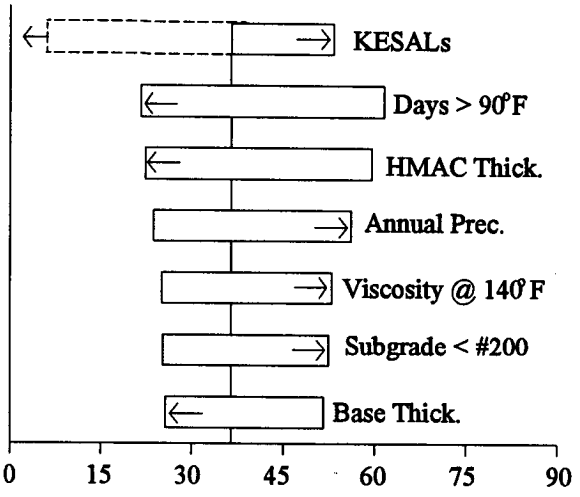

b. **Dry-No Freeze Data Set**

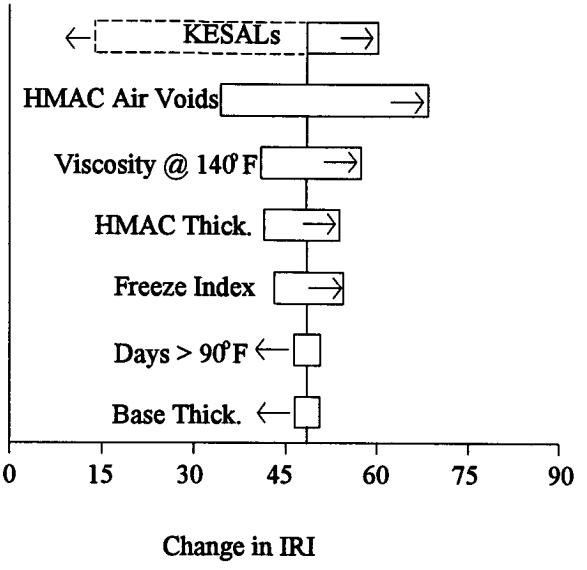

c. **Wet-Freeze Data Set**

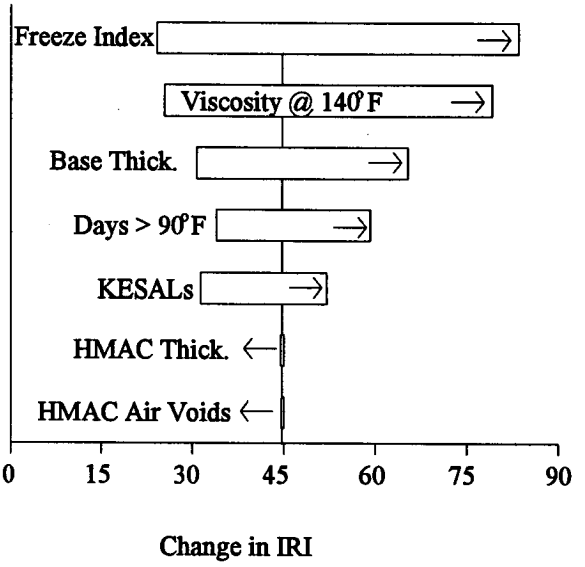

d. **Dry-Freeze Data Set**

Figure 7.26. Results From Sensitivity Analyses for Change in IRI in HMAC on Granular Base

Table 7.10. Calculated Changes in IRI for Various Combinations of Independent Variable Magnitudes, Wet-Freeze Equation

Independent Variable	Case Numbers													
	1	2	3	4	5	6	7	8	9	10	11	12	13	14
KESALs	100	5000	20,000	5000	5000	5000	5000	5000	5000	5000	5000	20,000	5000	5000
HMAC Air Voids	5	5	5	8	5	5	3	8	5	5	5	5	3	5
Asphalt Viscosity	1000	1000	1000	2000	1000	1000	1000	1000	2000	2000	2000	1000	1000	500
HMAC Thickness	6	6	6	10	10	2	6	6	6	6	6	10	6	10
Freeze Index	600	600	600	1000	1000	1000	1000	1000	1000	600	1000	1000	1000	1000
Days > 90°F	30	30	30	60	30	30	30	30	30	30	30	30	30	30
Base Thickness	12	12	12	4	12	12	12	12	12	12	20	20	12	4
Calculated ΔIRI	18	48	68	141	61	37	35	94	71	66	69	83	35	53

Figure 7.27 shows a plot of predicted versus actual changes in roughness for the full-depth HMAC model, and Figure 7.28 shows a plot of the residuals versus predicted log(change in roughness).

A plot of the change in IRI predicted by the equation in Table 7.11 appears as Figure 7.29. This plot appears to have much the same form as those in Figure 7.24 for HMAC on granular base.

The results from the sensitivity analysis appear in Figure 7.30. KESALs is again the most significant independent variable, but freeze index was also very significant. The other significant variables in order of significance were subgrade passing the #200 sieve, asphalt content, annual numbers of days experiencing a temperature greater than 90°F, and HMAC thickness. It is not clear why the combination of finer subgrade soil and log (freeze index +1) would decrease change in roughness, so this characteristic is assumed to result from the specific test sections in the data set.

Change in Roughness of HMAC Pavements on Portland Cement-Treated Base

Only thirty-seven of the sixty-six test sections in this data set had the data necessary for these analyses. Consequently, the analyses were conducted on the entire data set, producing the equation appearing in Table 7.12.

Figure 7.31 shows a plot of predicted versus actual changes in roughness for the HMAC over a portland cement-treated base model, and Figure 7.32 shows a plot of the residuals versus predicted log(change in roughness).

The predicted changes in IRI versus KESALs, with all other variables held at their means, appears in Figure 7.33. The general form of the equation appears to approximate those for the other models for change in roughness, except a large initial change in roughness occurs in the life of the pavement and the rate of change after that appears to be smaller than that for the other pavements without portland cement-treated bases. This appears similar to the differences noted for rutting.

The results from the sensitivity analysis appear in Figure 7.34. In this case, the subgrade material passing the #200 sieve was found to be the most significant variables, followed by KESALs and annual number of days with temperatures greater than 90°F.

Table 7.11. Coefficients for Regression Equations Developed to Predict Change in Roughness in Full-Depth HMAC Pavement, Entire Data Set

$\Delta IRI = N^B 10^C$ (In./Mile)

Where: N = Number of Cumulative KESALs

$B = b_0 + b_1 x_1 + b_2 x_2 + ... + b_n x_n$

$C = c_0 + c_1 x_1 + c_2 x_2 + ... + c_n x_n$

Explanatory Variable or Interaction (x_i)	Units	Coefficients for Terms n	
		b_i	c_i
Constant Term	-	0.373	-0.0126
Log (HMAC Thickness)	Inches	0	-0.145
Log (Annual Number of Days > 90°F)	Number	0	-0.102
(Subgrade < #200 * Log (Freeze Index + 1))	% by Weight Degree-Days	0	-0.00189
((Log (Asphalt Content)) * (Log Freeze Index + 1))	% by Weight Degree-Days	0	0.531

n = 33 R^2 = 0.76 Adjusted R^2 = 0.71 RMSE in $Log_{10}(\Delta IRI)$ = 0.39

Summary of Sensitivity Analyses for Change in Roughness of HMAC Pavements

Table 7.13 lists the rankings for the individual independent variables, in terms of relative sensitivities, for each of the seven separate models and sensitivity analyses. One column indicates the number of models for which a specific independent variable was found to be significant. The far right column gives average rankings, with a rank of 10 arbitrarily assigned for cases when the variable was not found to be significant and was not included in the model (same logic as for rutting, Table 7.8).

The independent variables are listed below in order of combined rankings, one list is based on average rankings, and one is based on the number of models in which the variable was included:

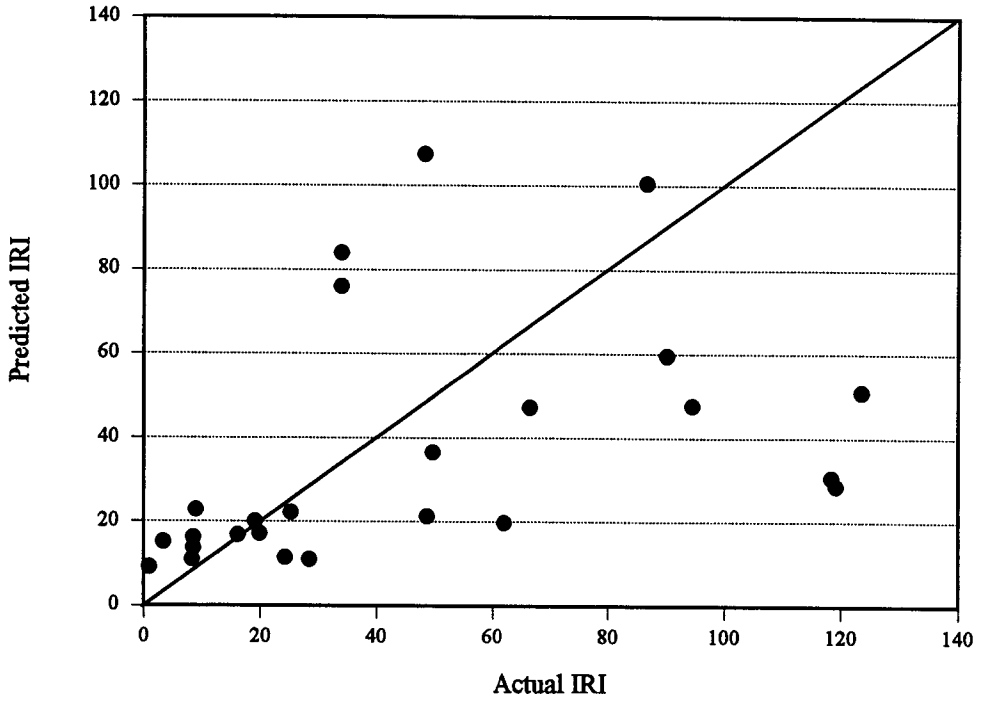

Figure 7.27. Plots of Predicted vs. Actual Change in IRI for Full-Depth HMAC Pavement Data Set

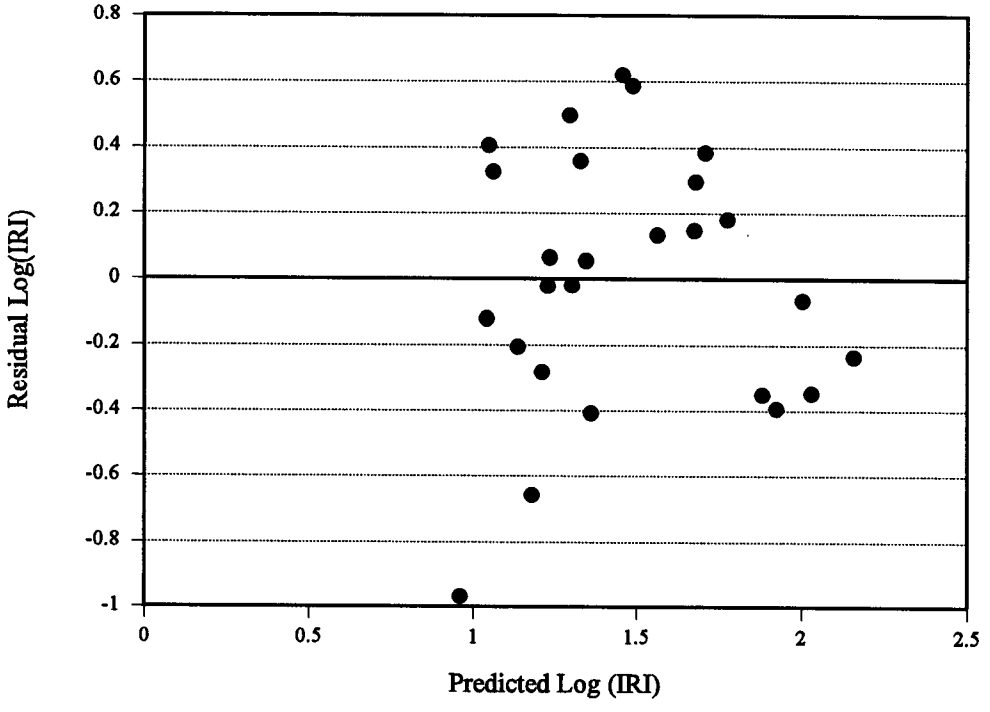

Figure 7.28. Plots of Residual vs. Predicted Log(Change in IRI) for Full-Depth HMAC Pavement Data Set

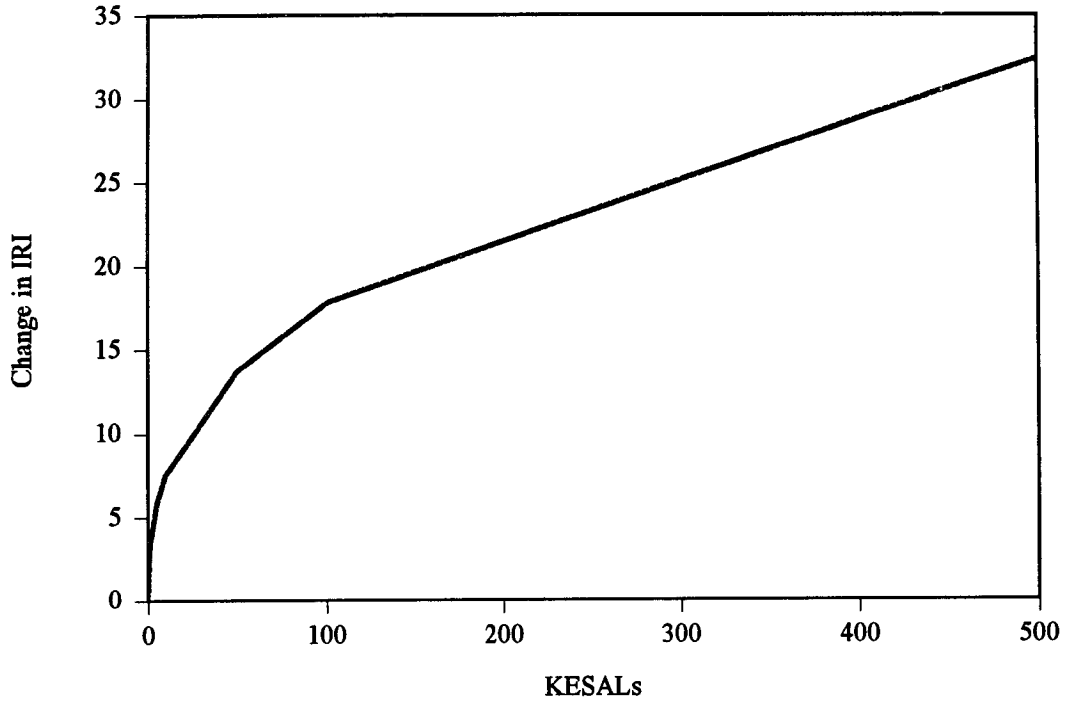

Figure 7.29. Predicted Change in IRI vs. KESALs, With All Other Independent Variables at Their Means, Full-Depth HMAC Pavement

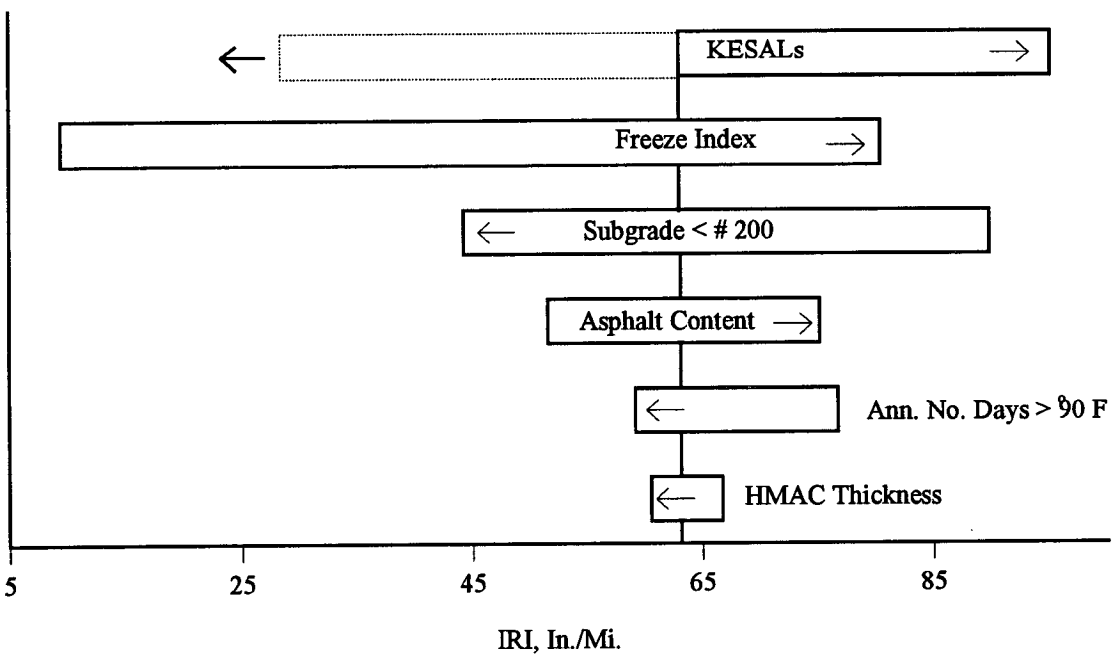

Figure 7.30. Results From Sensitivity Analyses for Change in IRI in Full-Depth HMAC Pavement

Table 7.12. Coefficients for Regression Equations Developed to Predict Change in Roughness in HMAC on Portland Cement-Treated Base, Entire Data Set

$\Delta IRI = N^B 10^C$ (In./Mile)

Where: N = Number of Cumulative KESALs

$B = b_0 + b_1 x_1 + b_2 x_2 + \ldots + b_n x_n$

$C = c_0 + c_1 x_1 + c_2 x_2 + \ldots + c_n x_n$

Explanatory Variable or Interaction (x_i)	Units	Coefficients for Terms in	
		b_i	c_i
Constant Term	-	0.126	-0.00394
Log (Base Thickness)	Inches	0	0.560
Log (Annual Number of Days > 90°F)	Number	0	0.0394
(Log (HMAC Thickness) Log (Base Thickness))	Inches Inches	0	-0.501
(Air Voids in HMAC * Annual Precipitation)	% by Volume Inches	0	0.000287
(Subgrade < #200 Sieve * Log (Annual Number of Days > 90°F))	% by Weight Number	0	0.00717
(Annual Precipitation * Freeze Index)	Inches Degree-Days	0	-1.502×10^{-5}
(Freeze Index * Log (Annual Number of Days > 90°F))	Degree-Days Number	0	0.00039

$n = 37$ $R^2 = 0.80$ Adjusted $R^2 = 0.75$ RMSE in Log_{10} (ΔIRI) = 0.33

Ranking by Averages

KESALs
Asphalt Viscosity
Days With Temp. > 90°F
HMAC Thickness
Base Thickness
Freeze Index
Subgrade < #200 Sieve
Air Voids in HMAC
Base Compaction
Annual Precipitation
Daily Temp. Range
Annual Freeze-Thaw Cycles
Asphalt Content
HMAC Aggregate < #4 Sieve

Ranking by Number of Models Found Significant

KESALs
Days With Temp. > 90°F
HMAC Thickness
Base Thickness
Asphalt Viscosity
Freeze Index
Air Voids in HMAC
Subgrade < #200 Sieve
Annual Precipitation
Base Compaction
Daily Temp. Range
Asphalt Content
Annual Freeze-Thaw Cycles
HMAC Aggregate < #4 Sieve

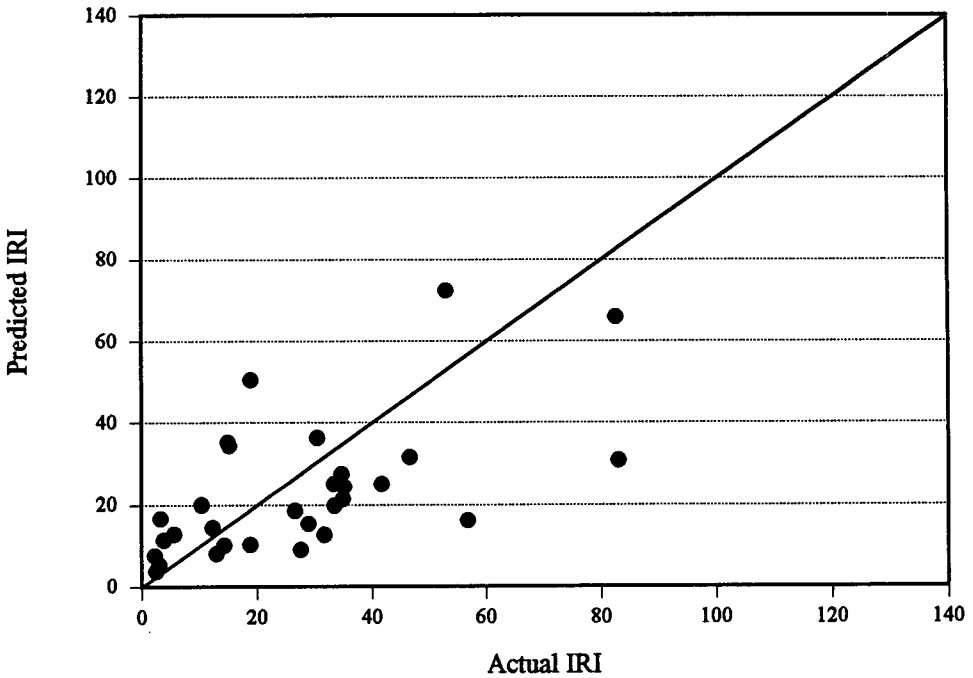

Figure 7.31. Plots of Predicted vs. Actual Change in IRI for HMAC on Portland Cement-Treated Base Data Set

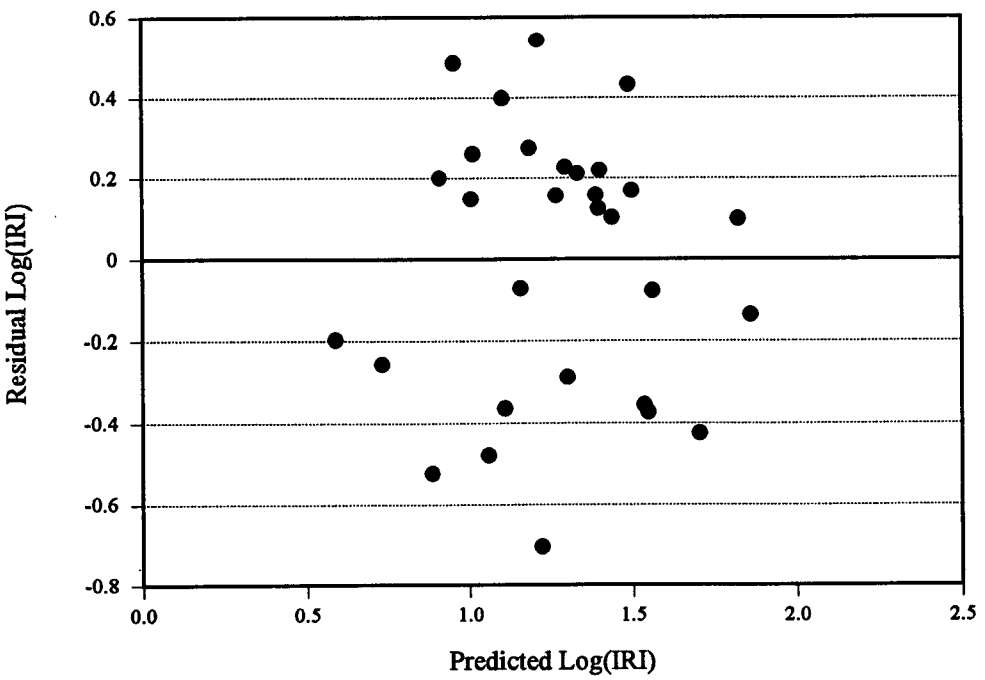

Figure 7.32. Plots of Residual vs. Predicted Log(Change in IRI) for HMAC on Portland Cement-Treated Base Data Set

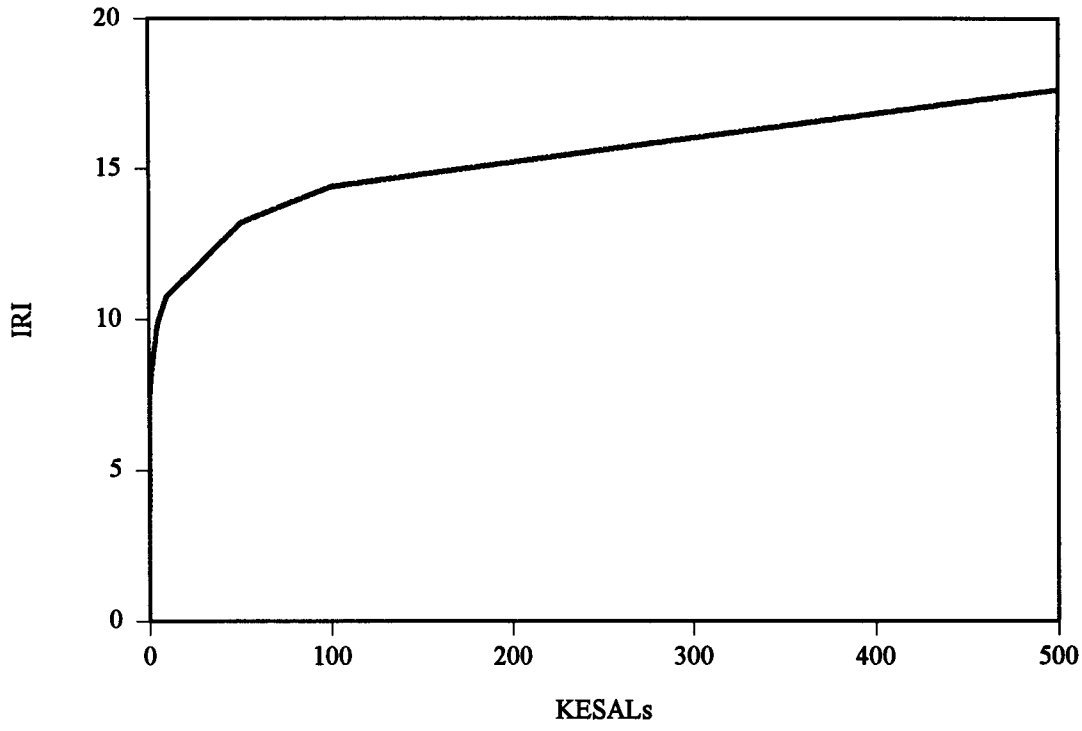

Figure 7.33. Predicted Change in IRI vs. KESALs, With All Other Independent Variables at Their Mean Values, HMAC Over Portland Cement-Treated Base

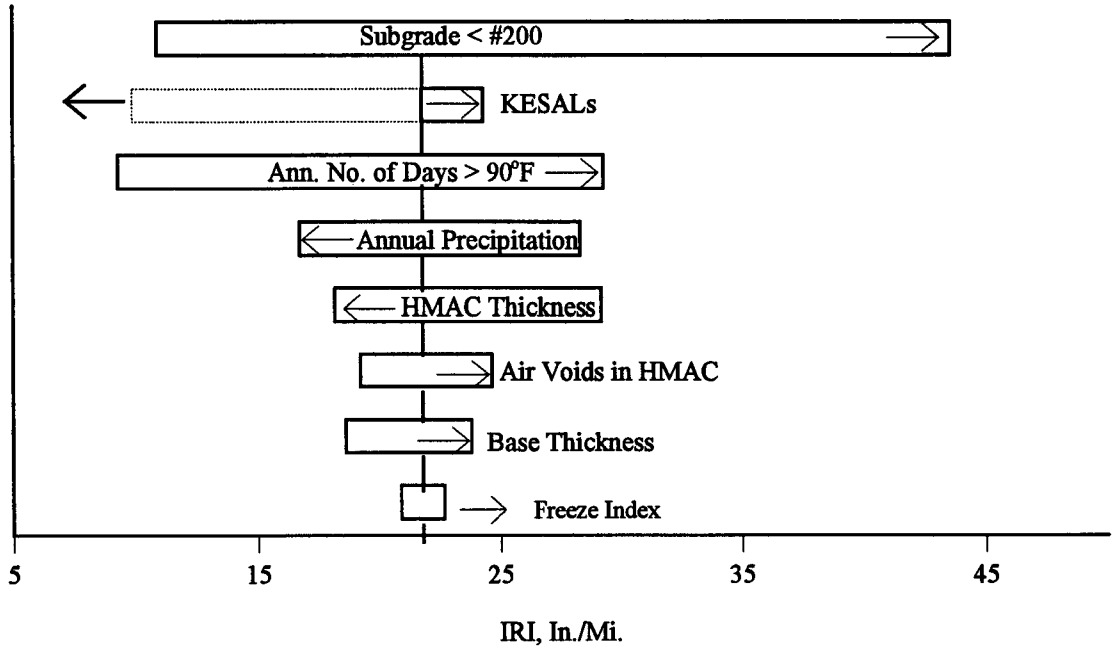

Figure 7.34. Sensitivity Analyses of Change in IRI in HMAC Over Portland Cement-Treated Base

Table 7.13. Orders of Significance for Independent Variables, All Models for Change in Roughness of HMAC Pavement

Independent Variables	HMAC on Granular Base					Full-Depth HMAC	HMAC on Portland Cement-Treated Base	No. of Models Found Significant	Average Ranking
	All Zones	WNF Zones	WF Zones	DNF Zones	DF Zones				
KESALs	1	3	1	1	5	1	2	All	2.0
Air Voids in HMAC	9	8	2	-	7	-	6	5	7.4
HMAC Thickness	5	5	4	3	6	6	5	All	4.9
HMAC Aggr. < #4	-	5	-	-	-	-	-	1	9.3
Asphalt Viscosity	6	7	3	5	2	-	-	5	3.9
Asphalt Content	. 10	-	-	-	-	4	-	2	9.1
Base Thickness	7	2	7	7	3	N/A	6	All	5.5
Base Compaction	4	10	-	-	-	N/A	1	3	7.5
Subgrade < #200	8	4	-	6	-	3	-	4	7.3
Days > 90°F	2	9	6	2	4	5	3	All	4.4
Annual Precipitation	11	4	-	4	-	-	4	4	7.6
Freeze Index	3	-	5	-	1	2	8	5	5.6
Annual Freeze-Thaw Cycles	-	1	-	-	-	-	-	1	8.7
Daily Temp. Range	-	6	-	-	-	4	-	2	8.6

Note: N/A = Variable not in equation

It can be seen that four of the fourteen independent variables have the same rankings for both bases, and the others varied only one to three positions. These rankings also appear logical.

Transverse Cracking of HMAC Pavements on Granular Base and Full-Depth HMAC Pavements

There were not sufficient test sections with transverse cracking in some environmental zones for separate analyses for HMAC on granular base and full-depth HMAC, so these data sets were combined. In addition, any pavements which had not experienced transverse cracking were deleted from the data set. As was the case for rut depth and change in roughness, the multiple regressions were conducted with the common log of the dependent variable, with the same equation forms. The resulting predictive equations appear in Table 7.14. The dependent variable used is transverse crack spacing.

Figure 7.35 shows plots of predicted versus actual transverse crack spacing for the combined HMAC over granular base and full-depth HMAC models by environmental zones. Figure 7.36 shows plots of residuals versus predicted log(transverse crack spacing).

Figure 7.37 shows predicted crack spacing versus age for the entire data set and for each environmental zone when the independent variables appearing in the five separate data sets are held at their means. It appears from these graphs that there was more early transverse cracking (closer crack spacing) for the pavements in the dry zones than for those in the wet zones, and the predicted crack spacing after about 6 to 10 years was close to the same for all environmental zones. The predictions for mean conditions in the wet-no freeze zone indicate that the crack spacing will eventually be closer than for the other zones. This scenario does not appear likely and probably results from only having seventeen observations to use in developing the model for this zone.

The results from the sensitivity analyses conducted on the equations in Table 7.14 appear in Figures 7.38 and 7.39.

As for rutting and change in roughness, fourteen cases were examined for the dry-freeze zone to study the effects of variations in the magnitudes of the independent variables in various combinations on transverse crack spacing. The magnitudes of variables for each case study and the resulting calculated crack spacings appear in Table 7.15.

Case 1 represents a typical case for the dry-freeze zone, which had a predicted crack spacing of 56 ft (17m). Case 4 represented the worst case, which had a predicted crack spacing of 7 ft (2 m). Case 12 represents a highway with a heavy pavement structure, heavy traffic (for this zone), and an age of 17 years. Its predicted crack spacing was 75 ft (23m). In general, the predicted crack spacings appeared to be reasonable.

Table 7.14. Coefficients for Regression Equations Developed to Predict Transverse Crack Spacing in HMAC on Granular Base and Full-Depth HMAC Pavement

Crack Spacing (Ft) $= N^B 10^C$ Where N = Age, Years

$B = b_0 + b_1 x_1 + b_2 x_2 + \ldots + b_n x_n$

$C = c_0 + c_1 x_1 + c_2 x_2 + \ldots + c_n x_n$

a. Entire Data Set

Explanatory Variable or Interaction (x_i)	Units	Coefficients for Terms n	
		b_i	c_i
Constant Term	-	-0.205	0.282
Log (HMAC Thickness)	Inches	0	0.341
Air Voids in HMAC	% by Volume	0	0.00686
Log (Base Thickness +1)	Inches	0	-0.00310
Base Compaction (Mod. AASHTO)	% of Max. Density	0	0.00646
(Asphalt Viscosity at 140°F * Log (Base Thickness +1))	Poise Inches	0	0.00013
(Log (Annual Precipitation) * Log (Base Thickness +1))	Inches Inches	0	0.301

$n = 118$ $R^2 = 0.37$ Adjusted $R^2 = 0.33$ RMSE in Log_{10} (Crack Spacing)= 0.53

b. Wet-No Freeze Data Set

Explanatory Variable or Interaction (x_i)	Units	Coefficients for Terms In	
		b_i	c_i
Constant Term	-	-1.12	0.0131
Log (Freeze Index +1)	Degree-Days	0	0.733
Log (Annual Precipitation)	Inches	0	0.534
(HMAC Thickness * Log (Asphalt Viscosity at 140°F))	Inches Poise	0	0.0109
(Base Thickness * Asphalt Content)	Inches % by Weight	0	-0.00587
(Base Compaction * Daily Temperature Range)	% of Max. Density °F	0	0.000295

$n = 17$ $R^2 = 0.85$ Adjusted $R^2 = 0.75$ RMSE in Log_{10} (Crack Spacing)= 0.52

Table 7.14(continued). Coefficients for Regression Equations Developed to Predict Transverse Crack Spacing in HMAC on Granular Base and Full-Depth HMAC Pavement

Crack Spacing (Ft) = $N^B 10^C$ Where N = Age, Years

$B = b_0 + b_1 x_1 + b_2 x_2 + ... + b_n x_n$

$C = c_0 + c_1 x_1 + c_2 x_2 + ... + c_n x_n$

c. Wet-Freeze Data Set

Explanatory Variable or Interaction (x_i)	Units	Coefficients for Terms n	
		b_i	c_i
Constant Term	-	-0.106	-0.0201
HMAC Aggregate < #4	% by Weight	0	-0.0131
HMAC Thickness	Inches	-0.00474	0
Log (Annual Precipitation)	Inches	0	1.84
Annual No. of Days > 90°F	Number	-0.0540	0
(Base Thickness * Log (Annual Precipitation))	Inches Inches	0	-0.0159
(Base Thickness * Annual No. of Days > 90°F)	Inches Number	0	0.00240
(Subgrade < #200 * Log (Annual Precipitation))	% by Weight Inches	0	0.00408

n = 44 R^2 = 0.86 Adjusted R^2 = 0.83 RMSE in Log_{10} (Crack Spacing) = 0.30

d. Dry-No Freeze Data Set

Explanatory Variable or Interaction (x_i)	Units	Coefficients for Terms n	
		b_i	c_i
Constant Term	-	-0.241	-0.00155
HMAC Thickness	Inches	0	-0.0282
Log (Base Thickness +1)	Inches	-0.147	0
Log (Annual Precipitation)	Inches	0	1.89

n = 23 R^2 = 0.86 Adjusted R^2 = 0.83 RMSE in Log_{10} (Crack Spacing) = 0.35

Table 7.14(continued). Coefficients for Regression Equations Developed to Predict Transverse Crack Spacing in HMAC on Granular Base and Full-Depth HMAC Pavement

Crack Spacing = $N^B 10^C$ (Ft) Where N = Age, Years

$B = b_0 + b_1 x_1 + b_2 x_2 + ... + b_n x_n$

$C = c_0 + c_1 x_1 + c_2 x_2 + ... + c_n x_n$

e. Dry-Freeze Data Set

Explanatory Variable or Interaction (x_i)	Units	Coefficients for Terms n	
		b_i	c_i
Constant Term	-	-0.425	0.0468
Log (Annual Traffic)	KESALs	0	0.854
Base Thickness	Inches	0	-0.00853
Freeze Index	Degree-Days	0	0.00013
(HMAC Thickness * Base Thickness)	Inches Inches	0	0.00398
(HMAC Thickness * Asphalt Viscosity at 140°F)	Inches Poise	0	1.64×10^{-5}
(HMAC Thickness * Log (Subgrade < #200 +1))	Inches % by Weight	0	-0.0350
(Asphalt Viscosity at 140°F * Log (Subgrade < #200 +1))	Poise % by Weight	0	0.000109

n = 34 R^2 = 0.78 Adjusted R^2 = 0.72 RMSE in Log_{10} (Crack Spacing) = 0.44

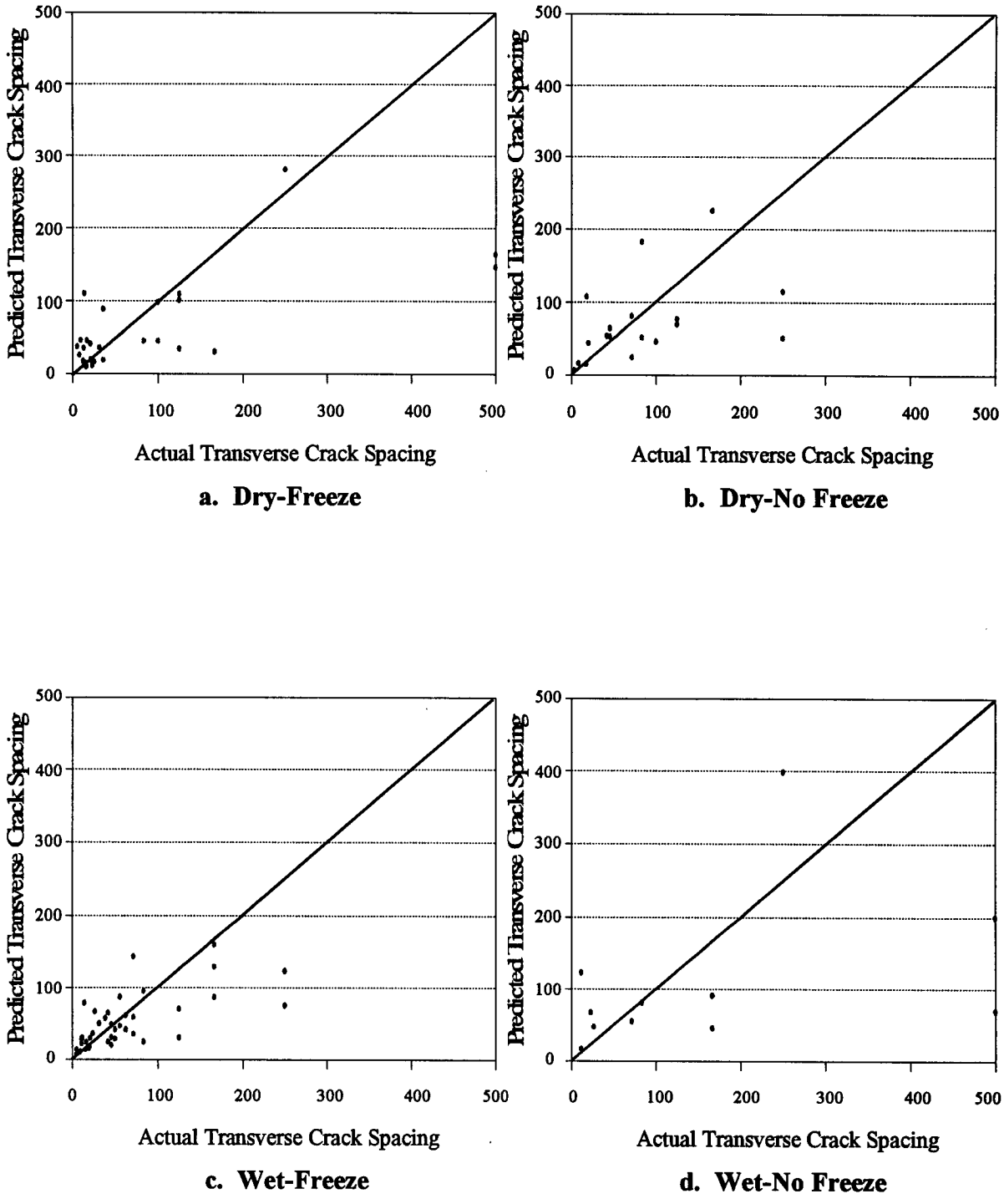

Figure 7.35. Plots of Predicted vs. Actual Transverse Crack Spacing for HMAC Over Granular Base and Full-Depth HMAC Pavement Data Sets

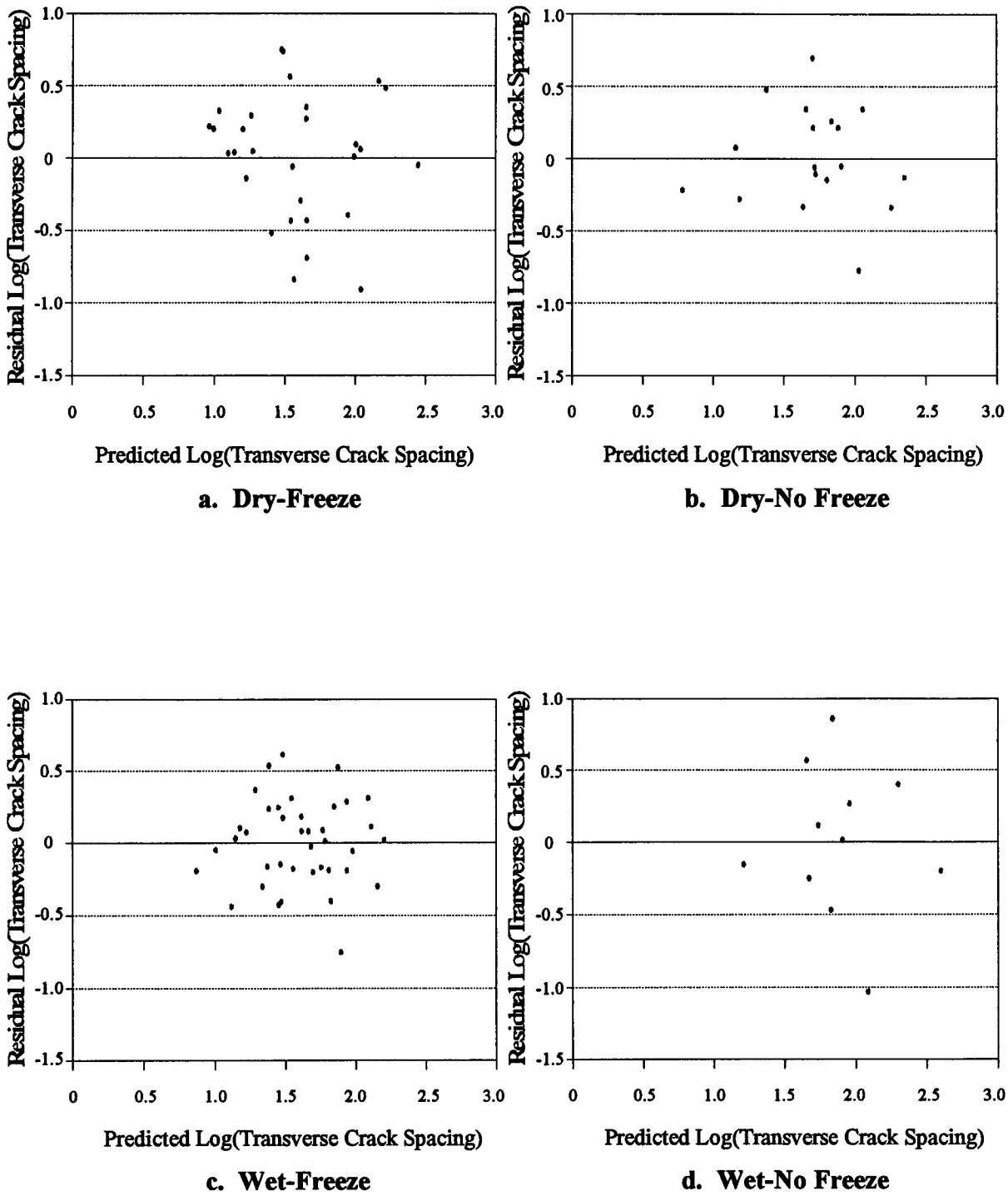

Figure 7.36. Plots of Residuals vs. Predicted Log(Transverse Crack Spacing) for HMAC Over Granular Base and Full-Depth HMAC Pavement Data Sets

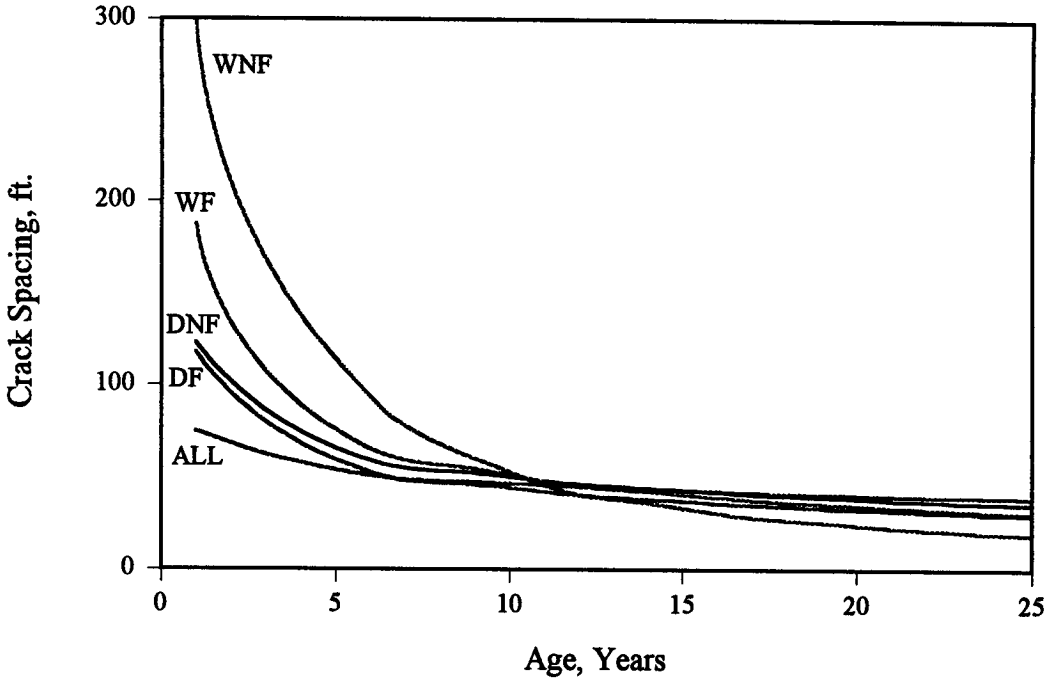

Figure 7.37. Predicted Transverse Crack Spacing vs. Age for HMAC Pavements Over Granular Base and Full-Depth HMAC

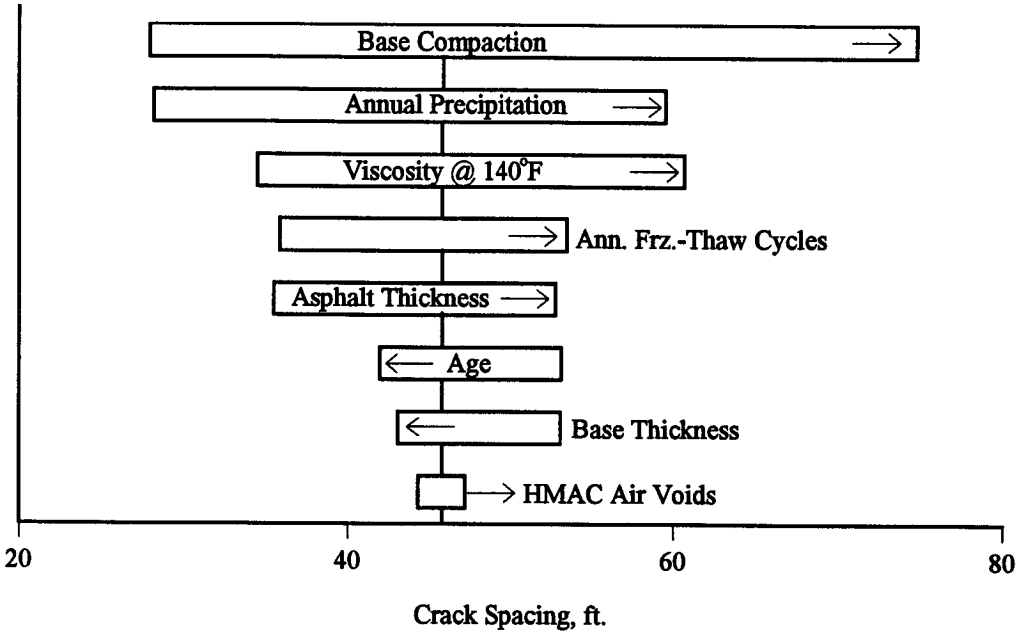

Figure 7.38. Results From Sensitivity Analyses for Transverse Crack Spacing in HMAC Pavements on Granular Base and Full-Depth HMAC Pavements, North American Data Set

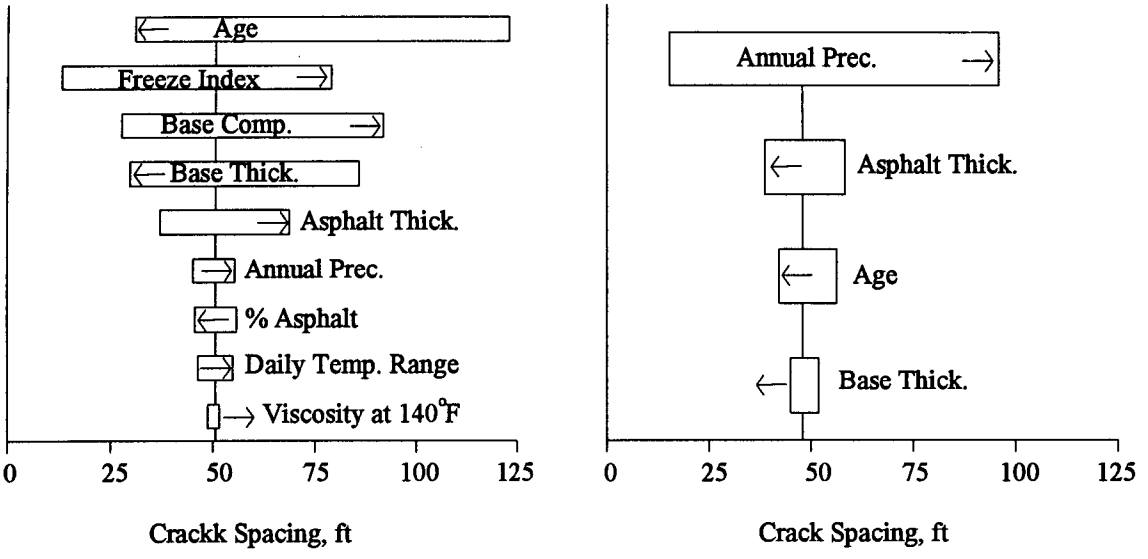

a. Wet-No Freeze Data Set

b. Dry-No Freeze Data Set

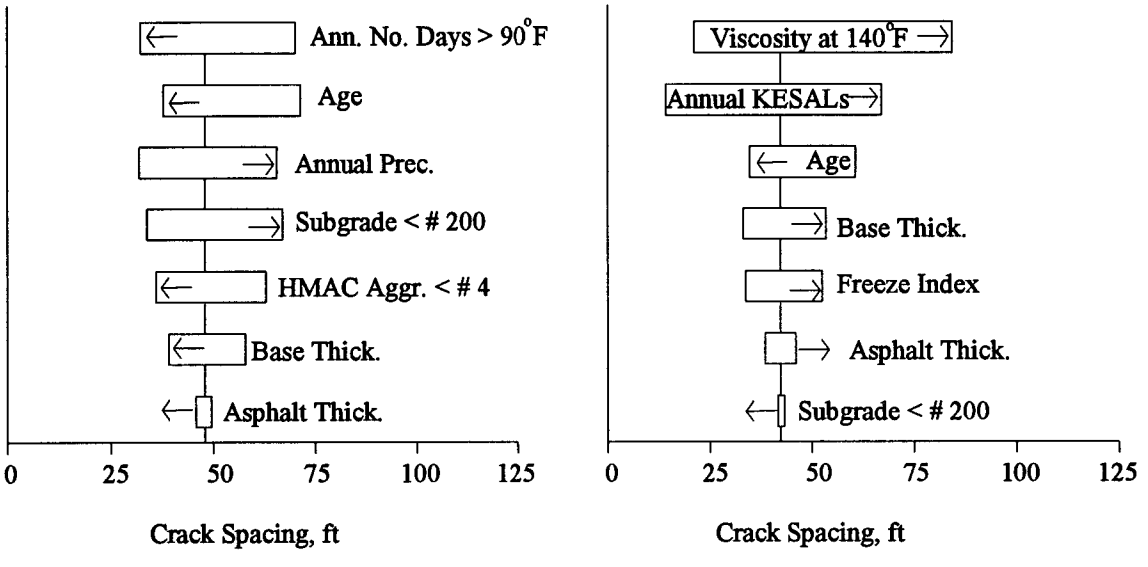

c. Wet-Freeze Data Set

d. Dry-Freeze Data Set

Figure 7.39. Results From Sensitivity Analyses of Transverse Crack Spacing for HMAC Pavements on Granular Base and Full-Depth HMAC Pavements

Table 7.15. Calculated Crack Spacing for Various Combinations of Independent Variable Magnitudes, Dry-Freeze Equation

Independent Variable	Case Numbers													
	1	2	3	4	5	6	7	8	9	10	11	12	13	14
Age	30	10	17	17	10	10	10	10	10	10	10	17	10	10
Annual KESALs	90	90	90	30	90	150	90	90	90	90	90	150	90	90
HMAC Thickness	6	6	6	2	2	10	6	6	6	10	6	10	6	10
Base Thickness	12	12	12	4	12	12	12	12	12	12	20	20	12	4
Asphalt Viscosity	1000	1000	1000	500	1000	1000	2000	500	1000	1000	1000	1000	2000	1000
Subgrade < #200	60	60	60	100	60	60	100	100	20	20	20	60	60	20
Freeze Index	1000	1000	1000	500	1000	1000	1000	1000	1000	1000	1000	1000	1000	1000
Calculated Crack Spacing	56	33	27	7	33	53	32	22	37	44	49	75	66	25

Summary of Sensitivity Analyses for Transverse Cracking in HMAC Pavements

Table 7.16 lists the rankings for the individual independent variables, in terms of relative sensitivities, for each of the five separate models and sensitivity analyses. One column indicates the number of models for which a specific independent variable was found to be significant. The far right column gives average rankings; a rank of 10 was arbitrarily assigned for cases when the variable was not found to be significant and was not included in the model (same logic as for rutting, Table 7.8).

The independent variables are listed below in order of combined rankings. One list is based on average rankings, and one is based on the number of models in which the variable was included:

Rankings by Averages	Ranking by Number of Models Found Significant
Age	Age
Annual Precipitation	HMAC Thickness
HMAC Thickness	Base Thickness
Base Thickness	Annual Precipitation
Asphalt Viscosity	Asphalt Viscosity
Base Compaction	Base Compaction
Freeze Index	Freeze Index
Days With Temp. > 90°F	Subgrade < #200 Sieve
Subgrade < #200 Sieve	Days With Temp. > 90°F
Annual KESALs	Annual KESALs
Annual Freeze-Thaw Cycles	Annual Freeze-Thaw Cycles
HMAC Aggregate < #4 Sieve	HMAC Aggregate < #4 Sieve
Asphalt Content	Asphalt Content
HMAC Air Voids	HMAC Air Voids
Daily Temperature Range	Daily Temperature Range

It can be seen from Table 7.16 that three of the variables appeared in all five models, one appeared in four models, one in three models, three in two models, and seven of the fifteen variables appeared in only one model each. However, the environmental variables are generally correlated with each other, so different combinations may represent the climate in the different environmental zones.

Table 7.16. Orders of Significance for Independent Variables, All Models for Transverse Cracking in HMAC Pavements

Independent Variables	HMAC on Granular Base and Full-Depth HMAC					No. of Models Found Significant	Average Rankings
	All	WNF	WF	DNF	DF		
Annual KESALs	-	-	-	-	2	1	8.4
Air Voids in HMAC	8	-	-	-	-	1	9.6
HMAC Thickness	5	5	7	2	6	All	5.0
HMAC Aggr. < #4	-	-	5	-	-	1	9.0
Asphalt Viscosity	3	9	-	-	1	3	6.6
Asphalt Content	-	7	-	-	-	1	9.4
Base Thickness	7	4	6	4	4	All	5.0
Base Compaction	1	3	-	-	-	2	6.8
Subgrade < #200	-	-	4	-	7	2	8.2
Days > 90°F	-	-	1	-	-	1	8.2
Annual Precipitation	2	6	3	1	-	4	4.4
Freeze Index	-	2	-	-	5	2	7.4
Annual Freeze-Thaw Cycles	4	-	-	-	-	1	8.8
Daily Temp. Range	-	8	-	-	-	1	9.6
Age	6	1	2	3	3	All	3.0

Summary of Sensitivity Analysis Results for HMAC Pavements

Tables 7.8, 7.13, and 7.16 list rankings for individual independent variables, in terms of relative sensitivities, for rutting, change in roughness, and transverse cracking, respectively. Much more detail for individual pavement types and environmental zones has been provided earlier in this chapter.

The twelve most significant variables from the sensitivity analyses for HMAC pavements are listed below by distress type, in order of relative ranking with the most significant variable at the top and the least at the bottom:

Rutting	Change in Roughness	Transverse Cracking
KESALs	KESALs	Age
Air Voids in HMAC	Asphalt Viscosity	Annual Precipitation
HMAC Thickness	Days With Temp. > 90°F	HMAC Thickness
Base Thickness	HMAC Thickness	Base Thickness
Subgrade < #200 Sieve	Base Thickness	Asphalt Viscosity
Days With Temp. > 90°F	Freeze Index	Base Compaction
HMAC Aggregate < #4 Sieve	Subgrade < #200 Sieve	Freeze Index
Asphalt Viscosity	Air Voids in HMAC	Days With Temp. > 90°F
Annual Precipitation	Base Compaction	Subgrade <#200 Sieve
Freeze Index	Annual Precipitation	KESALs
Base Compaction	Daily Temp. Range	Annual Freeze-Thaw Cycles
Average Annual Min. Temp.	Annual Freeze-Thaw Cycles	HMAC Agg. <#4 Sieve

It can be seen that nine of these variables are significant for all three distress types. The following are exceptions:

- Air voids in HMAC was not significant for transverse cracking.
- HMAC aggregate passing a #4 sieve was not significant for change in roughness.
- Annual number of freeze-thaw cycles was not significant for rutting.
- Average annual minimum temperature and daily temperature range were significant only for rutting and change in roughness, respectively.

It can also be seen that four environmental variables were found to be significant for rutting, five for change in roughness, and four for transverse cracking.

Some recommendations and comments that result from the sensitivity analyses follow:

- The majority of the rutting occurred for these pavements right after the pavement was opened to traffic; however, these pavements do not represent cases in which deterioration has advanced; water is entering the base, subbase, and subgrades; and the rate of rutting is increasing rapidly.

- It is important not to overcompact HMAC, because this will reduce the air flow through the mix, which appears to result in early hardening that stiffens the mix and substantially reduces the rate of compaction under traffic. (It is also important to get sufficient compaction so that the early compaction under traffic is not excessive.)

- The HMAC aggregate passing a #4 sieve was selected to represent the effects of gradation. Within its inference spaces in the separate data sets, increasing amounts of aggregate passing a #4 sieve appeared beneficial to reducing rutting.

- As expected, traffic loading is the strongest contributor to the occurrence of rutting and roughness, and pavement age had the strongest effect on transverse cracking.

- Thicker HMAC surfaces and granular base layers may be expected to generally decrease all three types of distress (again expected).

There are some results that are difficult to explain. For example, Figures 7.38 and 7.39 indicate that increasing base compaction, annual precipitation, asphalt viscosity, or annual freeze-thaw cycles (or freeze index) tends to increase transverse crack spacing (reduce cracking). These results are difficult to understand and cannot be explained entirely in terms of reliabilities of the equations, because the regional equations had fairly good statistics.

In summary, most results from the sensitivity analyses appear reasonable; however, others are surprises that may (1) have resulted from the specific characteristics of the data sets upon which they are based, (2) represent mechanisms we do not yet understand, or (3) result from interactions not explained by the equation forms.

8

Predictive Models for Distress Types and Results of Sensitivity Analyses for Portland Cement Concrete Pavements

Similar to the work described in the previous chapter, a major part of this study was the development of predictive models for key concrete pavement distress types and roughness indicators. The methodology used to select the significant data elements considered in the development of the models, the initial data exploratory analysis to assemble the data into the appropriate sets for analysis, and the model development procedure used for concrete pavements have been discussed in the previous chapters. The approach used to perform a sensitivity analysis on each of these models has also been described. The results obtained from these activities for portland cement concrete (PCC) pavements are presented in this chapter.

Predictive models were developed for ten key distress and roughness indicators, and sensitivity analyses were conducted on each of them individually. The models include joint faulting of doweled and non-doweled joints; transverse cracking of jointed plain concrete pavement (JPCP); transverse crack deterioration of jointed reinforced concrete pavement (JRCP); joint spalling of JPCP and JRCP; and International Roughness Index (IRI) of doweled JPCP, and non-doweled JPCP, JRCP, and continuously reinforced concrete pavement (CRCP). The development of these models and the results of the sensitivity analyses conducted to show the relative effects of the explanatory variables on the distress and roughness indicators are described. The development of the first model, joint faulting of doweled pavements, is described in detail to illustrate more fully the general approach used (described in Chapter 6). All the prediction models are based on nationwide data obtained from the Strategic Highway Research Program (SHRP) Long-Term Pavement Performance (LTPP) Database. Because of the limited amount of data available for this early concrete pavement analysis, regional models could not be developed.

Joint Faulting of Doweled Concrete Pavements

Faulting of doweled transverse joints of concrete pavements contributes greatly to longitudinal roughness, and thus to user discomfort and the needs for rehabilitation. It is directly related to water pumping and the erosion of the material beneath the slab and/or treated base. Another contributing factor is poor load transfer across the joint. Previous studies have shown that the faulting of doweled joints is controlled so much by dowels that other factors have much less effect[9]. These factors were all taken into account in the development of the model.

Database, Dependent Variables, And Explanatory Variables

Data on the pavement sections with doweled joints from both General Pavement Studies (GPS)-3 (JPCP) and GPS-4 (JRCP) experiments were combined to provide the initial database used for this model. The mean faulting of all doweled joints in a pavement section, FAULTD, was the dependent variable used in the prediction model. The potential explanatory variables initially selected for consideration were chosen from those identified by experts to be significant as described in Chapter 2, provided they were available in the LTPP Database. The explanatory variables that were initially considered are as follows:

THICK:	slab thickness, in.
EPCC:	slab modulus of elasticity, psi (laboratory measured)
PCCAGG:	gradation of aggregate in concrete
BASETYP:	base type (0 = untreated aggregate; 1 = treated aggregate)
BASETHK:	base thickness, in.
BCOMP:	percentage of compaction of base
BAGG:	coarse aggregate gradation of base
CESAL:	cumulative 18,000-lb. (80N) equivalent single axle loads (ESALs) in traffic lane, millions
AGE:	time since construction, years
JTSPACE:	mean transverse joint spacing, ft
JEFF:	falling weight deflectometer (FWD) measured joint efficiency, %
DOWDIA:	diameter of dowels in transverse joints, in.
EDGESUP:	edge support (1 = tied concrete shoulder; 0 = any other shoulder type)
DRAIN:	drainage provisions (0 = no subdrainage; 1 = subdrainage)
SUBGRADE:	subgrade soil classification (0 = fine grained; 1 = coarse grained)
KSTATIC:	static backcalculated k-value, psi/in.
PM200:	subgrade soil passing #200 sieve, %
PRECIP:	average annual precipitation, in.
DAYS32:	number of days/year with temperature less than 32°F (0°C)
DAYS90:	number of days/year with temperatures greater than 90°F (32°C)
FT:	number of air freeze-thaw cycles

TRANGE: mean monthly temperature range (mean maximum daily temperature minus mean minimum daily temperature for each month averaged over the year), °F

Since there were very little data for several of these variables in the database, it was not possible to consider all of them (e.g., PCCAGG, BAGG, BCOMP). In addition, the maximum dowel/concrete bearing stress (BSTRESS, psi), which had been determined to be a cluster variable that influences faulting, was considered. It was calculated for each section by using the conventional Bradbury approach and the data for the above inputs and an assumed 9000 lb (40 kN) load located at the corner directly over one dowel.[7] However, BSTRESS was found to correlate strongly with dowel diameter as shown in Table 8.1, so only dowel diameter was considered in the analysis.

Data Review and Evaluation

The data for each section were reviewed to determine if any data expected to be significant were missing. Examples of data missing from some test sections included joint faulting, CESALs, joint spacing, and FWD data. The pavement sections with such data missing were not used in this early analysis. Data exploration started with a determination of the mean, minimum, maximum, and standard deviation of each dependent and independent variable. All data were then assembled into a matrix and sorted several ways including increasing faulting, increasing age, and increasing traffic. These results were studied and any abnormalities or obviously erroneous data were identified.

Two-dimensional scatter plots of all variables were prepared and examined. Some of these plots are shown as examples in Figures 8.1, 8.2, and 8.3. Figure 8.3 is of special interest since it contains mostly climatic variables. The results show that several of the climatic variables correlate well with each other, as also indicated in the correlation matrix, Table 8.1. For example, TRANGE and DAYS32 correlate very strongly with each other. There is also a strong correlation among the temperature variables, and some of the temperature variables also correlate well with PRECIP. Other variables that show some correlation with FAULTD include AGE, KSTATIC, JTSPACE, and CESAL.

Three-dimensional plots of the raw data were also directly generated to help show the general trends of FAULTD with AGE, CESAL, and other variables. Examples of two such plots are given in Figures 8.4 and 8.5. Figure 8.4 shows the relationship among FAULTD, CESAL, and AGE. This plot also shows an obvious area with no data in the CESAL—AGE plane. Figure 8.5 shows the relationship among FAULTD, JTSPACE, and CESAL. A number of sharp peaks in the generated surface point to abrupt variations in data that require further investigation. The pavement sections causing such unusual peaks or reverse slopes were identified.

Table 8.1. Correlation Matrix for Selected Variables for Doweled Joint Faulting

	CESAL	BSTRESS	JTSPACE	KSTATIC	AGE	FI	PRECIP	TRANGE	OPENING	DAYS32	THICK	EDGESUP	DRAIN	DOWDIA	FAULTD
CESAL	1.000	-0.118	0.377	-0.158	0.553	-0.025	0.110	0.017	0.349	0.007	0.117	-0.037	-0.071	0.022	0.485
BSTRESS	-0.118	1.000	-0.169	0.234	-0.151	-0.183	0.079	-0.255	-0.175	-0.240	-0.621	-0.265	0.347	-0.849	-0.024
JTSPACE	0.377	-0.169	1.000	-0.251	0.549	-0.182	0.357	-0.059	0.950	-0.125	-0.011	0.159	-0.282	0.004	0.399
KSTATIC	-0.158	0.234	-0.251	1.000	-0.403	-0.155	-0.143	-0.191	-0.283	-0.031	0.223	0.129	0.140	0.086	-0.224
AGE	0.553	-0.151	0.549	-0.403	1.000	-0.105	0.305	0.043	0.493	-0.079	-0.039	-0.073	-0.369	-0.132	0.523
FI	-0.025	-0.183	-0.182	-0.155	-0.105	1.000	-0.516	0.790	-0.057	0.859	-0.187	-0.323	-0.099	0.201	-0.129
PRECIP	0.110	0.079	0.357	-0.143	0.305	-0.516	1.000	-0.621	0.220	-0.627	0.171	-0.010	0.018	-0.200	0.283
TRANGE	0.017	-0.255	-0.059	-0.191	0.043	0.790	-0.621	1.000	0.130	0.907	-0.215	-0.193	-0.320	0.142	-0.080
OPENING	0.349	-0.175	0.950	-0.283	0.493	-0.057	0.220	0.130	1.000	0.014	-0.059	0.165	-0.330	0.002	0.327
DAYS32	0.007	-0.240	-0.125	-0.031	-0.079	0.859	-0.627	0.907	0.014	1.000	-0.156	-0.230	-0.183	0.220	-0.151
THICK	0.117	-0.621	-0.011	0.223	-0.039	-0.187	0.171	-0.215	-0.059	-0.156	1.000	0.397	-0.020	0.575	0.041
EDGESUP	-0.037	-0.265	0.159	0.129	-0.073	-0.323	-0.010	-0.193	0.165	-0.230	0.397	1.000	-0.015	0.329	-0.120
DRAIN	-0.071	0.347	-0.282	0.140	-0.369	-0.099	0.018	-0.320	-0.330	-0.183	-0.020	-0.015	1.000	-0.175	-0.159
DOWDIA	0.022	-0.849	0.004	0.086	-0.132	0.201	-0.200	0.142	0.002	0.220	0.575	0.329	-0.175	1.000	-0.177
FAULTD	0.485	-0.024	0.399	-0.224	0.523	-0.129	0.283	-0.080	0.327	-0.151	0.041	-0.120	-0.159	-0.177	1.000

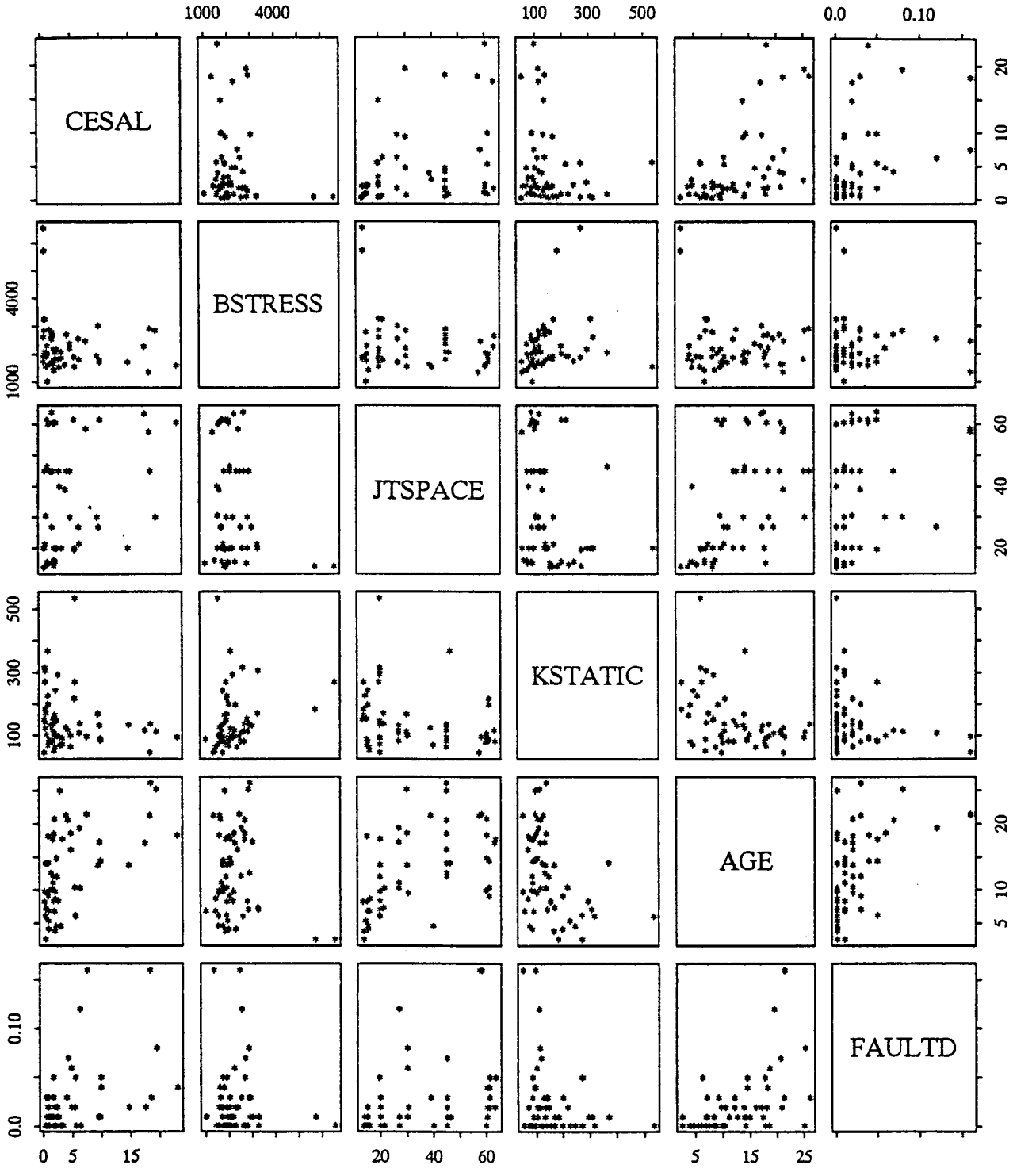

Figure 8.1. Two-Dimensional Plots of Selected Design Variables for Doweled Joint Faulting

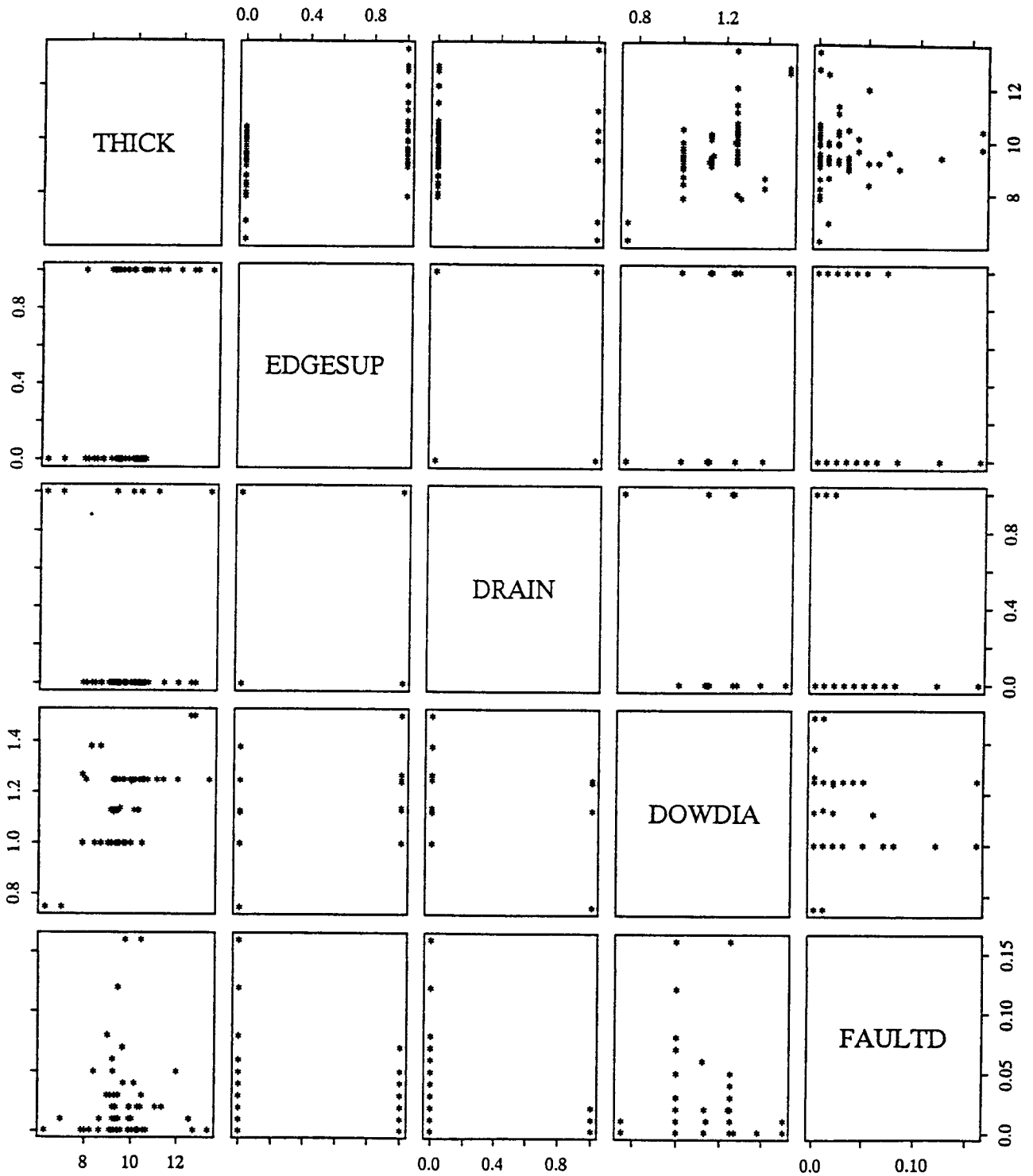

Figure 8.2. Two-Dimensional Plots of Additional Design Variables for Doweled Joint Faulting

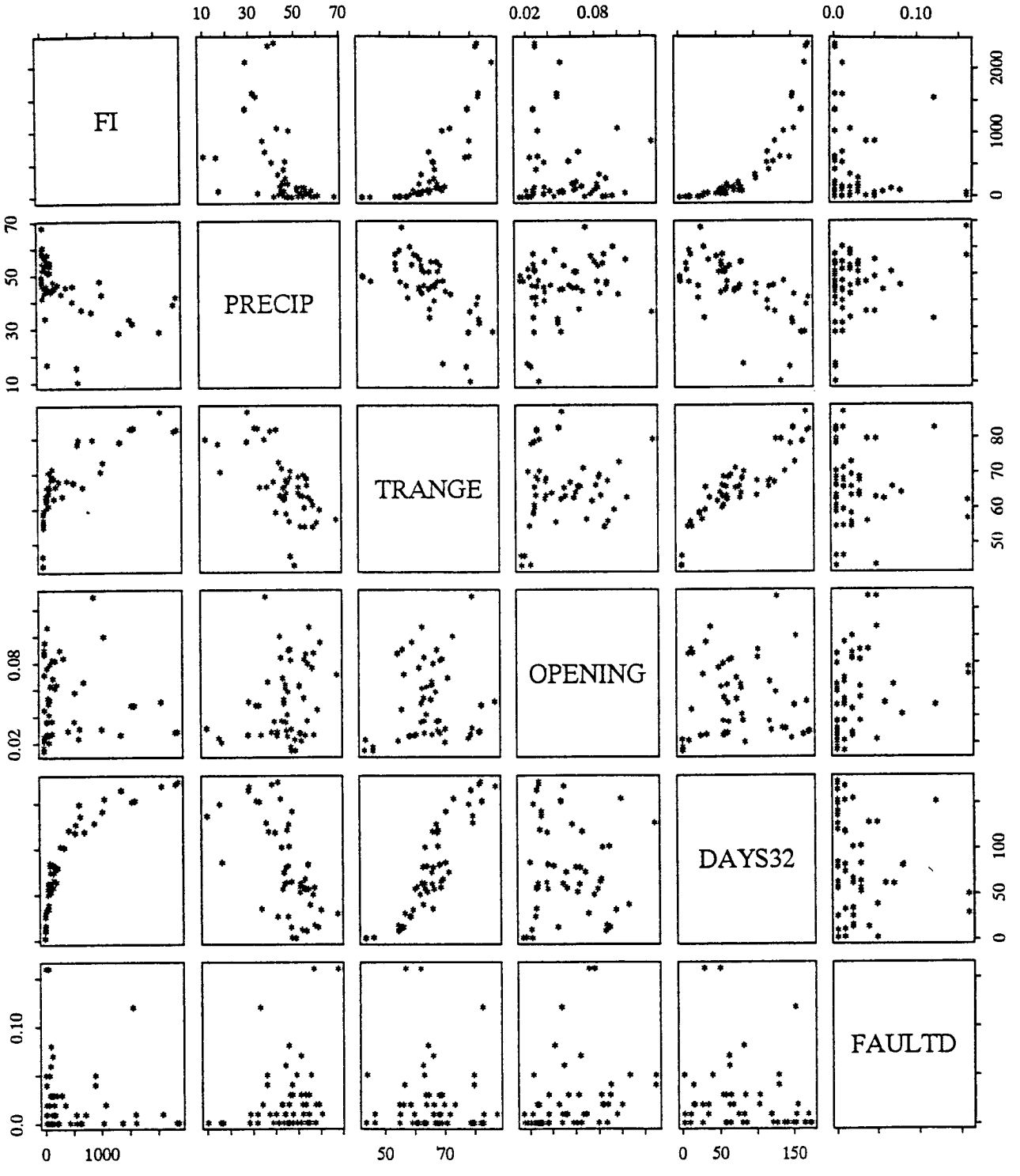

Figure 8.3. Two-Dimensional Plots of Selected Climatic Variables for Doweled Joint Faulting

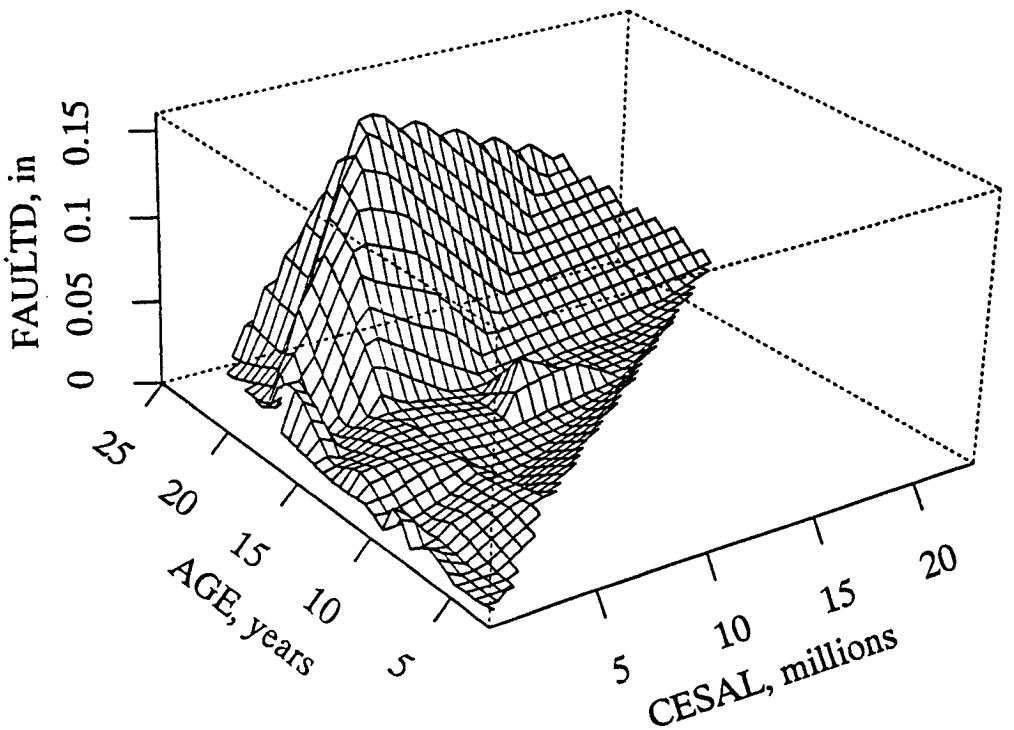

Figure 8.4. Three-Dimensional Plot (FAULTD, AGE, CESAL) of Doweled Joint Faulting

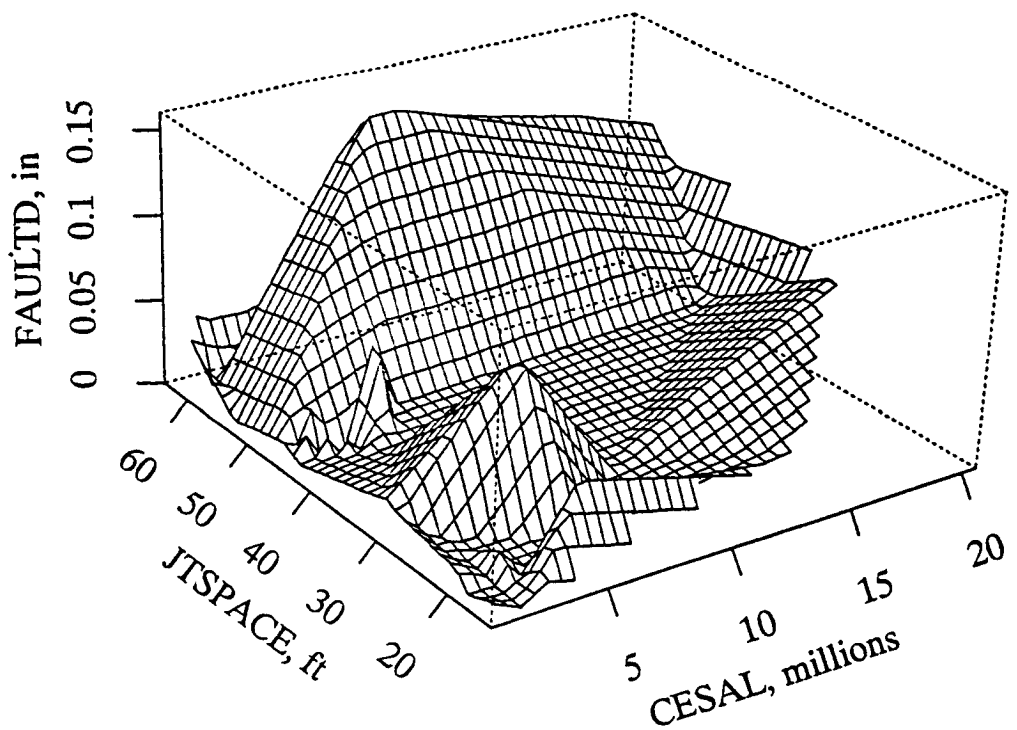

Figure 8.5. Three-Dimensional Plot (FAULTD, JTSPACE, CESAL) of Doweled Joint Faulting

Based on all these results, specific sections were identified that had missing, erroneous, or questionable data. The sections with missing and erroneous data were deleted, and those with questionable data were marked for observation and evaluation during the actual model development. These data reviews provided valuable understanding of the data and the type of relationships among variables that needed to be explored in detail. Fifty-nine pavement sections remained for model development after the data review and evaluation.

Model Development

The first step in model development for transverse dowel joint faulting was to identify the general functional form of the distress with respect to time and traffic. Previous studies have shown that faulting increases rapidly with traffic loadings at first, and then levels off at a much decreased rate[9, 10]. In previous studies where time series faulting data were available, the following model form that meets this criteria has been used.

$$FAULTD = CESAL^{P} * [\text{Explanatory Variables}] \quad (8.1)$$

This form of the model meets logical boundary conditions with the faulting equal to zero when CESAL is zero (i.e., prior to opening to traffic). The exponent P is usually less than 1. To allow the use of linear regression techniques, this form of the model was transformed by dividing both sides of the equation by $CESAL^{P}$, to make the ratio $FAULTD/CESAL^{P}$ the dependent variable. Other transformations of the model, such as a logarithmic transformation, were tried but did not improve results.

Based on expert judgment and previous data observations, several explanatory variables were selected for testing in the above model. Regression analyses were conducted with a variety of techniques to develop the most useful faulting prediction model. The following briefly describe the techniques used in the analyses:

- Many explanatory variables were tested to determine their actual significance in the overall model. Even though some of these variables were expected to have an effect on faulting, they were eliminated if they were not significant to the prediction of joint faulting.

- Several interactions between the variables were evaluated and found not to be significant.

- Tests for collinearity between explanatory variables were conducted throughout the development phase. When significant collinearity was found, one of the variables was eliminated from the model (except for AGE, which is explained below).

- The two- and three-dimensional plots were studied, and these studies indicated that some variables were not linearly related to faulting. These included CESAL, KSTATIC, JTSPACE, and AGE. The best exponents for these variables were determined by using the Alternating Conditional Expectations (ACE) algorithm introduced by Breiman and Friedman along with the Box-Cox transformation. Detailed descriptions of these techniques are provided in "Design of Joints in Concrete Pavements."[7]

The final model for transverse joint faulting is as follows:

$$FAULTD = CESAL^{0.25} * \left[0.0238 + 0.0006 * \left(\frac{JTSPACE}{10} \right)^2 + 0.0037 * \left(\frac{100}{KSTATIC} \right)^2 + 0.0039 * \left(\frac{AGE}{10} \right)^2 - 0.0037 * EDGESUP - 0.0218 * DOWDIA \right] \quad (8.2)$$

where FAULTD = mean transverse doweled joint faulting, in.
CESAL = cumulative 18,000 lb. (80N) ESALs in traffic lane, millions
JTSPACE = mean transverse joint spacing, ft
KSTATIC = mean backcalculated static k-value, psi/in.
AGE = age since construction, years
EDGESUP = edge support (1-tied concrete shoulder; 0-any other shoulder type)
DOWDIA = diameter of dowels in transverse joints, in.

Statistics:
N = 59 sections
R^2 = 0.534
RMSE = 0.028 in. (0.7 mm)

Figure 8.6 shows a plot of the predicted versus actual faulting for this model, and Figure 8.7 shows a plot of the residuals versus predicted faulting. A sensitivity analysis of the model was conducted with the procedures described in Chapter 6. The results in Figure 8.8 show that CESALs, joint spacing, age, and the static k-value have the greatest effects on doweled joint faulting, and increases in the significant variables appear to result in logical increases or decreases in the dependent variable.

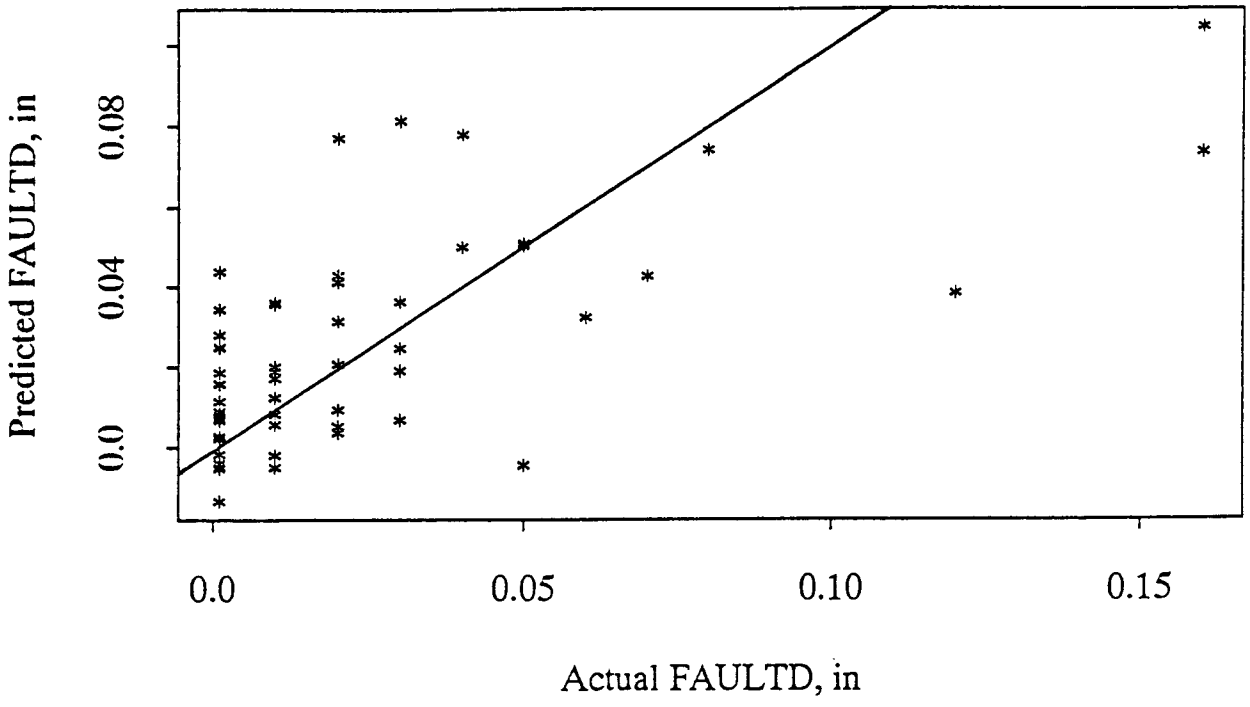

Figure 8.6. Predicted FAULTD vs. Actual FAULTD

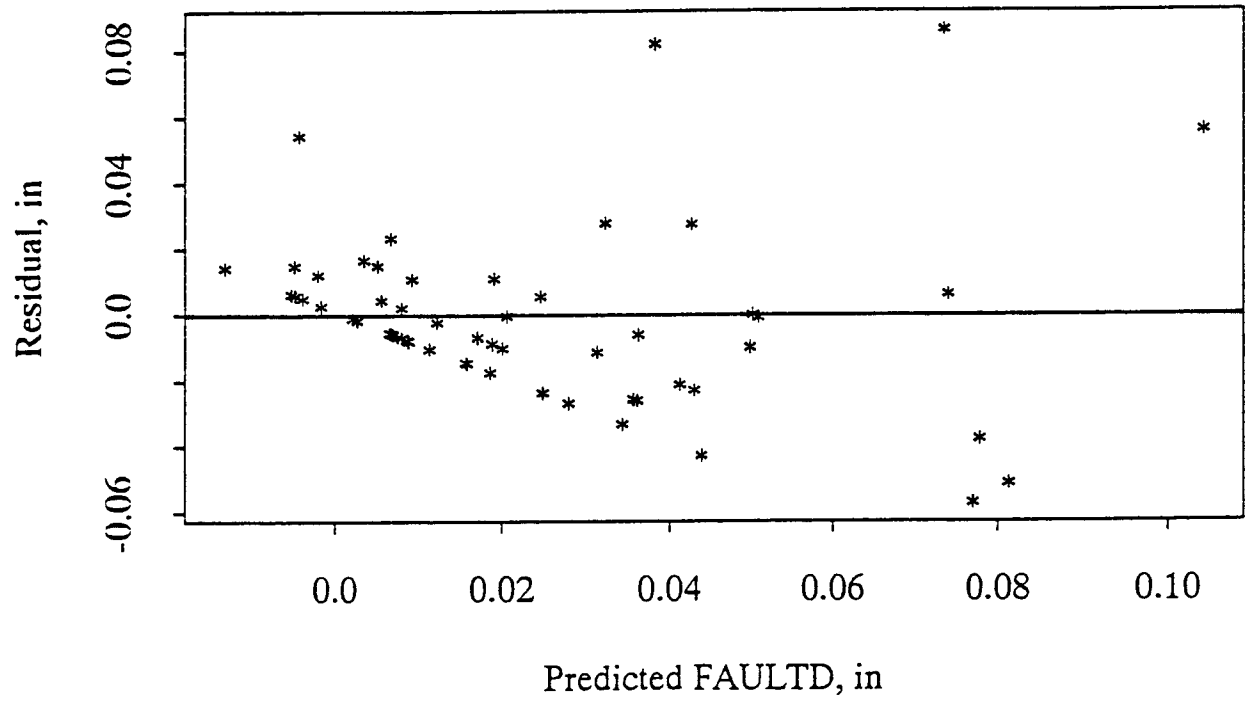

Figure 8.7. Plot of Residuals vs. Predicted FAULTD

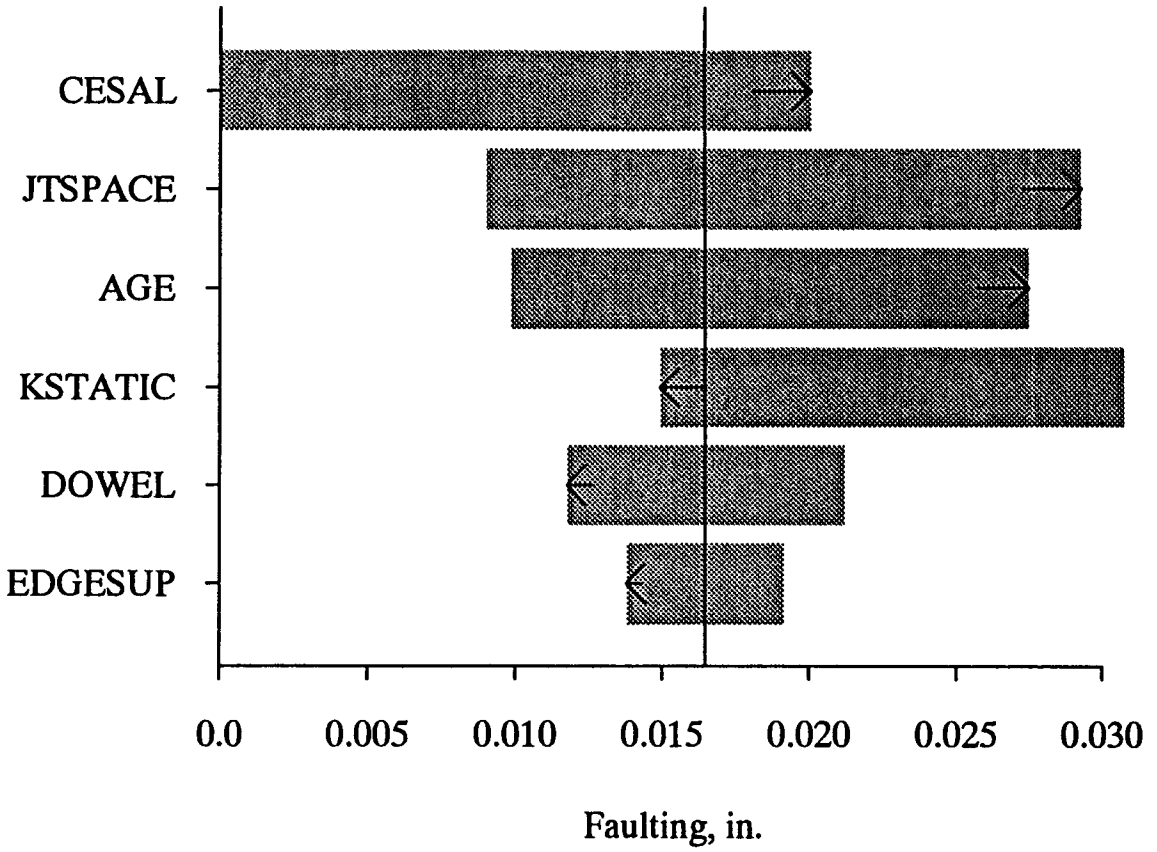

Figure 8.8. Sensitivity Analysis for Doweled Joint Faulting Model

Predicted faulting increases with increasing CESALs, joint spacing, and age. An increase in static k-value, which shows the effect of subgrade stiffness on the development of faulting, results in a decrease in faulting. Edge support provided by a tied concrete shoulder also causes a slight reduction in faulting. In addition, faulting decreases as dowel diameter increases, which reflects the reduction in dowel/concrete bearing stress brought about by the use of the larger dowels.

Three-dimensional plots of the response surface of this model, generated to show the predicted relationship between faulting and CESALs and age, and joint spacing are shown in Figures 8.9 and 8.10. As CESALs increase, faulting increases rapidly at first and then the rate of increase decreases. Faulting also increases with age and as joint spacing increases.

Although AGE and CESAL were found to be positively correlated with a coefficient of correlation of 55%, AGE was included in the model due to its apparent strong individual effect. It is believed that AGE reflects the effects of the cycles of climatic changes such as joint opening/closing and thermal curling cycles. None of the climatic variables were significant enough to appear in the doweled faulting model itself.

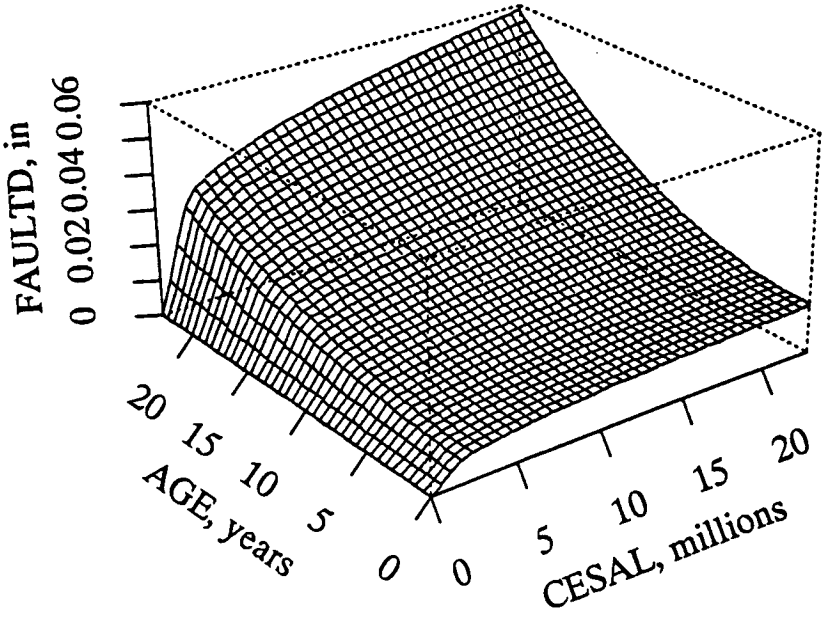

Figure 8.9. Three-Dimensional Plot (FAULTD, AGE, CESAL) of Doweled Joint Faulting Model

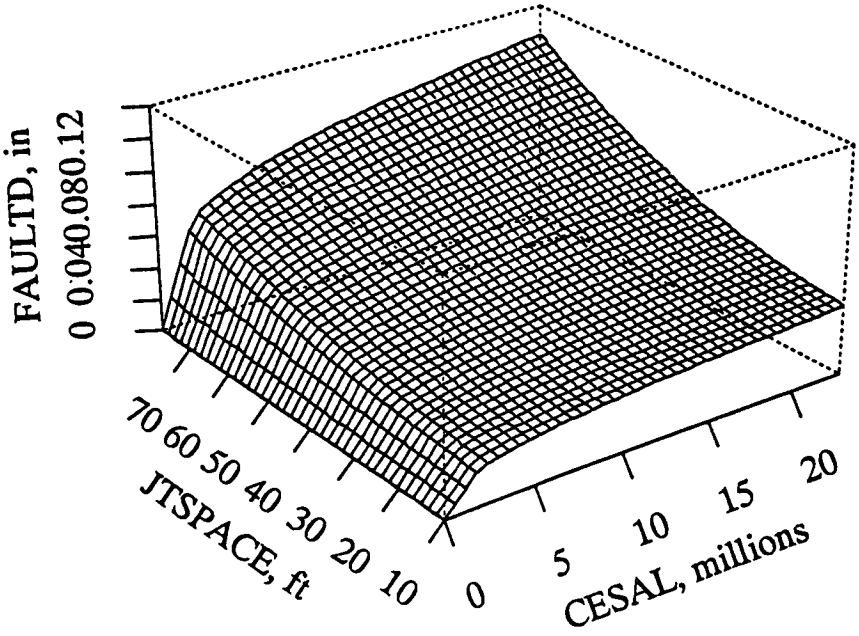

Figure 8.10. Three-Dimensional Plot (FAULTD, JTSPACE, CESAL) of Doweled Joint Faulting

The model includes several variables known from previous studies to affect faulting and the effects of these variables appear logical. However, there are several potentially significant variables that are missing from the model. For example, base type (untreated versus treated) and climate did not show much significance, although they were expected from previous studies to be significant. With a coefficient of determination (R^2) of only 0.53 and root mean square error (RMSE) of 0.028 inches (0.7 mm), there is considerable room for improvement of this model.

Joint Faulting of Non-Doweled Concrete Pavements

The phenomenon of faulting of non-doweled transverse joints is similar to that described in the preceding section for doweled joints. Faulting of non-doweled joints also contributes greatly to longitudinal roughness and thus to user discomfort. Several factors that have been shown in previous studies to influence the faulting of non-doweled joints include traffic, design, materials, and climatic factors.[9] Faulting is directly related to water pumping and erosion of the support material beneath the slab and/or treated base of a concrete pavement. Another major contributing factor to non-doweled joint faulting is poor load transfer across the joint, since aggregate interlock is often the only medium of load transfer available. Faulting of non-doweled joints, therefore, depends much more on several other variables, such as climate and base type. The general procedure outlined in Chapter 6 for model development was used to obtain the non-doweled joint faulting model described here.

Database, Dependent Variables, and Explanatory Variables

The initial database used for this model was obtained from all the pavement sections with non-doweled joints from the GPS-3 (JPCP) experiment. The mean faulting of all non-doweled joints in a pavement section, FAULTND, was the dependent variable used in the model. Potential explanatory variables were chosen as those identified by the experts to be significant, provided they were available in the LTPP Database. The initial explanatory variables that were considered are as follows:

THICK:	slab thickness, in.
EPCC:	modulus of elasticity of PCC from laboratory testing, psi
PCCAGG:	gradation of aggregate in concrete
BASETYP:	base type (0 = untreated aggregate; 1 = treated aggregate)
BASETHK:	base thickness, in.
BCOMP:	percentage of compaction of base
BAGG:	coarse aggregate gradation of base
CESAL:	cumulative 18,000 lb. (80kN) ESALs in traffic lane, millions
AGE:	time since construction, years
JTSPACE:	mean transverse joint spacing, ft

JEFF:	FWD-measured joint efficiency, %
EDGESUP:	edge support (1 = tied concrete shoulder; 0 = any other shoulder type)
DRAIN:	drainage provisions (0 = no subdrainage, 1 = if subdrainage)
SUBGRADE:	subgrade soil classification (0 = fine grained; 1 = coarse grained)
KSTATIC:	static backcalculated k-value, psi/in.
PM200:	subgrade soil passing #200 sieve, %
DAYS90:	number of days/year with temperatures greater than 90°F (32°C)
PRECIP:	average annual precipitation, in.
FT:	number of air freeze-thaw cycles
TRANGE:	mean monthly temperature range (mean maximum daily temperature minus mean minimum daily temperature for each month averaged over the year), °F
FI:	freeze index, degree-days below freezing

Since there were very little data for several of these variables (e.g., PCCAGG, BAGG, BCOMP, PM200) in the database, it was not possible to consider all of them in the model development.

Data Review and Evaluation

The data from the GPS-3 test sections were reviewed to determine if data expected to be significant were missing. Examples of data missing for some test sections included joint faulting, CESALs, joint spacing, and FWD data. These sections with missing data could not be used in this early analysis. Data evaluation included an examination of the mean, minimum, maximum, and standard deviation of each dependent and independent variable. These values appear in SHRP-P-684, Early Analyses of LTPP General Pavement Studies Data, Data Processing and Evaluation.

The data were also assembled into matrix form and sorted several ways, such as increasing faulting, increasing age, and increasing traffic, and studied in order to identify any abnormalities or obviously erroneous data. Bivariate plots of all significant variables were prepared and examined. A correlation matrix was then obtained to show the strength of the correlation between all of dependent and independent variables. This correlation matrix is shown in Table 8.2.

A three-dimensional plot which shows the relationship between faulting, CESALs, and age is given in Figure 8.11. This plot shows there are a few abnormal peaks in the plots that point to abrupt variations in data. The sections causing the unusual peaks or reverse slopes were identified and examined. Twenty-five sections remained for model development after the sections identified as having missing and erroneous data identified were deleted.

Table 8.2. Correlation Matrix for Selected Variables for Non-Doweled Joint Faulting

	CESAL	JTSPACE	KSTATIC	AGE	FI	PRECIP	OPENING	DAYS32	TRANGE	THICK	EDGESUP	BASETHK	DRAIN	FAULTND
CESAL	1.000	-0.042	0.064	-0.060	-0.110	-0.159	-0.020	0.123	0.083	0.164	0.284	-0.531	0.007	-0.019
JTSPACE	-0.042	1.000	0.169	0.364	-0.250	0.643	0.497	-0.279	-0.335	0.031	-0.088	0.008	-0.173	0.131
KSTATIC	0.064	0.169	1.000	0.073	-0.260	0.069	-0.120	-0.109	-0.259	0.175	0.209	0.128	0.033	-0.138
AGE	-0.061	0.364	0.073	1.000	-0.400	0.329	0.069	-0.397	-0.344	0.055	0.020	0.277	-0.118	0.289
FI	-0.105	-0.245	-0.264	-0.400	1.000	0.039	0.122	0.863	0.664	-0.134	-0.028	0.080	-0.086	0.202
PRECIP	-0.159	0.643	0.069	0.329	0.039	1.000	0.153	-0.092	-0.284	-0.132	-0.115	0.113	-0.297	0.459
OPENING	-0.020	0.497	-0.120	0.069	0.122	0.153	1.000	0.263	0.503	-0.002	0.146	-0.111	0.029	-0.127
DAYS32	0.123	-0.279	-0.109	-0.400	0.863	-0.092	0.263	1.000	0.827	-0.035	0.145	-0.084	-0.194	0.159
TRANGE	0.083	-0.335	-0.259	-0.340	0.664	-0.284	0.503	0.827	1.000	0.006	0.176	-0.070	0.047	-0.072
THICK	0.164	0.031	0.175	0.055	-0.130	-0.132	-0.002	-0.035	0.006	1.000	0.204	0.243	0.000	0.075
EDGESUP	0.284	-0.088	0.209	0.020	-0.030	-0.115	0.146	0.145	0.176	0.204	1.000	-0.080	0.071	-0.083
BASETHK	-0.531	0.008	0.128	0.277	0.080	0.113	-0.111	-0.084	-0.070	0.243	-0.080	1.000	-0.062	0.236
DRAIN	0.007	-0.173	0.033	-0.120	-0.090	-0.297	0.029	-0.194	0.047	0.000	0.071	-0.062	1.000	-0.269
FAULTND	-0.019	0.131	-0.138	0.289	0.202	0.459	-0.127	0.159	-0.072	0.075	-0.083	0.236	-0.269	1.000

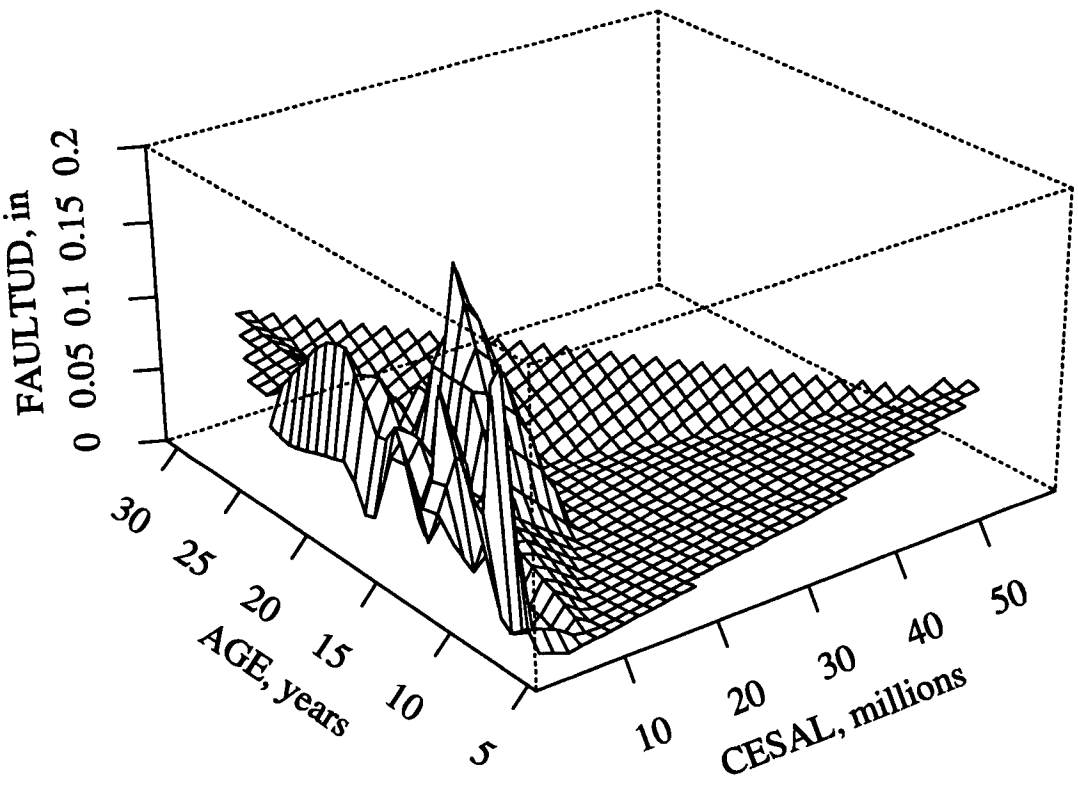

Figure 8.11. Three-Dimensional Plot (e.g., FAULTND, AGE, CESAL) of Doweled Joint Faulting

Model Development

The general functional form identified for faulting of nondoweled joints is the same as the one identified for faulting of doweled transverse joints in Equation 8.2. It shows faulting increasing with traffic loadings at a rapid rate at first and then at a reduced rate as time passes. The model also meets the necessary boundary conditions with faulting equal to zero when CESALs are equal to zero (e.g., prior to opening to traffic). For non-doweled pavements, the exponent P is also usually less than 1 for faulting. In order to use linear regression techniques, both sides of the equation were divided by $CESAL^P$ and the ratio $FAULTND/CESAL^P$ was used as the dependent variable. Other transformations of the data were tried but were not successful in improving the results.

With several explanatory variables selected for testing in the above model, regression analyses were conducted with a variety of techniques to try to develop the most suitable faulting prediction model for sensitivity analysis. The techniques used included the following:

- The explanatory variables were tested to determine their significance in the overall faulting model. Those that were not significant were eliminated, even though they were expected to affect faulting.

- Interactions between the explanatory variables were evaluated, but only the interaction between freeze index and precipitation was found to be significant.

- Tests for collinearity between the explanatory variables were conducted throughout the development phase, and the results were used to identify some of the variables that had to be eliminated from the model.

- The two- and three-dimensional plots were studied, and these studies indicated that there were some variables that are not linearly related to faulting of non-doweled transverse joints. These included CESAL, AGE, and PRECIP. The ACE algorithm was used to determine the best exponents for these variables to use in the model.

The model finally selected for transverse non-doweled joint faulting, based on the data for the JPCP sections of GPS-3, is as follows:

$$FAULTND = CESAL^{0.25} * \left[-0.0757 + 0.0251 * \sqrt{AGE} + 0.0013 * \left(\frac{PRECIP}{10} \right)^2 + 0.0012 * \left(\frac{FI * PRECIP}{1000} \right) - 0.0378 * DRAIN \right] \quad (8.3)$$

where FAULTND = mean transverse non-doweled joint faulting, in.
CESAL = cumulative 18,000 lb. (80kN) ESALs in traffic lane, millions
PRECIP = mean annual precipitation, in.
FI = mean freeze index, degree-days < freezing
AGE = age since construction, years
DRAIN = 1=longitudinal subdrainage; 0=otherwise

Statistics:

N = 25 sections
R^2 = 0.550
RMSE = 0.047 in. (1.2 mm)

The limited number of sections available for the development of this model clearly limits its adequacy. Figure 8.12 shows a plot of the predicted versus actual faulting, and Figure 8.13 shows a plot of the residuals versus predicted faulting. A sensitivity analysis of the model was conducted with the procedures described in Chapter 6. The results are shown in Figure 8.14. The variables that significantly affect the prediction of non-doweled joint faulting include CESALs, age, precipitation, freeze index, and drainage. The senses of these effects (increase in variables increases or decreases faulting) were consistent with results from previous studies and theory[9].

The form of the model produces physically logical predictions of faulting with traffic loadings. Faulting is known to increase rapidly at first, and then level off with continued traffic loadings. In addition, this form matches the boundary conditions of zero faulting at zero traffic loadings. Although AGE and CESALs are strongly correlated, both were kept in the models due to their apparent strong individual effects. It is believed that AGE in this model represents the effects of cycles of climatic changes such as joint opening/closing and thermal curling cycles. The model indicates an increase in faulting with increasing age. A three-dimensional plot of the predicted response surface generated with this model that shows the relationship between FAULTND, AGE, and CESAL is presented in Figure 8.15.

Two climatic variables, precipitation and freeze index, were also sufficiently significant to enter the model. According to the model, increased precipitation will result in increased faulting, and pavements located in areas with a higher freeze index (FI) combined with a higher mean annual precipitation (PRECIP) will experience more faulting. The model also indicates that the provision of subdrainage will decrease faulting. However, it should be noted that most of the non-doweled JPCP sections included in this study did not have subdrainage, and had a high potential for erosion and pumping, especially because they did not have dowels to limit corner deflections. With only five of the sections with subdrainage in the form of longitudinal pipes, the subdrainage variable DRAIN included in the model must be viewed with caution. None of the pavement sections used in this analysis had a permeable base.

The model developed includes several variables known from previous studies[9, 10] to affect faulting, and the senses (increase in variable increases or decreases faulting) appear to be logical. However, there were several variables expected to be significant that were not found to be so. For example, neither base type (untreated versus treated) or joint spacing showed up as significant, even though other studies have shown them to be so. [9, 10] There is much room for improvement of this model, which has an R^2 of 0.55 and a fairly high RMSE.

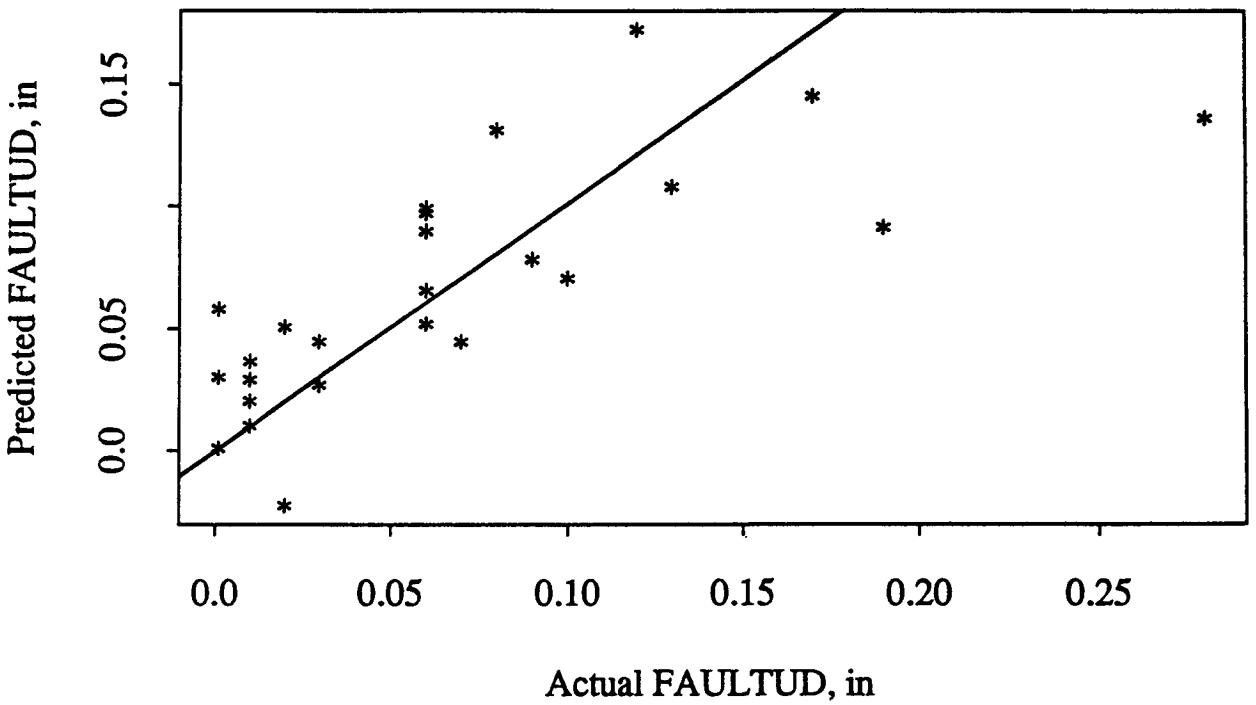

Figure 8.12. Predicted vs. Actual FAULTND

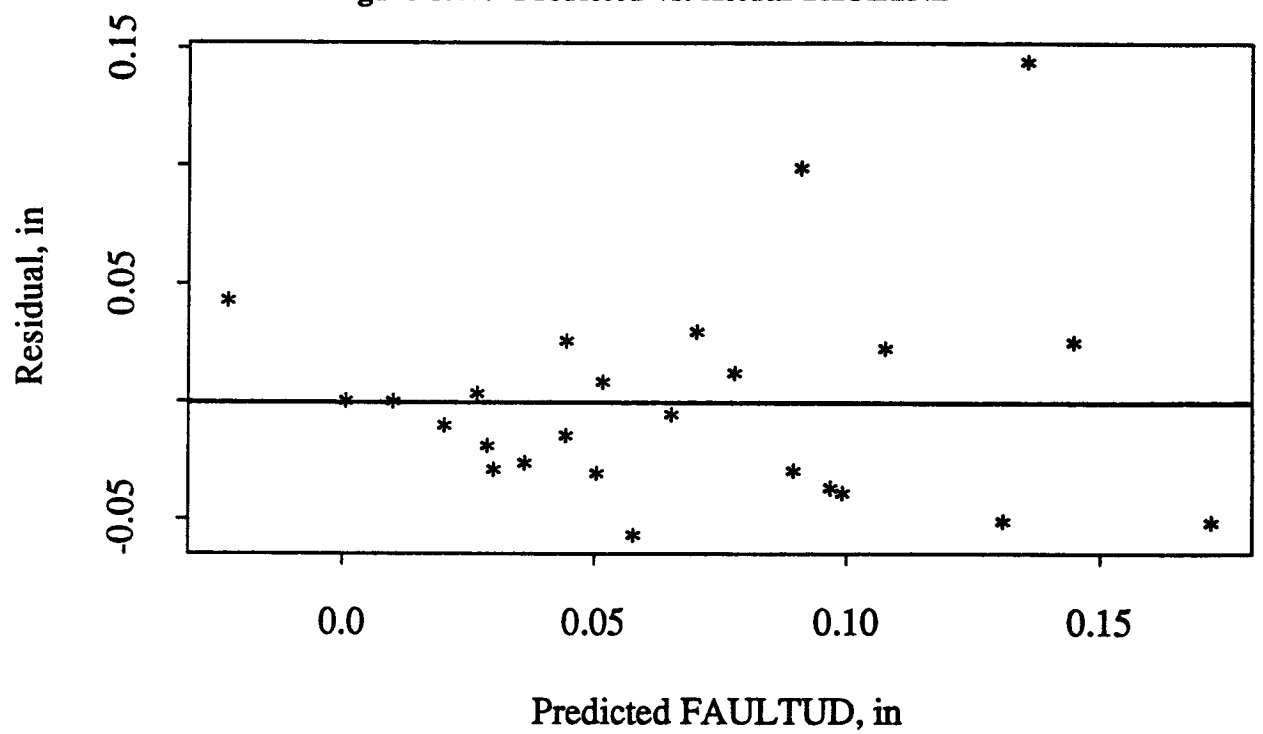

Figure 8.13. Plot of Residuals vs. Predicted FAULTND

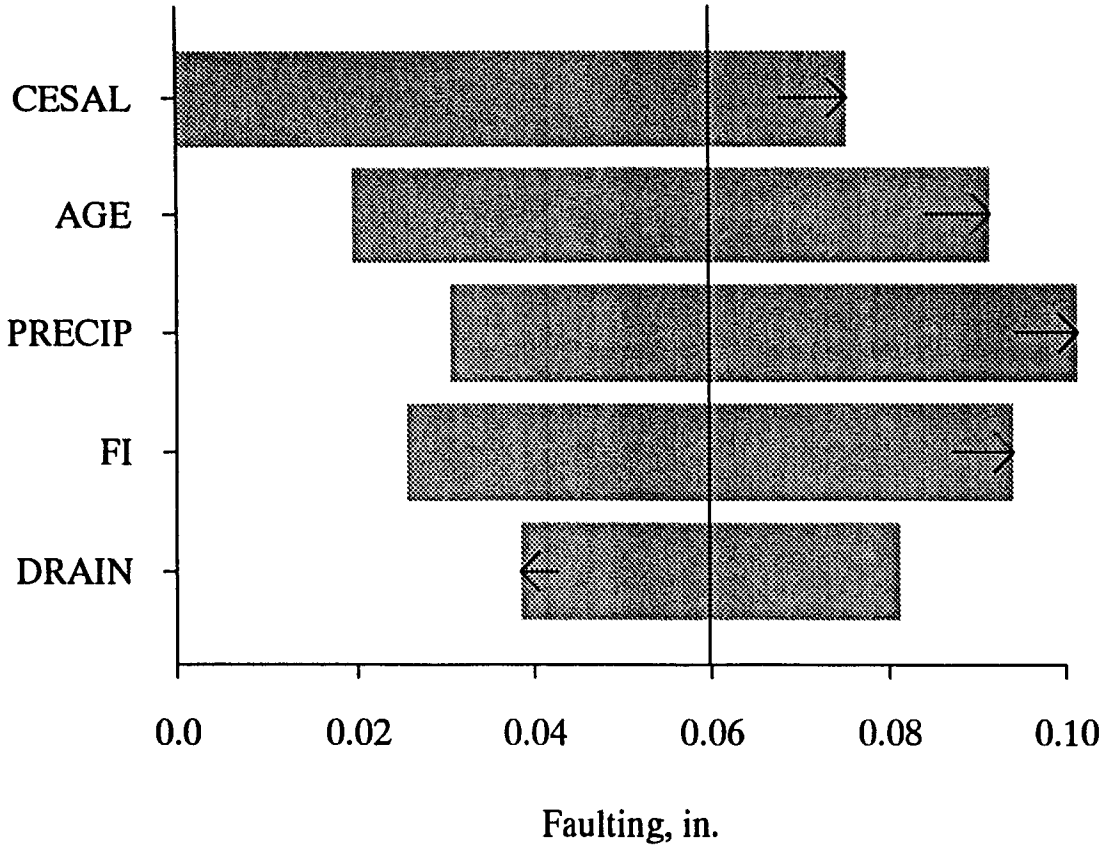

Figure 8.14. Sensitivity Analysis for Non-Doweled Joint Faulting Model

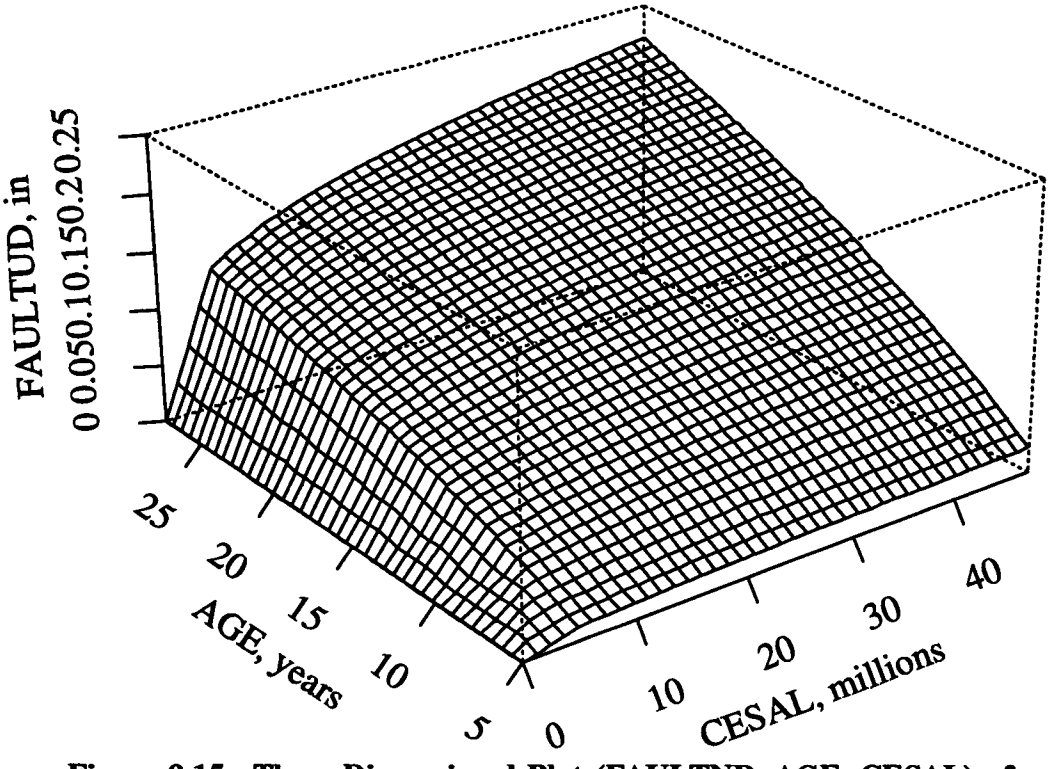

Figure 8.15. Three-Dimensional Plot (FAULTND, AGE, CESAL) of Non Doweled Joint Faulting Model

Transverse Cracking of JPCP

For this study, transverse cracking of JPCP was defined as all severity levels of cracks occurring transversely across the traffic lane. Such transverse cracks eventually spall and fault, and lead to longitudinal profile roughness, user discomfort, and the need for rehabilitation. The general procedure outlined in Chapter 6 for model development had to be modified to obtain a transverse cracking model for JPCP. Since there were only a few sections that contained transverse cracking data, the general approach could not be used to produce a model. However, this opportunity allowed for a demonstration of the development of a more mechanistic type model. The model developed is presented for illustration and must not be used for prediction because of the limited number of sections actually used to develop it.

The mechanistic model is based on the principle that transverse cracking results from fatigue damage brought on by repeated tensile slab stresses. These tensile stresses are caused by a combination of repeated heavy loads, thermal gradient curling, and moisture gradient warping (and perhaps temperature and drying shrinkage). By combining all these variables into a single calculated fatigue damage value over a pavement's service life, the fatigue damage can be related to transverse cracking. This type of approach has been used several times in the past and has produced useful results[9, 11]. The use of this fatigue damage approach is described in this section.

Database, Dependent Variables, and Explanatory Variables

The initial database consisted of sections from the GPS-3 (JPCP) experiment. The percentage of slabs cracked (all severities of cracks) in a pavement section (PCRACKED) was the dependent variable used in the model. All potential explanatory variables identified to be significant by the experts, provided they were available in the LTPP Database and could be included in the mechanistic analysis, were used. The initial explanatory variables that were considered are as follows:

THICK:	slab thickness, in.
PCCSTR:	indirect tensile strength of PCC (cores) converted to flexural strength, psi
EPCC:	modulus of elasticity of PCC measured in the laboratory, psi
JTEFF:	longitudinal lane/shoulder joint load transfer efficiency
JTSPACE:	mean transverse joint spacing, ft
KSTATIC:	static backcalculated k-value, psi/in.
LNWIDTH:	traffic lane width, ft
CESAL:	cumulative 18,000 lb. (80kN) ESALs in traffic lane, millions
TGRAD:	mean temperature gradients through slab for different geographical regions, °F/in. thickness slab
PRECIP:	average annual precipitation, in.

Data Review and Evaluation

The usual review of each of the sections was conducted to determine if any critical data were missing. The sections with such missing data were then eliminated. A comprehensive evaluation of the data and interrelationships was conducted. The goal of this evaluation was to identify data that appeared to be inconsistent with a majority of the data. These sections were not deleted at this stage, but were simply identified as potential errors to be examined further.

The mean, minimum, maximum, and standard deviation of each dependent and independent variable were examined, as were the data that were assembled into a matrix and sorted several ways (increasing PCRACKED, increasing CESALS, and increasing JTSPACE). Bivariate plots of all the variables were examined, and a correlation matrix of all dependent and independent variables was obtained. This correlation matrix is shown in Table 8.3.

Table 8.3. Correlation Matrix for Selected Variables for JPCP Transverse Cracking

	PCRACKED	THICK	PCCSTR	JTSPACE	CESAL	TGRAD	PRECIP	JTEFF	EPCC	KSTATIC
PCRACKED	1	-0.02	-0.06	0.03	0.37	0.01	0.20	-0.05	-0.16	0.13
THICK	-0.02	1	-0.1	0.112	0.036	0.072	0.08	0.079	-0.13	0.201
PCCSTR	-0.06	-0.1	1	-0.441	0.014	0.013	-0.346	0.069	-0.043	0.018
JTSPACE	0.03	0.112	-0.441	1	0.219	0.318	0.532	0.019	0.175	0.031
CESAL	0.37	0.036	0.014	0.219	1	0.332	0.032	-0.006	0.037	0.025
TGRAD	0.01	0.072	0.013	0.318	0.332	1	0.3	0.075	0.243	0.12
PRECIP	0.20	0.08	-0.346	0.532	0.032	0.3	1	-0.059	0.131	0.003
JTEFF	-0.05	0.079	0.069	0.019	-0.006	0.075	-0.059	1	0.025	0.073
EPCC	-0.16	-0.13	-0.043	0.175	0.037	0.243	0.131	0.025	1	-0.203
KSTATIC	0.13	0.201	0.018	0.031	0.025	0.12	0.003	0.073	-0.203	1

These results were studied and any abnormalities or obviously erroneous data were identified. For example, one clear abnormality was a thick 12 in. (305 mm) slab, which was only 5 years old, did not carry very heavy traffic, and had over 50% cracking. It was obvious that the cracking observed was related to construction (such as late joint sawing) and not load fatigue. A total of 128 sections remained for the model development after the sections with missing and erroneous data had been deleted. Only twelve of these sections had experienced any transverse cracking.

Mechanistic Inputs

For the mechanistic-based model developed for transverse cracking of JPCP, the critical stress and fatigue damage had to be calculated for each of the pavement sections. The critical edge stress was calculated to account for the combined effect of loading and positive (daytime) temperature gradient curling. The stress prediction models used are based on finite element analyses and are described in "Mechanistic Design Models of Loading and Curling in Concrete Pavements"[12]. The variables used in the edge stress calculation include slab thickness, modulus of elasticity, Poisson's ratio, slab length, thermal gradients through the slab, subgrade k-value, single axle load at edge of slab and the thermal coefficient of expansion of concrete. Some of these inputs, such as thermal coefficient of expansion of concrete and Poisson's ratio, had to be assumed.

Temperature gradients were based on mean positive gradients during daylight hours. The following values obtained from *Design for Zero-Maintenance Plane Jointed Concrete Pavement*[11] were used in the analysis:

Environmental Zone	Slab Thick (in.)	Mean Annual Thermal Gradient (°F/in. slab)
Non freeze	8	1.40
	9	1.30
	10	1.21
	11	1.11
	12	1.01
Freeze	8	1.13
	9	1.05
	10	0.96
	11	0.87
	12	0.79

(1 in. = 25.4 mm; °F/in. = 0.0458 °C/mm)

With these inputs the free edge stress was calculated and then adjusted for load transfer for a tied concrete shoulder (i.e., approximately 75% deflection transfer, which results in a 15% reduction in edge stress).

Miner's fatigue damage model was used to determine the accumulated damage over the life of each pavement section. Fatigue damage was calculated as follows:

$$\text{Fatigue Damage} = n/N$$

where n = expected number of applied edge stresses considering CESAL loadings and thermal daytime curling

= CESAL * percentage of loads at edge * percentage of trucks in daytime hours (with 5% loads at edge for regular width lanes, and 0.1% for widened traffic lanes assumed; 75% percent trucks assumed in daytime)

N = mean number of allowable edge stress loads that causes slab cracking

$= 10^{\{2.13 *(1/RATIO)^{1.2}\}}$

RATIO = STRESS/STRENGTH

STRESS = f [EPCC, THICK, POISSON'S RATIO, KSTATIC] (computed with finite element techniques described in "Portland Cement Concrete Pavement Evaluation System-COPES".)

STRENGTH = mean 28 day flexural strength, psi (estimated from split tensile strengths of cores taken during LTPP data collection, adjusted to 28 days)

Both n and N were computed for each section in the database in this manner from the time the pavements were opened to traffic to the time when transverse cracking was measured. The ratio n/N was used as the estimated fatigue damage at the slab edge.

Model Building

The first step in builing the model was to identify the general functional form of the occurrence of transverse cracking over time. From field observations, transverse cracking has been shown to develop slowly in pavements during their early life, then increase more rapidly as time passes, and eventually level off as all slabs become cracked. The lower limit of cracking is 0% of slabs cracked, and the maximum amount of cracking is 100% of slabs cracked. Any cracking that occurs very early in a pavement's life is usually the result of inadequate forming of transverse joints or other construction problems.

Two previous studies show that this progression of transverse cracking follows an s-shaped curve with traffic or time.[9, 10] Rehabilitation is usually performed by the time 50% of the slabs have cracked, so most pavements never experience greater than 50% slabs cracked. With percentage of slabs cracked, PCRACKED, as the dependent variable, Figure 8.16 was prepared to show the relationship of percentage of cracked slabs versus accumulated fatigue damage (n/N) on a logarithmic scale.

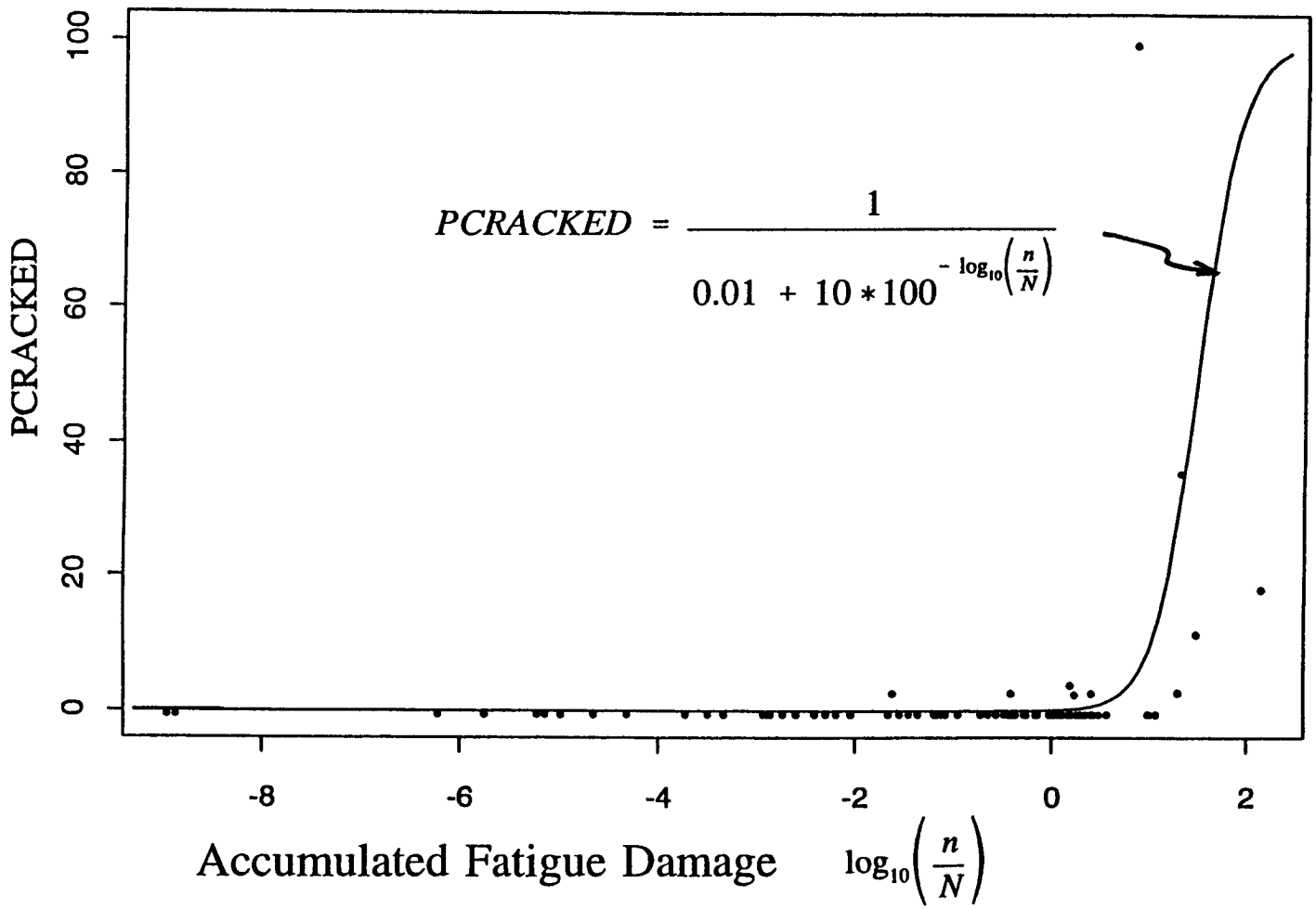

Figure 8.16. Percentage of Slabs Cracked vs. Accumulated Fatigue Damage for JPCP

This plot shows very little cracking for accumulated fatigue damage less than about 1.0. Cracking develops for accumulated fatigue damage beyond 1.0. Although there are a limited number of cracked sections, there exists a general trend that follows the s-shaped curve. Similar results have been obtained in previous studies with far more data than were available for this study.

Conceptually, an s-shaped curve that satisfies the proper boundary conditions should be fitted through this data. However, fitting such a curve by regression techniques was not successful because of the limited number of cracked sections. Therefore, *for illustrative purposes only*, the best s-shaped curve was fitted through the data with a curve-fitting method and is shown in Figure 8.16. The equation of this curve is given below:

$$PCRACKED = \frac{1}{0.01 + 10 * 100^{-\log_{10}\left(\frac{n}{N}\right)}} \qquad (8.4)$$

where

PCRACKED	=	percentage of cracked slabs (all severities)
n	=	expected number of applied edge stresses, considering ESALs and thermal daytime curling
N	=	mean number of allowable edge stress loads that cause slab cracking

The results of a sensitivity analysis of this model are shown in Figure 8.17. Slab thickness (THICK) has by far the greatest effect on transverse cracking, followed distantly by concrete flexural strength at 28 days. This model is based upon too few data points and should only be considered illustrative. As more LTPP data become available, especially sections with more slabs cracked, it will be possible to develop a much more reliable model for predicting transverse slab cracking for JPCP.

Another important point to note is that the fatigue damage calculation algorithm used was not comprehensive. A much more comprehensive fatigue damage analysis can be developed and applied in the future. Such an analysis should consider axle load spectra (not CESALs), increased concrete strength over time, erosion beneath the slab, a far more accurate representation of thermal gradient over a year, and moisture gradients through the slab. Placement of the axle at the slab corner should also be considered along with a negative (nighttime) thermal gradient on transverse cracking.

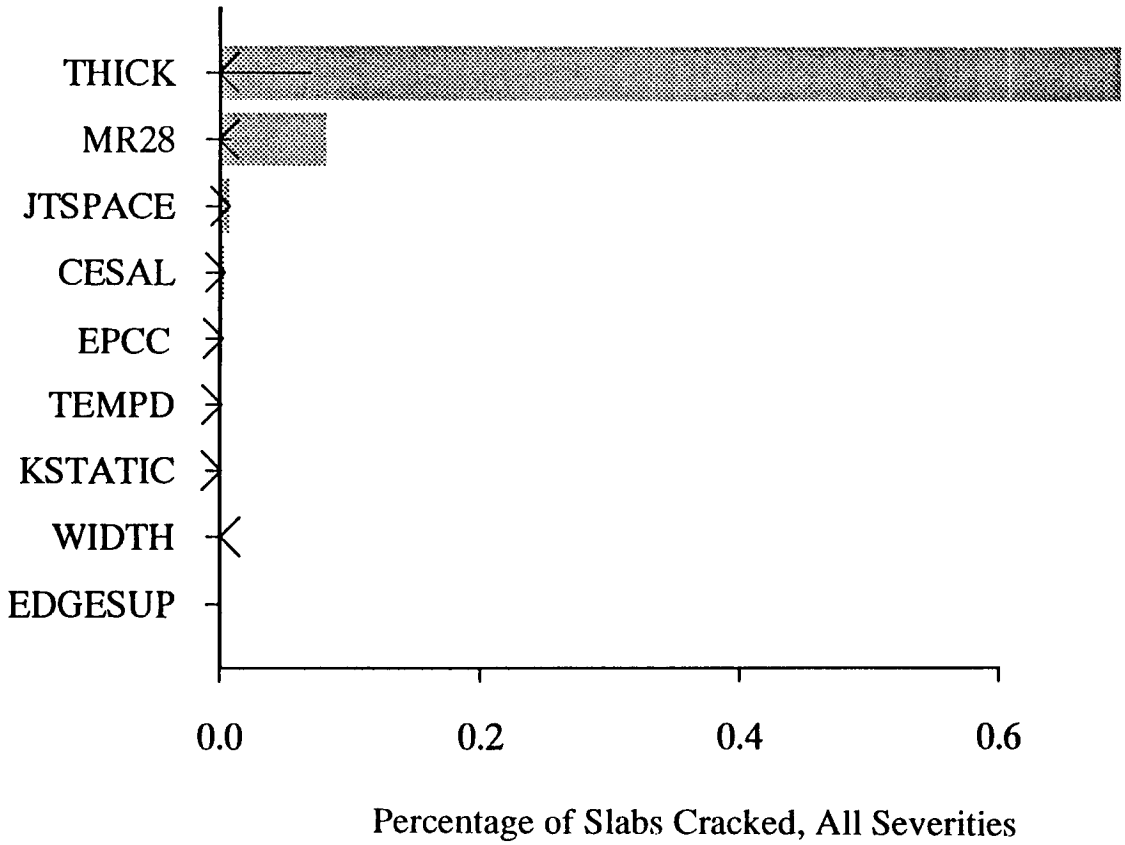

Figure 8.17. Sensitivity Analysis for Slab Cracking of JPCP (PCRACKED) Model

Three-dimensional plots illustrating the relationship between CESALs, slab thickness, and percentage of slabs with transverse cracks (PCRACKED) for this model are given in Figure 8.18. The plots show the effect of a widened traffic lane on transverse cracking of JPCP. Clearly, a widened lane decreases transverse cracking of JPCP.

Transverse Cracking of JRCP

Transverse cracks in JRCP are of concern when they deteriorate as a result of spalling and faulting. Low-severity transverse cracks are a normal occurrence in JRCP the reinforcement is designed to hold them tight and prevent deterioration. However, deterioration can be caused by repeated vertical shear stresses across the cracks from heavy wheel loads and increasing crack widths. As a crack widens, loss of aggregate interlock increases, which results in deterioration of the crack. The deterioration of such cracks causes longitudinal profile roughness, user discomfort, and the need for premature rehabilitation. As a result, only deteriorated (medium- and high-severity) transverse cracks were considered in the model development. The general procedure outlined in Chapter 6 for model development was utilized to obtain a deteriorated transverse crack model.

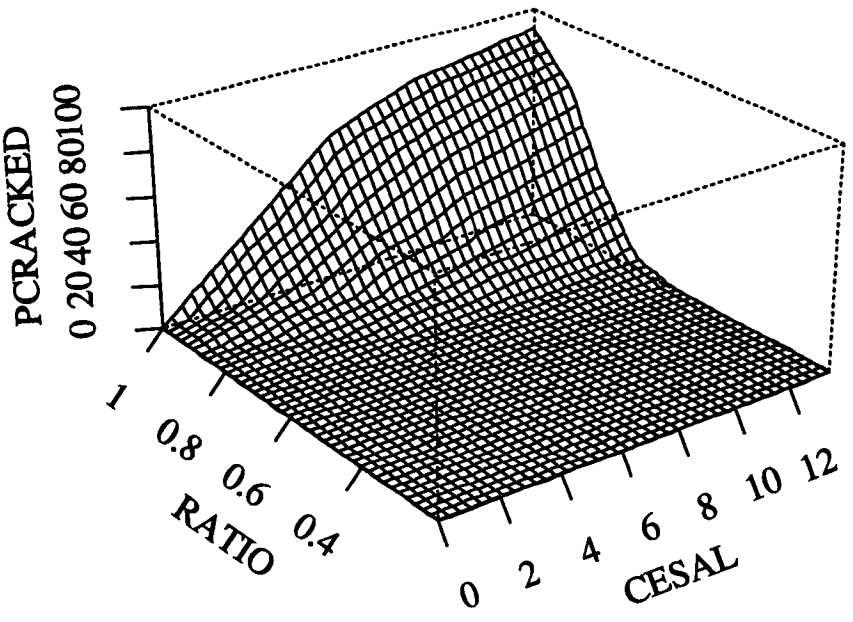

a). Widened Lane

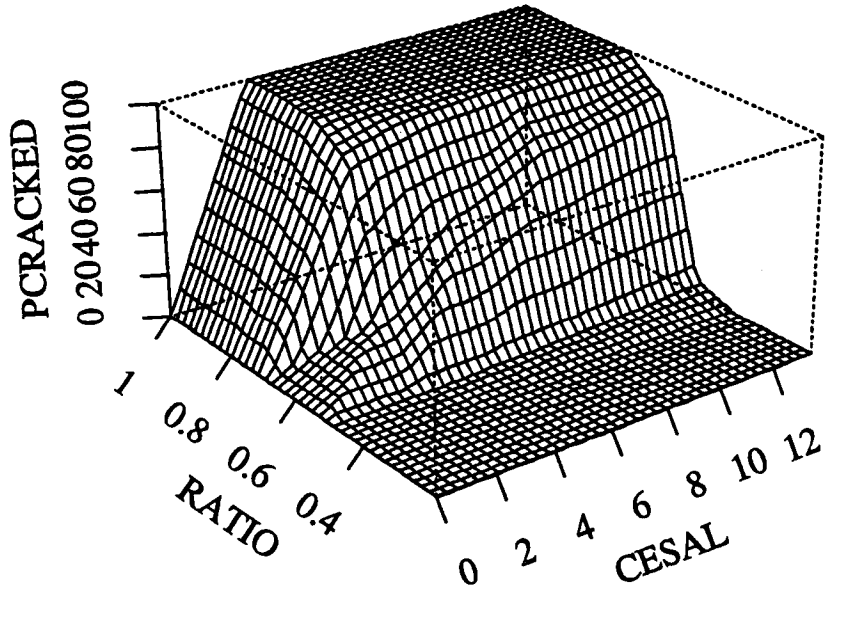

b). No Widened Lane

Figure 8.18. Three-Dimensional Plots of JPCP Transverse Cracking Model

Database, Dependent Variables, and Explanatory Variables

Previous studies have shown that the deterioration of transverse cracks in JRCP depends on traffic, design, materials, and climatic factors.[10] Data on pavement sections from the GPS-4 (JRCP) experiment were used to provide the initial database. The number of deteriorated cracks (defined as medium- and high-severity cracks) in a pavement section, CRACKJR, was the dependent variable used in the model. The initial explanatory variables that were considered are as follows:

THICK:	slab thickness, in.
EPCC:	slab modulus of elasticity of PCC measured in the laboratory, psi
TYPAGG:	type of coarse aggregate in concrete
PCCAGG:	maximum size of coarse aggregate in concrete
BASETYP:	base type (0 = untreated aggregate; 1 = treated aggregate)
BASETHK:	base thickness, in.
BCOMP:	percentage of compaction of base
BAGG:	coarse aggregate gradation of base
CESAL:	cumulative 18,000 lb. (80kN) ESALs in traffic lane, millions
AGE:	time since construction, years
JTSPACE:	mean transverse joint spacing, ft
EDGESUP:	edge support (1 = tied concrete shoulder; 0 = any other shoulder type)
PSTEEL:	percentage of longitudinal steel reinforcement, % area
DRAIN:	drainage provisions (0 = no subdrainage; 1 = subdrainage)
KSTATIC:	static backcalculated k-value, psi/in.
SUBGRADE:	subgrade soil classification (0 = fine grained; 1 = coarse grained)
PM200:	subgrade soil passing #200 sieve, %
FI:	freeze index, degree-days
FT:	number of air freeze-thaw cycles
PRECIP:	average annual precipitation, in.
TRANGE:	mean monthly temperature range (mean maximum daily temperature minus mean minimum daily temperature for each month averaged over year), °F

Data Review and Evaluation

A comprehensive evaluation of the data for each section was conducted to determine if any critical data were missing. Examples of such data missing for some test sections were deteriorated transverse cracks per mile (CRACKJR), CESALs, joint spacing, and percentage of steel. Sections with such data missing were eliminated from the study. The mean, minimum, maximum, and standard deviation of each dependent and independent variable were computed and examined. All data were then assembled into a matrix and studied in several ways to detect any abnormalities or obviously erroneous data. This study included the use of bivariate plots of all the variables. A correlation matrix that shows the strengths of the correlations between all the dependent and independent variables is shown in Table 8.4.

Table 8.4. Correlation Matrix for Selected Variables for Tranverse Crack Deterioration for JRCP

	CRACKJR	THICK	JTSPACE	CESAL	PRECIP	EPCC	KSTATIC	AGE	PSTEEL	TRANGE
CRACKJR	1	0.27	-0.09	0.0	-0.11	-0.02	0.11	0.02	-0.25	-0.02
THICK	0.27	1	-0.13	-0.061	0.513	-0.022	0.233	-0.162	-0.523	-0.635
JTSPACE	-0.09	-0.13	1	0.259	0.26	0.071	-0.152	0.097	0.496	-0.316
CESAL	0.0	-0.061	0.259	1	-0.094	-0.068	-0.257	0.449	0.116	0.034
PRECIP	-0.11	0.513	0.26	-0.094	1	0.364	-0.163	0.147	0.184	-0.898
EPCC	-0.02	-0.022	0.071	-0.068	0.364	1	-0.314	0.093	0.13	-0.371
KSTATIC	0.11	0.233	-0.152	-0.257	-0.163	-0.314	1	-0.39	-0.371	-0.035
AGE	0.02	-0.162	0.097	0.449	0.147	0.093	-0.39	1	0.422	-0.02
PSTEEL	-0.25	-0.523	0.496	0.116	0.184	0.13	-0.371	0.422	1	0.001
TRANGE	-0.02	-0.635	-0.316	0.034	-0.898	-0.371	-0.035	-0.02	0.001	1

Three-dimensional plots were also used to study the data further. Two examples of such plots are given in Figures 8.19 and 8.20. Figure 8.19 shows the relationship between CRACKJR, AGE, and CESALs, and Figure 8.20 shows the relationship between CRACKJR, PSTEEL, and CESALs. Any abrupt variations in the data indicated by unusual peaks in the surface or reverse slopes were identified and investigated. Twenty-seven sections remained for model development after sections with missing and erroneous data were deleted.

Model Building

The first step in building the model was to identify the general functional form of the occurrence of the distress over time. There were no time series data to clearly show the functional form of the progression of deteriorated transverse cracks. However, a model from a previous study shows that deteriorated transverse cracks develop almost linearly

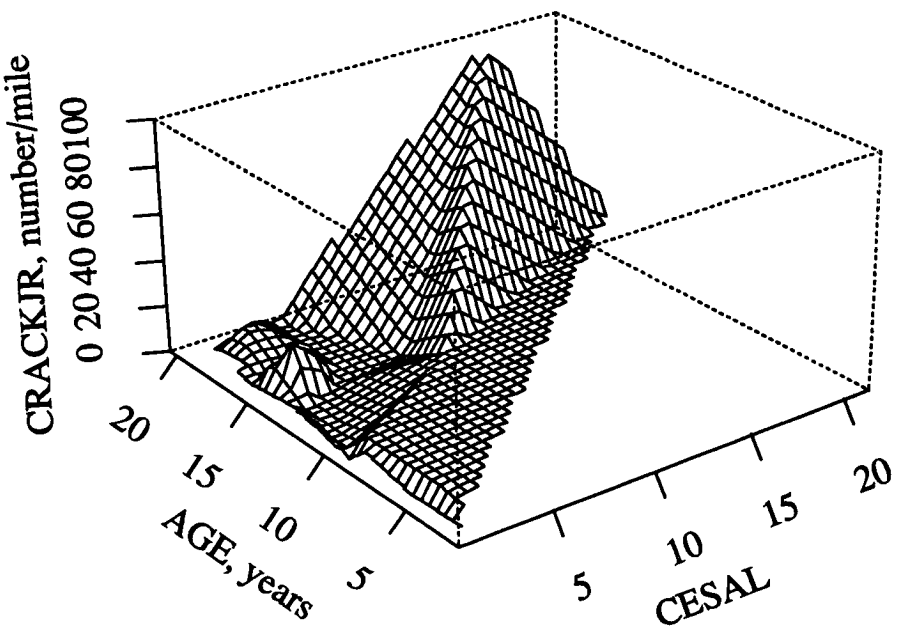

Figure 8.19. Three-Dimensional Plot (CRACKJR, AGE, CESAL) of Deteriorated JRCP Transverse Cracks

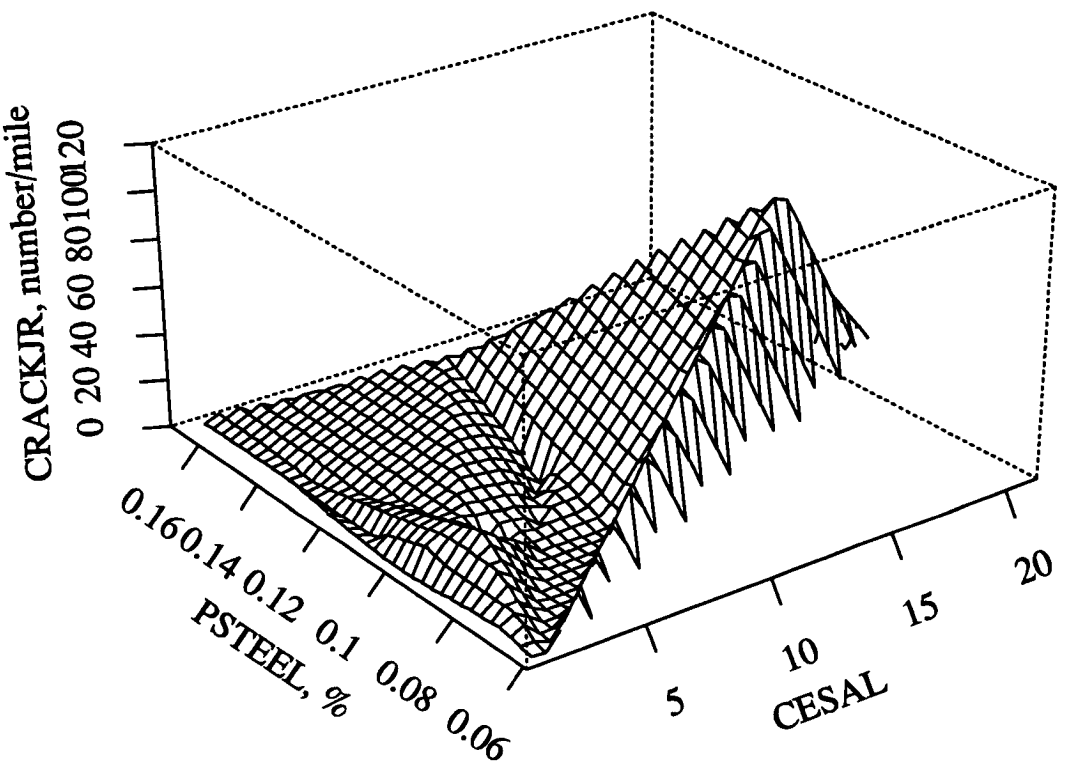

Figure 8.20. Three-Dimensional Plot (CRACKJR, PSTEEL, CESAL) of Deteriorated JRCP Transverse Cracks.

for several million applications of traffic loadings (CESALs), and then accelerate slightly with continual loadings.[10] It is also known that when CESALs and age are zero (prior to the pavement opening to traffic), deteriorated cracks are also zero.

Based upon expert judgment and the data evaluations, several explanatory variables were chosen for testing. Regression analyses were conducted with a variety of techniques to try to develop the most suitable model for deteriorated cracks prediction the sensitivity analysis. The following briefly describe the techniques utilized in the analyses:

- The explanatory variables were tested to determine their significance in the overall model. Those that showed a lack of significance on transverse cracking, even though they logically were expected to have an effect, were eliminated.

- Several interactions between variables were evaluated, but none were found to be significant.

- Tests for collinearity between the explanatory variables were conducted throughout the model development phase, and where significant collinearity was found, one of the variables was eliminated from the model.

- Observations of the previous two- and three-dimensional plots indicated some variables, including PSTEEL and KSTATIC, were nonlinearly related to CRACKJR. The appropriate exponents for these variables were determined from graphical observations and the ACE algorithm[6]. The result was a transformation of KSTATIC and PSTEEL to obtain a linear regression model.

The final model selected for predicting deteriorated transverse cracks for JRCP is as follows:

$$CRACKJR = -72.9 + 1.9\ CESAL + 0.182\left(\frac{1}{PSTEEL^2}\right) + 2473\left(\frac{1}{KSTATIC}\right) + 0.697\ PRECIP \qquad (8.5)$$

where

CRACKJR	=	number transverse cracks (medium-/high-severity)/mi.
CESAL	=	cumulative 18,000 lb. (80kN) ESALs in traffic lane, millions
PSTEEL	=	percentage of steel (longitudinal reinforcement)
PRECIP	=	annual precipitation, in.
KSTATIC	=	mean backcalculated k-value, psi/in.

Statistics:

N	=	27 sections
R^2	=	0.48
RMSE	=	20.8 cracks/mi. (12.5 cracks/km)

The limited number of sections available for the analysis clearly limits the adequacy of the model. Figure 8.21 shows a plot of the predicted versus actual CRACKJR, and Figure 8.22 shows a plot of the residuals versus predicted CRACKJR.

The results of a sensitivity analysis of the model are shown in Figure 8.23. KSTATIC has the greatest effect on CRACKJR. For low KSTATIC values (i.e., very soft subgrades), CRACKJR increases, which is logical since a low KSTATIC will lead to high deflection, which in turn will lead to crack deterioration. PSTEEL also has an effect on CRACKJR, with a lower PSTEEL resulting in a higher number of deteriorated cracks. This is also logical since lower steel content will result in increased crack width. The model indicates that deteriorated cracks will develop at a uniform rate with increased traffic loadings (CESALs). Crack deterioration is also shown to depend on climate: areas with higher precipitation have more crack deterioration. A three-dimensional plot that shows the predicted relationship between CRACKJR, CESALs, and PSTEEL from this model appears in Figure 8.24.

Although all the variables recommended by the experts that were available in the LTPP Database were examined, only the variables shown in the model were found to be significant. Other variables that have been found to be significant in previous studies include base type (untreated versus treated), slab thickness, joint spacing, and climatic variables.[9, 10] It is believed that consideration of these factors when more data are available will help improve the R^2 of 0.48 and RMSE of 21 cracks/mi. (13 cracks/km) obtained for the model.

Joint Spalling of JPCP

Joint spalling is defined as a breakdown of the concrete near the joint. Spalling eventually causes longitudinal profile roughness and user discomfort. Joint spalling can be caused by several mechanisms, including the following:

- infiltration of incompressibles into the joint over time, causing increased stresses in hot weather;
- misaligned dowels that create high stress concentration points, which leads to spalling of the concrete near the joint; and
- concrete durability problems, such as "D" cracking, that lead to deterioration of concrete near the joint.

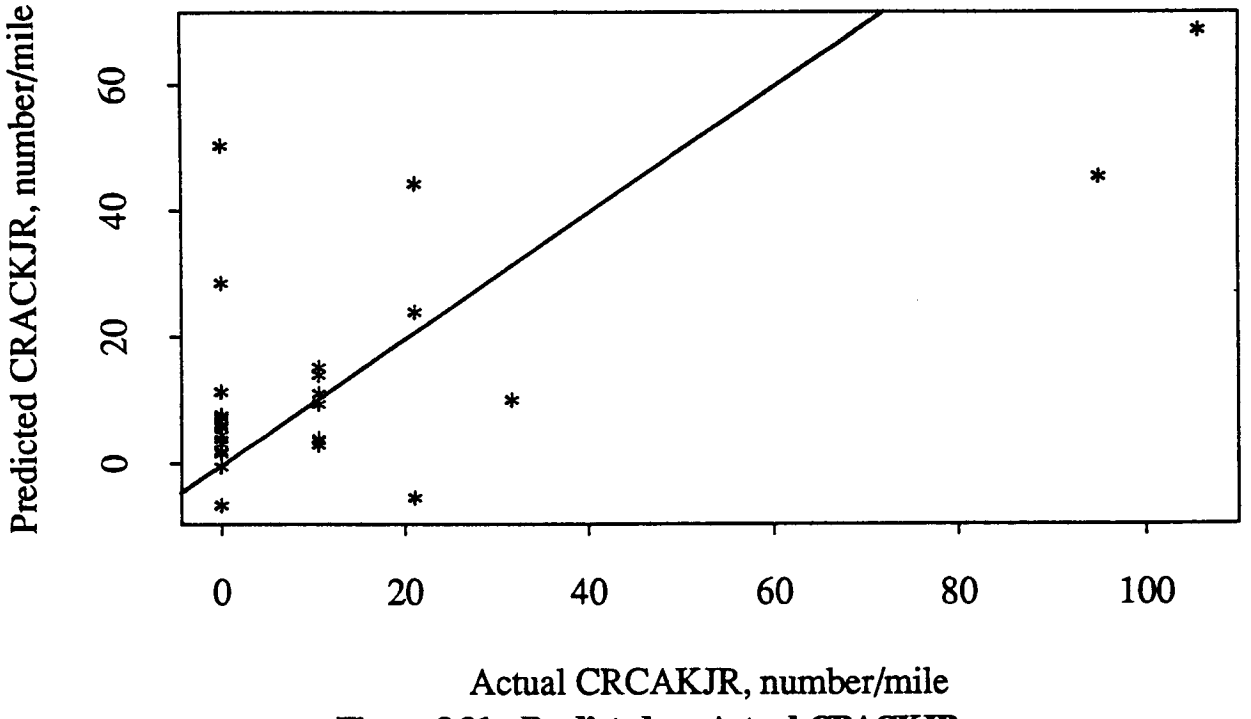

Figure 8.21. Predicted vs. Actual CRACKJR

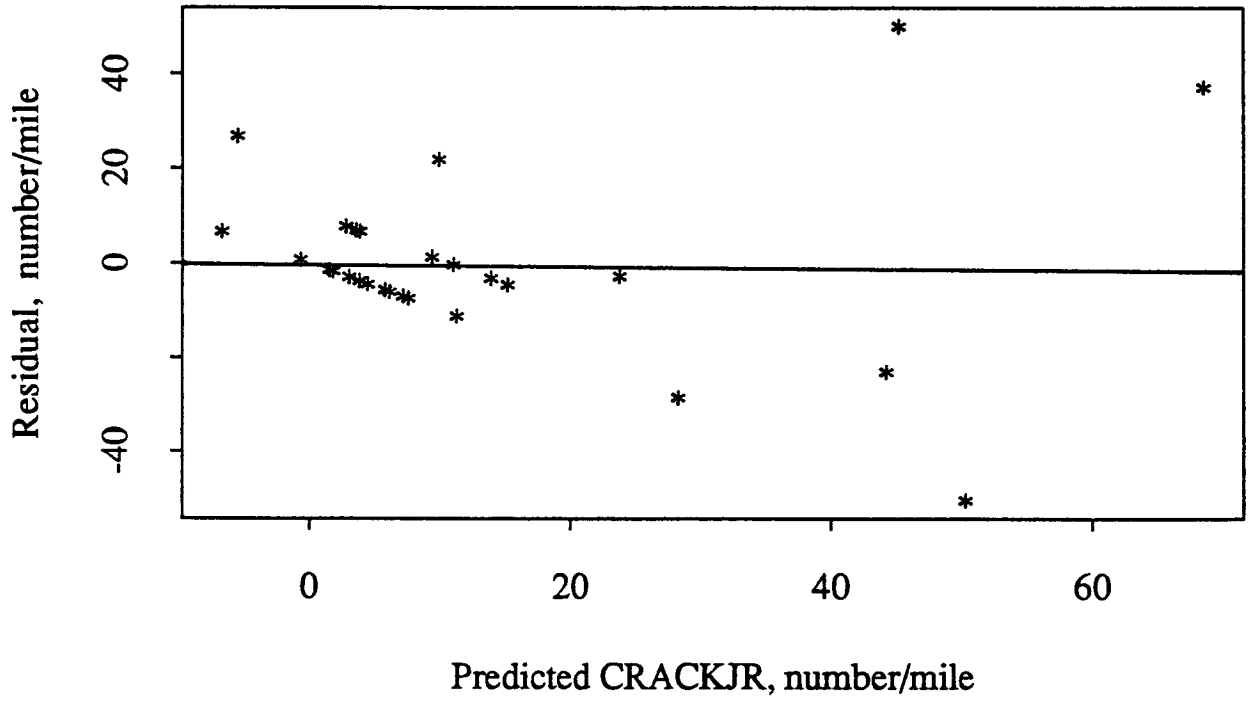

Figure 8.22. Plot of Residuals vs. Predicted CRACKJR

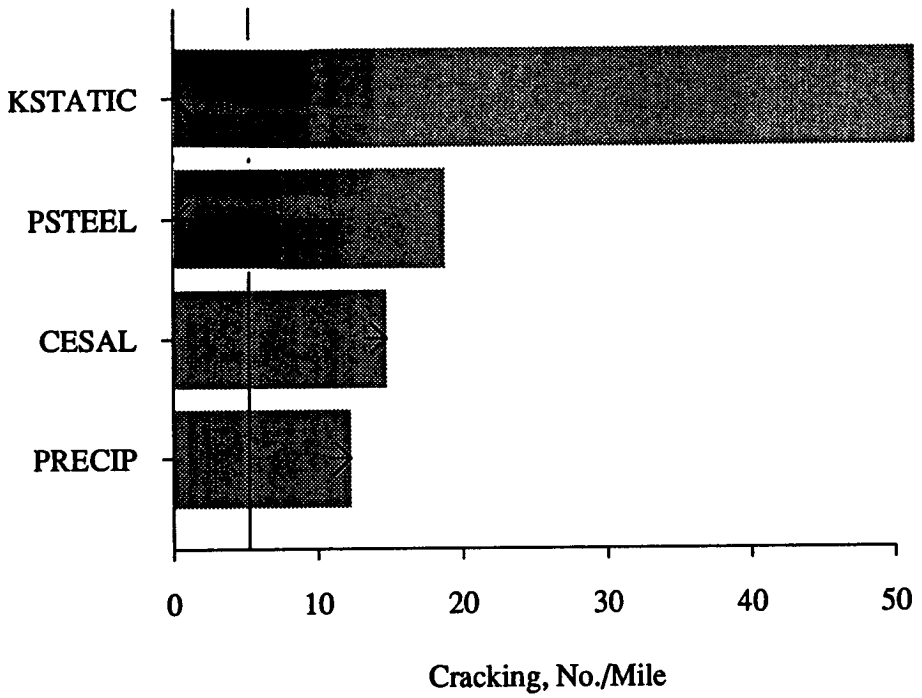

Figure 8.23. Sensitivity Analysis for the CRACKJR Model

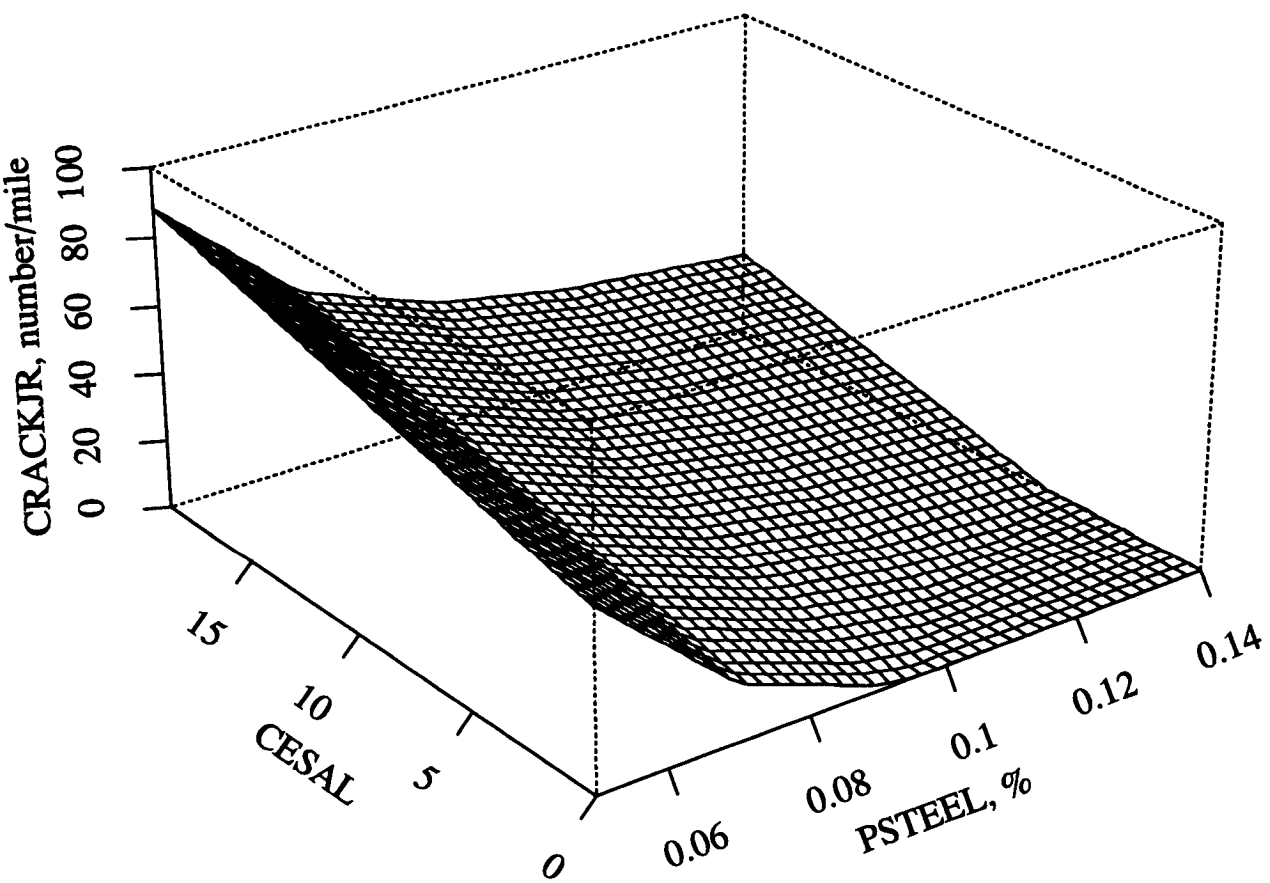

Figure 8.24. Three-Dimensional Plot Showing CRACKJR, CESAL, and PSTEEL

The general procedure outlined in Chapter 6 for model development was utilized to obtain a joint spalling model for JPCP.

Database, Dependent Variables, and Explanatory Variables

Data from sections from the GPS-3 (JPCP) experiment were used to provide the initial database. The percentage of low-, medium-, and high-severity spalled joints in a pavement section, SPALLJP, was the dependent variable used in the model. Those explanatory variables identified by the experts to be significant that were available in the LTPP Database were used. The initial explanatory variables that were considered are as follows:

THICK:	slab thickness, in.
PCCSTR:	indirect tensile strength of PCC (cores), psi
TYPAGG:	type of coarse aggregate in concrete
PCCAGG:	gradation of coarse aggregate in concrete
JTEFF:	joint load transfer efficiency
JTSPACE:	mean transverse joint spacing, ft
JTSEAL:	joint seal type (several types exist in the database)
DRAIN:	drainage provisions (0 = no subdrainage; 1 = if subdrainage)
BASETYP:	base type (0 = untreated aggregate; 1 = treated aggregate)
SUBGRADE:	subgrade soil classification (0 = fine grained; 1 = coarse grained)
PM200:	subgrade soil passing #200 sieve, %
CESAL:	cumulative 18,000 lb. (80kN) ESALs in traffic lane, millions
AGE:	time since construction, years
FI:	freeze index, degree-days
DAYS90:	number of days temperature is greater than 90°F
PRECIP:	average annual precipitation, in.
FT:	number of air freeze-thaw cycles
TRANGE:	mean monthly temperature range (mean maximum daily temperature minus mean minimum daily temperature for each month averaged over year), °F.

There were very little data for several of these variables in the database, which made it impossible for them to be considered. These included PCCAGG and PM200.

Data Review and Evaluation

Several of the techniques described previously for the other models were used in a comprehensive evaluation of the data. This included an examination of the statistics for each dependent and independent variable. A correlation matrix of the dependent and independent variables is shown in Table 8.5. Two-dimensional plots of all variables were prepared and examined. A three-dimensional plot, which shows the relationship between SPALLJP, AGE, and FT is presented in Figure 8.25. After deleting the sections with missing data and those with any abnormalities or obvious errors, fifty-six sections remained for the model development.

Table 8.5. Correlation Matrix for Selected Variables for JPCP Joint Spalling

	THICK	JTSPACE	CESAL	PRECIP	DRAIN	FT	DAYS90	DAYS32	AGE	TRANGE	SPALLJP
THICK	1.000	0.127	0.137	0.072	-0.065	-0.084	0.190	-0.104	0.006	-0.082	-0.162
JTSPACE	0.127	1.000	0.147	0.504	-0.080	-0.136	0.048	-0.227	0.229	-0.197	-0.165
CESAL	0.137	0.147	1.000	-0.012	-0.155	-0.264	0.339	-0.274	0.414	-0.181	0.111
PRECIP	0.072	0.504	-0.012	1.000	0.262	-0.529	0.067	-0.477	0.091	-0.543	-0.290
DRAIN	-0.065	-0.080	-0.155	0.262	1.000	-0.472	0.308	-0.425	-0.248	-0.504	-0.116
FT	-0.084	-0.136	-0.264	-0.529	-0.472	1.000	-0.647	0.925	-0.013	0.839	0.330
DAYS90	0.190	0.048	0.339	0.067	0.308	-0.647	1.000	-0.727	-0.123	-0.448	-0.055
DAYS32	-0.104	-0.227	-0.274	-0.477	-0.425	0.925	-0.727	1.000	-0.080	0.879	0.264
AGE	0.006	0.229	0.414	0.091	-0.248	-0.013	-0.123	-0.08	1.000	-0.095	0.312
TRANGE	-0.082	-0.197	-0.181	-0.543	-0.504	0.839	-0.448	0.879	-0.095	1.000	0.263
SPALLJP	-0.162	-0.165	0.111	-0.290	-0.116	0.330	-0.055	0.264	0.312	0.263	1.000

Model Building

An examination of the results from the exploration of the data showed that joint spalling develops slowly over the first few years, and then increases more rapidly with age. Two models developed from previous studies also show similar results.[9, 10] It is also known that when age is zero (at completion of construction), joint spalling is zero unless early joint sawing causes some spalling. Based on expert judgment and evaluation of the data, several of the explanatory variables were selected for testing. Regression analyses were conducted with a variety of the techniques previously described to develop the most useful joint spalling prediction model.

Many of the explanatory variables tested did not show any significance nor did any of the interactions between them. Where tests showed collinearity between explanatory variables, one of the variables was eliminated from the model. This often occurred with

the climatic variables. The observations of the previous two- and three-dimensional plots indicated that freeze-thaw cycles were not linearly related to SPALLJP. An exponent of 2 was found to provide a best fit for the limited data.

With this information, the following model was developed for transverse joint spalling:

$$SPALLJP = 9.79 + 10.09 * \left[- 1.227 + 0.0022 * (0.9853 * AGE + 0.1709 * FT)^2 \right] \quad \textbf{(8.6)}$$

where SPALLJP = predicted mean percentage of transverse joint spalling (all severities), percentage of total joints
FT = mean annual air freeze-thaw cycles
AGE = age since construction, years

Statistics: N = 56 sections
R^2 = 0.335
RMSE = 11.05 % joints

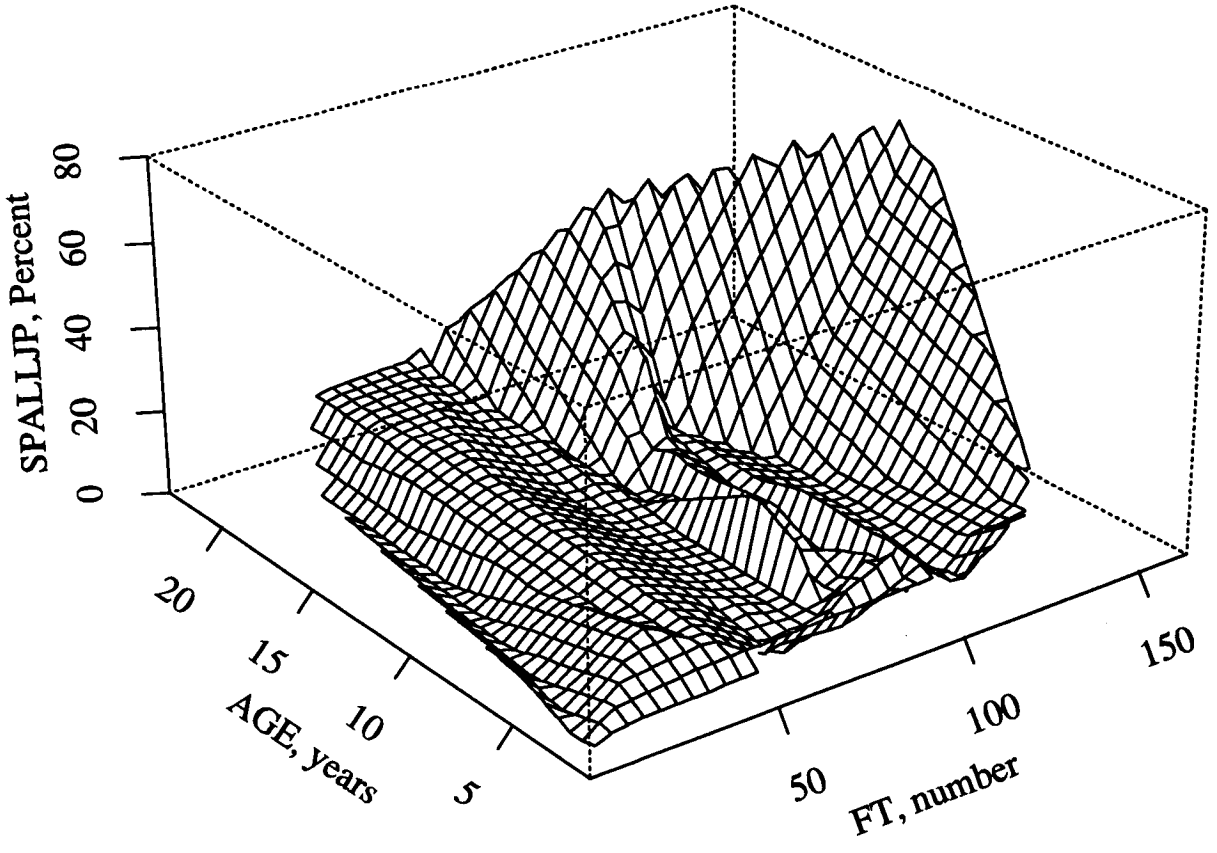

Figure 8.25. Three-Dimensional Plot (SPALLJP, AGE, FT) for JPCP Joint Spalling

Figure 8.26 shows a plot of the predicted versus actual SPALLJP, and Figure 8.27 shows a plot of the residuals versus predicted SPALLJP.

Only two variables were found to be strongly related to joint spalling of JPCP. The results from a sensitivity analysis of the model are shown in Figure 8.28. Both number of freeze-thaw cycles and age significantly affect joint spalling. The model predictions for joint spalling are generally consistent with those from previous studies[9, 10]. A three-dimensional plot showing the predicted relationship between joint spalling, number of freeze-thaw cycles, and age is presented in Figure 8.29.

The model indicates that spalling generally increases slowly at first and then increases more rapidly after several years. A high number of freeze-thaw cycles will tend to increase spalling. This is logical since it takes time for the incompressible materials, which increase compressive stresses in hot weather, to infiltrate the joints. A high number of freeze-thaw cycles of saturated concrete may also slowly weaken the concrete near the joints over time, and bring about dowel bar corrosion and subsequent joint lockup that may contribute to joint spalling.

The model includes only two of the several variables known to affect spalling from previous studies[9, 10]. However, it is believed that with an R^2 of only 0.34 and RMSE of 11%, there is considerable room for improvement of this model as more data become available.

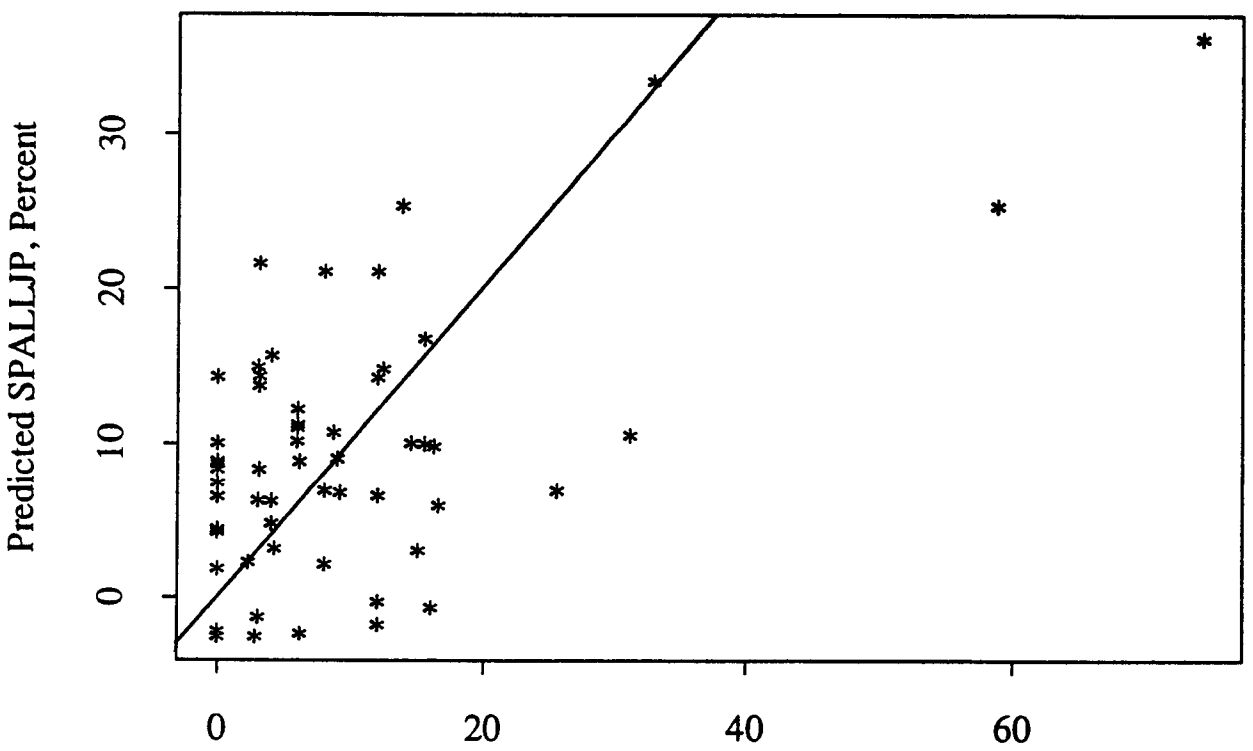

Figure 8.26. Predicted SPALLJP vs. Actual SPALLJP for JPCP

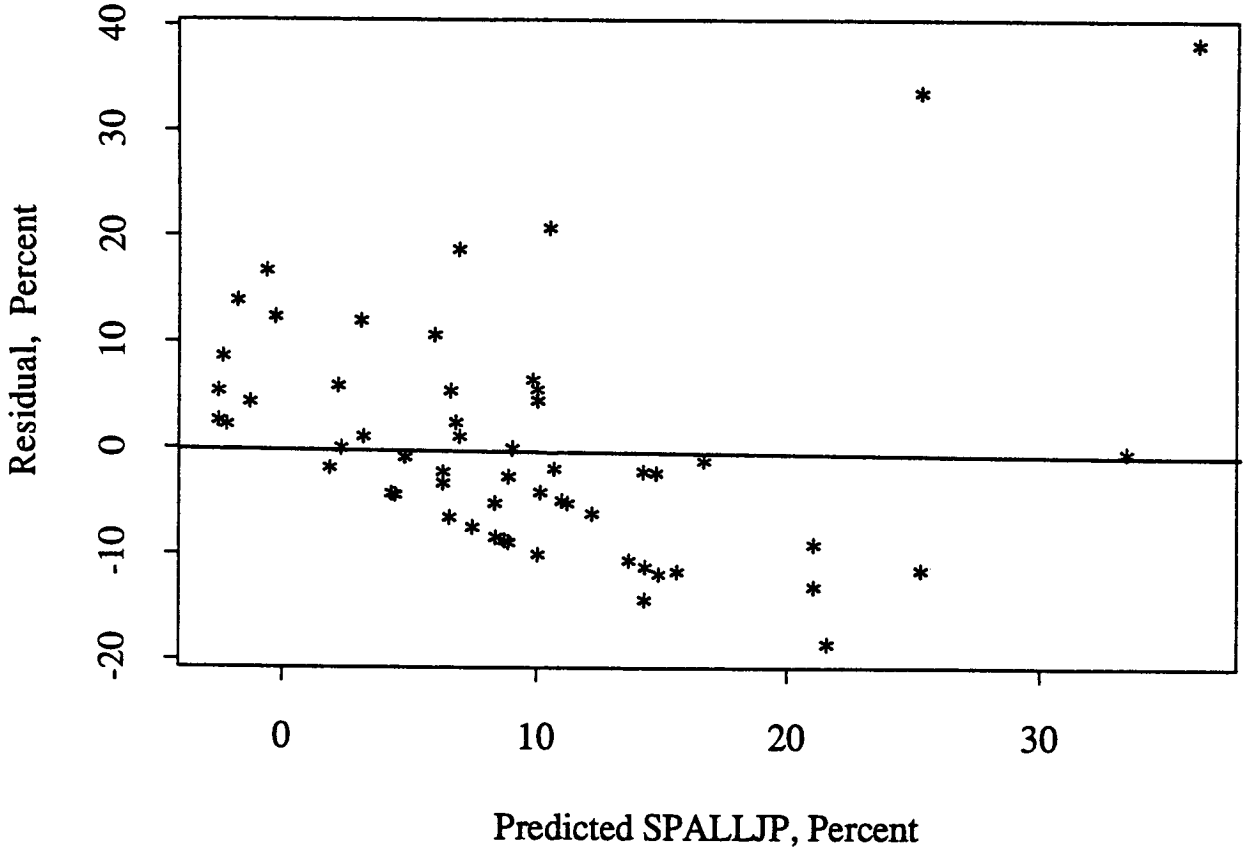

Figure 8.27. Plot of Residuals vs. Predicted SPALLJP for JPCP

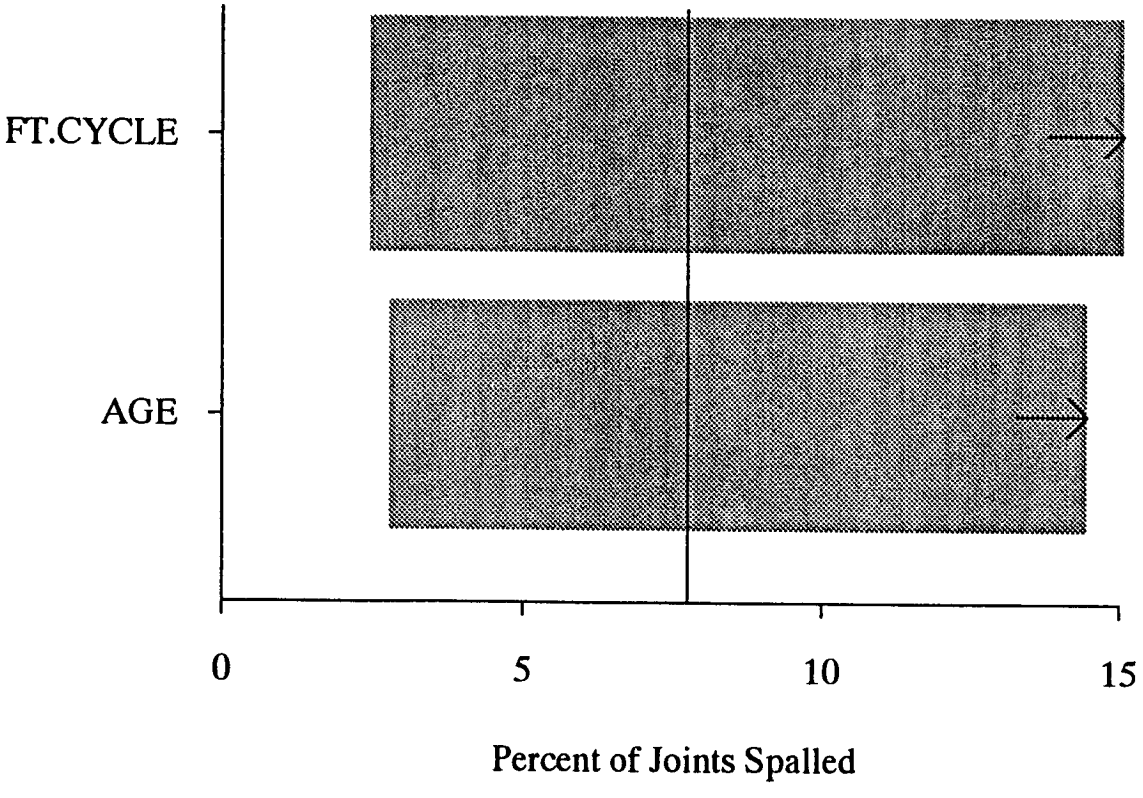

Figure 8.28. Sensitivity Analysis for Joint Spalling of JPCP (SPALLJP) Model

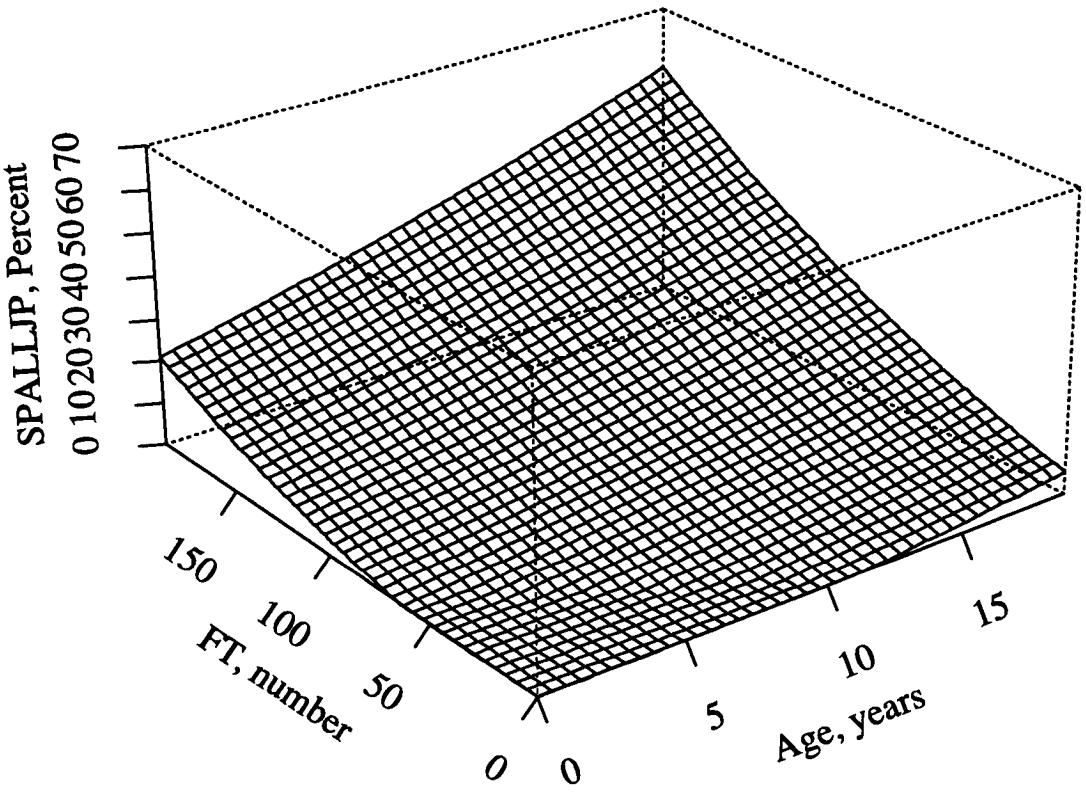

Figure 8.29. Three-Dimensional Plot of Joint Spalling Model for JPCP

Joint Spalling of JRCP

Joint spalling is defined as a breakdown of the concrete near the joint that results in loose pieces. Spalling eventually causes longitudinal profile roughness, user discomfort, and the need for rehabilitation. Joint spalling can be caused by several mechanisms, including the following:

- infiltration of incompressibles into the joint over time, which in hot weather can lead to a buildup of stresses when the concrete slabs expand;
- misaligned dowels that create high stress concentration points, which leads to spalling of the concrete near the joint; and
- concrete durability problems, such as "D" cracking that lead to a breakdown of concrete near the joint.

The general procedure outlined in Chapter 6 for model development was utilized to obtain a joint spalling model for JRCP.

Database, Dependent Variables, and Explanatory Variables

The initial database comprised data from sections of the GPS-4 (JRCP) experiment. The percentage of low-, medium-, and high- severity spalled joints in a pavement section (SPALLJR) was the dependent variable used in the prediction model. The explanatory variables identified by the experts to be significant were selected for consideration, provided they were available in the LTPP Database. The initial explanatory variables that were considered follow:

THICK:	slab thickness, in.
PCCSTR:	indirect tensile strength of PCC (cores), psi
TYPAGG:	type of coarse aggregate in concrete
PCCAGG:	gradation of coarse aggregate in PCC
JTSPACE:	mean transverse joint spacing, ft
JTEFF:	joint load transfer efficiency
JTSEAL:	joint seal type (several types are listed in the database)
DRAIN:	drainage provisions (0 = no subdrainage; 1 = subdrainage)
BASETYP:	base type (0 = untreated aggregate; 1 = treated aggregate)
SUBGRADE:	subgrade soil classification (0 = fine grained; 1 = coarse grained)
PM200:	subgrade soil passing #200 sieve, %
CESAL:	cumulative 18,000 lb. (80kN) ESALs in traffic lane, millions
AGE:	time since construction, years
PRECIP:	average annual precipitation, in.
FT:	mean number of annual air freeze-thaw cycles
TRANGE:	mean monthly temperature range (mean maximum daily temperature minus mean minimum daily temperature for each month averaged over the year), °F
FI:	freeze index, degree-days (°F) below freezing
DAYS90:	number of days temperature greater than 90°F

There were very little data for several of these variables (e.g., PCCAGG and PM200) in the database, which made it impossible to consider many of them. Each pavement section was reviewed to determine if any data were missing. Examples of missing data included SPALLJR, JTSPACE, and TRANGE data. Sections with missing data could not be used in the analysis.

Data Review and Evaluation

A comprehensive evaluation of the data was conducted to identify those sections with data outliers or influential observations. These sections were not deleted at this stage, but were simply identified as sections with potential errors to be examained further. The mean, minimum, maximum, and standard deviation of each dependent and independent

variable were computed and examined. All data were then assembled into a matrix, sorted several ways, and studied to identify any abnormalities or obviously erroneous data.

Two-dimensional plots of all variables were prepared and examined. A correlation matrix that shows the strength of the correlation between all the dependent and independent variables is shown in Table 8.6. Three-dimensional plots were also generated to show the relationships between the dependent variable and several of the selected explanatory variables. One example of the three-dimensional plots is given in Figure 8.30 that shows the relationship between SPALLJR, AGE, and TRANGE. There are a few sharp peaks in the surface that indicated abrupt variations in the data. The sections causing these unusual peaks or reverse slopes were identified. In the end only twenty-five sections remained for model development after sections with missing and erroneous data were deleted.

Model Building

The first step in building the model was to identify the general functional form of JRCP spalling with time and traffic. Two previous studies show that joint spalling develops slowly over the first few years, and then increases more rapidly with AGE.[9, 10] It is also known that when AGE is zero (at construction), joint spalling is zero unless early joint sawing causes some spalling. Based on this information, expert judgment, and the previous data observations, several explanatory variables were chosen for testing in this model. Regression analyses were conducted with a variety of techniques to try to develop the most suitable model for joint spalling prediction for the sensitivity analysis. The following briefly describe the techniques utilized in the analyses:

- The explanatory variables were tested to determine their significance in the overall model. Due to their lack of significance, many were eliminated, even though they were known from previous studies to affect joint spalling.

- The variables were evaluated to determine the existence of significant interactions between them, but none of the interactions were found to be significant.

- Tests for collinearity between the explanatory variables were performed throughout the model development phase. When such collinearities were found, one of the variables was eliminated from the model. This was found to be the case for some of the climatic variables such as FT and TRANGE. For this model, TRANGE was retained as it was more closely correlated to spalling than FT.

Table 8.6. Correlation Matrix for Selected Variables for JRCP Joint Spalling.

	THICK	JTSPACE	CESAL	PRECIP	DRAIN	SEAL	FT	DAYS90	DAYS32	AGE	TRANGE	SPALLJR
THICK	1.000	-0.048	-0.234	0.560	0.075	-0.106	-0.531	0.424	-0.607	-0.173	-0.676	-0.510
JTSPACE	-0.048	1.000	0.438	0.312	-0.123	-0.096	-0.083	0.082	-0.242	0.306	-0.331	-0.097
CESAL	-0.234	0.438	1.000	0.058	-0.166	-0.088	0.108	-0.170	0.118	0.614	0.034	0.169
PRECIP	0.560	0.312	0.058	1.000	0.120	-0.457	-0.792	0.696	-0.894	0.240	-0.918	-0.424
DRAIN	0.075	-0.123	-0.166	0.120	1.000	-0.167	0.084	-0.136	0.006	-0.156	-0.109	0.013
SEAL	-0.106	-0.096	-0.088	-0.457	-0.167	1.000	0.381	-0.277	0.392	-0.192	0.284	0.174
FT	-0.531	-0.083	0.108	-0.792	0.084	0.381	1.000	-0.870	0.917	-0.279	0.746	0.233
DAYS90	0.424	0.082	-0.170	0.696	-0.136	-0.277	-0.870	1.000	-0.873	0.087	-0.633	-0.220
DAYS32	-0.607	-0.242	0.118	-0.894	0.006	0.392	0.917	-0.873	1.000	-0.177	0.890	0.354
AGE	-0.173	0.306	0.614	0.240	-0.156	-0.192	-0.279	0.087	-0.177	1.000	-0.092	0.385
TRANGE	-0.676	-0.331	0.034	-0.918	-0.109	0.284	0.746	-0.633	0.890	-0.092	1.000	0.505
SPALLJR	-0.510	-0.097	0.169	-0.424	0.013	0.174	0.233	-0.220	0.354	0.385	0.505	1.000

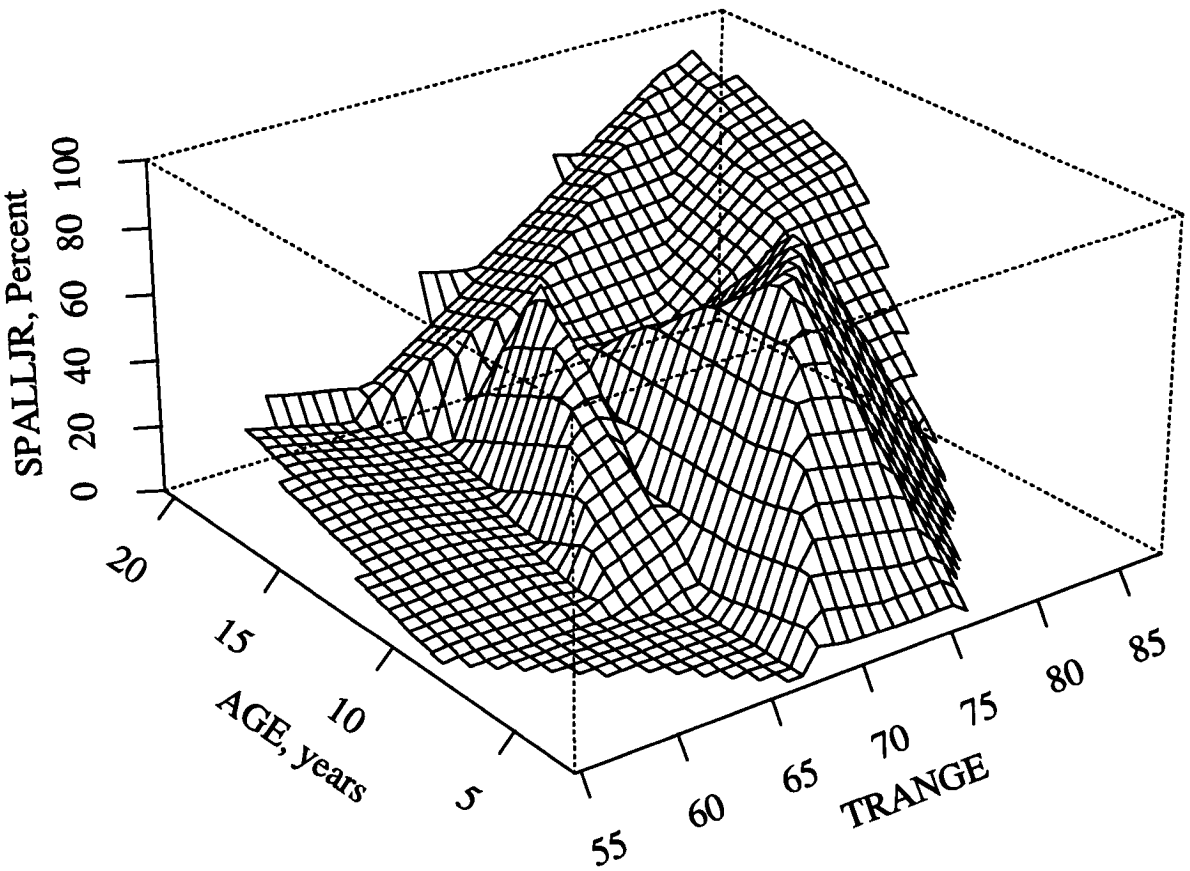

Figure 8.30. Three-Dimensional Plot (AGE, SPALLJR, TRANGE) for JRCP Joint Spalling.

- The observations of the previous two- and three-dimensional plots indicated that TRANGE and AGE were not linearly related to SPALLJR. An exponent of 1.5 for both AGE and TRANGE was found to provide a best fit to the limited data.

The following model was developed for all severities of transverse joint spalling of JRCP based on the data from the GPS-4 sections:

$$SPALLJR = -79.0 + 0.604 * (AGE)^{1.5} + 0.129 * (TRANGE)^{1.5} \quad (8.7)$$

where SPALLJR = predicted mean percentage of transverse joint spalling (all severities), percentage of total joints

TRANGE = mean monthly temperature range (mean maximum daily temperature minus mean minimum daily temperature for each month over a year)

AGE = age since construction, years

Statistics:

N =	25 sections
R^2 =	0.644
RMSE =	16.6% joints

The limited number of sections available for the analysis clearly limits the adequacy of the model. Although all the variables that were recommended by the experts that were available in the database were evaluated, only a few were found to be significant. Figure 8.31 shows a plot of the predicted versus actual SPALLJR, and Figure 8.32 shows a plot of the residuals versus predicted SPALLJR. The results from the sensitivity analysis of the model are shown in Figure 8.33. Both AGE and TRANGE have a large and approximately equal effect on joint spalling of JRCP.

The form of the model shows a curvilinear increase in spalling with AGE and with more severe temperature conditions (TRANGE). A three-dimensional plot that shows the relationship among the predicted SPALLJR, TRANGE, and AGE is shown in Figure 8.34. This form of the model is generally consistent with the measured development of spalling with age in other studies.[9, 10]

The AGE variable in the model may represent factors such as cycles of climatic changes such as joint opening/closing, thermal curling cycles, cold/hot cycles, freeze-thaw cycles, and progressive corrosion of dowels. The TRANGE variable reflects daily and monthly temperature ranges to which the pavement is subjected. The higher the TRANGE (northern US and Canada), the higher the joint spalling. Greater ranges in temperature generally cause increased joint openings, that increase the infiltration of incompressibles in cold weather and high compressive stresses in hot weather. TRANGE also correlates strongly with other thermal variables, including the number of freeze-thaw cycles, number of days above 90°F (32°C), and the freeze index.

This model includes only two of several variables known to affect spalling from previous studies. For example, joint seal type and base type were not found to be significant, but have been found to be significant in other studies. Also, data on concrete durability were not available in the database, but durability is known to be significant to the occurrence of D cracking. Joint spacing, which ranged from 13 to 30 ft (4 to 9 m), is implicitly included in the model, because the dependent variable is expressed as the percentage of joints spalled. This means that as the number of joints per mile increases, there will be more joints that can spall. The R^2 of 0.64 and the RMSE of 17% indicate that there is considerable room for improvement of the model.

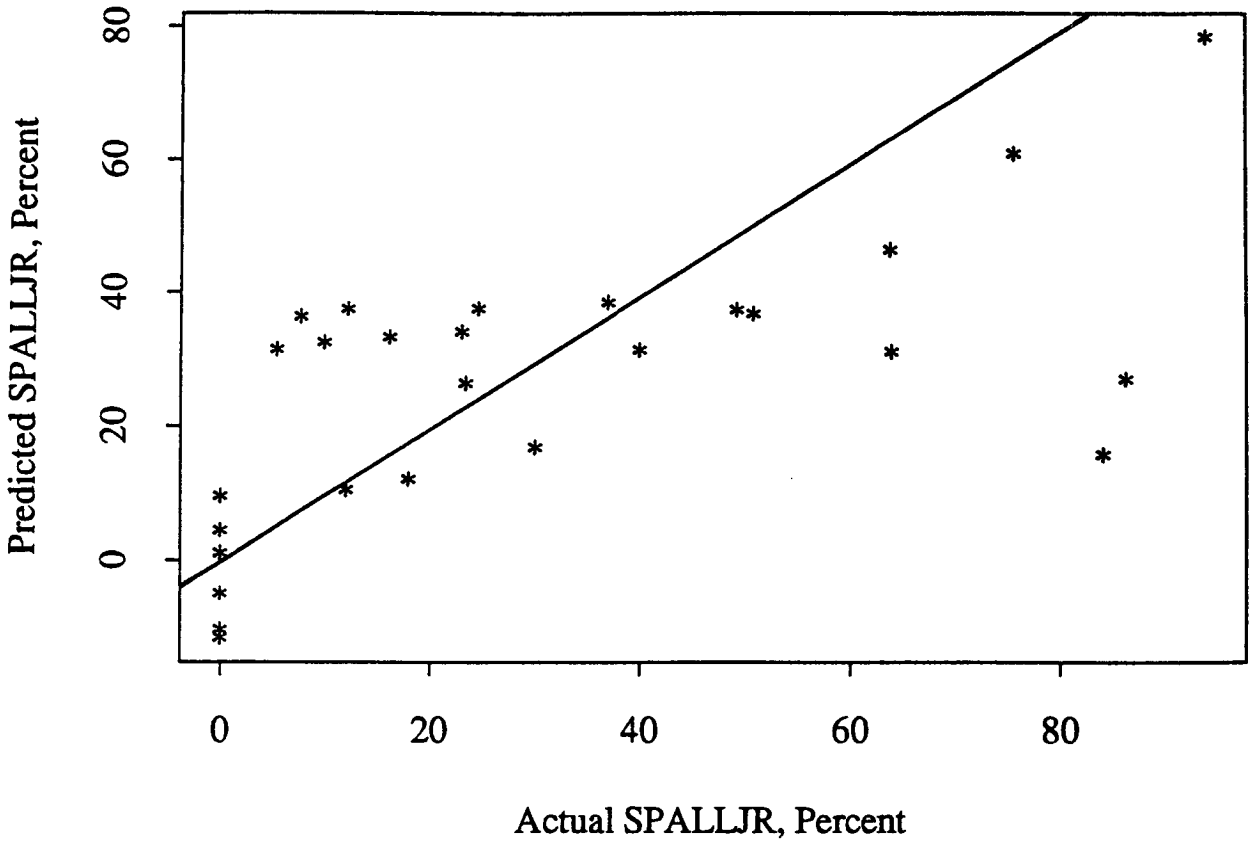

Figure 8.31. Predicted vs. Actual SPALLJR

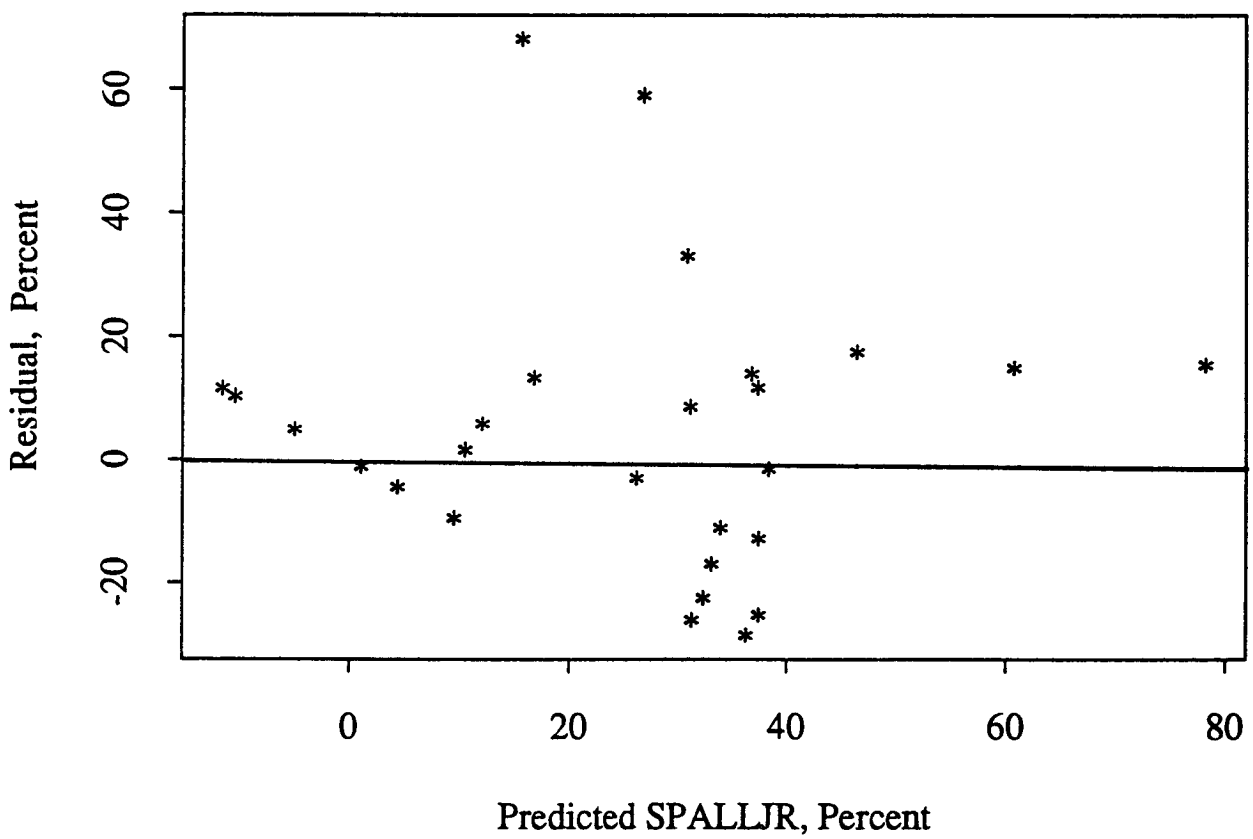

Figure 8.32. Plot of Residuals vs. Predicted SPALLJR

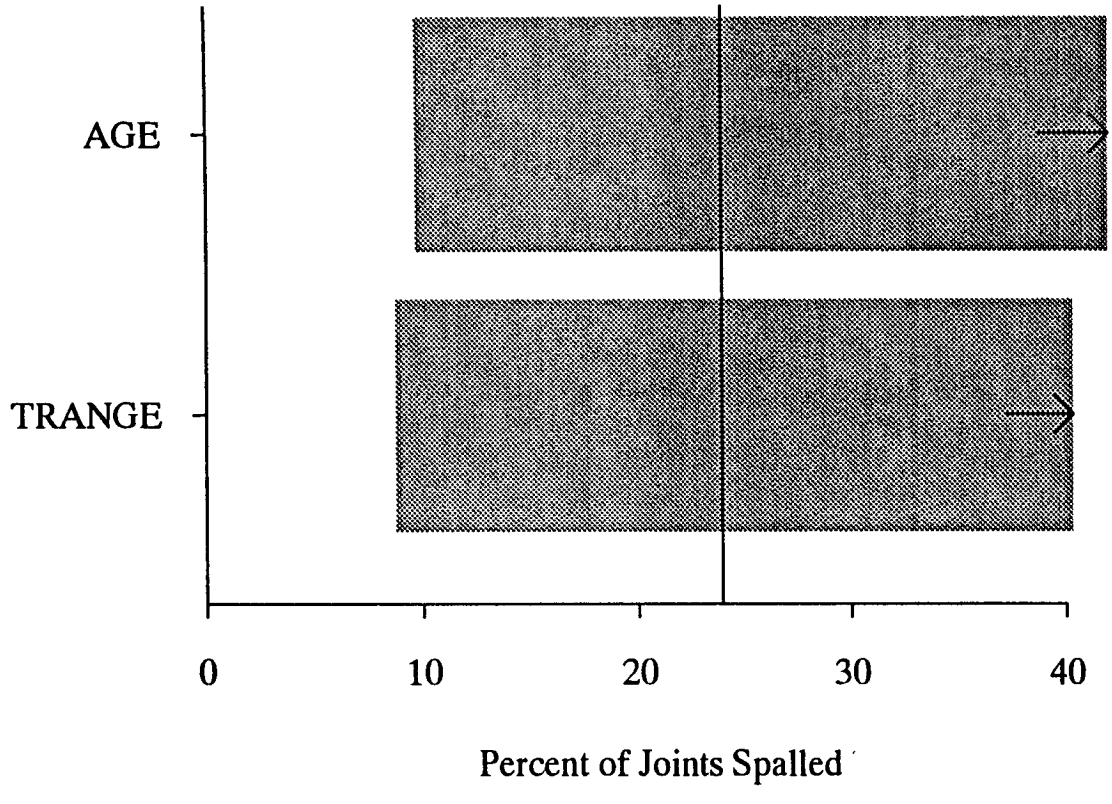

Figure 8.33. Sensitivity Analysis for Joint Spalling of JRCP (SPALLJR) Model

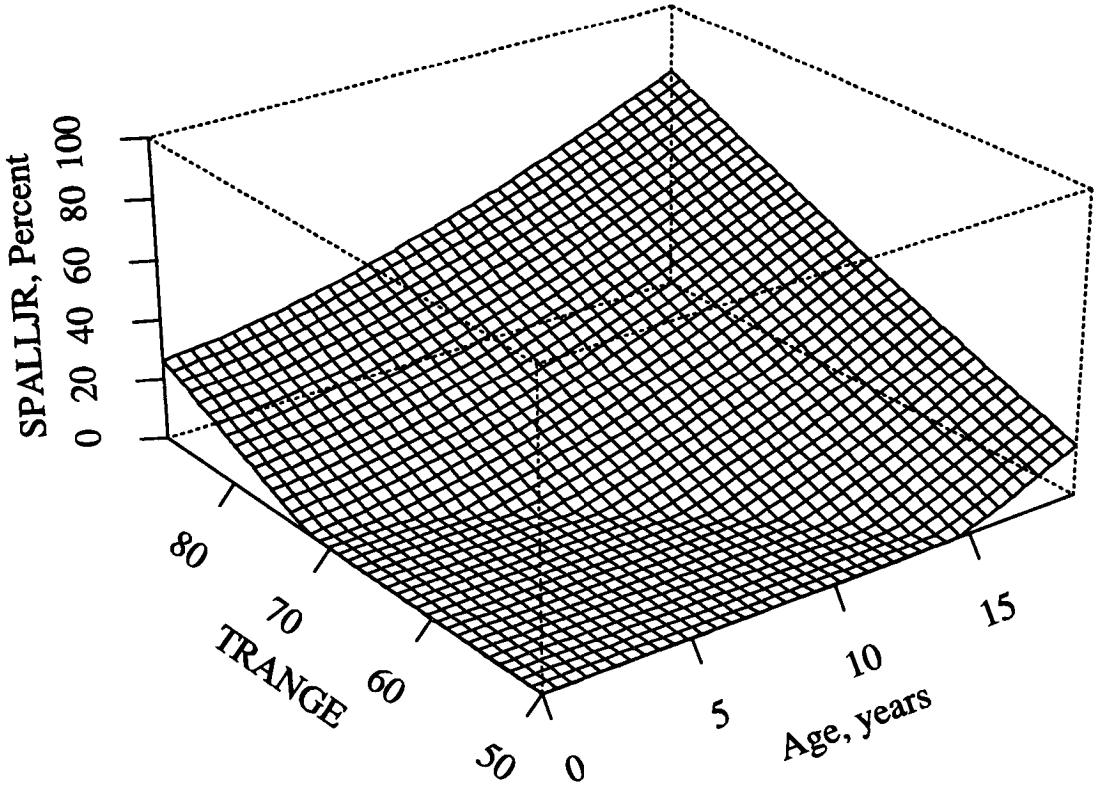

Figure 8.34. Three-Dimensional Plot (SPALLJR, TRANGE, AGE) for Joint Spalling Model for JRCP

IRI of Doweled JPCP

The IRI is calculated from the longitudinal profile and is reported in units of in./mi., m/km, or cm/km. IRI has been shown to correlate well with the subjective rating of highway users. An IRI of zero represents a perfectly smooth plane. However, a typical IRI for new construction is about 26 in./mi. (41 cm/km) which correlates to a Present Serviceability Index (PSI) of approximately 4.5. A typical IRI of a pavement showing considerable roughness is approximately 169 in./mi. (267 cm/km), which correlates to a PSI of 2.5. (An increase in IRI with time after construction is caused by the development of distresses and also any movement of the foundation.) Thus, IRI is an indicator of the highway users' response to the pavement and thus to the needs for rehabilitation based on roughness. The general procedure outlined in Chapter 6 for model development was used to obtain an IRI model for JPCP.

Database, Dependent Variables, And Explanatory Variables

Data on the doweled pavement sections from the GPS-3 (JPCP) experiment provided the initial database used in the development of this model. The values of IRI measured over the LTPP sections were used to represent the dependent variable. The potential explanatory variables selected for investigation were those identified by the experts to be significant, provided they were available in the LTPP Database. The initial explanatory variables that were considered are as follows:

THICK:	slab thickness, in.
PCCSTR:	indirect tensile strength of PCC (cores), psi
TYPAGG:	type of coarse aggregate in concrete
PCCAGG:	gradation of coarse aggregate in PCC
JTEFF:	joint load transfer efficiency
JTSPACE:	mean transverse joint spacing, ft
JTSEAL:	joint seal type (several types exist in the database)
EDGESUP:	edge support (1 = tied PCC shoulder; 0 = other shoulder types)
DRAIN:	subdrainage provisions (0 = no subdrainage; 1 = subdrainage)
BASETYP:	base type (0 = untreated aggregate; 1 = treated aggregate)
KSTATIC:	align subgrade with static backcalculated k-value, psi/in.
SUBGRADE:	subgrade soil classification (0 = fine grained; 1 = coarse grained)
PM200:	subgrade soil passing #200 sieve, %
CESAL:	cumulative 18,000 lb. (80kN) ESALs in traffic lane, millions
AGE:	time since construction, years
PRECIP:	average annual precipitation, in.
FT:	mean number of annual air freeze-thaw cycles

TRANGE:	mean monthly temperature range (mean maximum daily temperature minus mean minimum daily temperature for each month averaged over the year), °F
FI:	freeze index, degree-days (F) below freezing
DAYS90:	number of days temperature greater than 90°F (32°C)

Sufficient data were not available for some variables even though they were expected to be significant. Examples include PCCAGG and PM200. Examples of other data missing for some of the test sections include IRI, JTSPACE, CESAL, and TRANGE. Sections with such data missing could not be used in the analysis.

Data Review and Evaluation

Evaluation of the data was conducted to identify anomalies and errors. Various statistics of the dependent and independent variables, such as the mean, minimum, maximum, and standard deviation, were computed and examined. All data were then assembled, sorted, and studied in several ways to determine any abnormalities or obvious errors. Two-dimensional plots of all variables were also prepared and examined to determine the bivariate relationships between selected variables. A matrix that shows the strengths of the correlations between dependent and independent variables appears in Table 8.7.

Three-dimensional plots that show the trends of IRI with AGE, CESALs, and other variables were also prepared and examined. One example of such a plot appears in Figure 8.35 to show the relationship between IRI, JTSPACE, and AGE. There are a few unusual peaks and reverse slopes in the plot that indicate the existence of abnormal data. Twenty-one sections remained for model development after the sections with missing and erroneous data had been deleted.

Model Building

Model building started with an attempt to identify the general functional form of IRI in relation to time and traffic. Although time series data were not available to identify a typical functional form for change in IRI, two previous studies on in-service pavements show that PSI drops somewhat rapidly at first, and then levels out for a long time, which may then be followed by another rapid drop as severe deterioration occurs.[9, 10] Because PSI is primarily a measure of roughness, this form was assumed for model building.

Table 8.7. Correlation Matrix for Selected Variables for Doweled JPCP IRI.

	THICK	FT	BASETYP	CESAL	DAYS32	EDGESUP	DWLDIA	JTSPACE	KSTATIC	AGE	PCCSTR	SUBGRADE	TRANGE	PRECIP	IRI
THICK	1.000	-0.400	-0.211	-0.037	-0.318	0.442	0.537	-0.105	0.346	-0.300	-0.187	-0.013	-0.460	0.300	0.010
FT	-0.373	1.000	-0.202	-0.207	0.917	-0.221	-0.120	0.088	0.042	0.430	-0.095	-0.245	0.774	-0.133	0.320
BASETYP	-0.211	-0.200	1.000	0.044	-0.323	-0.084	-0.012	0.156	-0.084	-0.300	-0.176	-0.258	-0.151	-0.025	0.120
CESAL	-0.037	-0.200	0.044	1.000	-0.266	0.023	-0.034	0.434	-0.096	0.330	-0.291	-0.062	-0.160	-0.161	0.000
DAYS32	-0.318	0.920	-0.323	-0.266	1.000	-0.235	-0.105	-0.093	-0.079	0.500	-0.095	-0.138	0.865	-0.162	0.280
EDGESUP	0.442	-0.200	-0.084	0.023	-0.235	1.000	0.670	-0.407	0.125	-0.500	-0.164	-0.022	-0.162	-0.351	0.000
DWLDIA	0.537	-0.100	-0.012	-0.034	-0.105	0.670	1.000	-0.266	0.209	-0.300	-0.127	-0.168	-0.173	-0.179	0.290
JTSPACE	-0.105	0.090	0.156	0.434	-0.093	-0.407	-0.266	1.000	-0.066	0.480	-0.201	-0.291	-0.197	0.371	0.380
KSTATIC	0.346	0.040	-0.084	-0.096	-0.079	0.125	0.209	-0.066	1.000	-0.600	-0.125	0.168	-0.157	0.057	-0.100
AGE	-0.321	0.430	-0.316	0.330	0.501	-0.469	-0.304	0.480	-0.556	1.000	-0.069	-0.185	0.392	0.162	0.340
PCCSTR	-0.187	0.00	-0.176	-0.291	-0.095	-0.164	-0.127	-0.201	-0.125	0.000	1.000	0.097	-0.064	0.156	0.000
SUBGRADE	-0.013	-0.200	-0.258	-0.062	-0.138	-0.022	-0.168	-0.291	0.168	-0.200	0.097	1.000	-0.114	-0.187	-0.700
TRANGE	-0.460	0.770	-0.151	-0.160	0.865	-0.162	-0.173	-0.197	-0.157	0.390	-0.064	-0.114	1.000	-0.406	0.190
PRECIP	0.300	-0.100	-0.025	-0.161	-0.162	-0.351	-0.179	0.371	0.057	0.160	0.156	-0.187	-0.406	1.000	0.170
IRI	0.012	0.320	0.119	-0.047	0.278	-0.059	0.287	0.383	-0.117	0.340	-0.033	-0.659	0.193	0.166	1.000

It is also known that immediately after construction when AGE is zero, IRI is not necessarily zero due to construction variation. Since the initial IRI was not measured for any of the sections, however, it was not possible to utilize the change in IRI as the dependent variable. In addition, there is no maximum value of IRI. As a result, the measured IRI was selected as the dependent variable for the model to be developed.

Based upon expert judgment and previous data observations, several explanatory variables were selected for testing in the model. Regression analyses were conducted with a variety of techniques to try to develop the most suitable IRI prediction model for the sensitivity analysis. The following briefly describes the techniques utilized in the analyses:

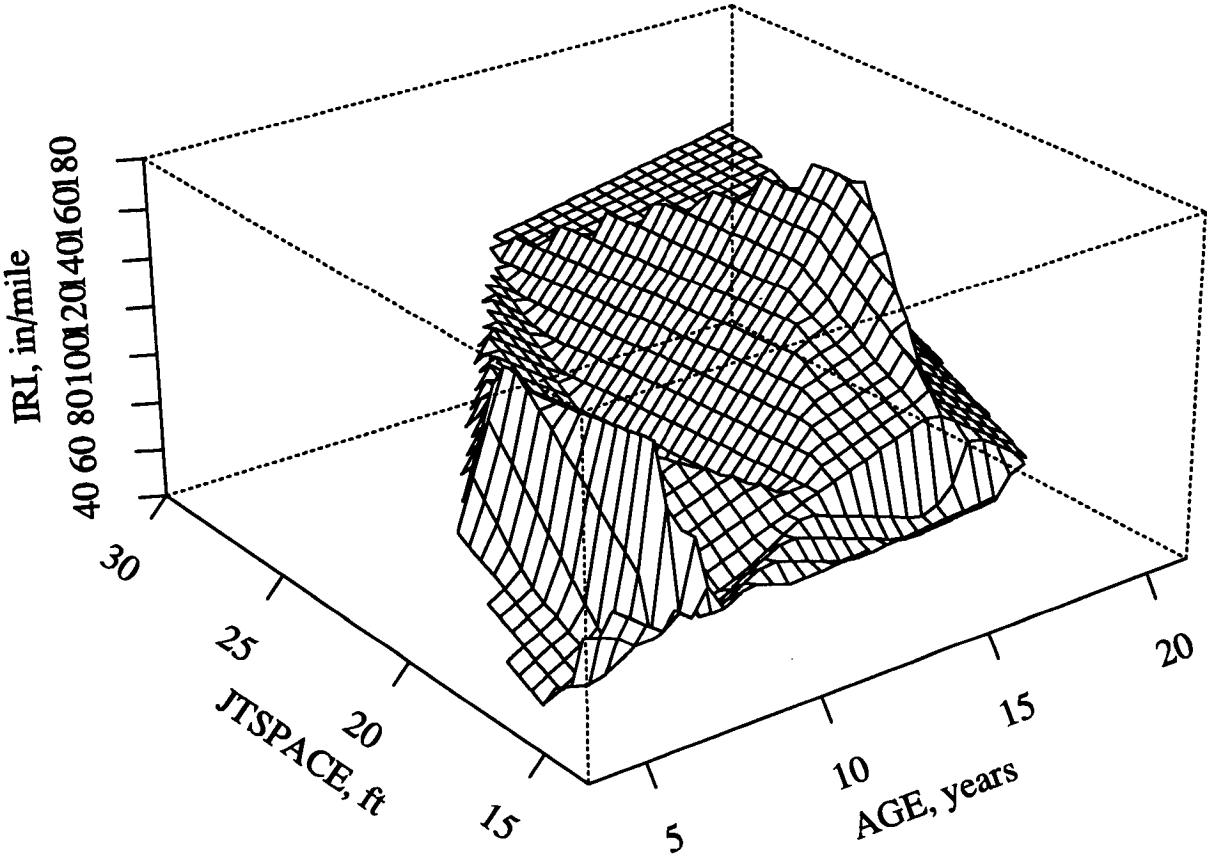

Figure 8.35. Three-Dimensional Plot (IRI, JTSPACE, AGE) for JPCP

- The explanatory variables were tested to determine their significance in the overall model. Those that were not found to be significant were eliminated, even if they should logically affect IRI.

- Interactions between the variables were evaluated. One interaction that was found to be significant was that between AGE and KSTATIC.

- Tests for collinearity between the explanatory variables were conducted throughout the development of the model. Where such collinearity was found, one of the variables was eliminated from the model.

- Observations of the previous two- and three-dimensional plots indicated that KSTATIC was not linearly related to IRI. The relationship was linearized by using 1/KSTATIC as the independent variable.

With these techniques and regression analysis, the following model was developed for predicting the IRI of doweled JPCP sections with data from the GPS-3 sections:

$$IRI = 105.9 + 159.1 * \left(\frac{AGE}{KSTATIC}\right) + 2.167 * JTSPACE - 7.127 * THICK + 13.49 * EDGESUP \quad (8.8)$$

where

IRI	=	International Roughness Index, in./mi.
AGE	=	age since construction, years
THICK	=	concrete slab thickness, in.
KSTATIC	=	mean backcalculated static k-value, psi/in.
EDGESUP	=	1 = tied concrete shoulder; 0 = any other shoulder type
JTSPACE	=	mean transverse joint spacing, ft

Statistics:

N	=	21 sections
R^2	=	0.548
RMSE	=	19.06 (in./mi.) (30.6 cm/km)

Figure 8.36 is a plot of the predicted versus actual IRI, and Figure 8.37 shows a plot of the residuals versus predicted IRI for this model. Although all variables recommended by the experts that were available in the database were evaluated, only a few were found to be significant. The results of a sensitivity analysis of the model showing the level of significance of the variables in the model is presented in Figure 8.38. JTSPACE has the largest effect on IRI of doweled JPCP, followed closely by THICK, EDGESUP, AGE, and KSTATIC. The form of the model provides for a linear increase in IRI over time.

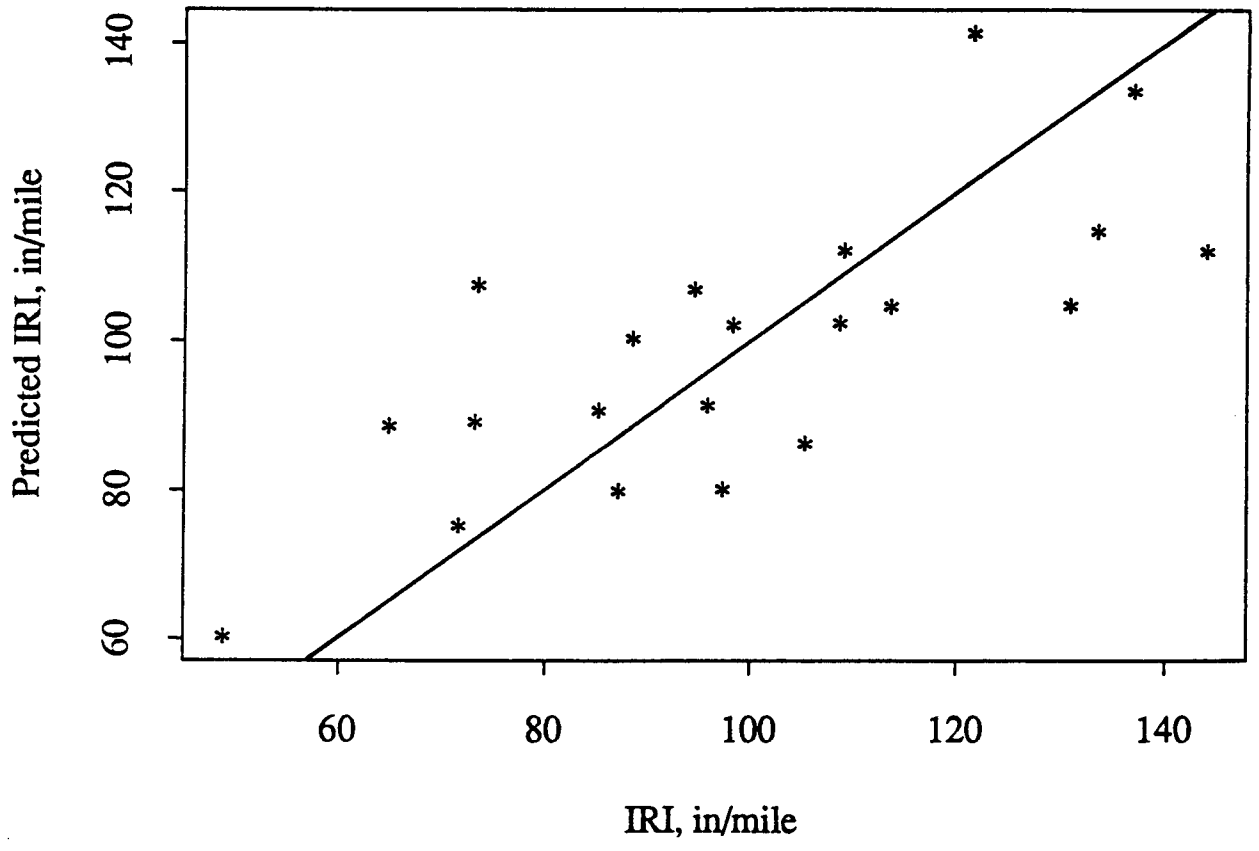

Figure 8.36. Predicted vs. Actual IRI for Doweled JPCP

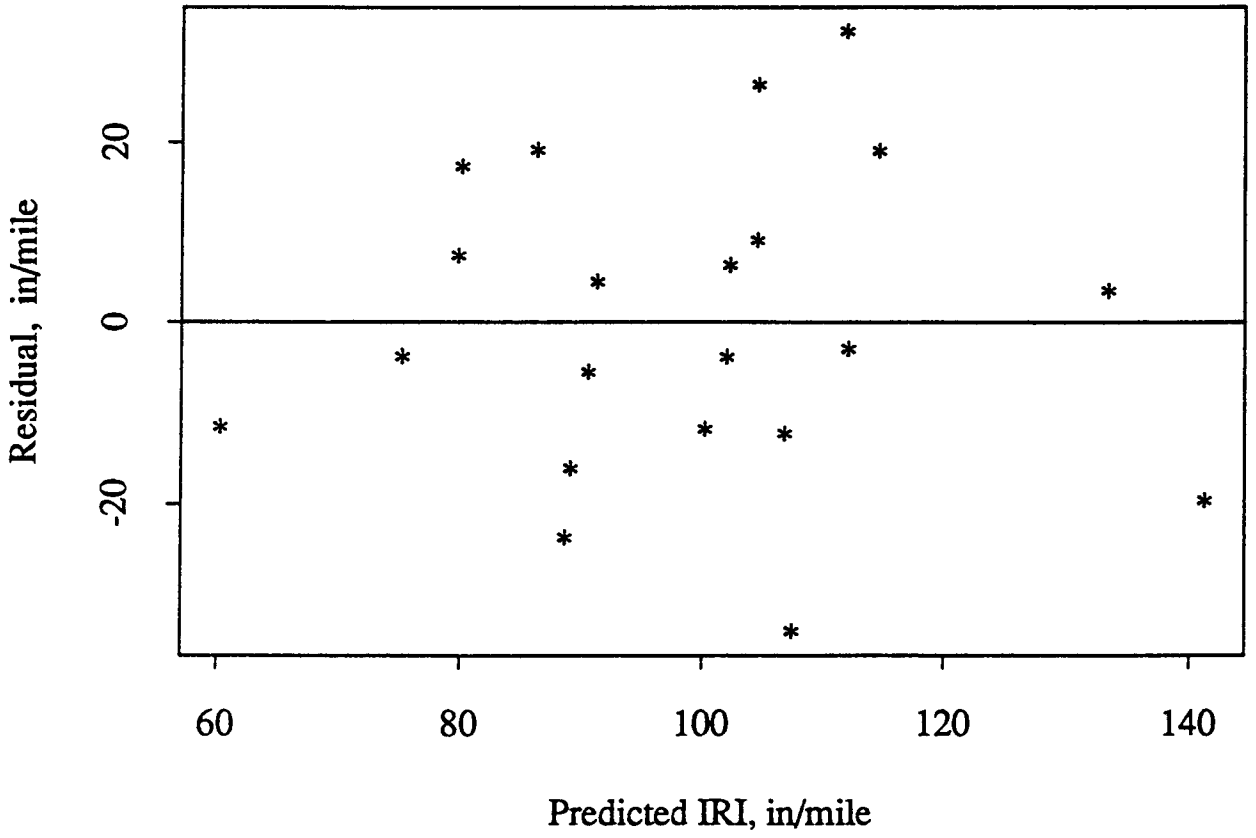

Figure 8.37. Plot of Residuals vs. Predicted IRI for Doweled JPCP

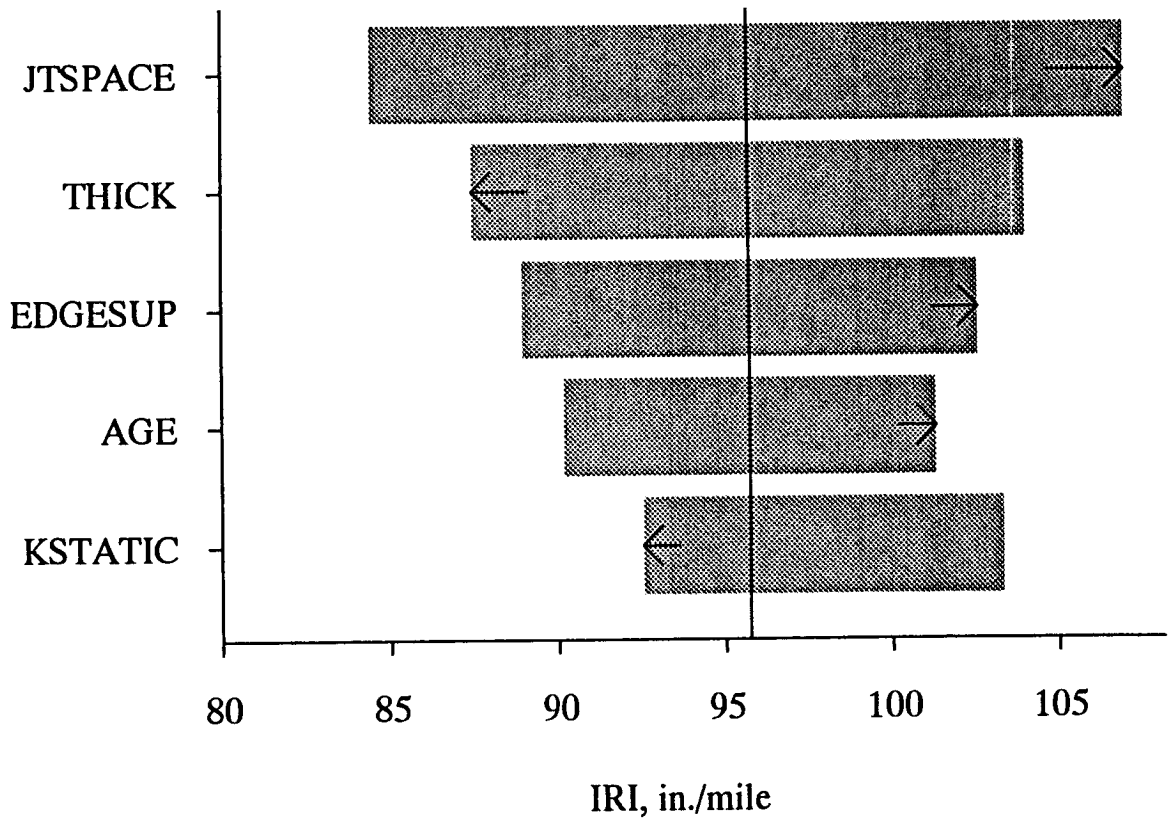

Figure 8.38. Sensitivity Analysis for IRI Model for Doweled JPCP

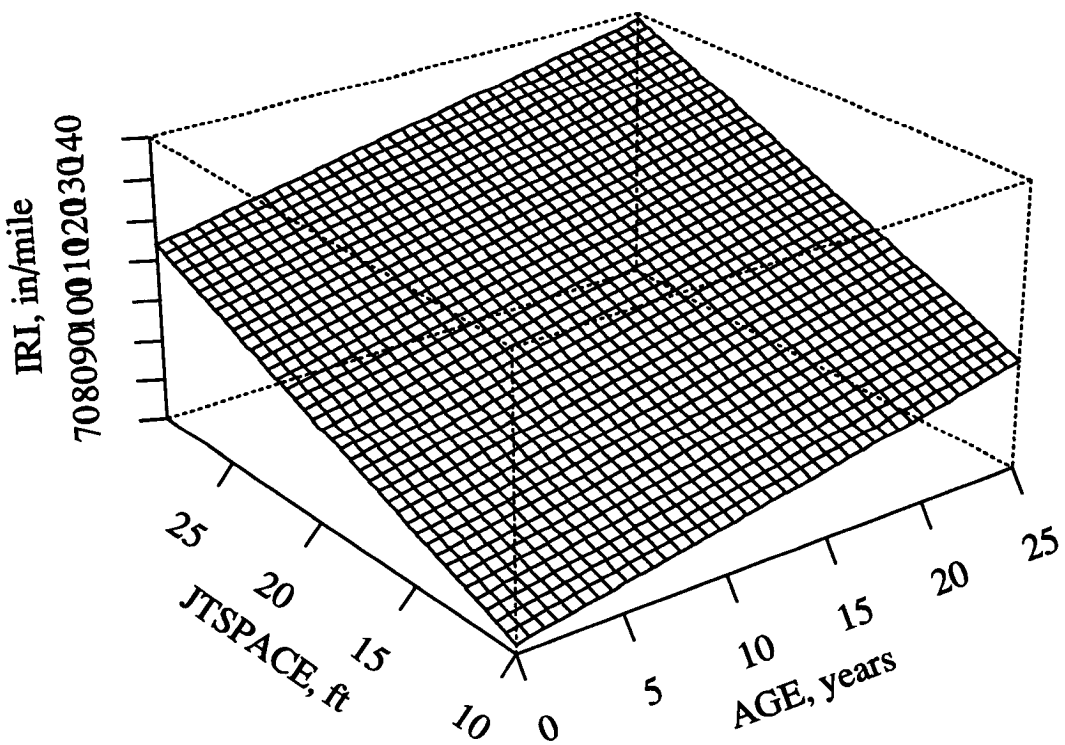

Figure 8.39. Three-Dimensional Plot of IRI Model for Doweled JPCP

According to the model, as joint spacing increases, IRI increases. (This result may relate to the faulting model for doweled JPCP and JRCP, where increased joint spacing resulted in increased faulting.) As THICK increases, IRI decreases, perhaps indicating that thicker slabs develop fewer distresses such as transverse cracking that cause roughness. The indication that the presence of a tied concrete shoulder, EDGESUP, results in an increase in IRI is difficult to explain.

AGE probably represents a combination of factors, including traffic loadings and the effect of cycles of climatic changes, such as joint opening/closing, thermal curling cycles, and freeze-thaw cycles, on the pavement. AGE may also represent time-dependent settlements or heaves of the foundation. (No climatic variables were sufficiently strong enough to appear in the model.) Similar to the results for several of the distress types such as faulting and cracking, the model shows that a stiffer subgrade, as measured by the backcalculated KSTATIC, lowers the IRI. A three-dimensional plot showing the relationship between the predicted IRI, JTSPACE, and AGE is shown in Figure 8.39.

This model for predicting the IRI of doweled JPCP includes several variables known to affect roughness from previous studies, and the senses of the effects (increase with variable magnitude increases or decreases the predicted distress) appear logical. There are, however, several variables that were expected to have an effect that are not represented in the model, including base type (untreated versus treated) and several climatic variables. With only an R^2 of 0.55 and a RMSE of 19 in./mi. (30.6 cm/km), there is considerable room for improvement of this model.

IRI of Non-Doweled JPCP

The IRI for non-doweled JPCP is also calculated from the longitudinal profile and is reported in units of in./mi., m/km, or cm/km. As in the previous case, the IRI for non-doweled JPCP has been shown to correlate with the subjective rating of highway users and thus to rehabilitation needs based on roughness. The development of a model for predicting the IRI of non-doweled JPCP, with the procedure outlined in Chapter 6, is described in this section.

Database, Dependent Variables, and Explanatory Variables

The data used for the development of an IRI model for non-doweled sections were obtained from GPS-3 (JPCP) sections. The IRI measured over the LTPP section was used as the dependent variable.

The potential explanatory variables for the model were chosen as those identified by the experts to be significant, provided they were available in the LTPP Database. The initial explanatory variables that were considered are as follows:

THICK: slab thickness, in.
PCCSTR: indirect tensile strength of PCC (cores), psi
TYPAGG: type of coarse aggregate in concrete
PCCAGG: gradation of coarse aggregate in PCC
JTSEAL: joint seal type (several types are listed in the database)
JTSPACE: mean transverse joint spacing, ft
JTEFF: joint load transfer efficiency
DRAIN: drainage provisions (0 = no subdrainage; 1 = subdrainage)

EDGESUP: edge support (1 = tied PCC shoulder; 0 = other shoulder types)
BASE: base type (0 = untreated aggregate; 1= treated aggregate)

KSTATIC: static backcalculated k-value, psi/in.
SUBGRADE: subgrade soil classification (0 = fine grained; 1 = coarse grained)
PM200: subgrade soil passing #200 sieve, %

CESAL: accumulative 18,000 lb. (80kN) ESALs in traffic lane, millions
AGE: time since construction, years

PRECIP: average annual precipitation, in.
FT: mean number of annual air freeze-thaw cycles
TRANGE: mean monthly temperature range (mean maximum daily temperature minus mean minimum daily temperature for each month averaged over the year), °F
FI: freeze index, degree-days (°F) below freezing
DAYS90: number of days temperature greater than 90°F (32°C)

There were little or no data for some of these variables, including PCCAGG and PM200, and these variables were, therefore, not considered in the model development. Review of the data for individual test sections indicated that data were missing that were expected to be significant to the predictions of IRI of nondoweled JPCP. Examples of the variables for which data were missing include IRI, JTSPACE, CESAL, and TRANGE. Sections missing such data could not be used in the analysis.

Data Review and Evaluation

Various statistical properties of the data were determined and examined. These included the mean, minimum, maximum, and standard deviation of each dependent and independent variable to determine their distributions. All data were also assembled, sorted several ways, and studied to detect any abnormalities or obvious errors. Two-dimensional plots of all the variables were prepared and the bivariate relationships were examined. A correlation matrix that shows the strength of the relationship between all dependent and independent variables is presented in Table 8.8.

Table 8.8. Correlation Matrix for Selected Variables for Non-Doweled JPCP IRI

	THICK	FT	BASE	CESAL	DAYS32	EDGESUP	KSTATIC	AGE	PCCSTR	SUBGRADE	TRANGE	PRECIP	IRI
THICK	1.000	0.000	0.020	0.587	-0.036	-0.004	0.252	0.400	0.492	-0.490	-0.008	-0.137	0.460
FT	-0.001	1.000	-0.401	-0.264	0.932	0.337	0.031	-0.300	-0.013	-0.018	0.878	-0.215	0.000
BASE	0.020	-0.400	1.000	0.112	-0.558	0.000	0.370	0.260	0.196	0.041	-0.540	-0.338	-0.300
CESAL	0.587	-0.300	0.112	1.000	-0.281	-0.206	0.089	0.520	0.213	-0.162	-0.321	0.069	0.600
DAYS32	-0.036	0.930	-0.558	-0.281	1.000	0.290	-0.186	-0.400	-0.050	0.046	0.931	-0.136	0.040
EDGESUP	-0.004	0.340	0.000	-0.206	0.290	1.000	0.441	-0.100	-0.011	-0.062	0.223	-0.102	-0.100
KSTATIC	0.252	0.030	0.370	0.089	-0.186	0.441	1.000	0.370	0.257	-0.151	-0.251	-0.127	0.000
AGE	0.400	-0.300	0.263	0.523	-0.381	-0.136	0.372	1.000	-0.116	-0.217	-0.314	0.324	0.410
PCCSTR	0.492	0.000	0.196	0.213	-0.050	-0.011	0.257	-0.100	1.000	-0.196	0.000	-0.597	0.000
SUBGRADE	-0.490	0.000	0.041	-0.162	0.046	-0.062	-0.151	-0.200	-0.196	1.000	0.023	0.014	-0.200
TRANGE	-0.008	0.880	-0.540	-0.321	0.931	0.223	-0.251	-0.300	0.000	0.023	1.000	-0.159	0.000
PRECIP	-0.137	-0.200	-0.338	0.069	-0.136	-0.102	-0.127	0.320	-0.597	0.014	-0.159	1.000	0.470
IRI	0.455	0.000	-0.274	0.602	0.044	-0.111	-0.005	0.410	-0.052	-0.248	-0.025	0.474	1.000

The effects of multiple explanatory variables on the IRI of non-doweled JPCP were also studied by using three-dimensional plots to display general trends in IRI with two selected explanatory variables. One example of such a plot is given in Figure 8.40, which shows the relationship between IRI, PRECIP, and CESAL. The unusual peaks and reverse slopes in the surface of this plot point to anomalies in the data. The data causing such abnormalities were identified and closely examined to determine if they required any special attention. Twenty-eight sections remained for the development of the model after the deletion of sections with missing and erroneous data.

Model Building

Model development started with an effort to determine the general functional form of IRI over time and traffic. Since time series data were not available to identify a typical functional form for change in IRI with time and traffic, the functional form of PSI, which is closely related to IRI, was used as a starting point. Two previous studies on in-service pavements show a rapid drop in PSI at the beginning of service and then a leveling off for a long period thereafter, which may then be followed by another rapid drop as severe deterioration sets in.[9, 10] This functional form was assumed for IRI of non-doweled JPCP.

Because IRI is not zero when AGE is zero (immediately after construction due to construction) because of construction variation, it was not possible to use the change in IRI as the dependent variable since the initial IRI was not measured for any of the sections. Therefore, the measured IRI was selected as the dependent variable for the model to be developed.

Based on expert judgment and previous data observations, several explanatory variables were selected for testing. Regression analyses were conducted with a variety of techniques to try to develop the most appropriate IRI prediction model. The following briefly describes the techniques used in the analyses:

- The explanatory variables were tested to determine their significance in the overall model. Those that were not found to be significant were not considered further, even in cases where the variables were expected to be significant to the occurrence of IRI.

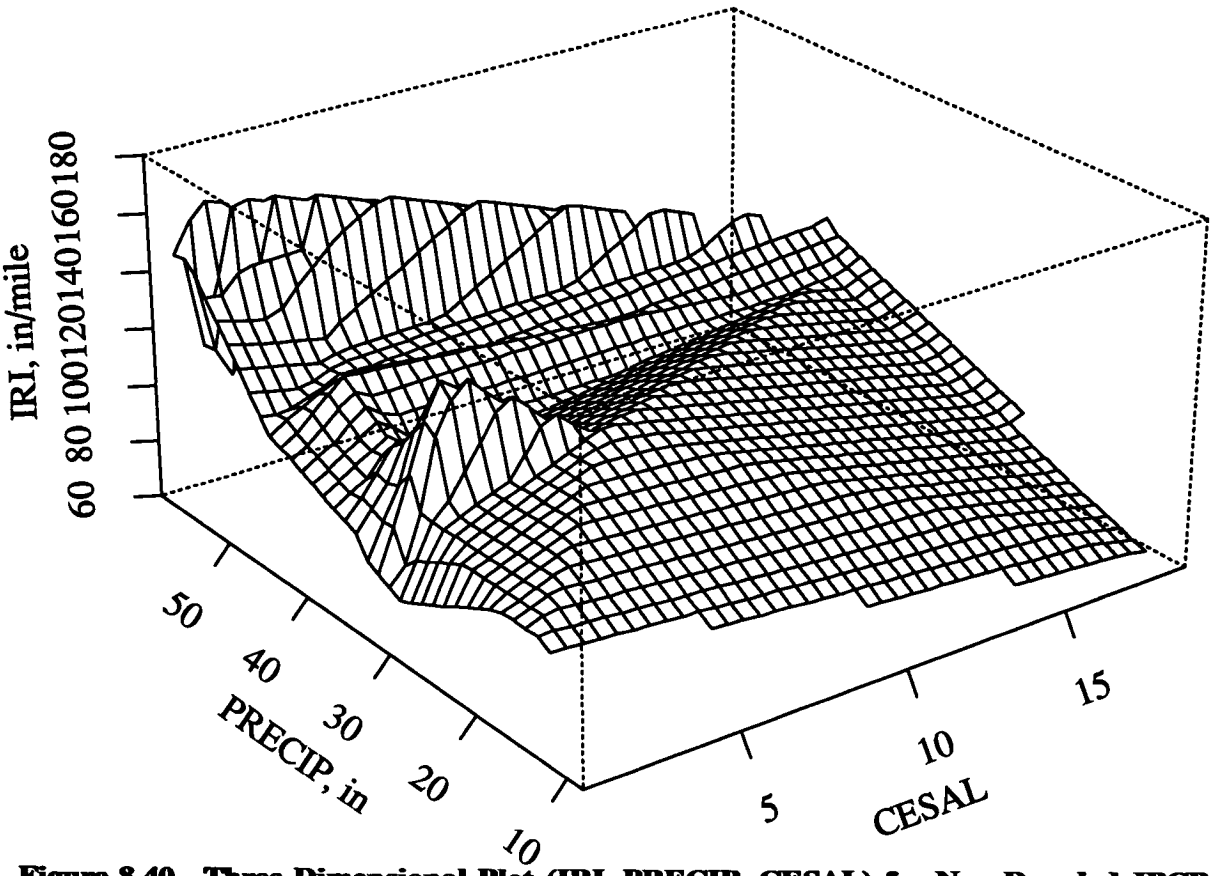

Figure 8.40. Three-Dimensional Plot (IRI, PRECIP, CESAL) for Non-Doweled JPCP

- The variables were examined to determine if there were any significant interactions between them. None were found to be significant.
- Tests for collinearity between the explanatory variables were conducted throughout the model development phase. When such collinearity was found, one of the variables was eliminated from the model.
- Observations of the previous two- and three-dimensional plots indicated that, generally, all the variables were linearly related to IRI.

Through the application of these techniques, the following model was developed for predicting IRI for non-doweled JPCP sections with data from the GPS-3 pavement sections:

$$IRI = 38.85 + 12.89 * CESAL + 0.2217 * FT + 1.498 * PRECIP - 10.96 * BASE - 13.69 * SUBGRADE \quad (8.9)$$

where

IRI	=	International Roughness Index, in./mi.
CESAL	=	cumulative 18,000 lb. (80kN) ESALs in traffic lane, millions
PRECIP	=	mean annual precipitation, in.
FT	=	mean annual air freeze-thaw cycles
BASE	=	1 = treated granular material (with asphalt oement) or lean concrete; 0 = if untreated granular material
SUBGRADE	=	1 = AASHTO classification (A-1, A-2, A-3 coarse grained); 0 = if AASHTO classification (A-4, A-5, A-6, A-7 fine grained)

Statistics:

N	=	28 sections
R^2	=	0.644
RMSE	=	31.29 (in./mi.) (50 cm/km)

Figure 8.41 shows a plot of the predicted versus actual IRI, and Figure 8.42 shows a plot of the residuals versus predicted IRI for this model. The results of a sensitivity analysis of the model are presented in Figure 8.43. The results indicate that CESAL has the largest effect on IRI of non-doweled JPCP, followed closely by PRECIP, FT, SUBGRADE, and BASE. The form of the model indicates a linear increase in IRI with cumulative ESALs.

Specifically, IRI increases linearly as CESAL increases. This result is related to the various distress types such as faulting and cracking that develop with increased traffic loadings. As PRECIP and FT increase, the IRI increases, which indicates the significant effects a severe climate has on the deterioration of non-doweled JPCP.

Base type (BASE) affects IRI in that treated bases result in a decrease in IRI in comparison to untreated bases. Subgrade soil classification (SUBGRADE) also affects IRI; coarse-grained soils result in a lower IRI over time than do fine-grained soils. These results support the common belief that better subgrades and bases result in smoother pavements.

A three-dimensional plot that shows the relationship between the predicted IRI, PRECIP and CESAL, is shown in Figure 8.44.

Several variables, such as joint spacing, that are known from previous studies to affect IRI do not appear in the model. The small number of sections (28) that were available for the development of the model also limited its adequacy. The R^2 of 0.64 and RMSE of 31 in./mi. (50 cm/km) indicate that there is considerable room for improvement of this model.

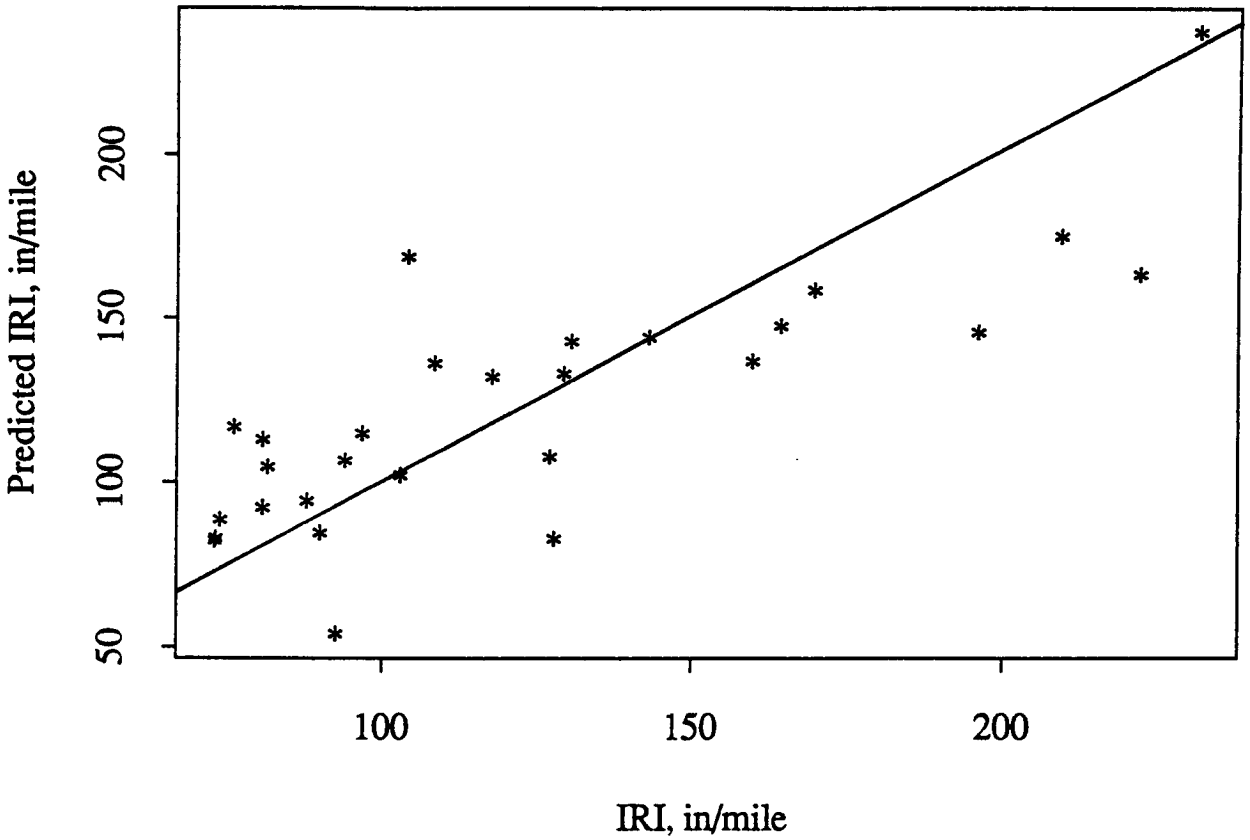

Figure 8.41. Predicted vs. Actual IRI for Non-Doweled JPCP Model

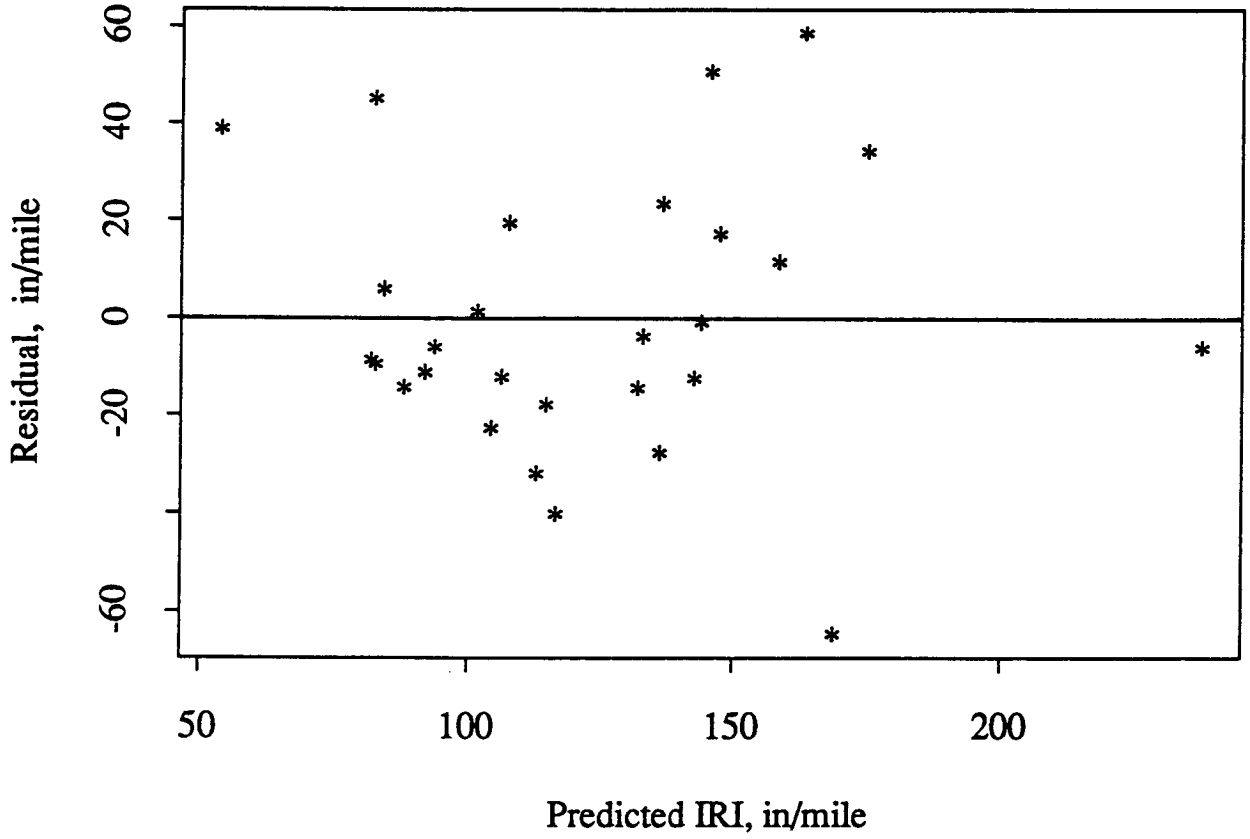

Figure 8.42. Plot of Residuals vs. Predicted IRI for Non-Doweled JPCP Model

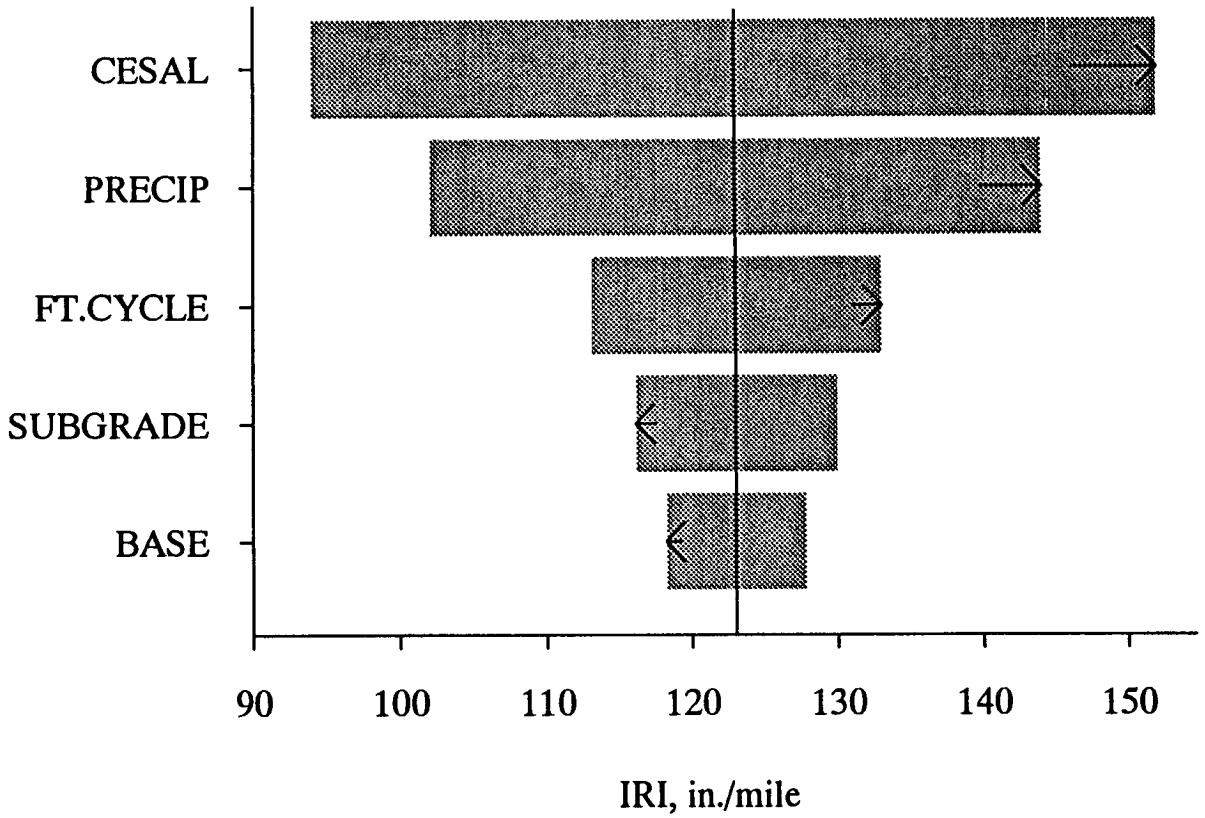

Figure 8.43. Sensitivity Analysis for IRI Model for Non-Doweled JPCP

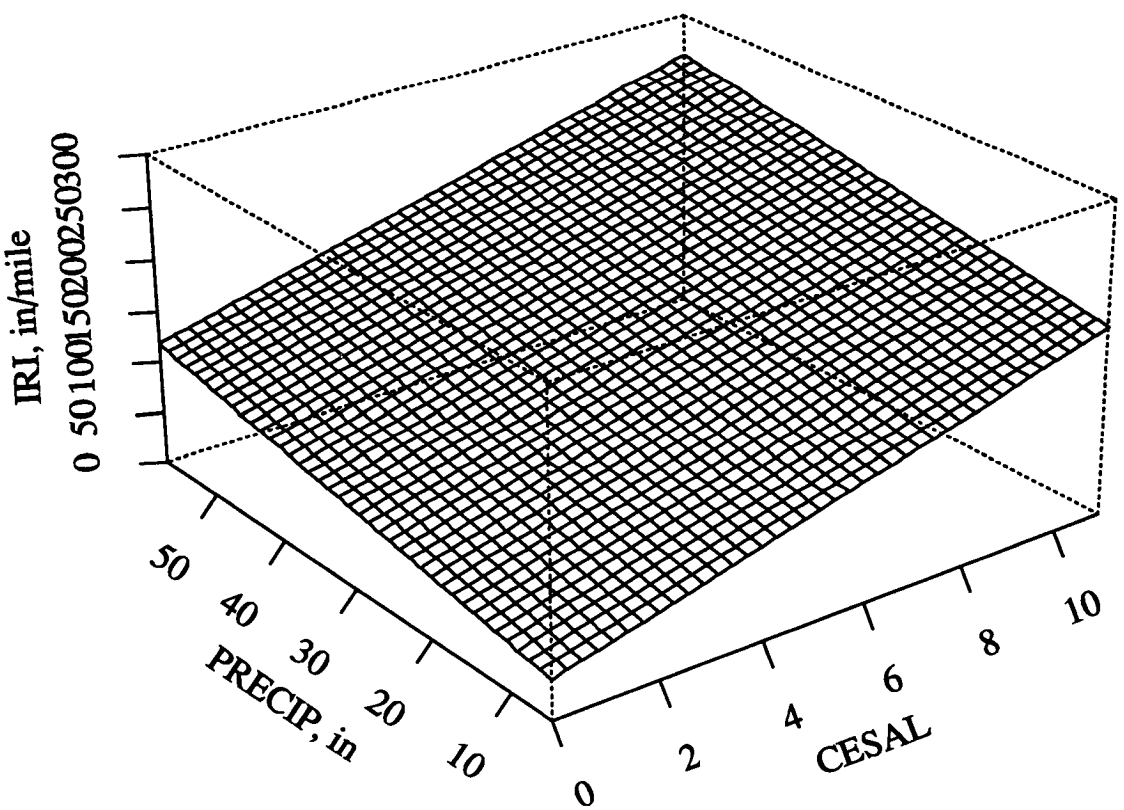

Figure 8.44. Three-Dimensional Plot of IRI Model for Non-Doweled JPCP

IRI of JRCP

The IRI of JRCP is also calculated from the longitudinal profile and is reported in units of in./mi., m/km, or cm/km. It also correlates well with the subjective rating of highway users and therefore is a good indicator of highway users' response to the pavement and of rehabilitation needs based on roughness. The general procedure outlined in Chapter 6 for model development was utilized to obtain an IRI model for JRCP.

Database, Dependent Variables, and Explanatory Variables

Data from the GPS-4 (JRCP) sections of the LTPP Database were used to form the initial database for the development of this IRI model. The IRIs measured over these sections were used to represent the dependent variable.

The explanatory variables identified by the experts to be significant to the IRI of JRCP were selected for consideration, provided they were available in the LTPP Database. The initial explanatory variables that were considered are as follows:

THICK:	slab thickness, in.
PCCSTR:	indirect tensile strength of PCC (cores), psi
TYPAGG:	type of coarse aggregate in concrete
PCCAGG:	gradation of coarse aggregate in PCC
JTEFF:	joint load transfer efficiency
JTSPACE:	mean transverse joint spacing, ft
JTSEAL:	joint seal type (several types are listed in the database)
PSTEEL:	percentage of longitudinal reinforcement, percentage of area
EDGESUP:	edge support (1 = tied PCC shoulder; 0 = other shoulder types)
DRAIN:	subgrade provisions (0 = no subdrainage; 1 = if subdrainage)
BASETYP:	base type (0 = untreated aggregate; 1 = treated aggregate)
KSTATIC:	static backcalculated k-value, psi/in.
SUBGRADE:	subgrade soil classification (0 = fine grained; 1 = coarse grained)
PM200:	subgrade soil passing #200 sieve, %
CESAL:	cumulative 18,000 lb. (80kN) ESALs in traffic lane, millions
AGE:	time since construction, years
PRECIP:	average annual precipitation, in.
FT:	mean number of annual air freeze-thaw cycles
FI:	freeze index, degree-days (°F) below freezing

DAYS90: number of days temperature greater than 90°F
TRANGE: mean monthly temperature range (mean maximum daily temperature minus mean minimum daily temperature for each month averaged over the year), °F

There were little or no data for several of these variables, such as PCCAGG and PM200; therefore, these could not be considered in the development of the model. The data for each section were also reviewed to determine if any data expected to be significant were missing. Examples of such missing data for some of the sections include IRI, JTSPACE, CESAL, and TRANGE. Sections with such missing data could not be used in the analysis.

Data Review and Evaluation

Evaluation of the data consisted of examination of the mean, minimum, maximum, and standard deviation of each dependent and independent variable to determine its distribution. The data were then assembled into matrix form, sorted several ways, and studied to determine any abnormalities or obviously erroneous data. The bivariate relationships between all the variables were also studied with two-dimensional plots. A correlation matrix obtained to show the strengths of the correlations among all the dependent and independent variables is presented in Table 8.9.

Three-dimensional plots were used to visualize the general trends of IRI with several of the explanatory variables. Figure 8.45, which shows the relationship between IRI, PRECIPS, and AGE, is one example of these plots. With such plots, unusual peaks and reverse slopes that correspond to atypical data were investigated. Thirty-two test sections remained for the model development after sections with missing and erroneous data had been deleted.

Model Building

The first step in building the model was to identify the general functional form of the IRI of JRCP over time and traffic. Similar to the other IRI models for the other pavement types, the known functional form for PSI was used as a basis. In two previous studies on in service pavements, PSI was shown to drop somewhat rapidly at first and then level out for a long period, which may then be followed by another rapid drop as severe pavement deterioration occurs.[9, 10]

It is also known that when AGE is zero at construction, the IRI is not zero due to construction variation. The initial IRI was not measured for any of the sections and, therefore, could not be used in the model development. Based on all these considerations, the measured IRI on the pavement sections was selected as the dependent variable to use in the model.

Table 8.9. Correlation Matrix for Selected Variables for IRI for JRCP

	THICK	FT	BASETYP	CESAL	DAYS32	DRAIN	EDGESUP	JTSPACE	KSTATIC	AGE	PCCSTR	SUBGRADE	TRANGE	PRECIP	IRI
THICK	1.000	-0.200	0.230	0.078	-0.221	0.009	0.118	0.318	0.138	0.060	0.182	-0.133	-0.320	0.155	0.670
FT	-0.241	1.000	-0.423	-0.099	0.935	0.128	-0.106	-0.247	0.230	-0.300	-0.538	0.214	0.827	-0.799	-0.400
BASETYP	0.230	-0.400	1.000	-0.126	-0.450	-0.149	0.318	0.029	-0.013	-0.200	0.150	-0.115	-0.401	0.316	0.320
CESAL	0.078	0.000	-0.126	1.000	-0.048	-0.119	-0.194	0.334	-0.182	0.530	0.084	-0.084	-0.105	0.066	0.090
DAYS32	-0.221	0.940	-0.450	-0.048	1.000	0.173	-0.256	-0.334	0.215	-0.300	-0.376	0.216	0.900	-0.869	-0.400
DRAIN	0.009	0.130	-0.149	-0.119	0.173	1.000	0.180	-0.085	-0.082	-0.300	-0.114	-0.139	0.354	-0.166	0.000
EDGESUP	0.118	-0.100	0.318	-0.194	-0.256	0.180	1.000	-0.017	-0.057	-0.300	-0.071	-0.129	-0.179	0.195	0.430
JTSPACE	0.318	-0.200	0.029	0.334	-0.334	-0.085	-0.017	1.000	-0.230	0.450	0.164	-0.206	-0.397	0.366	0.340
KSTATIC	0.138	0.230	-0.013	-0.182	0.215	-0.082	-0.057	-0.230	1.000	-0.200	-0.142	0.123	-0.052	-0.190	-0.300
AGE	0.055	-0.300	-0.229	0.529	-0.321	-0.276	-0.264	0.445	-0.222	1.000	0.291	0.041	-0.377	0.410	0.300
PCCSTR	0.182	-0.500	0.150	0.084	-0.376	-0.114	-0.071	0.164	-0.142	0.290	1.000	-0.288	-0.378	0.363	0.170
SUBGRADE	-0.133	0.210	-0.115	-0.084	0.216	-0.139	-0.129	-0.206	0.123	0.040	-0.288	1.000	0.130	-0.076	-0.100
TRANGE	-0.320	0.830	-0.401	-0.105	0.900	0.354	-0.179	-0.397	-0.052	-0.400	-0.378	0.130	1.000	-0.852	-0.500
PRECIP	0.155	-0.800	0.316	0.066	-0.869	-0.166	0.195	0.366	-0.190	0.410	0.363	-0.076	-0.852	1.000	0.480
IRI	0.666	-0.400	0.319	0.094	-0.440	-0.063	0.425	0.340	-0.256	0.300	0.172	-0.126	-0.453	0.480	1.000

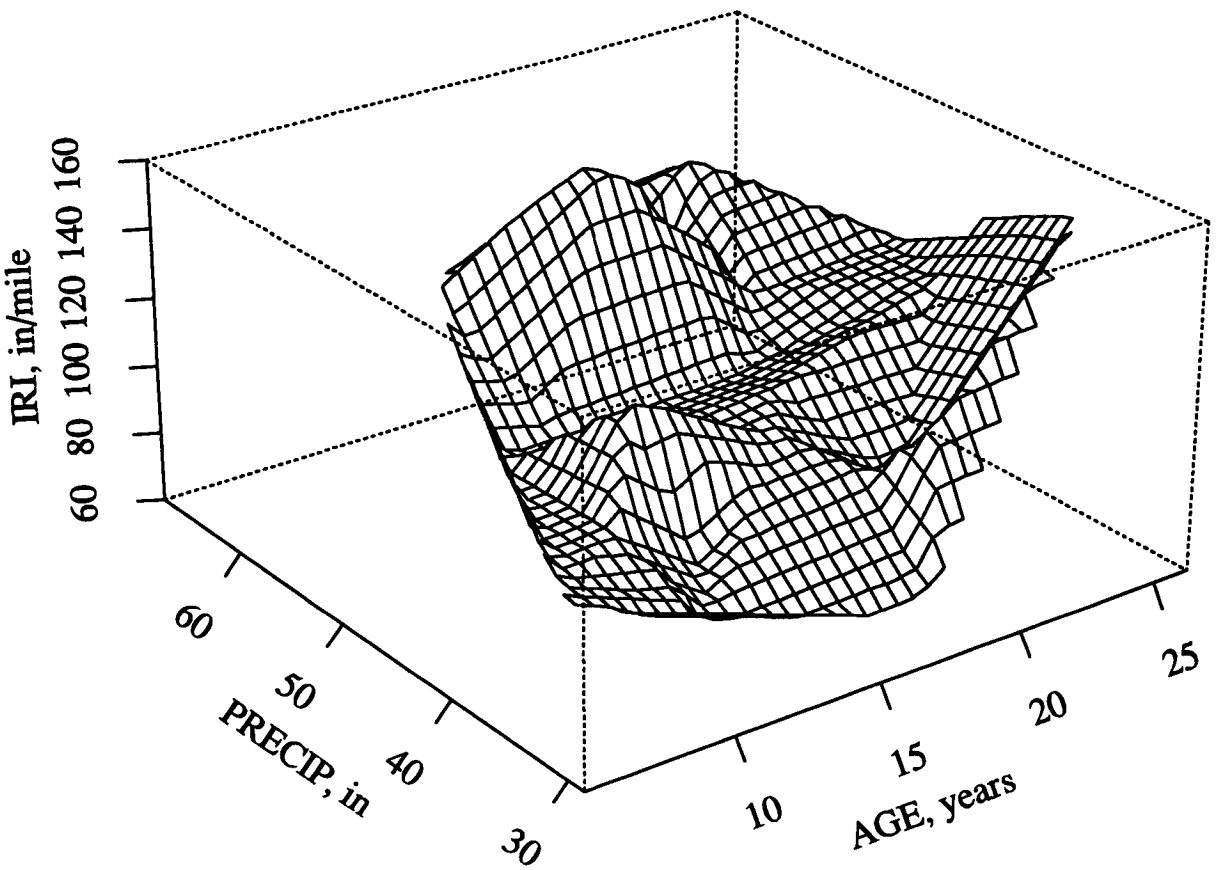

Figure 8.45. Three-Dimensional Plot (IRI, PRECIP, AGE) for JRCP

Several explanatory variables were chosen for testing based on the results of expert judgment and previous data observations. Regression analyses were then conducted with a variety of techniques to relate the explanatory variables to the predicted IRI. The following briefly describe the techniques utilized in the analyses:

- All the explanatory variables were tested to determine their significance in the overall model. Those that were not significant were deleted.
- Several interactions between variables were evaluated, but none were found to be significant.
- Tests for collinearity between the explanatory variables were conducted throughout the model development phase. When such collinearity was found, one of the variables was eliminated from the model.
- Observations of the previous two- and three-dimensional plots indicated that KSTATIC was not linearly related to IRI. The relationship was linearized by using 1/KSTATIC as the independent variable.

Based on using these techniques and the data from the GPS-4 sections, the following model was developed for predicting IRI for JRCP sections:

$$IRI = -141 + 0.849 * AGE + 0.347 * PRECIP + 1390 * \left(\frac{1}{KSTATIC}\right) + 21.2 * THICK + 15.1 * EDGESUP \quad (8.10)$$

where

IRI	=	International Roughness Index, in./mi
AGE	=	age since construction, years
THICK	=	concrete slab thickness, in.
KSTATIC	=	mean backcalculated static k-value, psi/in.
PRECIP	=	mean annual precipitation, in.
EDGESUP	=	1 = tied concrete shoulder; 0 = any other shoulder type

Statistics:

N	=	32 sections
R^2	=	0.78
RMSE	=	9.86 (in./mi.) (15.6 cm/km)

A plot of the predicted IRI based on this model versus actual IRI is shown in Figure 8.46. Figure 8.47 shows a plot of the residuals versus predicted IRI. The results of a sensitivity analysis of the model are shown in Figure 8.48. THICK has the largest effect on IRI of JRCP, followed closely by KSTATIC, EDGESUP, AGE, and PRECIP. The form of the model shows a linear increase in IRI over time.

The specific trends shown by the model include an increase in IRI when slab thickness increases. While this may seem illogical, one possible explanation may be that the thicker slabs in the GPS-4 database may have been constructed rougher originally. According to the model, the presence of a tied concrete shoulder increases the IRI slightly, which may also be related to initial construction.

AGE probably represents a combination of factors, including traffic loadings and the effect on pavements of cycles of climatic changes such as joint opening/closing, thermal curling cycles, and freeze-thaw cycles. IRI is shown to increase with time, or AGE. One climatic variable, PRECIP, also showed a sufficient effect to be included in the model. As PRECIP increases, IRI increases.

The model indicated that the stiffer the subgrade, as measured by the backcalculated KSTATIC, the lower the IRI. This result correlates with models developed for several key distress types that showed that stiffer subgrades resulted in decreased faulting and cracking. A three-dimensional plot that shows the relationship between the predicted IRI, PRECIP, and AGE is presented in Figure 8.49.

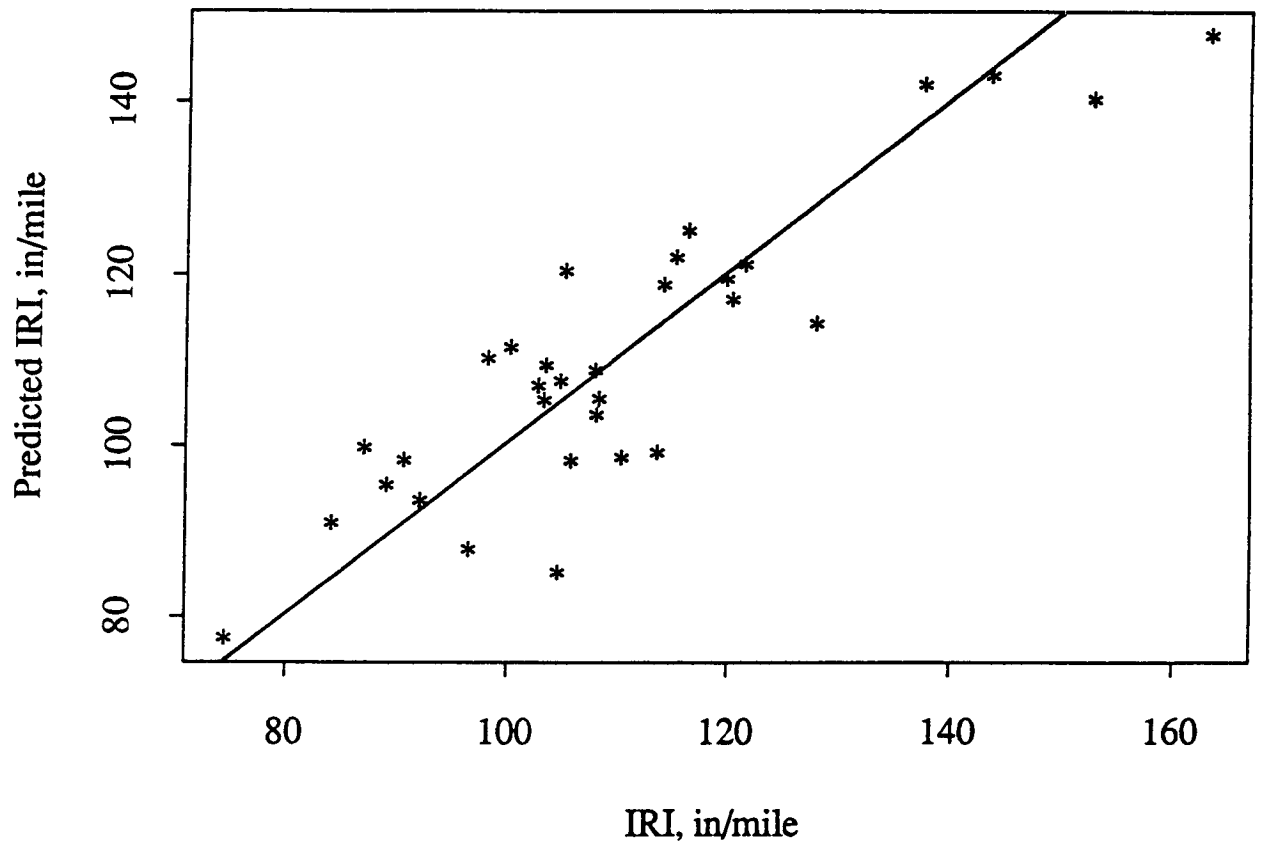

Figure 8.46. Predicted vs. Actual IRI for JRCP

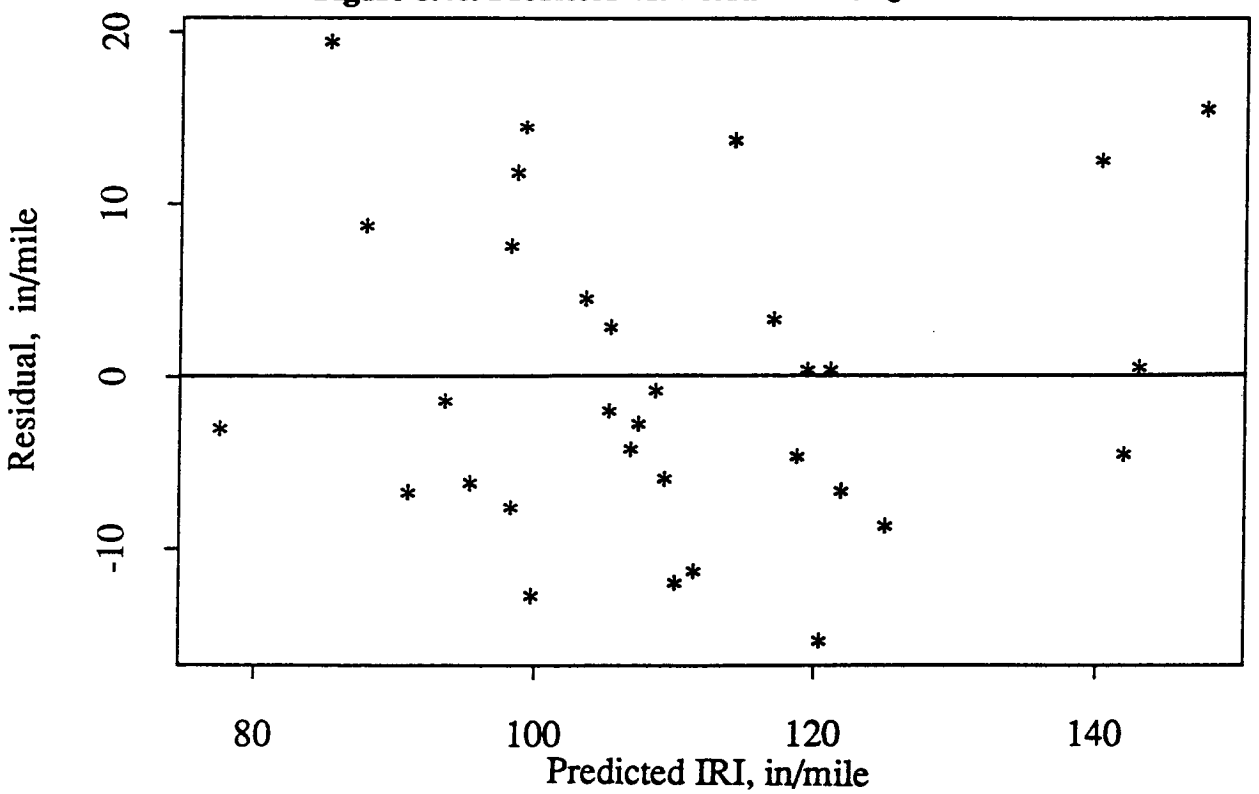

Figure 8.47. Plot of Residuals vs. Predicted IRI for JPCP

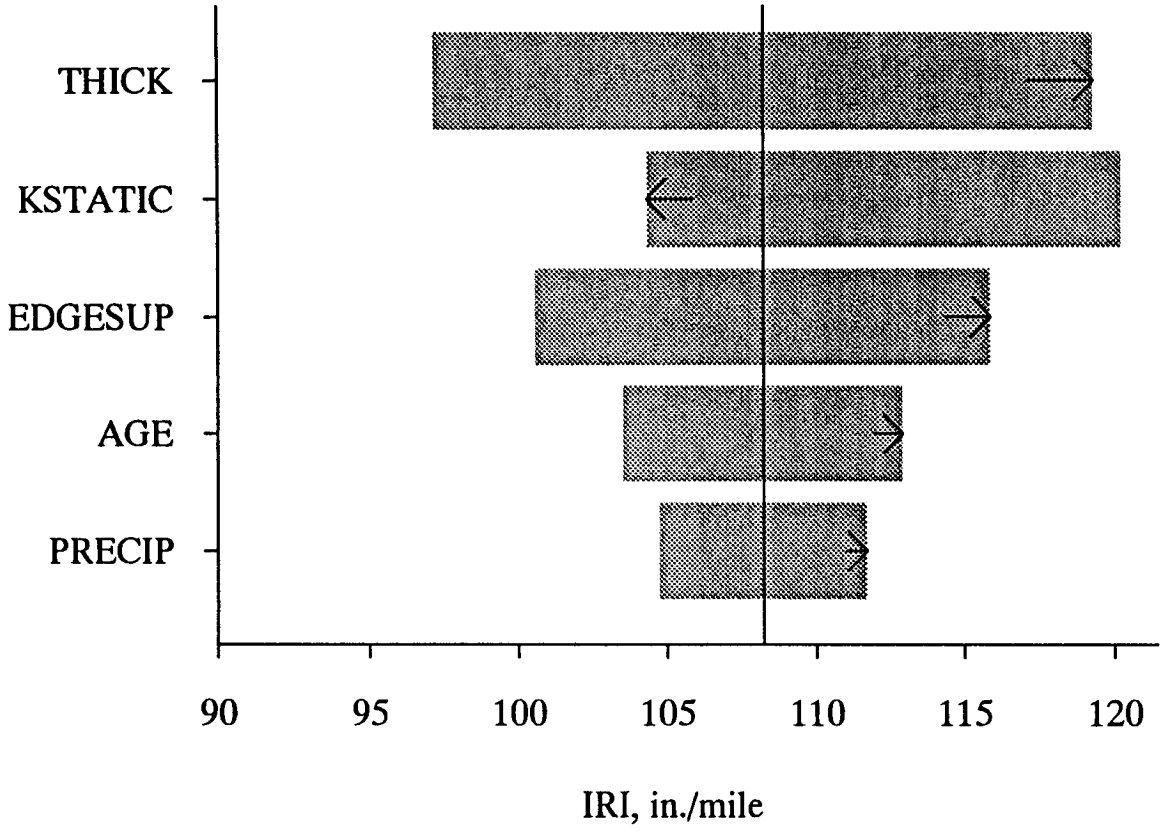

Figure 8.48. Sensitivity Analysis for IRI Model for JRCP

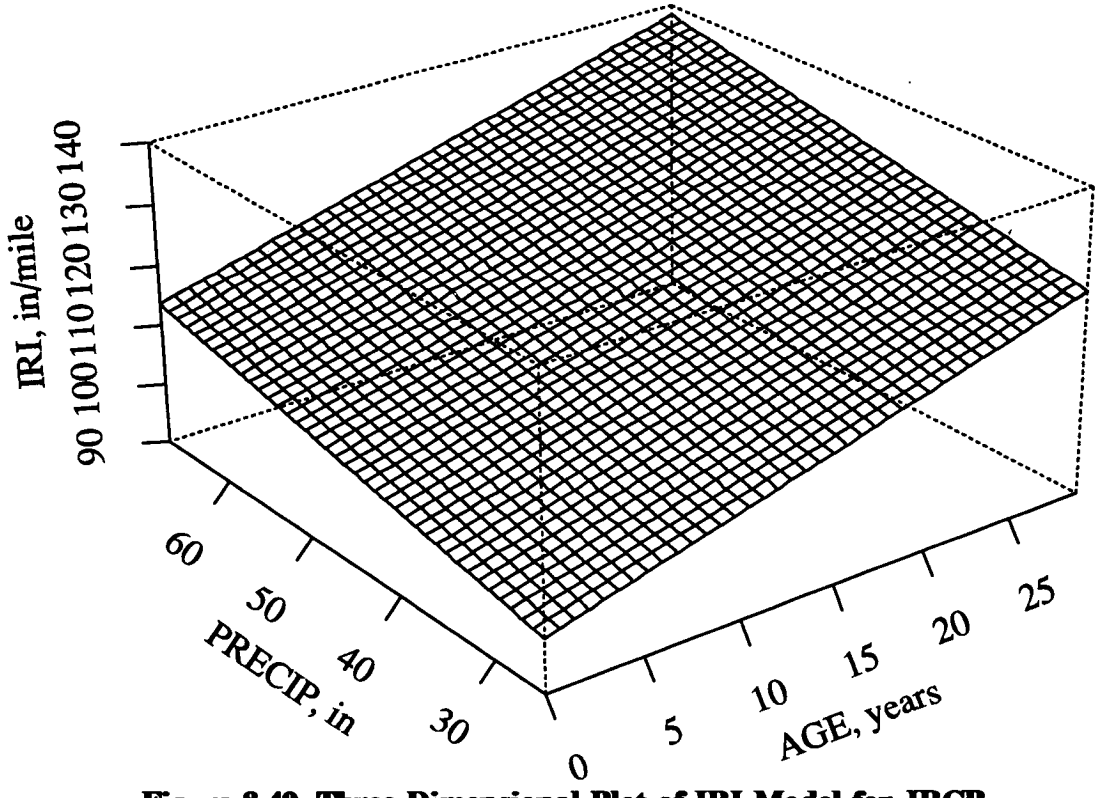

Figure 8.49. Three-Dimensional Plot of IRI Model for JRCP

The model developed for predicting the IRI of JRCP includes several variables that are known from previous studies, to affect roughness and the senses of these effects (increase in variables increases or decreases IRI) were consistent with results from previous studies. However, there are several other variables, including base type (untreated versus treated) and climatic variables, missing from the model that were expected to have an effect on IRI.

IRI of CRCP

The IRI for CRCP is calculated from the longitudinal profile and is reported in units of in./mi., m/km, or cm/km. The IRI for CRCP has also been shown to correlate well with the subjective rating of highway users and is a good indicator of highway users' response to the pavement and, consequently, of rehabilitation needs based on roughness. The general procedure outlined in Chapter 6 for model development was used to obtain an IRI model for CRCP.

Database, Dependent Variables, and Explanatory Variables

Data for the GPS-5 (CRCP) sections in the LTPP Database were used to provide the initial database. The IRIs measured over the sections were available to represent the dependent variable.

The potential explanatory variables that were selected for consideration in the model were those identified by the experts to be significant, provided they were available in the LTPP Database. The initial explanatory variables that were considered are as follows:

THICK: slab thickness, in.
PCCSTR: indirect tensile strength of PCC (cores), psi
TYPAGG: type of coarse aggregate in concrete
PCCAGG: gradation of coarse aggregate in PCC

JTEFF: joint load transfer efficiency
PSTEEL: percentage of longitudinal reinforcement, % area
EDGESUP: edge support (1 = tied PCC shoulder; 0 = other shoulder types)
JTSEAL: joint seal type (several types are listed in the database)
DRAIN: subdrainage provisions (0 = no subdrainage; 1 = if subdrainage)

BASETYP: base type (0 = untreated aggregate; 1 = treated aggregate)

KSTATIC: static backcalculated k-value, psi/in.
SUBGRADE: subgrade soil classification (0 = fine grained; 1 = coarse grained)
PM200: subgrade soil passing #200 sieve, %

AGE: time since construction, years

CESAL:	cumulative 18,000 lb. (80kN) ESALs in traffic lane, millions
PRECIP:	average annual precipitation, in.
FT:	mean number of annual air freeze-thaw cycles
FI:	freeze index, degree-days (°F) below freezing
DAYS90:	number of days temperature greater than 90°F
TRANGE:	mean monthly temperature range (mean maximum daily temperature minus mean minimum daily temperature for each month averaged over the year), °F

Among these variables, were several for which little or no data were available in the database, which made it impossible for them to be considered in the model development. These included PCCAGG and PM200. Data for test sections in the initial database were also reviewed to determine if any sections had data missing that were expected to be specific. Those test sections with such data missing could not be included in the model development. Examples of such missing data included IRI, PSTEEL, CESAL, and TRANGE.

Data Review and Evaluation

Evaluation of the data in the database included examination of the distribution of each dependent and independent variable. This included an examination of the values of various statistics for the variables, including the mean, minimum, maximum, and standard deviation. The data were also assembled into matrix form, sorted several ways, and studied to identify any abnormalities or obvious errors. Two-dimensional plots of all variables were also used to examine the bivariate relationships between them. A correlation matrix that shows the strength of the relationship between all the dependent and independent variables is presented in Table 8.10.

Several three-dimensional plots were generated to help visualize the general trends between IRI and various combinations of the explanatory variables. An example of a three-dimensional plot that shows the relationship between IRI, PSTEEL, and AGE is presented in Figure 8.50. From such plots, the data causing unusual peaks and reverse slopes were identified for further examination. Forty-two sections remained for the model development after the sections identified to have missing and/or erroneous data were deleted.

Table 8.10. Correlation Matrix for Selected Variables for IRI for CRCP

	THICK	FT	BASETYP	CESAL	DAYS32	DRAIN	EDGESUP	KSTATIC	PSTEEL	AGE	PCCSTR	SUBGRADE	TRANGE	WETDAYS	WIDENED	PRECIP	IRI
THICK	1.000	0.000	0.089	0.141	-0.068	0.393	-0.078	-0.133	-0.153	-0.700	0.620	0.122	-0.249	0.383	0.718	-0.052	-0.300
FT	-0.020	1.000	-0.237	0.178	0.918	0.129	-0.216	-0.281	0.356	0.020	0.088	-0.166	0.695	-0.059	-0.085	-0.458	0.000
BASETYP	0.089	-0.200	1.000	0.144	-0.249	0.274	0.105	0.238	-0.164	-0.200	0.060	-0.248	-0.136	-0.259	0.014	-0.185	0.380
CESAL	0.141	0.180	0.144	1.000	0.145	-0.045	-0.171	-0.127	-0.117	0.190	-0.069	-0.063	-0.062	0.242	0.158	-0.001	0.230
DAYS32	-0.070	0.920	-0.249	0.145	1.000	0.141	-0.276	-0.270	0.489	0.140	0.095	-0.127	0.859	-0.081	-0.189	-0.464	-0.100
DRAIN	0.393	0.130	0.274	-0.045	0.141	1.000	-0.104	-0.143	0.096	-0.500	0.309	-0.074	-0.024	0.354	0.469	-0.010	-0.200
EDGESUP	-0.080	-0.200	0.105	-0.171	-0.276	-0.104	1.000	0.107	0.008	0.000	-0.082	-0.303	-0.132	-0.197	-0.196	0.184	0.200
KSTATIC	-0.130	-0.300	0.238	-0.127	-0.270	-0.143	0.107	1.000	-0.007	-0.100	-0.289	-0.039	-0.076	-0.225	-0.072	-0.058	0.120
PSTEEL	-0.150	0.360	-0.164	-0.117	0.489	0.096	0.008	-0.007	1.000	0.070	-0.052	-0.259	0.541	-0.141	-0.404	-0.148	-0.400
AGE	-0.650	0.020	-0.231	0.187	0.142	-0.463	0.001	-0.127	0.071	1.000	-0.481	-0.217	0.239	-0.141	-0.525	0.119	0.210
PCCSTR	0.620	0.090	0.060	-0.069	0.095	0.309	-0.082	-0.289	-0.052	-0.500	1.000	0.025	-0.056	0.213	0.473	-0.004	-0.300
SUBGRADE	0.122	-0.200	-0.248	-0.063	-0.127	-0.074	-0.303	-0.039	-0.259	-0.200	0.025	1.000	-0.257	0.161	0.277	0.055	-0.300
TRANGE	-0.250	0.700	-0.136	-0.062	0.859	-0.024	-0.132	-0.076	0.541	0.240	-0.056	-0.257	1.000	-0.393	-0.449	-0.575	0.000
WETDAYS	0.383	0.000	-0.259	0.242	-0.081	0.354	-0.197	-0.225	-0.141	-0.100	0.213	0.161	-0.393	1.000	0.479	0.577	-0.200
WIDENED	0.718	0.000	0.014	0.158	-0.189	0.469	-0.196	-0.072	-0.404	-0.500	0.473	0.277	-0.449	0.479	1.000	0.078	-0.200
PRECIP	-0.050	-0.500	-0.185	-0.001	-0.464	-0.010	0.184	-0.058	-0.148	0.120	-0.004	0.055	-0.575	0.577	0.078	1.000	0.000
IRI	-0.300	0.000	0.378	0.229	-0.134	-0.157	0.199	0.121	-0.418	0.210	-0.250	-0.311	0.006	-0.207	-0.238	-0.062	1.000

Model Building

As with the other models, the first step in model building was the identification of the general functional form of IRI with time and traffic. Since IRI and PSI are correlated and previous studies[9, 10] on in-service pavements have shown the functional form of PSI with time and traffic, this equation form for PSI was used as the basis for this model.[9, 10] The previous studies indicated that IRI drops rapidly at first, then levels off for a long period, and may then drop rapidly again as severe deterioration occurs.

That IRI is not zero when AGE is zero at construction is also true for CRCP. Since the initial IRI was not measured for any of the sections, it was not possible to utilize the change in IRI as the dependent variable. Based on these considerations, the measured IRI on the pavement sections was selected as the dependent variable to use in the model development.

From the list of potential explanatory variables selected by the experts to be significant and the previous data observations, several explanatory variables were chosen for testing. Regression analyses were conducted, with a variety of techniques to attempt to develop the most suitable model for IRI prediction for CRCP. The following briefly describe the techniques utilized in the analyses:

- The explanatory variables were tested to determine their significance in the overall models, and those that were determined not to be significant were eliminated from consideration.

- The interactions between the variables were evaluated, but none were found that could be considered in the model to be developed.

- Tests for collinearity between the explanatory variables were conducted throughout the development phase. When such collinearity was found between a pair of variables, one of the variables was eliminated from consideration.

- The two- and three-dimensional plots were studied, and these studies indicated that all variables to be considered in the model were linearly related to IRI and did not need to be transformed.

Based on these principles, the following model was developed for predicting the of CRCP with the data from the GPS-5 test sections in the LTPP Database:

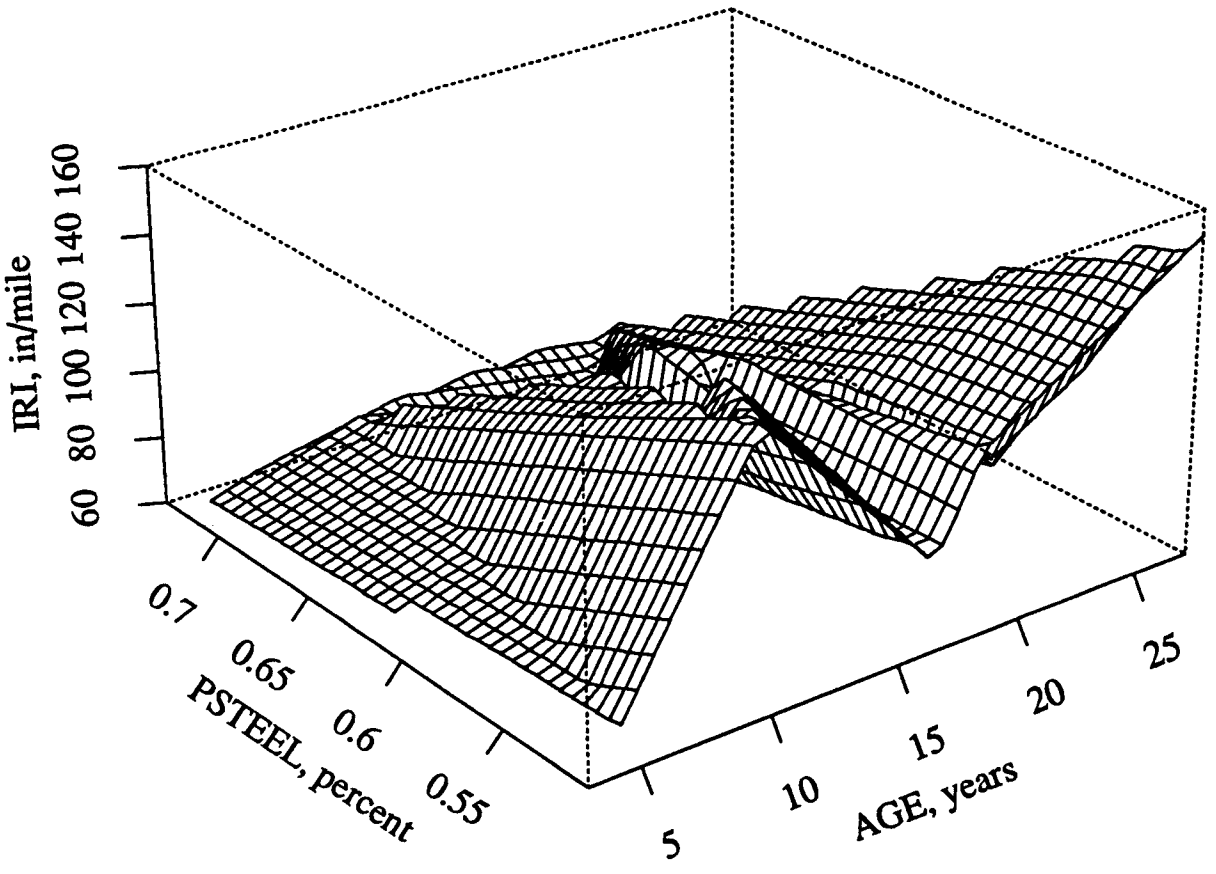

Figure 8.50 Three-Dimensional Plot (IRI, PSTEEL, AGE) for CRCP

$$IRI = 262 + 1.47 * CESAL - 2.94 * THICK - 232.3 * PSTEEL - 29.8 * WIDENED - 16.8 * SUBGRADE \quad (8.11)$$

where

IRI	=	International Roughness Index, in./mi.
CESAL	=	cumulative 18,000 lb. (80kN) ESALs in traffic lane, millions
PSTEEL	=	percentage of steel (longitudinal reinforcement), %
THICK	=	concrete slab thickness, in.
WIDENED	=	1 = widened traffic lane; 0 = normal width traffic lane
SUBGRADE	=	1 = AASHTO classification is A-1, A-2, or A-3 (i.e., coarse grained); 0 = if AASHTO classification is A-4, A-5, A-6, or A-7 (i.e., fine grained)

Statistics:

N	=	42 sections
R^2	=	0.546
RMSE	=	17.19 (in./mi) (27 cm/km)

Figure 8.51 shows a plot of the predicted versus actual IRI, and Figure 8.52 shows a plot of the residuals versus predicted IRI. The results of a sensitivity analysis of the model is shown in Figure 8.53. PSTEEL has by far the largest effect on IRI, followed by SUBGRADE, WIDENED, CESAL, and THICK. The form of the model provides for a linear increase in IRI with time. No climatic variables were sufficiently significant to be included in the model.

According to the model, as the percentage of reinforcement increases, the IRI decreases considerably. Increased reinforcement holds cracks tighter which reduces the number of punchouts. The number of punchouts has been strongly related to the percentage of reinforcement in other field studies.[9, 10] A coarse-grained subgrade soil type (SUBGRADE) results in a lower IRI in comparison to a fine-grained soil, and a widened lane reduces IRI. Increasing traffic (CESAL) results in an increase in IRI, and thicker slabs decrease IRI. A three-dimensional plot that shows the relationship between predicted IRI, CESAL, and PSTEEL is presented in Figure 8.54. All of the effects and trends indicated by the model are correct in sense (increases in explanatory variable increases or decreases the dependent variable).

The IRI model developed for CRCP includes several variables known to affect roughness from previous studies. However, there are additional variables that are known to affect IRI that are missing from the model. Examples include base type (untreated versus treated) and several climatic variables. With an R^2 of only 0.55 and a RMSE of 17 in./mi. (27 cm/km), the model has considerable room for improvement.

Summary of Sensitivity Analysis Results for PCC Pavements

Table 8.11 lists the rankings for individual explanatory (independent) variables, in terms of relative sensitivities, for each of the ten separate models and sensitivity analyses. One column indicates the number of models for which a specific explanatory variable was found to be significant. The far right column gives average rankings, with a rank of 8 arbitrarily assigned for cases when the variable was not found to be significant. The numbers of explanatory variables ranged from 2 to 6 per model, with a mean of 4.1, so the assigned priority had to be greater than 6. As there could be other relatively nonsignificant variables having stronger impacts on the occurrence of distress, the value of 8 appeared logical.

The independent variables are listed below in order of combined rankings. One list is based on average rankings, and one is based on number of models in which the variable was included (in the case of a tie, the other ranking basis was used to order the two variables):

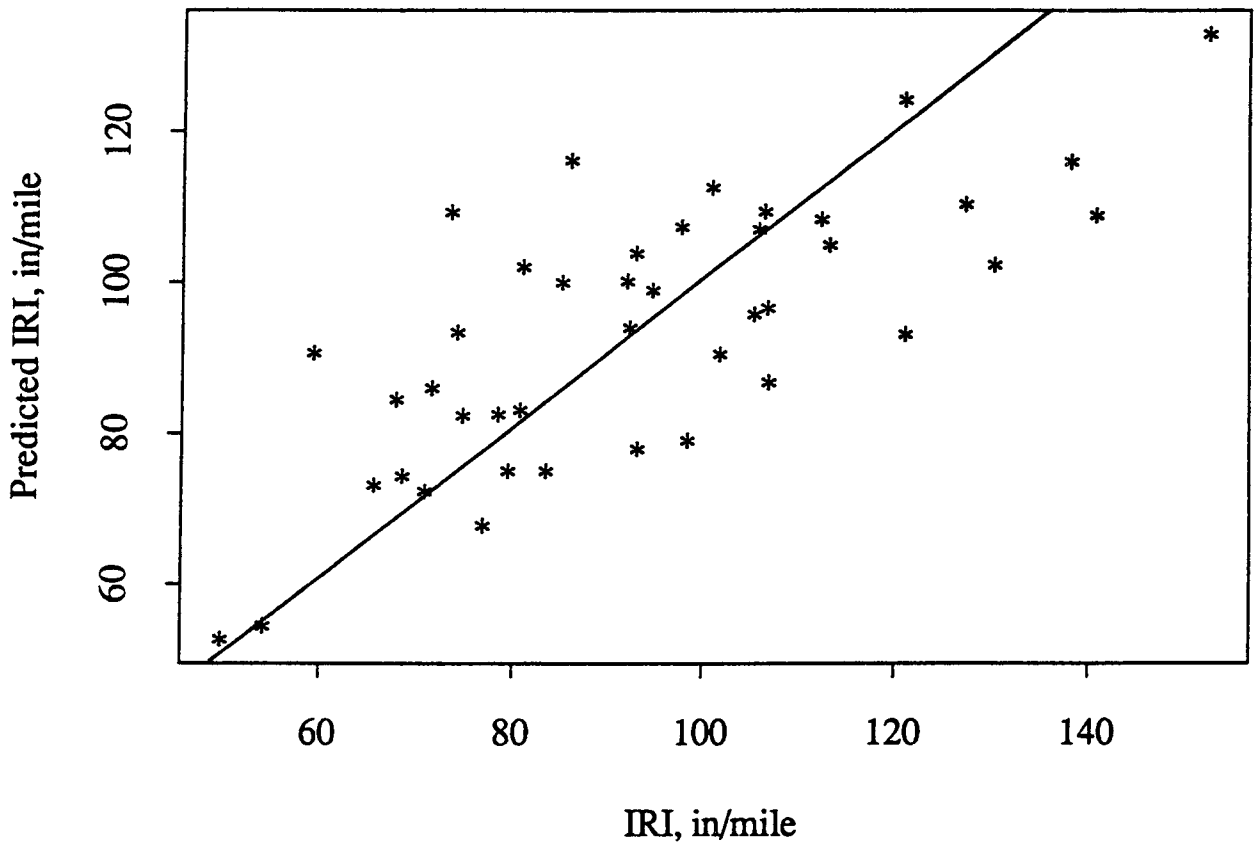

Figure 8.51. Predicted vs. Actual IRI for CRCP

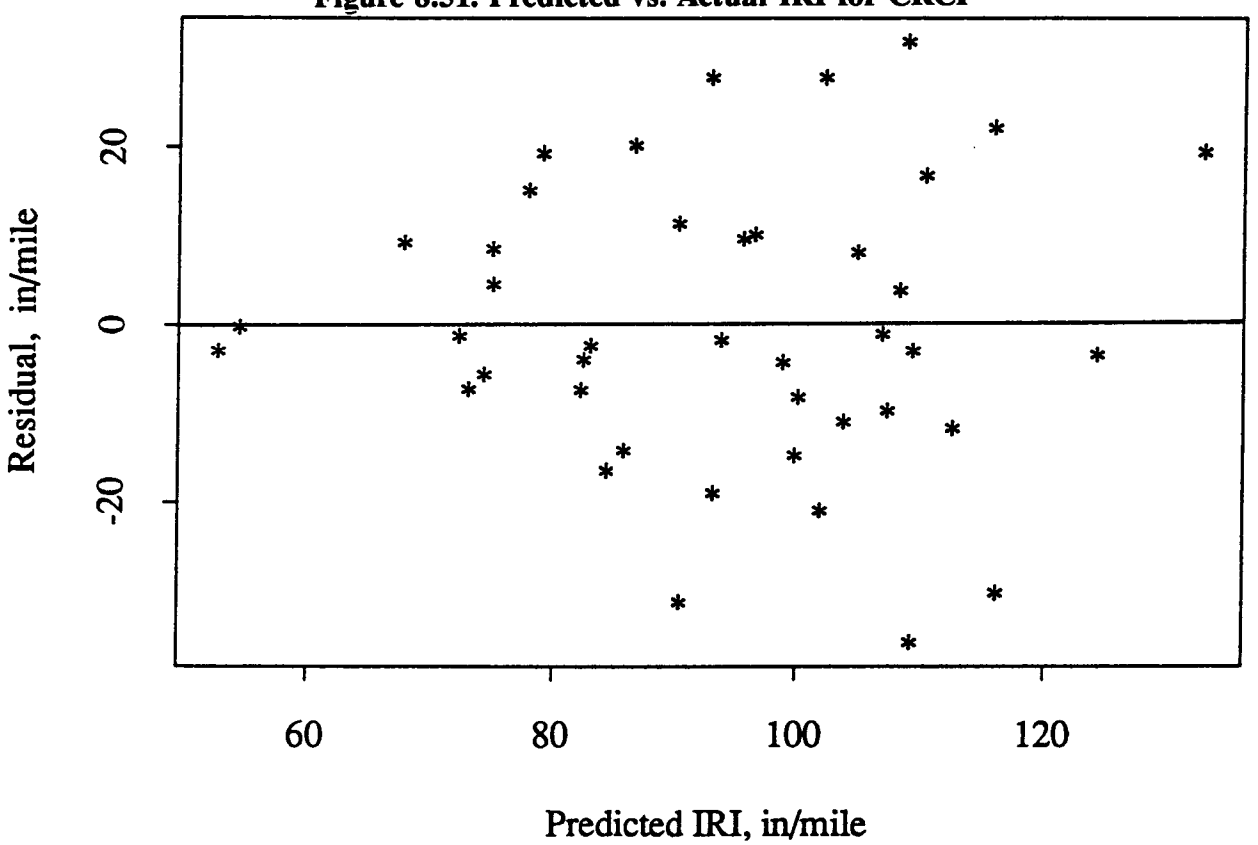

Figure 8.52. Plot of Residuals vs. Predicted IRI for CRCP

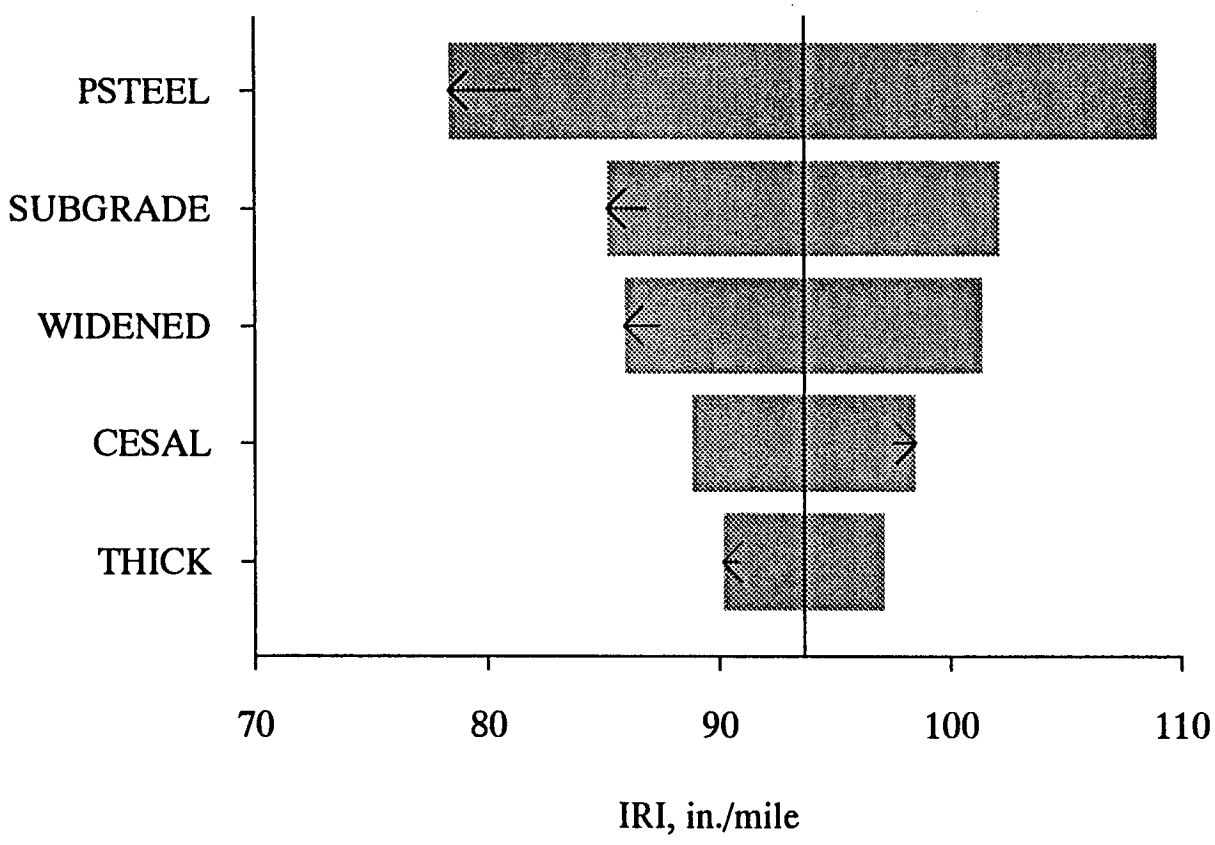

Figure 8.53. Sensitivity Analysis for IRI Model for CRCP

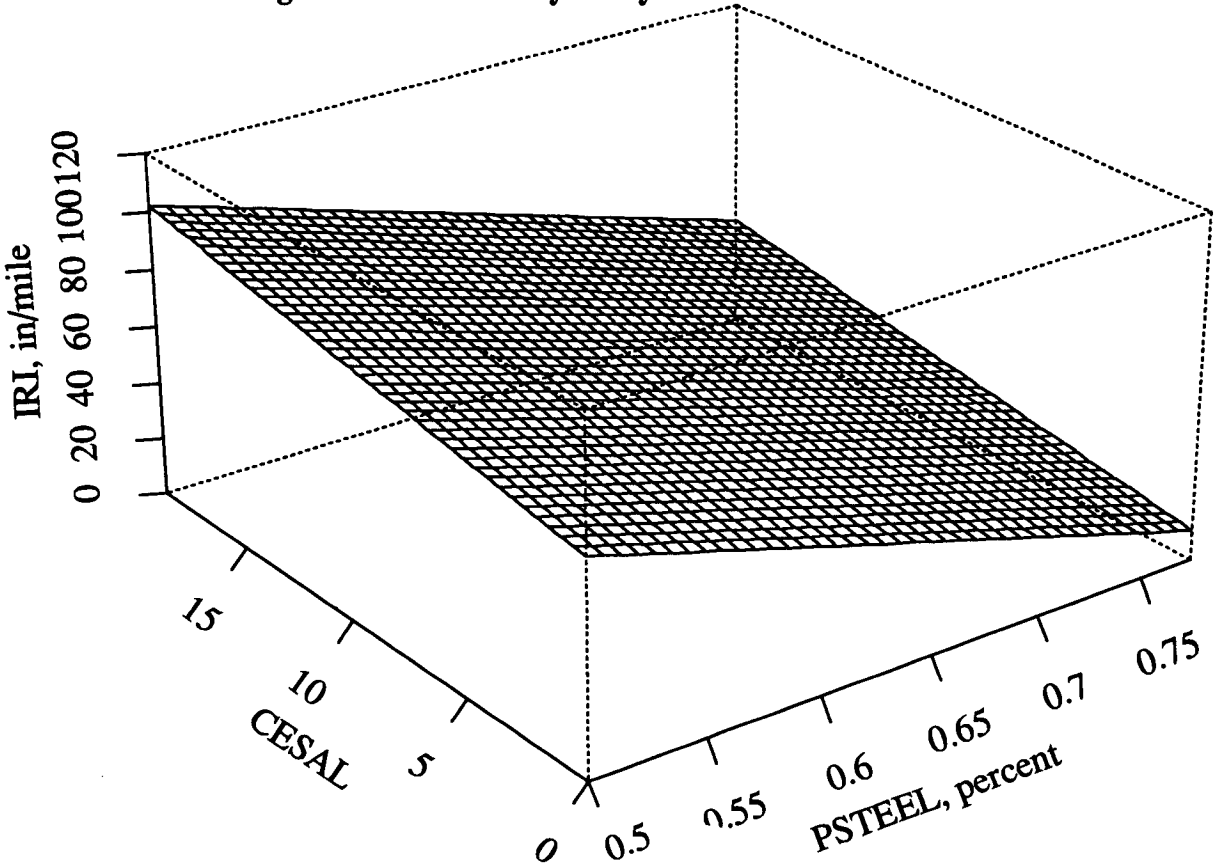

Figure 8.54. Three-Dimensional Plot of IRI Model for CRCP

Ranking by Average	Ranking by Number of Models Found Significant
Age	Age
CESALs	CESALs
Slab Thickness	Slab Thickness
Static k-Value	Static k-Value
Precipitation	Precipitation
Joint Spacing	Edge Support (Tied Shoulders)
Percentage of Steel	Joint Spacing
Edge Support (Tied Shoulders)	Percentage of Steel
Annual Freeze-Thaw Cycles	Annual Freeze-Thaw Cycles
Type of Subgrade	Type of Subgrade
PCC Flexural Strength	PCC Flexural Strength
Monthly Temperature Range	Monthly Temperature Range
Widened Traffic Lane	Widened Traffic Lane
Freeze Index	Freeze Index
Dowel Diameter	Dowel Diameter
Subdrainage	Subdrainage
Type of Base	Type of Base

As can be seen, the rankings are almost identical for both methods. However, this set of rankings does not tell the whole story, because the rankings are very dependent on type of pavement and type of distress. Conclusions drawn from the sensitivity analyses (and partially from past experience) are presented below:

Related Comments and Observations for JPCP

- The use of sufficiently sized dowels for the traffic loadings (the larger the dowel diameter, the less faulting) will ensure that faulting will not become significant and cause severe roughness. Dowel use is particularly important for heavy traffic in cold and wet climates. Thicker slabs by themselves do not reduce faulting significantly. Longitudinal subdrainage will help reduce faulting of non-doweled joints. A tied concrete shoulder will reduce doweled joint faulting.

- Increased slab thickness has a strong effect on reducing transverse slab cracking and providing a smoother JPCP (lower IRI) over time.

- Provision of increased subgrade support, as indicated by the backcalculated k-value, results in a lower IRI and a smoother pavement. Increased support over an existing soft subgrade would likely require either treatment of the soil or a thick granular layer over the subgrade.

Table 8.11. Significance Rankings for Explanatory Variables, by Distress Type and Pavement Type, for PCC Pavements

Explanatory Variables	Joint Faulting JCP w/ Dowels	Joint Faulting JCP w/o Dowels	Transverse Crack Deterioration, JPCP	Transverse Crack Deterioration, JRCP	Joint Spalling, JPCP	Joint Spalling, JRCP	IRI, JPCP w/ Dowels	IRI, JPCP w/o Dowels	IRI, JRCP w/o Dowels	IRI, CRCP	No. Models Significant	Average Ranking
CESALS	1	1		3				1		4	5	5.0
Joint Spacing	2						1				2	6.7
Age	3	2			2	1	4		4		6	4.8
Static k-Value	4			1			5		2		4	5.9
Dowel Diameter	5										1	7.7
Edge Support	6						3		3		3	6.8
Precipitation		3		4				2	5		4	6.2
Freeze Index		4									1	7.6
Longitudinal Subdrainage		5									1	7.7
Slab Thickness			1				2		1	5	4	5.7
PCC Flexural Strength			2								1	7.4
Percent Steel				2						1	2	6.7
Annual Freeze-Thaw Cycles					1			3			2	6.8
Monthly Temp. Range						2					1	7.4
Type of Subgrade (Granular or Clay)								4		2	2	7.0
Type of Base (Treated or Untreated)								5			1	7.7
Traffic Lane (Widened or Not)										3	1	7.5

Note: Empty cells are considered as 8 for averaging

- Use of shorter slabs for JPCP will reduce the amount of joint faulting and transverse cracking and will result in a smoother pavement (lower IRI) over time.

- Specification of durable concrete in freeze climates is desirable, so that freezing and thawing and other climatic factors do not result in significant joint spalling.

Related Comments and Observations for JRCP

- The use of sufficiently sized dowels for the traffic loadings (the larger the dowel diameter the less faulting) will ensure that faulting will not become significant and cause severe roughness. A tied concrete shoulder and shorter joint spacing also help to reduce joint faulting.

- The use of an increased percentage of longitudinal reinforcement will help control the deterioration of transverse cracks.

- Increased subgrade support will result in fewer deteriorated transverse cracks and a smoother pavement (lower IRI). Increased support over an existing soft subgrade would likely require either treatment of the soil or a thick granular layer over the subgrade.

- Shorter JRCP slabs will reduce the amount of joint faulting.

Related Comments and Observations for CRCP

- Increases in the percentage of longitudinal reinforcement will provide a smoother CRCP (lower IRI) over time. The increased percentage of steel reduces the amount of punchouts and the deterioration of transverse cracks.

- Increased subgrade support will result in fewer deteriorated transverse cracks and a lower IRI (smoother pavement). Increased support over an existing soft subgrade would likely require either treatment of the soil or a thick granular layer over the subgrade.

- A widened traffic lane will provide a smoother CRCP (lower IRI) over time.

- Increased slab thickness will result in somewhat smoother CRCP (lower IRI) over time. This is probably due to fewer punchouts as a result of the thicker slab.

9

General Discussions of Results From Sensitivity Analyses

The constraints imposed on the results that could be expected from these sensitivity analyses have been previously discussed in considerable detail in the Introduction and other locations throughout the previous chapters. While those planning for the sensitivity analyses knew that the timing of these first analyses critically reduced the utility of the database, it was hoped that the distribution of ages would partially offset the lack of adequate time sequence data and help to explain the curvatures in the relationships. This hope proved to be at least partially satisfied, even though few of the equations derived can be claimed to be highly reliable.

A general discussion of the results in the sensitivity analyses is presented below.

Limitations of Sensitivity Analyses Imposed by Database Limitations

Because there is a substantial discussion in Chapter 1 under "Analytical Limitations Resulting From Data Shortcomings," those limitations previously discussed are only listed below:

- The values of cumulative equivalent single axle loads (ESALs) were simply estimates from State Highway Agencies (SHAs), and are not believed to be very reliable.

- Initial roughness in terms of the International Roughness Index (IRI) had to be estimated for hot mix asphalt concrete (HMAC) pavements. This was done by using the estimated values of initial Pavement Serviceability Index (PSI) in an equation, developed by the World Bank.[8]

- There was generally only one measurement of each distress for each test section, plus an initial estimated or assumed value. For all distresses except roughness, it could be assumed that the distress was zero at the time the pavement was opened to traffic. Two values are generally not enough to explain the curvature in the relationships; however, as mentioned previously, we also had the advantage of the ages of the pavements at the times the distresses were observed being distributed reasonably over twenty years (see Figure 1.3).

- At the time the data arrived, important inventory data were missing for a number of test sections. When reasonable values could not be inferred, these test sections had to be omitted from the analyses.

- There were not enough test sections displaying some types of distress to support effective model development. In general, only data from test sections displaying a distress of interest were included in the analysis database for that distress type.

- There were not enough overlaid pavements for which the condition prior to overlay was known to support model building and sensitivity analyses. Consequently, these data were only used to evaluate existing design procedures (see SHRP-P-394, Early Analyses of LTPP General Pavement Studies Data, Evaluation of the AASHTO Design Equations and Recommended Improvements).

- It was intended that current knowledge be integrated into the process by use of mechanistic clusters of variables in the regression equations, but this plan was thwarted by a lack of layer stiffness data, which was required for the development of the mechanistic clusters.

- Test sections had not been found for all the cells within the sampling templates, which tends to introduce biases.

It is probable that any missing inventory data that can be obtained is now in the database, because Quality Assurance/Quality Control procedures have been developed and applied to identify such deficiencies, and the regional offices have been instructed to obtain and enter the data wherever possible. However, the test sections that could not be used because of missing data are identified in SHRP-P-684, Early Analyses of General Pavement Studies Data, Data Processing and Evaluation of this report; efforts may be made to obtain the missing data, or perhaps decisions can be made to eliminate the test sections if it is believed that this lack of data will unacceptably limit the sections use in future analyses.

Some of the mising data are easily determined, such as joint spacing for jointed concrete pavement (JCP) and other data that can simply be measured in the field. For those test sections missing deflection data, these data are now available for all or virtually all the test sections.

The research staff was able to deal with some of the problems of missing inventory data. For instance, tables from the Asphalt Institute[13] were used to approximate asphalt viscosity when the asphalt grade was known. In a few cases where data on base densities were not available, it was assumed that they were compacted at 95% of modified American Association of State Highway and Transportation Officials (AASHTO) compaction.

It became obvious early in the development of the predictive equations that adequate equations could generally not be developed on the basis of the overall inference space (the U.S. plus part of Canada). For most of the distress types studied for HMAC pavements, there were sufficient test sections to allow development of limited regional models. These were typically more accurate than the models based on all the data. Unfortunately, there were really not enough portland cement concrete (PCC) pavement test sections that had both sufficient data and the distress types of interest to allow development of regional models.

For HMAC pavements, only 14 to 27% of the test sections in the analysis databases rested on clay subgrade (see Table 9.1), so there is a bias toward pavements on granular subgrades. Studies should be initiated *for the individual analysis databases* to study distributions of test sections within the sampling templates that could be used for the separate analyses (pavement type and distress type combinations). Entries could be made on the sampling template factorial of interest to indicate for each cell whether its test section(s) were on clay or on granular subgrades. Such a study would display the degree of the bias and identify cells where test sections with clay subgrades should be sought. Such plots would display other biases as well.

Table 9.1. HMAC Pavement Test Sections With Clay Subgrade Within Databases Used for the Analyses

Type of Pavement	Distress Type	Numbers of Test Sections		% With Clay Subgrade
		Total	Clay Subgrade	
HMAC Over Granular Base	Rutting	152	33	22
	Change in IRI	108	26	24
Full-Depth HMAC	Rutting	44	8	18
	Change in IRI	33	6	18
HMAC Over Granular Base and Full-Depth HMAC	Transverse Cracking	118	17	14
HMAC Over Portland Cement-Treated Base	Rutting	49	10	20
	Change in IRI	37	10	27
	Transverse Cracking	35	8	23

In summary, a number of the data limitations experienced during this early data analysis will not seriously constrain future analyses. As time passes, time sequence data on the occurrence and severity levels of distress will accumulate, substantial traffic monitoring will tend to improve the estimates for ESALs, and the availability of data for the Specific Pavement Studies (SPS) projects will enhance the databases. It is also hoped that some additional General Pavement Studies (GPS) test sections will be selected and brought into the studies to reduce biases in the databases. Unfortunately, some test sections may continue to be unusable when significant inventory data are missing.

Reliability of Results

Tables 9.2 through 9.6 have been prepared to provide the pertinent statistical values for the various predictive equations developed for use in the sensitivity analyses. For the data available, the development of these equations was limited to statistical linear regressions for the sensitivity analyses. It is almost certain that better models could have been developed if the research team was free to use nonlinear regression techniques.

It can be seen by reviewing the several tables that the coefficient of determination (R^2) varied for flexible pavements from 0.33 to 0.75 for the entire data set. Those for rutting varied from 0.41 to 0.54. Those for ΔIRI range from 0.62 to 0.75, and the one for transverse cracking was the lowest at 0.33. As discussed previously, these equations were not considered sufficiently reliable, so data sets were developed for the four individual environmental zones and were regressed separately.

The R^2's for the regional models for rutting varied from 0.55 to 0.81. The R^2's for ΔIRI varied from 0.81 to 0.93, and those for transverse cracking varied from 0.72 to 0.83. While a number of these models appear very promising, it must be remembered that the RMSE shown is for the common log of the distress. As explained early in Chapter 7, the confidence interval for these equations is quite broad. Consequently, the research team has not recommended that these early equations be used in design procedures or pavement management systems. However, it may be worthwhile to use them to check pavement structure designs obtained by other means and to use them in pavement management systems as placeholders when more reliable predictive equations are not available.

The statistics for the PCC pavement predictive equations appear in Table 9.6. Because the number of test sections with usable data was considerably less for the PCC pavements than for the HMAC pavements, the research staff did not have the luxury of developing regional models, but instead had to try to explain the variations in distress caused by environmental variables, and their interactions with other variables, across the entire United States and part of Canada. Consequently, the R^2's are somewhat lower for these models, varying from 0.34 to 0.78. Although these models cannot be claimed to be very reliable, they may also be useful for checking designs developed by other means and serve as placeholders in pavement management systems.

Table 9.2. Statistics for Predictive Equations for Rutting and ΔIRI, Developed for Sensitivity Analyses for HMAC Pavements Over Granular Base

Distress Type	Entire Data Set			Wet-No Freeze			Wet-Freeze			Dry-No Freeze			Dry-Freeze		
	N	R^2	RMSE	N	R^2	RMSE	N	R^2	RMSE	N	R^2	RMSE	N	R^2	RMSE
Rutting	152	0.41	0.18	41	0.66	0.18	41	0.68	0.19	36	0.70	0.16	34	0.81	0.11
ΔIRI	108	0.62	0.34	32	0.81	0.31	35	0.84	0.27	27	0.93	0.18	14	0.92	0.21

Notes: N = No. of test sections in data set; R^2 (coefficient of determination) is the adjusted R^2; RMSE (root mean square error) is in $\log_{10}$ (Distress).

Table 9.3. Statistics for Predictive Equations for Rutting and ΔIRI, Developed for Sensitivity Analyses for Full-Depth HMAC Pavements

Distress Type	Entire Data Set			Wet			Dry			No Freeze			Freeze		
	N	R^2	RMSE	N	R^2	RMSE	N	R^2	RMSE	N	R^2	RMSE	N	R^2	RMSE
Rutting	42	0.54	0.20	27	0.73	0.17	13	0.79	0.10	22	0.55	0.14	18	0.78	0.15
ΔIRI	33	0.71	0.39												

Notes: N = No. of test sections in data set, R^2(coefficient of determination) is the adjusted R^2; RMSE (root mean square error) is in $\log_{10}$ (distress).

Table 9.4. Statistics for Predictive Equations for Rutting and ΔIRI, Developed for Sensitivity Analyses of HMAC Over Portland Cement-Treated Base

Distress Types	Entire Data Base		
	N	R^2	RMSE
Rutting	49	0.51	0.21
ΔIRI	37	0.75	0.33

Notes: N = No. of test sections in data set; R^2 (coefficient of determination) is the adjusted R^2; RMSE (root mean square error) is in $\log_{10}$ (distress).

Table 9.5. Statistics for Predictive Equations for Transverse Cracking, Developed for Sensitivity Analyses of HMAC Over Granular Base and Full-Depth HMAC Pavements (Combined Data Set)

Distress Type	Entire Data Set			Wet-No Freeze			Wet-Freeze			Dry-No Freeze			Dry-Freeze		
	N	R^2	RMSE	N	R^2	RMSE	N	R^2	RMSE	N	R^2	RMSE	N	R^2	RMSE
Transverse Cracking	118	0.33	0.53	17	0.75	0.52	44	0.83	0.30	23	0.83	0.35	34	0.72	0.44

Notes: N = No. of test sections in data set; R^2 (coefficient of determination) is the adjusted R^2; RMSE (root mean square error) is in Log_{10} (Distress).

Table 9.6. Statistics for Predictive Equations for PCC Pavement Distress, Developed for Sensitivity Analyses

Pavement Type	Distress Type	N	R^2	RMSE
JPCP & JRCP With Dowels	Joint Faulting	59	0.53	0.028
JPCP & JRCP Without Dowels	Joint Faulting	25	0.55	0.047
JPCP	Transverse Crack Deterioration	N/A	N/A	N/A
JRCP	Transverse Crack Deterioration	27	0.48	20.8
JPCP	Joint Spalling	56	0.34	11.0
JRCP	Joint Spalling	25	0.64	16.7
JPCP With Dowels	IRI	21	0.55	19.1
JPCP Without Dowels	IRI	28	0.64	31.3
JRCP Without Dowels	IRI	32	0.78	9.9
CRCP	IRI	42	0.55	17.2

Note: N = No. of test sections in data set, R^2 is not the adjusted R^2, and RMSE = root mean square error.
N/A = Not Applicable

Actions Recommended to Repair Limitations in the LTPP GPS Database

Because of the late arrival of the data, not all the planned studies could be accomplished within the time available. In addition, hindsight has produced some ideas for improving the data for future analyses. The following recommendations propose subsequent work to improve the database:

- Carefully review the data deficiencies for those test sections that could not be used for these analyses. If the data have since been obtained or can be obtained, eliminate the deficiency so that the data for these test sections can be used in future analyses.

- Evaluate those test sections for which apparently critical data cannot be obtained to see if the available data are sufficient for any anticipated research. If a test section does not have the critical data, consider eliminating it from the studies.

- In recognition of the fact that the databases of primary interest are those that can be used for specific analyses, separate all available data into data sets by pavement types and environmental zones. These data sets can then be used for more detailed studies in terms of specific data required for specific analyses; e.g., those that exhibit specific distresses or those with mix designs with various characteristics. Observe the distributions of the significant data elements within these data sets to determine if the data sets are adequate for the desired analyses. SHRP-P-684, Early Analyses of General Pavement Studies Data, Data Processing and Evaluation of this report contains numerous plots that indicate distributions for specific GPS experiments and environmental zones. While these aren't the exact data sets that were used, they will be useful to a study such as that proposed here.

- Use plots similar to the sampling template factorial plots for the various data sets so that the gaps in the factorials can be studied to decide where additional test sections are needed.

- Consider the test sections that have been built, and to the extent possible those that will be built, for the SPS, and add them to the factorials for the GPS before seeking to fill gaps in the GPS. The data for the SPS should be much more complete, because they will not depend on old SHAs records, and a more detailed materials testing program will be applied.

To summarize, it is recommended that the period between this data analysis and the next major data analysis be used to rectify deficiencies in the data and to conduct further limited analyses to improve the products from these early studies. Some examples of useful analyses follow:

- Based on the layer modulus data that were not available for these studies, apply the mechanistic variable clusters that the research team was unable to use for this analysis and nonlinear regression techniques to develop improved predictive equations. Monitoring data from an additional 3 or so years could be included to reap the benefits of time sequence data.

- Utilize mechanistic responses from models such as MICHPAVE[14] that was used by the Michigan SHA in its data analyses along with other data, to develop mechanistic-empirical models. Such regression models that include mechanistic responses can be used in combination with mechanistic response models, or regression models that have been developed from response models, to predict the occurrence of distress.

- Utilize the data available in existing mechanistic-empirical distress models to identify deficiencies and to improve or calibrate these models to provide more reliable predictions.

The implementation of the recommendations offered above will likely lead to other useful studies and applications.

10

Summary and Conclusions

The steps leading to the sensitivity analyses, the process of developing suitable models for sensitivity analyses, the procedures for conducting the sensitivity analyses, and the results from the sensitivity analyses have been discussed in detail in the preceding chapters. The limitations for the results and their causes have also been identified and discussed. The Long-Term Pavement Performance (LTPP) studies are indeed long-term and improved analytical results can be expected in the future. The question at this time is; How can these results be used to benefit the highway community? The purpose of this chapter is primarily to identify potential benefits from these early analyses.

Use of Sensitivity Analysis Results by the Highway Community

It should be noted again that the results from the sensitivity analyses, like load equivalence factors, depend heavily on the predictive equations from which they are derived. Therefore, it is important to determine whether these predictive equations reasonably represent the performance of pavement structures while those structures are subjected to the traffic loadings and the environment in which they exist. Are the independent variables those that truly control the occurrence of distresses in pavements? If so, are the equation forms sufficiently realistic? If so, are the relative sensitivities of the independent variables themselves realistic? These questions probably cannot be answered precisely, but part of their answers can come from a review of the results in light of previous studies and experience.

Review of Chapters 7 and 8 indicates that the relative rankings of significance for the various distresses and pavement types are generally logical in terms of past studies and experience. While there is no doubt that the relative magnitudes of the sensitivities have been affected by the inevitable biases in any database such as this, they are believed to be generally reasonable.

There have also been cases where independent variables were not found to be significant; however, other studies have indicated that they were significant. There were also some mild surprises, but some of them had logical explanations. An example of such a surprise, is that it became apparent during the analyses that increasing hot mix asphalt concrete (HMAC) air voids decreased predicted rutting. This finding was not expected and caused considerable consternation until it was understood that the inference space included few pavements with really high air voids. Thus, it did not mean that 10% air voids will minimize rutting, but that air voids in the order of 5 to 7% offer better access for air flow within the pavement, compared to lower air voids, which in turn stiffen the mix and reduce rutting. This result has been reported in other studies as well.

If one can reach the conclusion that individual models are reasonably reliable for predicting the occurrence of the distress of interest, then the relative sensitivity rankings indicate where more or less emphasis should be placed in mix design, structural design, and construction control. For instance, the results for the portland cement concrete (PCC) studies indicate rather clearly that dowels should be used for jointed concrete pavements. Similarly, inspectors should strive to avoid overcompaction, as well as undercompaction, of HMAC mixes.

The results from these sensitivity analyses can be compared to results from previous studies to either corroborate that in-service pavements respond as expected from previous studies or experience, or that the relative significance of specific independent variables differs from that of current experience and past studies. In the latter case, the differences may point to other fruitful research to explore the differences.

Use of Linear Regression Distress Models for Design and/or Pavement Management

As previously stated, the development of the distress models was constrained by both data limitations and the requirement that the models be statistically linear for use in the sensitivity analyses. Consequently, they are not recommended for general use in design or in pavement management systems. However, the design procedures used by many highway agencies deal only with composite indices, such as the Present Serviceability Index considered in the American Association of State Highway and Transportation Officials (AASHTO) design procedures. As maintenance, repair, and rehabilitation decisions are more often based on the distresses noted in the pavements, it appears that it would be useful to check such pavement structure designs against predictions of specific distresses. If a pavement thickness design and planned construction control appear to suitably limit the occurrence of distresses over the design life, then confidence in the design tends to increase. If the predictive equations indicate that the pavement structure will not limit specific distresses to an acceptable level over the life of the pavement, designers can look into this aspect in more detail until they are satisfied with the reliability of the design or make changes to limit the predicted distress. This approach also provides experience for future design procedures, which are expected to

include consideration of several distress types rather than just one composite index.

It is recognized that the distress models for many pavement management systems do not include all these distresses or may be based on even less reliable predictive models. In these cases, it may be worthwhile to insert these distress models into the system as placeholders until better models are available.

References

1. Transportation Research Board, *Strategic Highway Research Program Research Plans*, Washington, DC, May 1986, P. TRA 2-6.

2. Pavement Management Systems, Limited, PROQUAL V1.4, Amherst, NY, 1992.

3. SAS Institute, Inc., SAS® System for Personal Computers, Release 6.04, Cary, NC, 1987.

4. Hocking, R.R., and O.J. Pendleton. "The Regression Dilemma-Variable Elimination, Coefficient Shrinkage and Robust Estimation," Communications in Statistics, Vol. 12, No. 5, 1983.

5. Freund, R.J., and R.C. Littell. *SAS System for Regression, SAS Series in Statistical Applications*, 2nd edition. SAS Institute Inc., Cary, N.C., 1991, p. 123-124.

6. Statistical Sciences, Inc. *S-PLUS User's Manual*, Seattle, WA, March 1993.

7. Bradbury, R.D. "Design of Joints in Concrete Pavements," Proceeding, 12th annual meeting of the Highway Research Board, Washington, DC, December 1932, pp. 105-137.

8. Paterson, William D.O. *Road Deterioration and Maintenance Effects, Models for Planning and Management*, published for the World Bank by the John Hopkins University Press, Baltimore, 1987.

9. Smith, K.D., A.L. Mueller, M.I. Darter, and D.G. Peshkin. "Performance of Jointed Concrete Pavements," FHWA-RD-89-137, Federal Highway Administration, McLean, VA, 1990.

10. Darter, M.I., J.M. Becker, M.B. Snyder, and R.E. Smith. "Portland Cement Concrete Pavement Evaluation System - COPES, " NCHRP Report No. 277, Transportation Research Board, Washington, DC, 1985.

11. Darter, M.I.. *Design for Zero-Maintenance Plain Jointed Concrete Pavement-Final Report.* Report FHWA-RD-77-111, FHWA, U.S. Department of Transportation, Washington, DC, June 1977.

12. Lee, Ying-Haur, and M.I. Darter. "Mechanistic Design Models of Loading and Curling in Concrete Pavements," Proceedings: ASCE Airfield Pavement Specialty Conference, Vicksburg, MS, 1993.

13. Puzinauskas, V.P. "Properties of Asphalt Cements," The Asphalt Institute Research Report No. 80-2, College Park, MD, November 1980.

14. Harichandren, R.S., G.Y. Baladi, M.S. Yeh, MICHPAVE, Michigan State University, East Lansing, MI, 1989.

Appendix A: Preliminary Identification of Data Elements to Be Included in P-020 Sensitivity Analyses of Pavements With Asphalt Concrete Surfaces (March 19, 1991)

There are some 117 data elements that may be entered into the National Information Management System (National Pavement Data Base) for pavements with flexible surfaces. It is necessary to considerably reduce the number of variables (data elements) from the 117 available in order to develop meaningful performance prediction equations and reasonable estimates of relative significance of the independent variables to occurrence of specific distresses (dependent variables). The approach adopted for preliminary elimination of insignificant variables was to obtain relative significance rankings from experts in pavement performance modeling. A table that lists the 117 data elements as rows and the six distresses for study as columns is attached. Space was provided to enter a significance ranking for each of the 117 data elements with respect to each of the six distresses. Space was also provided to enter the other data element numbers considered to be correlated with each specific data element.

The voluminous forms (11 pages) were filled out by Dr. Witczak, Dr. Mahoney, Dr. Baladi, Dr. Rauhut and Mr. Von Quintus. Data elements that were considered to be of importance to the occurrence of the distress in question, in the opinion of the rater, were marked with a "1". If considered to be moderately significant, a "2"was entered. If a data element was considered to have little or no significance to the occurrence of the distress, a "3" was entered. The five ratings were averaged for each box, and the average rating of significance entered on the attached set of forms, entitled "Significant Variables and Their Relative Importance to the Significant Distresses for Pavements with Asphalt Concrete Surfaces". Those boxes that are hatched are those that have been tentatively selected to be of sufficient significance that they should be included in the analysis, subject to the inclusion of one or more other data elements that are expected to provide sufficient correlation to allow "explanation" of essentially the same portion of the variation. Therefore, it is not expected that all of the data elements hatched will necessarily be included individually in the analysis if other data elements are included that are closely correlated.

The general approach that was used for selecting the data elements to be hatched was as follows:

1. All boxes with an average score of less than 2 were included.

2. Data elements with a score of 2 were included in some cases but not in others on the basis of judgement.

3. No data elements with a score greater than 2 were included.

None of these decisions are final and different combinations of data elements may be tried to achieve the best results possible. The 11-page table attached provides the results of this study, and has been further marked up to provide additional information for GPS

Experiment 1, Asphalt Concrete Pavements Over Unbound Base. Note that a number of boxes have been crossed out. This is to eliminate boxes involving overlays or bound base or subbase that are not included in GPS-1. The set of codes and some notes have been included on the right side of the forms to indicate relative importance (criticality) and source from which the data will be forthcoming. These codes are identified below:

CL	Critical - Available from Lab results
CI	Critical - Only available from Inventory Data
CT	Critical - Available from Traffic Data
IC	Important, but can be "explained" by other correlated variables indicated by No.
NC	Noncritical
DU	Sufficient data not available - have to obtain the data from SHA's or rely on correlations to other data elements.
CM	Critical - Available from Monitoring Data
CE	Critical - Available from Environmental Data

The forms have been further marked up to indicate the following:

1. Percentages have been provided in the left hand margin for a number of the data elements to indicate approximately the percent of test sections for which that data has been provided. This is very important because data elements cannot be included if it is missing for the majority of test sections in an experiment.

2. A check mark in a box representing a data element and a significant distress indicates that the current expectation is that that data element will be included in the study for that distress.

3. An "X"in the box indicates that we do not expect to have enough data for consideration of that data element for the distress indicated.

4. A "C" in a box indicates that this variable is tentatively expected to be represented by one or more other correlated variables, even though it may be available. As an example, asphalt grade (data element 25) and penetration (data element 29) are expected to be represented by viscosity of the asphalt cement (data element 28). Although each could reasonably be used to represent either of the other two, it is believed that viscosity is the more meaningful variable, and it can be estimated from the other two.

An analysis of these results has been summarized in another table entitled, "Evaluation of Numbers of Data Elements for GPS Experiment 1 that will be Available and will be Used for Contract P-020 Data Analysis". In this table, numbers of test sections in various

categories (availability, correlation, etc.) appear as rows and the six distresses to be studied appear as columns. The first row describes the number of significant data elements for each of the distresses. These are found by simply counting the hatched boxes for a particular distress in the relative significance forms. The second row indicates the number of significant data elements that will not be available in sufficient numbers. Specific data elements can be identified as they have an "X" in the box. The third row indicates a maximum number of significant data elements available for analyses, arrived at by subtracting the second row from the first.

The fourth row includes the estimated number of variables with correlation to other variables that will not be included in the analyses. These can be identified as a "C"appears in these boxes.

The fifth row indicates the number of deflection data elements not to be used for the P-020 analyses (even though rated as significant). Deflection data is not being included because it would amount to duplication as major deflections are the consequence of the other characteristics of the pavement structure that are included. The sixth row provides a number of data elements expected to be used for the P-020 analyses, arrived at by subtracting the fourth and fifth rows from the third row.

A separate row has been included at the bottom of the table to indicate the number of the missing data elements that are believed to be sufficiently correlated to other data elements that their absence would not have a significant effect on results. Fortunately, most of this missing data will be sufficiently correlated with other available data elements for four of the distresses, while other correlated data is not available for friction loss or raveling/weathering.

The information provided above can be usefully summarized for identification of specific data elements of inventory data that must be available for a test section to have value for the analyses (critical data elements). Data elements that are expected to be available in sufficient quantity for reasonable use are listed below to indicate the expected source of the data:

1. Critical data elements available from material sampling and testing: 1-13, 22, 41, 42 (air voids after traffic), 68, 72, 73, and 79.
2. Critical data elements available from inventory data: 14, 28, (or 25 or 29), 42 (initial air voids), and 113.
3. Critical data element available from National Traffic Data Base: 15.
4. Critical data elements available from environmental data: 89, 90, 91, 102-107.

This leaves a number of critical data elements that may be available for some test sections, but not in sufficient numbers to support the analyses. Some of these are expected to be represented to a reasonable level by correlations to other data elements. Those expected to be adequately "explained" are listed below, with the data elements that are expected to "explain" their effects:

Data Element Number	Correlated With	Expected Degree of Correlation
16, 18	22-24 and 8	Adequate
25, 29	28	Adequate
32	28	Reasonable
33	28	Limited
34	28	Adequate
35	28	Reasonable
36	28	Adequate
37	28	Limited
43-45	8, 22, 41 and 42	Adequate
51	8, 22, 25, 41, and 42	Adequate
52	42	Adequate
66, 67	9, 10, 57	Adequate
69, 70	13, 68, and 79	Adequate
81-83, 85, 86	68, 72, 73, and 79	Adequate

We have now accounted for most of the critical data elements, leaving a few that we could certainly use. The absence of some of these is not expected to greatly affect the development of performance equations (introduce error in equations), but those not included can not be evaluated directly as to sensitivity of predictions to their variations. The absence of a few will have serious impacts for some distresses. These remaining data elements are listed below, with indications as to the expected effects of their absence on the analyses for specific distresses:

Data Element Number	Level of Effect	Distress Type(s)
19 (Type of Mineral Filler)	Nominal	All
20 (Aggregate Durability)	Serious	Friction Loss and Raveling/Weathering
	Nominal	Other 4 Distresses
21 (Polish Value of Coarse Aggregate)	Serious	Friction Loss
	Nominal	Other 5 Distresses
30 (Type of Asphalt Modifiers)	Nominal	Friction Loss
	Moderate	Other 5 Distresses
31 (Quantity of Asphalt Modifiers)	Nominal	Friction Loss
	Moderate	Other 5 Distresses
49 (Moisture Susceptibility)	Nominal	Friction Loss
	Moderate	Other 5 Distresses

It can be seen from the discussions above that the expectation is that a reasonable array of data elements will be available for the sensitivity analyses for all of the distress types of interest, except for friction loss. Two of the most important variables, polish value and aggregate durability, will generally be missing, leaving only age of pavement, cumulative 18-kip ESAL, geological classification of coarse aggregate, and type of environment to explain variations in skid measurements.

Review of the data elements indicates a few data elements that should be available, if a test section is to prove very useful in the analyses. Those from inventory data believed to be necessary are listed below with the distress type for GPS-1 for which each is believe to be required:

Data Element Number	Description	Distress Types Necessary For
14	Age of Pavement	All
17	Geological Classification of Coarse Aggregate	For Friction Loss (Unless Polish Value is Available)
20	Aggregate Durability	Raveling/ Weathering and Friction Loss (Unless Polish Value is Available)
21	Polish Value of Coarse Aggregates	Friction Loss
25,28, or 29 (One of these)	Asphalt Grade, Viscosity, or Penetration	Alligator Cracking, Transverse Cracking, and Rutting
30, 31	Type and Amount of Asphalt Modifiers (if a modifier was used in sufficient quantity to seriously affect asphalt cement characteristics)	Alligator Cracking, Transverse Cracking, and Rutting

For GPS-2, other data elements describing bound base and subbase layers may also be critical as follows:

Data Element Number	Description	Distress Types Critical For
60, 61	Type and Percent of Stabilizing Agent	Transverse Cracking

For GPS-6 and GPS-7, data elements characterizing asphalt concrete (described above) will also be necessary for the overlay layer.

Considering the necessary data elements identified above in the previous three paragraphs, age of pavement will virtually always be available, although some may have used dates for original construction rather than for the overlay (GPS-6 and GPS-7). If geological classification of coarse aggregate is missing, this can likely be obtained from the State Highway Agency (SHA) or through observation of extracted aggregate in the laboratory.

Data on aggregate durability or polish value of coarse aggregates may not be available in project files, but local SHA personnel may be able to approximately relate other data for other projects to the project of interest, based on their knowledge of local materials in use.

Data on asphalt grade, viscosity, or penetration will generally be available. If it is not in project files, local SHA personnel may know what asphalt grade was specified or in common use at the time of construction.

Data on type and amount of modifiers may be difficult, if not available in project files, but this data should be pursued if there is reason to think a modifier was used.

Where a bound base is known to exist, the type of stabilizer at least should be identified. This can probably be ascertained by inspection in the laboratory. Amount of stabilizer would be good to have, but likely could be omitted without serious consequence, if the type is known.

Similar evaluations can be made for Experiments GPS-3, GPS-4 and GPS-5. Drs Darter and Owusu-Antwi are conducting similar evaluations on these experiments to establish relative significance of data elements.

GPS-1

SIGNIFICANT VARIABLES AND THEIR RELATIVE IMPORTANCE TO THE SIGNIFICANT DISTRESSES FOR PAVEMENTS WITH ASPHALT CONCRETE SURFACES

SIGNIFICANT VARIABLES		SIGNIFICANT DISTRESSES						BELIEVED TO BE CORRELATED WITH VARIABLE NUMBERS	
NO.	DESCRIPTION	Alligator Cracking	Transverse Cracking	Rutting	Roughness	Friction Loss	Raveling/ Weathering		
LAYER THICKNESSES:									
1	A.C. Overlay	~~1~~	~~1.2~~	~~1~~	~~1.2~~	3	2.8		CL
2	A.C. Surface	✓1	✓1.2	1✓	1✓	3	2.8		CL
3	Unbound Base	✓1	3	1✓	1✓	3	3		CL
4	Unbound Subbase	✓1	3	1✓	1.2✓	3	3		CL
5	Bound Base	~~1~~	~~1.8~~	~~1~~	~~1~~	3	3		CL
6	Bound Subbase	~~1~~	2	~~1~~	~~1~~	3	3		CL
LAYER STIFFNESSES:									
7	A.C. Overlay (w/temp.)	~~1~~	~~1~~	~~1~~	2	3	2.8		CL
8	A.C. Surface (w/temp.)	✓1	✓1	1✓	2.2	3	2.8		CL
9	Unbound Base	✓1	2.8	1✓	2.6	3	3		CL
10	Unbound Subbase	✓1.2	2.8	1.2✓	2.8	3	3		CL
11	Bound Base	~~1~~	~~1.8~~	~~1~~	2.6	3	3		CL
12	Bound Subbase	~~1.2~~	~~2.0~~	~~1.2~~	2.8	3	3		CL

SIGNIFICANT VARIABLES AND THEIR RELATIVE IMPORTANCE TO THE SIGNIFICANT DISTRESSES FOR PAVEMENTS WITH ASPHALT CONCRETE SURFACES CONT.

Percent Available

SIGNIFICANT VARIABLES		SIGNIFICANT DISTRESSES						BELIEVED TO BE CORRELATED WITH VARIABLE NUMBERS	
NO.	DESCRIPTION	Alligator Cracking	Transverse Cracking	Rutting	Roughness	Friction Loss	Raveling/ Weathering		
13	Subgrade	✓1.2	2.8	1.2 ✓	1.2 ✓	3	3		CL
AGE AND ESAL'S:									
14	Age of Pavement	✓1.2	✓1.2	1.4 ✓	1.6 ✓	1.6 ✓	1.8 ✓		CI
15	Cumulative 18-kip ESAL	✓1	✓1.8	1 ✓	1 ✓	2 ✓	2.2 ✓		CT
PLANT MIX AGGREGATE PROPERTIES:									
16	Composition of Coarse Aggregate	2.2	2.8	X 1.8	2.6	2	X 1.8	Generally only available from Inventory Data	
59% 17	Geological Classification of Coarse Aggregate	2.8	2.8	2.6	2.8	1.8 ✓	2.0		
18	Composition of Fine Aggregate	2.8	3	X 2	2.8	2.4	2.2		
19	Type of Mineral Filler	2.6	2.8	X 1.8	3	2	2.6		
20	Aggregate Durability	2.6	2.8	2.6	2.8	✓ 1.6	X 1.8		DU
8% 21	Polish Value of Coarse Aggregates	3	3	2.8	3	X 1.2	2.8		DU

SIGNIFICANT VARIABLES AND THEIR RELATIVE IMPORTANCE TO THE SIGNIFICANT DISTRESSES FOR PAVEMENTS WITH ASPHALT CONCRETE SURFACES CONT.

SIGNIFICANT VARIABLES		SIGNIFICANT DISTRESSES						BELIEVED TO BE CORRELATED WITH VARIABLE NUMBERS	
NO.	DESCRIPTION	Alligator Cracking	Transverse Cracking	Rutting	Roughness	Friction Loss	Raveling/ Weathering		
22	Gradation of Combined Aggregates	✓1.8	2.4	✓1.4	2.8	2	2.2		CL
23	Bulk Spec. Gravities	3	2.8	3	3	3	2.8		NC, CL
24	Effective Spec. Gravity-Aggregate Combination	3	2.8	3	3	3	2.4		NC, CL
PLANT MIX ASPHALT CEMENT PROPERTIES									
25	Asphalt Grade	C 1.4	C 1	C 1.4	2	3	2		IC-28-29
26	Source	2.2	2	2.2	2.6	2.8	2.4		NC
27	Specific Gravity	3	3	3	3	3	3		NC
ORIGINAL ASPHALT CEMENT PROPERTIES:									
28	Viscosity	✓1.6	✓1.2	✓1.4	2.2	2.8	2.4		IC-25, 29
29	Penetration	C 1.6	C 1.4	C 1.6	2.2	2.8	2.4		IC-25, 28
30	Type of Asphalt Modifiers	X 1.6	X 1.4	X 1.8	2.6	2.6	2.2		CI

95%
82%
77%
140°F 65%
72%

SIGNIFICANT VARIABLES AND THEIR RELATIVE IMPORTANCE TO THE SIGNIFICANT DISTRESSES FOR PAVEMENTS WITH ASPHALT CONCRETE SURFACES CONT.

SIGNIFICANT VARIABLES		SIGNIFICANT DISTRESSES						BELIEVED TO BE CORRELATED WITH VARIABLE NUMBERS
NO.	DESCRIPTION	Alligator Cracking	Transverse Cracking	Rutting	Roughness	Friction Loss	Raveling/ Weathering	
31	Quantity of Asphalt Modifiers	× 1.6	× 1.6	× 1.4	2.8	2.6	2.2	
32	Ductility	2	× 1.4	2.4	2.8	2.8	2.4	
33	Ring and Ball Softening Point	2	× 1.6	2	3	2.8	2.6	
LAB-AGED ASPHALT CEMENT PROPERTIES:								
34	Viscosity	1.2 ×	1 ×	1.2 ×	2.2	2.8	2.2	
35	Ductility	2 ×	1.4 ×	2.4	2.8	2.8	2.4	
36	Penetration	1.4 ×	1.2 ×	1.6 ×	2.2	2.8	2.2	
37	Ring and Ball Softening Point	2	1.6 ×	2	2.8	2.8	2.4	
38	Weight Loss	3	3	3	3	3	3	
ORIGINAL MIXTURE PROPERTIES:								
39	Max. Spec. Gravity	3	3	3	3	3	2.8	
40	Bulk Spec. Gravity	3	3	3	3	3	2.8	

77% 15%
4%
CI
CI
CI
43%
27%
23%
0%
DU
IC-25, 28-32
NC
50%
56%
NC
NC

SIGNIFICANT VARIABLES AND THEIR RELATIVE IMPORTANCE TO THE SIGNIFICANT DISTRESSES FOR PAVEMENTS WITH ASPHALT CONCRETE SURFACES CONT.

SIGNIFICANT VARIABLES		SIGNIFICANT DISTRESSES						BELIEVED TO BE CORRELATED WITH VARIABLE NUMBERS	
NO.	DESCRIPTION	Alligator Cracking	Transverse Cracking	Rutting	Roughness	Friction Loss	Raveling/ Weathering		
41	Asphalt Content	✓1	✓1.4	✓1	2.6	2.4	1.4 ✓		CL
42	Percent Air Voids	✓1	✓1.4	✓1.2	2.2	2.4	1.8 ✓	Initial from Inventory, At Time of Sampling from	Lab.
43	Marshall Stability - Blows	×1.8	2.3	×1.8	2.8	3	3	IC-7,8, 16-19,	22-25
44	Marshall Stability - Flow	×1.6	2.2	×1.6	2.6	3	3		
45	Hveem Cohesiometer Value	2.3	2.8	×1.8	2.8	3	3		
46	Type of Asphalt Plant	3	3	3	3	3	3		NC
47	Type of Antistripping Agent	2.8	3	2.8	3	2.8	2.3		NC
48	Amount of Antistripping Agent	2.8	3	2.3	3	2.5	2		NC
49	Moisture Susceptibility	2	2.8	2	3	2.2	1.2✓		DU
50	Mean Mixing Temp.	2.4	2.4	2.2	2.8	3	2.8		NC
51	Lay down Temp.	↗1.8	2.2	×1.8	2.6	3	2.4		DU
52	Percent Compaction	×1	×1.4	×1.4	2.2	2.4	2		DU, IC-42, 7,8
BASE/SUBBASE MATL. DATA:									
53	AASHTO Soil Class.	2.2	3	2.2	2.4	3	3		NC

SIGNIFICANT VARIABLES AND THEIR RELATIVE IMPORTANCE TO THE SIGNIFICANT DISTRESSES FOR PAVEMENTS WITH ASPHALT CONCRETE SURFACES CONT.

SIGNIFICANT VARIABLES		SIGNIFICANT DISTRESSES						BELIEVED TO BE CORRELATED WITH VARIABLE NUMBERS
NO.	DESCRIPTION	Alligator Cracking	Transverse Cracking	Rutting	Roughness	Friction Loss	Raveling/ Weathering	
54	Plasticity Index	2.6	2.8	2.2	2.2	3	3	
55	Max. Lab Dry Density	2.8	3	2.8	2.6	3	3	
56	Optimum Lab Moisture Content	3	3	3	2.8	3	3	
57	Percent Compaction	✓ 1.8	3	✓ 1.8	2.2	3	3	CI + plus one measurement of density in test pit
58	Gradation of Coarse Aggregate	2.2	3	2.2	2.4	3	3	
59	Gradation of Fine Aggregate	2.6	2.8	2.4	2.6	3	3	
60	Type of Stabilizing Agent (Bound)	2.2	~~1.4~~	2.2	2.6	3	3	
61	Percent Stabilizing Agent	2	~~1.8~~	2	2.6	3	3	
62	Type of Admixture	2.4	2.2	2.4	2.8	3	3	
63	Quantity of Admixture	2.4	2.4	2.4	2.8	3	3	
64	Compressive Strength (with confining press.).	2	2.6	✗ 1.6	2.2	3	3	Test Conducted DU Only for Treated Base/Subbase
65	Calcium Carbonate Content	3	3	2.8	2.8	2.8	3	
66	CBR	✗ 1.8	2.8	✗ 1.6	2.6	3	3	IC-9-11, 57-59
67	R-Value	✗ 1.8	2.8	✗ 1.6	2.6	3	3	

27% bound 47% base 41% 37%

NC NC NC CI NC NC CI CI NC NC 1% 1% 5%

SIGNIFICANT VARIABLES AND THEIR RELATIVE IMPORTANCE TO THE SIGNIFICANT DISTRESSES FOR PAVEMENTS WITH ASPHALT CONCRETE SURFACES CONT.

SIGNIFICANT VARIABLES		SIGNIFICANT DISTRESSES						BELIEVED TO BE CORRELATED WITH VARIABLE NUMBERS	
NO.	DESCRIPTION	Alligator Cracking	Transverse Cracking	Rutting	Roughness	Friction Loss	Raveling/ Weathering		
SUBGRADE DATA:									
68	AASHTO Soil Classification	2	3	1.8 ✓	1.6	3	3		CL
69	CBR	× 1.4	3	× 1.2	× 1.8	3	3	May be available from Inventory Data - IC-942	
70	R-Value	× 1.6	3	× 1.2	× 1.8	3	3		Tests Not Conducted
71	% Passing #40 Sieve	2.8	3	2.6	3	3	3		NC, CL
72	% Passing #200 Sieve	2.8	3	2.2	2 ✓	3	3		CL
73	Plasticity Index	2.4	3	2	2 ✓	3	3		CL
74	Liquid Limit	2.4	3	2	2	3	3		NC, CL
75	Max. Lab Dry Density	3	3	3	3	3	3		NC, CL
76	Optimum Lab Moisture Content	3	3	3	3	3	3		NC, CL
77	Percent Compaction	2.2	2.8	2	2.4	3	3		NC, CL
78	In Situ Dry Density	2.6	3	2.4	2.4	3	3		NC, CL
79	In Situ Moisture Content	2.2	3	1.8 ✓	2.2	3	3		CL

82% 9% 13% 40% 52% 40% 29% 23%

SIGNIFICANT VARIABLES AND THEIR RELATIVE IMPORTANCE TO THE SIGNIFICANT DISTRESSES FOR PAVEMENTS WITH ASPHALT CONCRETE SURFACES CONT.

SIGNIFICANT VARIABLES		SIGNIFICANT DISTRESSES						BELIEVED TO BE CORRELATED WITH VARIABLE NUMBERS
NO.	DESCRIPTION	Alligator Cracking	Transverse Cracking	Rutting	Roughness	Friction Loss	Raveling/ Weathering	
80	Relative Density (Cohesionless Soil)	2.4	3	2	2.2	3	3	
81	Soil Suction	2.4	2.8	2	× 1.8	3	3	IC- Correlated with 71-74, 77-77
82	Expansion Test	2.8	3	2.8	× 2	3	3	
83	Swell Pressure	3	3	3	× 1.8	3	3	
84	% by Wt. Finer Than 0.02 min.	2.4	3	2	1.8 ✓	3	3	
85	Av. Rate of Heave (Lab. Freeze Test)	2.4	3	2.2	× 1.6	3	3	IC-71-72
86	Frost Susceptibility Classification	2.4	3	2.2	× 1.6	3	3	
DEFLECTION DATA:								
87	Measured Deflections (normalized to stnd. temp.)	1.6	3	1.6	2.2	3	3	
88	Depth to "Rigid" Layer	1.8	3	1.8	2.4	3	3	Available at mid-point of test Section

0% 0% 1% 3% 1% 13%

NC DU DU DU CL DU CM

SIGNIFICANT VARIABLES AND THEIR RELATIVE IMPORTANCE TO THE SIGNIFICANT DISTRESSES FOR PAVEMENTS WITH ASPHALT CONCRETE SURFACES CONT.

SIGNIFICANT VARIABLES		SIGNIFICANT DISTRESSES						BELIEVED TO BE CORRELATED WITH VARIABLE NUMBERS	
NO.	DESCRIPTION	Alligator Cracking	Transverse Cracking	Rutting	Roughness	Friction Loss	Raveling/ Weathering		
ENVIRONMENTAL DATA:									
89	Type of Environment	C 2	C 1.2	1.4 ✓	1.8 ✓	2 ✓	1.6 ✓		CE
90	Freeze Index	2.4	✓ 1.4	2.4	1.8 ✓	2.8	2.4		CE
91	Thorthwaite Index	2.4	2.4	2.6	2 ✓	3	2.6		CE
92	Annual Precipitation	2.2	3	2.2	2.2	3	2.2		NC
93	Precipitation Days by Month	2.4	3	2.4	2.4	3	2.6		NC
94	Precipitation Days by Year	2.4	3	2.4	2.4	3	2.6		NC
95	No. of Days with High Solar Radiation	2.5	2.3	2.3	2.8	2.8	2.8		NC
96	Highest Annual Solar Radiation	2.8	2.6	2.6	3	2.8	2.8		NC
97	Lowest Annual Solar Radiation	3	2.6	2.6	3	3	3		NC
98	Elevation Above Sea Level	2.8	2.6	2.6	3	2.8	2.8		NC
99	% Sunshine (of Possible Time)	2.6	2.6	2.8	3	3	2.8		NC
100	Average Wind Speed by Month	2.8	2.8	2.8	3	3	3		NC
101	Average Dew Point by Month	3	3	3	3	3	3		NC
									NC

SIGNIFICANT VARIABLES AND THEIR RELATIVE IMPORTANCE TO THE SIGNIFICANT DISTRESSES FOR PAVEMENTS WITH ASPHALT CONCRETE SURFACES CONT.

SIGNIFICANT VARIABLES		SIGNIFICANT DISTRESSES						BELIEVED TO BE CORRELATED WITH VARIABLE NUMBERS	
NO.	DESCRIPTION	Alligator Cracking	Transverse Cracking	Rutting	Roughness	Friction Loss	Raveling/ Weathering		
TEMPERATURE:									
102	Monthly Average	C 1.8	C 1.4	C 1.2	C 2	3	2.4		CE
103	Average Max. Daily by Month	C 1.8	C 2	1.2 ✓	C 2	3	2.4		CE
104	Average Min. Daily by Month	C 1.8	C 1.6	C 2	C 2	3	2 ✓		CE
105	No. of Days with Max. Temp. Greater Than 90F	✓ 1.8	2.4	1.2 ✓	2 ✓	2.8	2.6		CE
106	No. of Days with Min. Temp. Less Than 32F	✓ 1.6	✓ 1.2	2.4	2.4	2.8	1.8 ✓		CE
107	No. of Freeze-Thaw Cycles/Year	✓ 2	✓ 1.4	2.2	1.8 ✓	2.8	1.4 ✓		CE
SHOULDER DATA:									
108	Shoulder Width	2.2	3	2.4	2.6	3	3		NC
109	Shoulder Surface Type	2.4	3	2.6	2.6	3	3		NC
110	Shoulder Surface Thickness	3	3	3	3	3	3		NC
111	Shoulder Base Type	2.6	3	2.8	2.8	3	3		NC

Note - These data are correlated with ...

SIGNIFICANT VARIABLES AND THEIR RELATIVE IMPORTANCE TO THE SIGNIFICANT DISTRESSES FOR PAVEMENTS WITH ASPHALT CONCRETE SURFACES CONT.

SIGNIFICANT VARIABLES		SIGNIFICANT DISTRESSES						BELIEVED TO BE CORRELATED WITH VARIABLE NUMBERS	
NO.	DESCRIPTION	Alligator Cracking	Transverse Cracking	Rutting	Roughness	Friction Loss	Raveling/ Weathering		
112	Shoulder Base Thickness	2.6	3	2.8	2.8	3	3		NC
SUBSURFACE DRAINAGE DATA:									
113	Type	2	2.6	1.6 ✓	1.6 ✓	3	3		CI
114	Location	2	2.4	2	1.6 ✗	3	3		CI
115	Diameter of Long. Drain Pipes	3	3	3	3	3	3		NC
116	Spacing of Laterals	2.6	3	2.6	2.2	3	3		NC
117	No. of Lanes in Travel Direction	2.8	3	2.8	3	3	3		NC

85%

EVALUATION OF NOS. OF DATA ELEMENTS FOR GPS EXPERIMENT 1 THAT WILL BE AVAILABLE AND WILL BE USED FOR CONTRACT P-020 DATA ANALYSIS

DESCRIPTION	ALLIGATOR CRACKING	TRANSVERSE CRACKING	RUTTING	ROUGHNESS	FRICTION LOSS	RAVELING/ WEATHERING
Maximum No. Of Significant Data Elements	38	25	44	27	6	11
No. Of Significant Data Elements That Will Not Be Available In Sufficient Nos.	13	9	17	8	2	3
Max. No. Of Significant Data Elements Available For Analyses	25	16	27	19	4	8
Est. No. Of Variables With Correlations To Other Variables, Not To Be Included In Analyses	6	6	5	4	0	0
No. Of Deflection Data Elements Not To Be Used For P-020 Analyses (Rated As Significant)	2	*	2	*	*	*
No. Of Data Elements Expected To Be Used For P-020 Analyses	17	10	20	15	4	8
No. Of Missing Data Elements Correlated To Other Available Data Elements	11	7	14	8	0	1

* Deflections Were Not Rated As Significant For These Distress Types.

EVALUATION OF NOS. OF DATA ELEMENTS FOR GPS EXPERIMENT 1 THAT WILL BE AVAILABLE AND WILL BE USED FOR CONTRACT P-020 DATA ANALYSIS

DESCRIPTION	ALLIGATOR CRACKING	TRANSVERSE CRACKING	RUTTING	ROUGHNESS	FRICTION LOSS	RAVELING/ WEATHERING
1. Maximum No. Of Significant Data Elements	38	25	44	27	6	11
2. No. Of Significant Data Elements That Will Not Be Available In Sufficient Nos.	13	9	17	8	2	3
3. Max. No. Of Significant Data Elements Available For Analyses (Row 1 - Row 2)	25	16	27	19	4	8
4. Est. No. Of Variables In Row 3 With Correlations To Other Variables, Not To Be Included In Analyses	6	6	5	4	0	0
5. No. Of Deflection Data Elements Not To Be Used For P-020 Analyses (Rated As Significant)	2	*	2	*	*	*
6. No. Of Data Elements From Row 3 Expected To Be Used For P-020 Analyses (Row 3 - Row 4 - Row 5)	17	10	20	15	4	8
7. No. Of Missing Data Elements From Row 2 Correlated To Other Data Elements That Are Available	11	7	14	8	0	1

* Deflections Were Not Rated As Significant For These Distress Types.

Appendix B

Technical Memorandum by Dr. Robert L. Lytton, March 31, 1992, "Clusters of Terms Relevant to Pavement Performance Prediction"

TECHNICAL MEMORANDUM

PROJECT: Contract SHRP 89-P-020
Data Analysis

DATE: March 31, 1992

DISTRIBUTION: Dr. Robert Raab, Dr. Brent Rauhut, Dr. Michael I. Darter, Dr. Emmanuel Owusu-Antwi, Dr. Olga Pendleton, Dr. Bill Hadley, Dr. Gil Baladi, and Dr. Peter Jordahl

AUTHOR: Robert L. Lytton

SUBJECT: Clusters of Terms Relevant to Pavement Performance Prediction

The prediction of pavement performance has been found empirically to be related to the "primary responses" of the pavement such as deflection and strains at specific points in the pavement. This is information that is known from previous studies and experience that should be carried forward into all future studies. Knowledge such as this can be used to make the task of developing future models of pavement performance much more efficient. In this memorandum, the use of relations taken from mechanics to make up terms that predict deflections and strains will be illustrated and the clusters of terms that result can be used as super, single variables in further regression analysis studies. This reduces the number of pavement sections on which data needs to be collected, reduces the number of independent variables in the regression equations, and best of all it makes use of what we already know.

Approximate Layered Elastic Theory

Odemark's assumption can be used to good advantage in this endeavor. Odemark found that in predicting pavement deflections of a multilayered pavement, a simplification could be used which transformed the layers of different materials into one layer of the same material. The thickness of the equivalent layer is h_s given by:

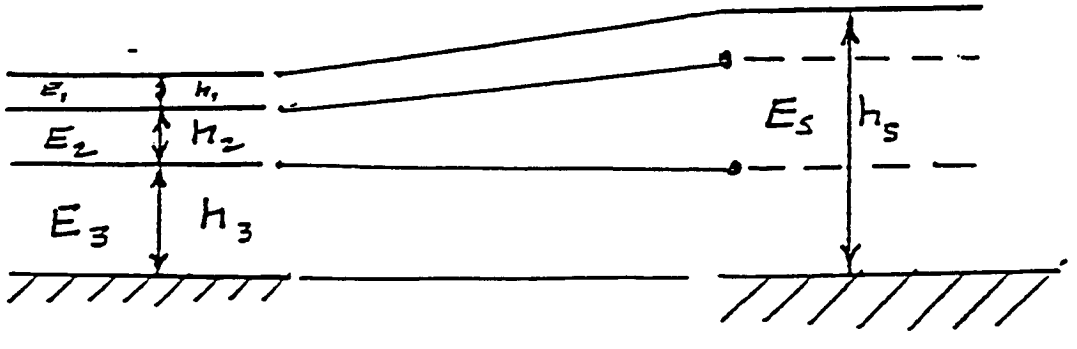

$$h_s = c \sum_{i=1}^{3} \left(\frac{E_i}{E_s}\right)^n h_i$$

where:

c	=	0.9
n	=	1/3
h_i	=	the thickness of layer i.
E_i	=	the Young's modulus of layer i.
E_s	=	the reference modulus. It can be selected to be the modulus of any layer.
h_s	=	the equivalent thickness of the reference material.

If layers on top of a subgrade with modulus, E_s , are all converted into equivalent thicknesses of subgrade material, then the Boussinesq equations may be used to calculate the deflections, strains, or stresses at any point in a pavement.

The Boussinesq equation for the deflection, Δ, of the surface of a half-space with a Poisson's ratio of 0.5 is:

$$\Delta = \frac{3P}{4\pi E_s r}$$

where

P	=	the load
r	=	the distance Δ is from the load

The vertical strain beneath the load in the center of each layer may be estimated using a combination of the Odemark assumption and the Boussinesq equations. The equation is of the form:

$$e_i = \frac{q}{E_i}\left[1 - \left(\frac{1}{1 + \left(\frac{a}{z_i}\right)^2}\right)^{3/2}\right]$$

where

$$\bar{z}_i = \frac{h_i}{2}\left(\frac{E_i}{E_s}\right)^{1/3} + \sum_{j=1}^{i-1} h_j \left(\frac{E_j}{E_s}\right)^{1/3}$$

$\bar{z}_i$	=	the Odemark - transformed distance to the center of each layer from the surface.
a	=	the diameter of the loaded area.
q	=	the uniform pressure on the loaded area (typical units: lbs/in.^{2})

The equation for the strain may be rewritten as:

$$e_i = \frac{q}{E_i}\left[1 - \frac{z_i^3}{(z_i^2 + a^2)^{3/2}}\right]$$

An estimate of the shearing strain at a radius, r, and depth, z, below the surface is:

$$\gamma = \frac{-3P}{4\,\pi\,E}\left[\frac{6rz_i^2}{R^5}\right]$$

where, in this case, z_i is defined differently as:

z_i = the Odemark transformed distance to the bottom of layer i from the surface.

$$z_i = \sum_{j=1}^{i} h_j \left(\frac{E_j}{E_s}\right)^{1/3}$$

and $R^2 = r^2 + z_i^2$

r = the radius from the center of the tire load.

This shearing strain is zero on the surface where r = z = 0 and is useful in estimating the fatigue life of the pavement surface. The number of load cycles to reach failure due to the propagation of a crack by shearing strains should be inversely proportional to the maximum value of the shearing strain that occurs at the bottom of the surface layer, that is, for a specific z_i, where:

$$\frac{\partial \gamma_i}{\partial r} = 0$$

This occurs where:

$$\frac{\partial \gamma}{\partial r} = \frac{-18P}{4\,\pi E}\,\frac{z_i^2}{R^7}\left[z_i^2 - 4r^2\right] = 0$$

That is where:

$$z_i = \pm 2r$$

Before running a regression analysis on fatigue it will be necessary at first to determine the value of r for which

$$\frac{\partial \gamma_i}{\partial r} = 0,$$

and then to determine the value of the shearing strain, γ_i, corresponding to it.

The equation for the deflection of a one-layered pavement resting on a rigid base is:

$$\Delta = c \frac{P}{E_s H}$$

where c = a constant of proportionality.
H = the thickness of the layers above the rigid base.

The equation for the deflection of a multilayered pavement above a rigid base is:

$$\Delta = c \frac{P}{E_s \sum_{i=1}^{l} \left(\frac{E_i}{E_s}\right)^n h_i}$$

where l = *the number of layers*

These simple equations give the form of the equation and the proper relationship among the variables, and because of this they are very valuable in determining the correct clusters of terms that relate a primary response of a pavement to the load, layer thicknesses and moduli on which it depends. Regression analysis can supply the value of the constant, C.

If it is assumed that rutting is due to:

1. Vertical compression and,

2. Horizontal displacement

in each layer, then more mechanistic terms may be added to the previous work. The forms of equation for vertical compression have already been worked out above.

Forms of equations for horizontal displacement are worked out below. Let us advance the hypothesis that the permanent horizontal displacement in each layer is proportional to the maximum shearing strain at the center of each layer. The shearing strain is given by

$$\gamma_{xy} = \frac{\partial u}{\partial z} + \frac{\partial w}{\partial r}$$

Displacements in a half-space

$$u = \frac{P}{2\pi} \frac{(1+\upsilon)(1-2\upsilon)}{E} \left[-\frac{1}{r} + \frac{z}{Rr} + \frac{rz}{(1-2\upsilon)R^3} \right]$$

$$w = \frac{P}{2\pi} \frac{(1+\upsilon)}{E} \left[\frac{z^2}{R^3} + \frac{2\,(1-\upsilon)}{R} \right]$$

$$R = (r^2 + z^2)^{1/2} \qquad R^3 = (r^2 + z^2)^{3/2}$$

If $\upsilon = 1/2$, *then* $(1-2\upsilon) = 0$ *and*

$$u = \frac{3P}{4\pi E} \frac{rz}{R^3}$$

$$w = \frac{3P}{4\pi E} \left[\frac{1}{R} + \frac{z^2}{R^3} \right]$$

$$\frac{\partial u}{\partial z} = \frac{3P}{4\pi E} \left[\frac{r}{R^3} - \frac{3rz^2}{R^5} \right]$$

$$\frac{\partial w}{\partial r} = \frac{3P}{4\pi E}\left[\frac{-r}{R^3} - \frac{3rz^2}{R^5}\right]$$

$$\gamma = \frac{\partial u}{\partial z} + \frac{\partial w}{\partial r} = \frac{3P}{4\pi E}\left[\frac{r}{R^3} - \frac{3rz^2}{R^5} - \frac{r}{R^3} - \frac{3rz^2}{R^5}\right]$$

$$\gamma = \frac{-3P}{4\pi E}\left[\frac{6rz^2}{R^5}\right]$$

Another useful set of relations comes from beam-on-elastic foundation theory. For example, the maximum moment in a beam beneath a uniform load of length, a, is:

$$M_{max} = \frac{q}{2\beta^2} e^{-\frac{\beta a}{2}} \sin\left(\frac{\beta a}{2}\right)$$

where q = the uniform load (example units: lbs/ft)
a = length

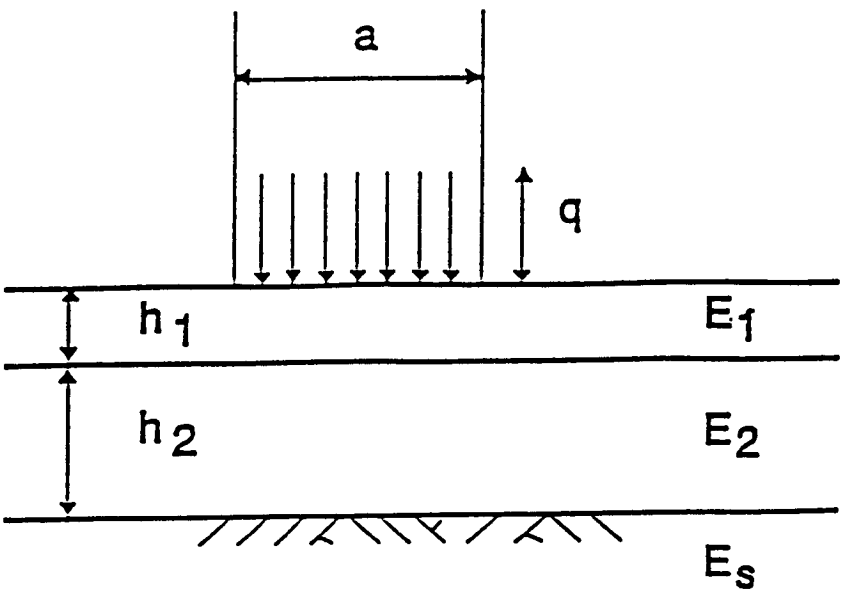

$$\beta = \sqrt[4]{\frac{E_s}{4a\,(\overline{EI})_{pavement}}}$$

$\overline{EI}$ = the flexural stiffness of the pavement per unit width.

$$= \sum_{i=1}^{l} \left(\frac{E_i h_i^3}{12} + E_i h_i d_i^2 \right)$$

d_i = the centroidal distance of each layer from the neutral axis of the layers above the subgrade.

l = number of pavement layers above the subgrade.

$\overline{d}$ = the distance to the neutral axis of the pavement from the surface.

$$\overline{d} = \frac{\sum_{i=1}^{l} E_i h_i \left(\frac{h_i}{2} + \sum_{j=1}^{i-1} h_j \right)}{\sum_{i=1}^{l} E_i h_i}$$

$$\textit{Thus, } d_1 = \overline{d} - \frac{h_1}{2}$$

$$d_2 = \overline{d} - h_1 - \frac{h_2}{2}$$

$$d_3 = \overline{d} - h_1 - h_2 - \frac{h_3}{2} \quad \textit{etc.}$$

The bending strain at the bottom of the top layer is:

$$\epsilon_1 = \frac{6 M_{max}}{E_1 h_1^2}$$

All of these equations provide relations among the load, tire pressure, diameter of the loaded area, layer thicknesses and moduli which are dictated by mechanics to predict the primary responses of deflection, strain and stress of a pavement. Regression analysis will provide the "scale factors" which link these primary responses to the different types of distress and deterioration in pavements.

Material Property Relations

Several useful material property relations have been found from previous studies in pavements and other materials. The studies have been in the areas of creep, fracture, and permanent deformation of materials. The relations will be presented here without the derivations.

In a creep test, a stress is applied to a material and held constant at σ_0 while the strain changes with time, $\epsilon(t)$. The quotient of the two is D(t), the creep compliance. This response of practically all materials of which pavements are built has been found to obey a power law:

$$\frac{\epsilon(t)}{\sigma_o} = D(t) = D_o + D_1 t^m$$

where D_o = the "elastic" or glassy part of the compliance.
D_1 = the constant related to the time-dependent part of the compliance.
m = the creep compliance exponent.

It has been found from fracture mechanics that the fatigue exponent, normally called K_2, is proportional to 2/m.

Furthermore, it has been found that the permanent deformation exponent, α, is given by 1-m. Other useful relations have been found which include m, the creep compliance exponent. Thus, it is useful to have a way of estimating it.

In asphaltic concrete, the greater the amount of asphalt that fills the voids in the mineral aggregate, the higher is the creep compliance exponent, m, which ranges between 0 and 1. It is never larger than 1.0. These facts may be used to estimate m. The block diagram of asphalt concrete is used for this purpose.

Volumetric Quantities			Weight Quantities	
Volume of Air	V_{air}	Air		
Volume of Asphalt	V_{as}	Asphalt	W_a	Weight of Asphalt
Volume of Solids	V_s	Solid (Aggregate)	W_s	Weight of Solids
Total Volume	V		W	Total Weight

VMA = $V_{air} + V_{as}$ = Voids in the Mineral Aggregate

An estimate of m is the ratio of the volume of asphalt to the volume of voids in the mineral aggregate, given by:

$$m = \frac{V_{as}}{VMA} = \frac{w_a \gamma_t}{w_a \gamma_t + (1-w_a) \gamma_a V_{air}}$$

where:
- w_a = asphalt content by weight
- γ_a = unit weight of asphalt
- γ_t = density of asphaltic concrete
- V_{air} = air voids, decimal, (V_a/VMA)

All of these data are recorded in the SHRP LTPP data base for each pavement section.

For base course and subgrade materials, the exponent of the creep compliance, m, has been found to depend upon the volumetric contents of the solids and water, according to the relation drawn from the rule of mixtures.

$$m = 0.02\ \theta_s + 0.60\ \theta_w$$

$$\theta_s = \frac{V_s}{V}, \quad \textit{the volumetric solids content}$$

$$\theta_w = \frac{V_w}{V}, \quad \textit{the volumetric water content}$$

These cannot be determined uniquely without knowing the water content, w, and the specific gravity of the solids, G_s.

$$\theta_w = \frac{G_s w}{1 + G_s w}$$

$$\theta_s = \frac{1}{1 + G_s w}$$

and thus,

$$m = \frac{0.02 + 0.60\ G_s w}{1 + G_s w}$$

The fatigue coefficient, K_1, has been found from fracture mechanics to be proportional to:

$$K_1 \propto \frac{h_1^{1-\frac{K_2}{2}}}{E_1^{K_2} A}$$

and the fracture coefficient, A, has been found proportional to:

$$A \propto \frac{1}{\sigma_t^2 E_1^{\frac{K_2}{2}} s}$$

where σ_t = the tensile strength of the fatiguing material
s = the speed of travel

Thus, the fatigue coefficient, K_1, is found to be proportional to:

$$K_1 \propto \frac{h_1^{1-\frac{K_2}{2}} \sigma_t^2 s}{E_1^{\frac{K_2}{2}}}$$

The fatigue exponent, K_2, as stated previously, is proportional to 2/m , and this allows the use of approximation of "m" that was developed previously:

$$K_2 = c \frac{2}{m} = c \frac{2[w_a \gamma_t + (1+w_a) \gamma_a V_{air}]}{w_a \gamma_t}$$

where c = a regression coefficient to be determined.
w_a, γ_t, γ_a, V_{air} = asphaltic concrete quantities that have been defined previously.

The permanent deformation exponent, α, for the asphalt layer is:

$$\alpha = 1-m = c \frac{(1+w_a) \gamma_a V_{air}}{w_a \gamma_t + (1+w_a) \gamma_a V_{air}}$$

where c = a regression coefficient to be determined.

The permanent deformation exponent, α, for base courses and subgrades is:

$$\alpha = 1-m = c\,\frac{0.98+0.40\,G_s\,w}{1+G_s\,w}$$

where c = a regression coefficient to be determined.
G_s, w = soil quantities previously defined.

The permanent deformation coefficient, μ, has been found to be proportional to:

$$\mu \propto (1-\alpha)\ (\Delta t)^{1-\alpha}$$

where Δt = the loading time, i.e., the time duration during which a point on the pavement is stressed by a moving load.

The loading time may be estimated by:

$$\Delta t = \frac{d}{s}$$

where d = the length of a deflection basin (approx. 10-20 feet).

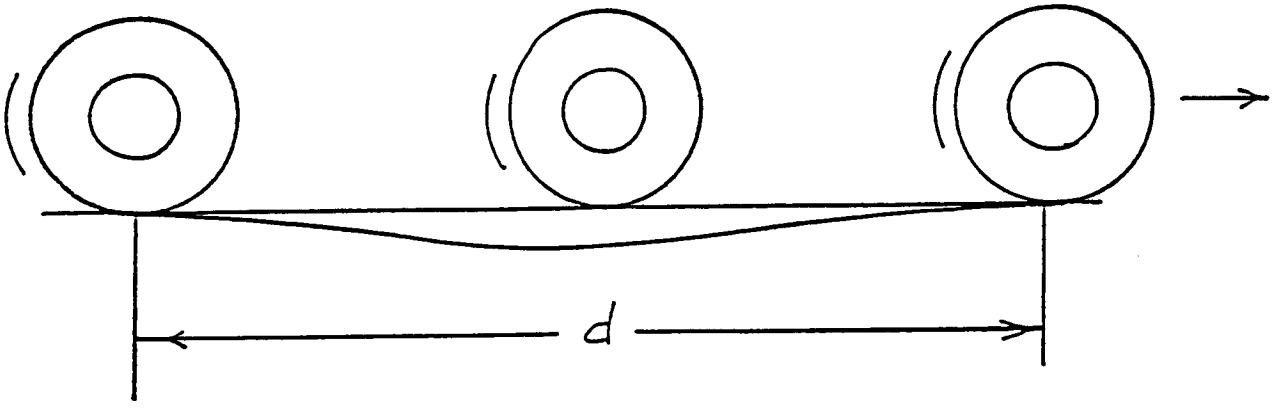

s = the speed of travel.

Thus, the permanent deformation coefficient, μ, is given by:

$$\mu = c\,(1-\alpha)\left(\frac{d}{s}\right)^{1-\alpha}$$

where c = a regression coefficient to be determined.
α, d, s = quantities that have been defined previously.

Pavement Performance Prediction Models

The kinds of pavement performance that need to be predicted include:

Alligator Cracking
Rutting
Damage due to the loss of serviceability index

Alligator Cracking

The number of load cycles to failure by alligator cracking is generally considered to be inversely dependent on the bending strain at the bottom of the asphalt layers, although recent results from fracture mechanics indicate that the maximum shearing strain may be more responsible. In either case, the number of load cycles to failure, N_f, is considered to be given by:

$$N_f = K_1 \left(\frac{1}{e_1}\right)^{K_2}$$

or

$$N_f = K_1 \left(\frac{1}{\gamma_1}\right)^{K_2}$$

Rutting

The rate of increase of permanent strain in each layer of a pavement due to repeated wheel loads is considered to be proportioned to the resilient strain according to the rule:

$$\frac{\partial \epsilon_a}{\partial N} = (\mu\, N^{-\alpha}) \cdot \epsilon_r$$

where
ϵ_a = the permanent strain
N = the number of load cycles
ϵ_r = the resilient vertical strain
μ = the permanent strain coefficient
α = the permanent strain exponent

The vertical compression of each pavement layer is:

$$\rho_i = \mu_i \, e_{ri} \, \frac{N^{1-\alpha_i}}{1-\alpha_i} \, h_i$$

where ρ_i = the contribution of layer i to the total vertical compression of a pavement.
ϵ_{ri} = the resilient vertical strain in each layer.
h_i = the thickness of each layer.

The total vertical compression is:

$$\rho = \sum_{i=1}^{l} \rho_i = \sum_{i=1}^{l} \frac{\mu_i \, e_{ri} \, h_i}{l-\alpha_i} \, N^{1-\alpha_i}$$

The rate of increase of the permanent lateral displacement in each layer is assumed to be of the same form.

$$\frac{1}{\gamma} \, \frac{\partial \gamma_a}{\partial N} = \mu \, N^{-\alpha}$$

$$\frac{\partial \gamma_a}{\partial N} = \gamma(r) \, \mu \, N^{-\alpha}$$

where: γ_a = the permanent shear strain
$\gamma(r)$ = the resilient shearing strain at a horizontal distance, r, from the center point of load application.

The lateral shear flow in layer i is given by:

$$\int_0^{r_i+a} h_i \, \frac{\partial \gamma_a}{\partial N} \, dr = h_i \int_0^{r_i+a} \int_0^{N} \gamma(r) \, \mu N^{-\alpha} \, \partial N \, dr$$

$$= h_i \, \frac{\mu N^{1-\alpha}}{1-\alpha} \int_0^{r_i+a} \gamma(r) \, dr$$

$$= h_i \ \mu \frac{N^{1-\alpha}}{1-\alpha} \left[\frac{-18Pz_i^2}{4\pi E} \right] \int_0^{r_i+a} \frac{r\,dr}{(r^2+z^2)^{5/2}}$$

where: a = the radius of the loaded tire footprint area

$$\int_0^{r_i+a} h_i \frac{\partial \gamma_a}{\partial N} dr = h_i \frac{\mu N^{1-\alpha}}{1-\alpha} \frac{3P}{2\pi E} \left\{ \frac{z_i^2}{[(r_i+a)^2 + z_i^2]^{3/2}} - \frac{1}{z_i} \right\}$$

The rut depth due to this lateral shear flow is proportional to it so that

$$\gamma_a \propto \frac{\partial w_a}{\partial r}$$

where: w_a = the accumulated vertical displacement due to lateral shear flow.

$$\gamma_a\, dr = \partial w_a$$

$$\int_{r=0}^{r=a+r_i} \gamma a \, dr = \int_{r=0}^{r=a+r_i} dw_a = w_a\,(a+r_i) - w_a(0)$$

For each layer, the increment of rut depth is proportional to

$$\Delta\ RD_{lateral\ flow} \propto \frac{3P}{2\pi E} h_i \frac{\mu N^{1-\alpha}}{1-\alpha} \left[\frac{z_i^2}{[(r_i + a^2) + z_i^2]^{3/2}} - \frac{1}{z_i} \right]$$

and the total rut depth due to lateral flow is proportional to

$$RD_{lateral\ flow} \propto \frac{3P}{2\pi} \sum_{i=1}^{n} \frac{h_i\, \mu_i\, N^{1-\alpha_i}}{E_i\,(1 - \alpha_i)} \left[\frac{z_i^2}{(z_i/2 + a)^2 + z_i^2]^{3/2}} - \frac{1}{z_i} \right]$$

If $P = \pi\, q\, a^2$ *then*

Because the permanent strain coefficient, μ_i, is approximated by

$$\mu_i = c\,(1-\alpha)\left(\frac{d}{s}\right)^{1-\alpha}$$

another expression for the rut depth due to lateral flow is

$$RD = C\,\frac{3qa^2}{2}\sum_{i=1}^{n}\frac{h_i}{E_i}\left(\frac{dN}{S}\right)^{1-\alpha_i}\left[\frac{z_i^2}{\left[\left(\frac{z_i}{z}+a\right)^2+z_i^2\right]}-\frac{1}{z_i}\right]$$

Damage

In general, damage is normalized distress, beginning at 0.0 and reaching an unacceptable value when it reaches 1.0. The loss of serviceability index is usually treated in this way.

$$g(N) = \frac{p_i - p(N)}{p_i - p_t}$$

where
- $g(N)$ = damage ratio
- p_i = the initial serviceability index
- p_t = the terminal serviceability index
- $p(N)$ = the current level of serviceability index

The damage ratio is considered to increase with the number of load cycles, N, and the deflection of the pavement under load:

$$g(N) = \left(\frac{N\Delta}{\rho}\right)^{\beta}$$

where ρ, β = regression coefficients

Clusters of Terms for Pavement Performance Prediction

Assembling all of the information that has been presented thus far permits the development of equations describing pavement performance and including clusters of terms that are dictated by what we have learned in mechanics.

Alligator Cracking Clusters

The number of load cycles to failure, N_f, is given by:

$$N_f = c_1(h_1\ \sigma_t^2\ s)^{c_2}\left(\frac{h_1\ E_1^{1/2}\ E_s^{1/2}}{qa^{1/2}}\right)^{c_3 K_2}\cdot\left[\frac{1}{\sum_{i=1}^{l} E_i\left(\frac{h_i^2}{12}+h_i\ d_i^2\right)}\right]^{c_4\frac{K_2}{2}}$$

where c_1, c_2, c_3, and c_4 are regression coefficients

The regression equation by which these coefficients are determined is:

$$\log N_f = \log c_1 + c_2 \log (x_1) + c_3 K_2 \log (x_2) + c_4 \frac{K_2}{2} \log (x_3)$$

where

$$x_1 = h_1\ \sigma_t^2\ s$$

$$x_2 = \frac{h_1\ E_1^{1/2}\ E_s^{1/2}}{qa^{1/2}}$$

$$x_3 = \frac{1}{\sum_{i=1}^{l} E_i\left(\frac{h_i^2}{12} + h_i\ d_i^2\right)}$$

The terms x_1, x_2, and x_3 are the clusters of terms which are appropriate to use in predicting the number of load cycles, N_f, to reach a specific level of alligator cracking.

If the maximum shearing strain criterion is used to relate to the number of load cycles to reach failure, the equation to be used is:

$$N_f = c_1\ (h_1\ \sigma_t^2\ s)^{c_2}\left(\frac{16}{3}\ \frac{E_s}{E_1^{1/2}\ h_1^{1/2}\ q\ a^2}\right)^{c_3 K_2}\cdot\left[\frac{(R_i^*)^5}{(r^*+z_i)^3\ r^* z_i (r^*+z_i)}\right]^{c_4 K_2}$$

where c_1, c_2, c_3, and c_4 are regression coefficients to be determined. The regression equation to be used for this purpose is:

$$\log N_f = \log c_1 + c_2 \log x_1 + c_3 K_2 \log x_2 + c_4 K_2 \log x_3$$

where the cluster variables x_1, x_2, and x_3 are:

$$x_1 = h_1 \sigma_t^2 s \quad \textit{as before}$$

$$x_2 = \frac{16}{3} \frac{E_s}{E_1^{1/2} h_1^{1/2} q a^2}$$

$$x_3 = \frac{(R_i^*)^5}{(r^*+z_i)^3 + r^* z_i (r^*+z_i)}$$

r^* = the radius at which the shearing strain, γ, is maximum at the transformed depth, z_i.

$(R^*_i)^2 = (r^*)^2 + (z_i)^2$

The value of K_2 to be used in either of these expressions is:

$$K_2 = \frac{2[w_a \gamma_t + (1+w_a)\gamma_a V_{air}]}{w_a \gamma_t}$$

where
- w_a = the asphalt content, by weight (decimal)
- V_{air} = the air voids (decimal)
- γ_a = the unit weight of asphalt cement
- γ_t = the density of asphalt concrete

Rutting Clusters

The regression equation for predicting rutting due to vertical compression is of the form:

$$RD = c_2 \left[q \sum_{i=1}^{l} \rho_i \right]^{c_3}$$

or

$$RD = c_1 + c_2 \left[q \sum_{i=1}^{l} \rho_i \right]$$

In either form of equation, the term $q\Sigma\rho_i$ represents the sum of the contributions to the total rut depth of each of the layers. When it is written out to show the cluster terms, it is as follows, in the preferred logarithmic form:

$$RD = c_2 \left\{ q \sum_{i=1}^{l} \frac{h_i}{E_i} \left(\frac{dN}{s} \right)^{1-\alpha_i} \left[\frac{(\bar{z}_i^{\,2} + a^2)^{3/2} - \bar{z}_i^{\,3}}{(\bar{z}_i^{\,2} + a^2)^{3/2}} \right] \right\}^{c_3}$$

The $\bar{z}_i$ used in this equation is different from the z_i used in the fatigue equations. Here, the $\bar{z}_i$ is the transformed depth to the center of layer i.

The regression equation that is used to determine the coefficients c_2 and c_3 is:

$$\log RD = \log c_2 + c_3 \log x_1$$

In this case, the single variable, x_1, is composed of the sum of clusters of terms, each cluster being related to one layer in the pavement. In other words,

$$x_1 = q\,[y_1 + y_2 + y_3 + \ldots + y_s]$$

where q = the tire pressure

$$y_1 = \frac{h_1}{E_1}\left(\frac{dN}{s}\right)^{1-\alpha_1}\left[\frac{(\bar{z}_1^{\,2} + a^2)^{3/2} - \bar{z}_1^{\,3}}{(\bar{z}_1^{\,2} + a^2)^{3/2}}\right]$$

$$y_2 = \frac{h_2}{E_2}\left(\frac{dN}{s}\right)^{1-\alpha_2}\left[\frac{(\bar{z}_2^{\,2} + a^2)^{3/2} - \bar{z}_2^{\,3}}{(\bar{z}_2^{\,2} + a^2)^{3/2}}\right]$$

.
.
.

$$y_s = \frac{h_s}{E_s}\left(\frac{dN}{s}\right)^{1-\alpha_s}\left[\frac{(\bar{z}_s^{\,2} + a^2)^{3/2} - \bar{z}_s^{\,3}}{(\bar{z}_s^{\,2} + a^2)^{3/2}}\right]$$

The terms d, N, s, a, h_i, and E_i have been defined previously, except for the term, h_s, the depth of the subgrade. Technically speaking this depth should be infinite and would imply an infinite depth of rutting. Since the rut depth is limited to the observed value, h_s (one value for <u>all</u> sections) must be selected to be a finite value which represents the depth within which significant rutting occurs in the subgrade.

However, it can also be used as a trial-and-error non-linear regression coefficient, altering h_s between regression runs to find the value that maximizes the R^2 and minimizes the sum of squared errors between the observed and predicted values.

The form of the equation for rut depth due to lateral flow, when written out in the preferred logarithmic form is

$$RD = C_4\left\{qa^2\sum_{i=1}^{l}\frac{h_i}{E_i}\left(\frac{dN}{S}\right)^{1-\alpha_i}\left[\frac{\bar{z}_i^{-2}}{\left[\left(\frac{\bar{z}_i}{z} + a\right)^2 + \bar{z}_i^{-2}\right]} - \frac{1}{\bar{z}_i}\right]\right\}^{C_5}$$

The regression equations that is used to determine the coefficients C_4 and C_5 is

$$\log RD = \log C_4 + C_5 \log x_2$$

In this case, the single variable, x_2, is composed of the sum of clusters of terms, each cluster being related to one layer in the pavement. In other words,

$$x_2 = qa^2 [t_1 + t_2 + t_3 + ... + t_s]$$

where

q = tire pressure

a = radius of tire footprint

$$t_1 = \frac{h_1}{E_1}\left(\frac{dN}{s}\right)^{1-\alpha_1}\left[\frac{\bar{z}_1^{-2}}{\left[\left(\frac{\bar{z}_1}{2}+a\right)^2+\bar{z}_1^{-2}\right]} - \frac{1}{\bar{z}_1}\right]$$

$$t_2 = \frac{h_2}{E_2}\left(\frac{dN}{s}\right)^{1-\alpha_2}\left[\frac{\bar{z}_2^{-2}}{\left[\left(\frac{\bar{z}_2}{2}+a\right)^2+\bar{z}_2^{-2}\right]} - \frac{1}{\bar{z}_2}\right]$$

$$\vdots$$

$$t_s = \frac{h_s}{E_s}\left(\frac{dN}{s}\right)^{1-\alpha_s}\left[\frac{\bar{z}_s^{-2}}{\left[\left(\frac{\bar{z}_s}{2}+a\right)^2+\bar{z}_s^{-2}\right]} - \frac{1}{\bar{z}_s}\right]$$

Combinations of the two models can be made by simply adding together the y_i - terms and the a^2 t_i - terms. An example of this would be

$$x_1 = q\left[y_1 + y_2 + y_3 + a^2 (t_1 + t_2 + t_3)\right]$$

Different combinations of the y_i - terms and the a^2 t_i - terms may be tried to determine which provides the best fit to the data.

Serviceability Loss Damage Clusters

The amount of damage to pavements represented by a loss of serviceability index from its initial value, p_i, to its present value, p, is:

$$g = \frac{p_i - p}{p_i - p_t}$$

The damage ratio, g, is considered to be proportional to the product of N, the number of load cycles, and the deflection under the load, Δ. The equation for serviceability index damage may be of the power law form or the exponential form.

$$g = \left(\frac{N\Delta}{\rho}\right)^{\beta} \qquad \textit{(Power Law)}$$

$$g = c\, e^{-\left(\frac{\rho}{N\Delta}\right)^{\beta}} \qquad \textit{(Exponential)}$$

In the exponential form, the coefficient, c, is $[p_i/p_i - p_t]$ and the coefficients ρ and β are to be found by regression analysis in both forms of equation. In the power law form, the regression equation is:

$$\ln g = \beta \ln x_1 - \beta \ln \rho$$

In the exponential form of equation, the regression equation is:

$$-\ln\left(\frac{g}{c}\right) = \beta \ln \rho - \beta \ln x_1$$

The single variable is x_1 which, when written to show the clusters of terms is:

$$x_1 = \frac{\pi}{4} \frac{N\, q\, a^2}{E_s \sum_{i=1}^{l} \left(\frac{E_i}{E_s}\right)^{1/3} h_i}$$

Here, as with the case of rutting, a depth of subgrade must be assigned, or may be found by a trial-and-error, non-linear regression analysis method. It is also possible, by having values of g corresponding to several values of N for a single pavement, that unique values of ρ and β may be determined for that single pavement. By determining values of ρ and β for a collection of pavements, regression equations for ρ and β which incorporate the layer thicknesses and moduli of the pavement may be developed.

Appendix A
Clusters due to Environmental Effects
Effect of Temperature

The moduli or the strength of materials E_0, E_1, ...E_j ..... all depend upon temperature as follows:

$$E_j = E_{dj}\ T^{-n} = \frac{E_{dj}}{T^n}$$

where

$$E_{dj} = \textit{the datum modulus or strength}$$

If the temperature varies, the modulus varies, and the average modulus is:

$$\bar{E}_j = \frac{1}{q} \sum_{k=1}^{q} \frac{E_{dj}}{T_k^n}$$

$$q = \textit{number of time periods}$$

$$\bar{E}_j = \frac{E_{dj}}{q} \sum_{k=1}^{q} \frac{1}{T_k^n}$$

define the mean temperature by the relation:

$$\frac{E_{dj}}{\bar{T}^n} = \frac{E_{dj}}{q} \sum_{k=1}^{q} \frac{1}{T_k^n}$$

Thus, the mean temperature is:

$$\frac{1}{\overline{T}} = \left[\frac{1}{q}\sum_{k=1}^{q} \frac{1}{T_k^n}\right]^{\frac{1}{n}}$$

This form of mean temperature equation needs to use a temperature datum that is below the lowest temperature that the pavement will experience.

$$\overline{T} = \frac{1}{\left[\frac{1}{q}\sum_{k=1}^{q} \frac{1}{T_k^n}\right]^{1/n}}$$

This value of T can be used in any regression equation where temperature affects the stiffness or strength of the material.

Another mean temperature relevant to rutting centers around the freezing point of water where the strength of soil material goes nearly to zero when thawing occurs.

$$S_j = S_{dj}\ (T-32)^n \qquad T \ in\ ^\circ F$$

or

$$S_j = S_{dj}\ (T)^n \qquad T \ in\ ^\circ C$$

The rutting or permanent strain or deflection that occurs is inversely proportional to the strength.

$$\Delta RD_j \propto \frac{1}{S_j}$$

$$RD_j = \sum_{k=1}^{q} \Delta RD_j = c \sum_{k=1}^{q} \frac{1}{S_{dj}\ (T_k-32)^n}$$

$$RD_j = \frac{c}{S_{dj}} \sum_{k=1}^{q} \frac{1}{(T_k-32)^n}$$

The average temperature factor, α, is given by

$$\overline{\alpha} = \frac{1}{\left[\frac{1}{q}\sum_{k=i}^{q}\frac{1}{(T_k - 32)^n}\right]^{1/n}}$$

Effect of Rainfall and Climatic Moisture

As the rainfall increases, the strength and stiffness of a moisture susceptible material decreases. Thus,

$$E_{jk} = E_{dj}\ (R_k)^{-n} = \frac{E_{dj}}{R_k^n}$$

where

R_k = the amount of rainfall in time period, k

E_{dj} = the datum modulus (or strength) for layer j

E_{jk} = the modulus (or strength) for layer j and time period k

The mean modulus (or strength) is

$$\overline{E_j} = \frac{E_{dj}}{q}\sum_{k=1}^{q}\frac{1}{R_k^n}$$

The mean rainfall is

$$\overline{R} = \frac{1}{\left[\frac{1}{q}\sum_{k=1}^{q}\frac{1}{R_k^n}\right]^{1/n}}$$

If monthly moisture balance is used to represent the climatic moisture and includes both rainfall and evapo - transpiration such as in the computation of the Thornthwaite Index, the calculations follow the same pattern as before.

$$E_{jk} = E_{dj}\ (T_k - T_d)^{-n}$$

where

T_k = the monthly moisture balance

T_d = the datum moisture balance which is lower than any other moisture balance amount. It will usually be negative.

The mean moisture balance is

$$\overline{\beta} = \frac{1}{\left[\frac{1}{q}\sum_{k=1}^{q}\frac{1}{(T_k - T_d)^n}\right]^{1/n}}$$

If what is to be represented has the strength or stiffness in the denominator, the average temperature, rainfall, or Thornthwaite Index moisture balance term to be used will be somewhat different.

$$\frac{1}{q}\sum_{k=1}^{q}\frac{1}{E_d\,T_k^{-n}} = \frac{1}{q\,E_d}\sum_{k=1}^{q}T_k^n$$

where q = the number of time periods
E_d = the datum modulus or strength

The mean value of the temperature in this case is obtained from

$$\overline{T^n} = \frac{1}{q}\sum_{k=1}^{q}T_k^n$$

and

$$\overline{T} = \left(\frac{1}{q}\sum_{k=1}^{q}T_k^n\right)^{1/n}$$

Appendix C

Technical Memorandum by Dr. Michael I. Darter and Dr. Emmanuel Owusu-Antwi, July 10, 1992, "Identification of Mechanistic Variables and Clusters for Concrete Pavement Distress Models"

TECHNICAL MEMORANDUM

TO: Robert Raab, Brent Rauhut, Robert L. Lytton

FROM: Michael Darter, Emmanuel Owusu-Antwi EOA
P020 Contract, ERES Consultants, Inc.

DATE: July 10, 1992

SUBJECT: **Identification of mechanistic variables and clusters for concrete pavement distress prediction models**

INTRODUCTION

This memorandum identifies the mechanistic variables and clusters of variables that are believed to be related to three concrete pavement distress types including transverse cracking, faulting of doweled joints and faulting of non-doweled joints. The mechanisms of other distress types are not as well known and, thus, prediction must be approached in a more empirical manner through conventional regression techniques, although some potential explanatory mechanistic variables may be included in these models to the extent possible.

Some Definitions As Used In This Memorandum

Dependent variable- pavement distress, such as transverse cracking and joint faulting.

Independent variable- any individual item such as slab thickness, concrete strength, mean annual temperature and number of single axle loadings of a certain weight.

Primary response variable- a mechanistic type variable such as slab stress, strain, or deflection; and horizontal opening and closing of joints/cracks.

ERES Consultants, Inc. 8 Dunlap Court Savoy, Illinois 61874-9501
Telephone (217) 356-4500 FAX (217) 356-3088

Cluster- a mathematical combination of two or more independent variables such as slab bending stress (a mathematical combination of slab thickness, k-value, wheel load, modulus of elasticity, etc. Note that stress is also a primary response variable.), the ratio of modulus values of successive layers (E1/E2), joint load transfer, concrete bending stress/strength, or joint opening/closing from temperature changes.

Mechanistic-Empirical (M-E) distress prediction model- a mathematical model relating a particular distress to one or more primary response variables, clusters and/or other variables. The functional form and boundary conditions are based upon past knowledge of theoretical studies and field observations of the distress, and the variables and clusters included in the model are based on knowledge of the engineering mechanics behind the distress phenomena. The unknowns (or constants) are derived from regression techniques using in-service highway pavement performance data.

Goals For The Predictive Models And Background Information

Main goal: to maximize the possibility that a predictive model will accurately predict the development of distress over a wide range of conditions in as much of a cause-and-effect relationship as possible. To achieve this, the following model characteristics are desired:(3)

- Correct overall functional form with time (age) and traffic applications.
- Proper boundary conditions at minimum and maximum points (e.g., at minimum point, 0 traffic gives 0 faulting).
- Proper direction of all variables (must not contradict the principles of engineering mechanics).
- Ideally, the independent variables included should be related to the distress in a cause-and-effect sense so that the models have as much of a rational scientific foundation as possible (this is the subject of this memo).

The independent variables included in the models are extremely important. Ideally, these variables should include one or more primary response variables (stress, strain, deformation) in a cause-and-effect relationship.

For example, transverse cracking in a concrete slab is believed to be related to the magnitude of tensile stresses caused by traffic load, thermal curling and other causes. However, slab cracking is also known to be related to other factors such as concrete strength and the number and magnitude of stresses applied. The exact relationship between the stress magnitudes, number of stress applications, the concrete strength and

the occurrence of cracking is obviously a very complicated mechanism and theory has not yet completely explained all of the mechanisms involved.

This is where field data becomes very valuable in bridging the gap between the limitations of theory and actual cracking as observed in the field. After the functional form and boundary conditions have been determined and the individual variables and clusters of variables have been identified, regression techniques are used to "calibrate" a prediction model (or solve for one or more constants using the field data). This M-E type model will have then some "built-in" scientific basis and may well provide better predictions outside of the relatively narrow inference space that the database provides.

PAVEMENT TYPES AND DISTRESSES

The SHRP LTPP P020 contract includes the development of predictive models for key distress types for three types of conventional concrete pavements:

Jointed plain concrete pavement (JPCP)

Transverse cracking, all severities
Longitudinal cracking, all severities
Pumping/erosion
Roughness, IRI
Friction loss
Joint faulting (doweled and non-doweled joints)
Joint spalling

Jointed reinforced concrete pavement (JRCP)

Transverse cracking, medium/high severities
Longitudinal cracking, all severities
Pumping/erosion
Roughness, IRI
Friction loss
Joint faulting (doweled joints)
Joint spalling

Continuously reinforced concrete pavement (CRCP)

Localized failures (punchouts, deteriorated transverse cracks)
Longitudinal cracking, all severities
Pumping/erosion
Roughness, IRI
Friction loss
Spalling of cracks

Previous research studies have determined that some of these distress types are related to "primary response variables" such as stresses, strains and deflections at specific points in the concrete slab (e.g., edges, corners, dowel/concrete interface). In addition, past research studies have also identified some of the mechanisms involved in their development. For these distress types, this knowledge will be very helpful in identifying the variables and mechanisms involved in formulating the M-E predictive models.

Distress Types Amenable To Mechanistic-Empirical Model Development

The following distress types are related to one or more primary response variables and are believed to be amenable to mechanistic-empirical analysis for jointed concrete pavements:

Transverse slab cracking: caused primarily by tensile and bending stresses from traffic loadings and climatic variables (note that this does not include the deterioration of cracks in JPCP or JRCP pavements which are caused by some different variables and mechanisms).

Transverse non-doweled joint faulting: caused primarily by large transverse joint differential deflections (under load) across the transverse joint under certain climatic conditions that leads to pumping action and erosion of the underlying layers.

Transverse doweled joint faulting: caused primarily by high dowel/concrete bearing stresses at the face of the joint when wheel load is directly above dowel which wears away the concrete creating a gap at the top and bottom of the dowel. Then, the same mechanism described for non-doweled joints develops to cause faulting.

Some of the other distress types such as joint spalling, the deterioration of transverse cracks in JRCP pavements, erosion/pumping and CRCP punchouts are also related to primary responses, but the mechanistic phenomena has not yet been adequately researched to consider them directly at this time.

USE OF DIMENSIONAL ANALYSIS TO IDENTIFY VARIABLES AND CLUSTERS

A useful concept that can assist in the identification of mechanistic type clusters that relate to primary response variables and thus to distress is that of dimensional analysis. Several publications have demonstrated that the principles of dimensional analysis can be utilized effectively in the interpretation of numerical data pertaining to pavement primary responses, such as stresses.(1, 2, 4, 5, 6, 9)

Dimensional analysis is encountered in the works of pavement researchers such as Westergaard, Bradbury, Burmister, Odemark, Pickett, and Losberg. Previous research

has also provided considerable knowledge in the identification of governing dimensionless parameters for a variety of mechanistic variables. Table 1 summarizes these findings.

The use of dimensionless variables to directly predict distresses may be useful when there does not exist a clear primary response variable, such as the case of faulting or joint spalling. It is not particularly useful for transverse cracking for example, because tensile stress can be calculated directly and used in the prediction model, rather than dimensional ratios such as a/l.

TRANSVERSE CRACKING VARIABLES AND CLUSTERS

Past research has shown that the development of transverse cracking distress in concrete slabs is the result of several external and internal tensile or bending stresses acting on the pavement slab. The major causes of these critical slab stresses are as follows:

- Traffic load repeated stresses with differing magnitudes and rates of loading.
- Thermal and moisture gradients through the slab causing tensile stresses at both top and bottom of the slab depending upon the gradient.
- Friction tensile stresses (maximum at mid-slab) that result when the slab contracts but is resisted by friction along the base to slab interface. The main causes of slab contraction include (1) drying shrinkage of the concrete and (2) temperature changes in the slab.
- Changes in slab support, either loss of support from pumping/erosion, foundation settlement or foundation heaving.

In addition to tensile stresses, concrete tensile or flexural strength is another variable that is closely related to transverse cracking of slabs. Variables and clusters relating to both of these are presented.

In conceptual form, transverse cracking is considered to be related to the following major variables:

TRCRACK = f (STRESS, STRENGTH, NO. LOAD APPLS.)

Where:

TRCRACK = Measure of transverse cracking (percent slabs, no. cracks/mi, ft./mi)

f = Functional relationship between cracking and independent variables, could be of several different forms (two different approaches will be considered: non-linear regression with proper functional form and incremental fatigue damage)

STRESS = Tensile stress in slab as function of traffic load, thermal curl and other variables

STRENGTH = Flexural strength of concrete slab at a given time after construction, psi

NO. APPLS = Number of applications applied at a given load level and axle type

Variables And Clusters For Tensile/Bending Stresses

Slab Stresses From Traffic Loads

There are two critical stress locations for transverse cracking: the longitudinal slab edge and the corner. The longitudinal slab edge (at the bottom of the slab) position is the conventional location of the critical stress that is used in design procedures for controlling transverse cracking. The corner load position can become critical under the following conditions: dowel bars are not used at the transverse joint or no tied concrete shoulder exists. In addition to this, any severe upward warping from moisture gradients or nighttime thermal gradients, or erosion of support beneath the slab will cause a very high tensile stress at the top of the slab that could result in a transverse or diagonal or corner crack.

The edge stress at the bottom of the slab that will be considered herein can be calculated from Westergaard's 1948 model.(10)

$$Se = [\, 3(1+u)P) \,/\, (\Pi(3+u)h^2) \,] * [\ln(Eh^3/100ka^4) + 1.84$$

$$- (4/3)u + (1-u)/2 + 1.18(1+2u)(a/l)]$$

Where:

Se= Edge stress for circular wheel load tangent to edge, psi
P = Applied wheel load (9,000 lbs., or 18-kip axle load)
k = Effective k-value beneath slab (from backcalculation)
a = Load radius (calculated using 9,000 lb. load and 100 psi pressure)
h = Slab thickness (database)
E = Slab modulus of elasticity (backcalculation)
u = Poisson's ratio (0.15 assumed)

This equation was extended by Salsilli using regression analysis techniques to establish relations between dimensionless parameters and the edge (bottom of slab) bending stress (Se) occurring in a slab-on-grade subjected to multiple-wheel loading along one of its edges, distance from edge to outside of tire, slab length and load transfer efficiency as summarized in Table 2. Most of the models in Table 2 can be considered as multiplicative "correction factors" which are applied sequentially to Westergaard's edge stress equation. The purpose of each factor is to eliminate one of Westergaard's restrictive assumptions.

Temperature Curling And Moisture Warping Stresses

A thermal gradient or a moisture gradient through a slab results in the movement of the slab corners and edges either upward or downward, depending upon the direction of the gradient. This movement is resisted by the weight of the slab and the bond to the base which results in tensile and compressive stresses in the slab. The tensile stresses can by themselves, or in combination with load stresses, cause slab cracking. The following model can be used to compute thermal curl stresses at the slab edge.(13)

$$S_{curl} = [B * E * C * DT] / 2$$

Where:

S_{curl}	=	curl stress, psi
B	=	coefficient that depends upon L/l ratio reproduced in Figure 1
E	=	modulus of elasticity of concrete, psi
C	=	coefficient of thermal contraction of concrete, degree F
DT	=	temperature differential through slab, degrees F

Moisture gradients through slabs begin at the time of construction due to the top becoming dryer than the bottom which is almost continually damp. In addition, if poor curing occurs resulting in a very dry slab surface, permanent severe warping of the slab will occur with the corners warped upward. If the base is relatively soft, the slab may settle somewhat into the base and relieve the effects of this warping, but this may not occur for stabilized bases. Very little work has been done in determining moisture gradients in slabs in different areas of the country. Mathematically, moisture warping can be considered similar to a negative thermal gradient in a slab, and thus the same cluster variables are involved. Moisture warping cannot be directly considered in this analysis due to a lack of data on moisture gradients.

Traffic Load And Temperature Curling Stresses

The stresses from load and temperature curling cannot be directly added together. In fact, the combining of these stresses is a highly non-linear problem due to the

changing support conditions beneath the slab as the slab curls upward or downward. The latest model for predicting the combined stress is that developed by Salsilli (9) under NCHRP Project 1-26. Models for stress caused by load and by thermal gradient were developed separately, and then they were combined using using the finite element program ILLISLAB.

$$S_{comb} = S_{load} + R * S_{curl}$$

Where:

S_{comb}	=	combined edge stress, psi
S_{load}	=	Westergaard solution for edge stress, psi
S_{curl}	=	curl stress given by following expression
	=	[B * E * C * DT] / 2
B	=	coefficient that depends upon L/l ratio reproduced in Figure1
E	=	modulus of elasticity of concrete, psi
C	=	coefficient of thermal contraction of concrete / degree F
DT	=	temperature differential through slab, degrees F
R	=	an adjustment factor

The combined edge stress was computed from the ILLISLAB finite element program. Then regression techniques were used to develop the R factor which depends on many pavement parameters, including L (joint spacing), DT, k, h, B, E and l (radius of relative stiffness.(9) Therefore, the S_{comb} can be calculated in a closed form solution over a wide range of pavement and load variables with good accuracy.

Stresses Caused By Slab Contraction (resisted by base friction)

Tensile stresses occur in a slab whenever the slab tries to contract because the movement is resisted by friction between the slab and base course. Slabs placed on a fine grained subgrade develop very little friction. Slabs placed on a stabilized stiff base develop a large amount of friction. Contraction of the slab can be caused by drying shrinkage during the early concrete curing time period, and also from decreasing temperatures.

The classical model used to predict the maximum friction stress at the center of the slab is given as follows:

$$S_{frict} = W L f / 24 h$$

Where:

S_{frict}	=	tensile stress at slab center, psi
W	=	weight of slab, lbs/sf

L = slab length, ft
f = average coefficient of friction between slab and base
h = slab thickness, in

This stress is almost negligible for short slab JPCP type of pavement, thus it is not included in this analysis.

Variables And Clusters Related To Concrete Strength

In addition to stress, concrete strength is the other primary variable related to slab cracking. Slab cracking can occur in two ways: (1) a high tensile stress due to some combination of critical loading, climate or material (contraction) situation occurs which exceed the slab strength, or (2) fatigue damage accumulates as a result of multiple applications of different levels of stress to the point that a crack develops.

One way in which to bring strength into the model is through the dimensionless stress/strength ratio. Flexural testing of concrete beams shows that the ratio of stress to strength produces a cluster term that relates linearly to the logarithm of applications to cracking as shown in Figure 2.

Variables And Clusters Related To Fatigue Damage

The stress to strength ratio provides a good dimensionless cluster to predict cracking when one level of stress is involved as previously shown. When multiple levels of stress exist, as in a concrete highway pavement, additional clusters must be included. Flexural testing of concrete beams has shown that Miner's (12) incremental damage ratio (Miners) provides a reasonable cluster that relates to cracking.

$$\text{DAMAGE SUM} = n_{ijkl} / N_{ijkl}$$

n_{ijkl} = Number of applied load applications having i^{th} axle type, j^{th} axle weight, k^{th} thermal gradient and l^{th} concrete strength.

N_{ijkl} = Number of allowable load applications to initial cracking for i^{th} axle type, j^{th} axle weight, k^{th} thermal gradient and l^{th} concrete strength.

This incremental damage ratio is actually a dimensionless "super cluster" of variables including all of those involved in slab stress and strength. The accumulated damage value is correlated with transverse slab cracking to provide for a prediction of cracking. This approach has been successfully applied since 1977 (7,9,11) for the prediction of transverse cracking caused by repeated load fatigue damage. Figure 3 shows an example of the damage ratio versus transverse cracking for a large number of field slabs.

This approach provides a predictive model that sums "damage" ratios over specific increments of time, where materials and soil properties, thermal and moisture characteristics and traffic are constant within the increments but can vary between increments (e.g., time increments could be as small as a few hours).

Example Model For Fatigue Cracking Of JPCP (S-Shaped Curve) (this curve form is based on the observation of cracking vs load repetitions or accumulated damage on actual pavements)(11)

$$\text{CRACKING (percent slabs)} = 1 / \{ 0.01 + a (b^{-\text{Log DAMAGE}}) \}$$

Where: a and b are determined from non-linear regression techniques.

- **Possible Increments Over Which Damage Is Accumulated** (due to database limitations, not all of these will be included)

  Thermal gradients (hourly thermal gradients over year)
  Moisture gradients (seasonal)
  Slab support (seasonal)
  Concrete strength (monthly)
  Traffic axle load distribution (single, tandem, tridem)
  Lateral truck traffic loadings (with regard to slab edge)

- **Data Required To Compute Damage** (not all are required for this initial analysis)

  Slab hourly thermal gradients over a year time period
  Slab seasonal moisture gradients over a year time period
  Slab support k-value and base layer modulus over a year
  Concrete slab thickness
  Concrete slab thermal coefficient of contraction
  Concrete slab strength increase over design life
  Concrete slab E and Poisson's ratio over design life
  Axle load distribution over design life
  Lateral truck loading distribution in traffic lane
  Load transfer of longitudinal joint (if tied PCC shoulder)

TRANSVERSE CRACK SUMMARY

Variables

The following variables are needed to develop the M-E models for transverse cracking. Where each will be obtained is given in parentheses.

P = Applied wheel load (9,000 lbs., or 18-kip axle load)
k = Effective k-value beneath slab (from backcalculation, estimate seasonal variation)
a = Load radius (calculated using 9,000 lb. load and 100 psi pressure)
h = Slab thickness (database)
E = Slab modulus of elasticity (backcalculation, backcast over time)
u = Poisson's ratio (0.15 assumed)
C = Thermal coefficient of contraction of PCC slab (assumed based upon coarse aggregate type)
L = Joint spacing (database)
N = Number of 18-kip ESALs accumulated in traffic lane (database)
FS = Flexural strength at 28 days, third point loading, psi (backcasted from data obtained from coring results, or backcasted from backcalculation of slab E)
G = Slab hourly thermal gradients over a year time period (computed using CMS program and data from climatic database)
D = Lateral truck loading distribution in traffic lane, distance from slab edge (assume from existing data)
LTs= Load transfer of longitudinal joint if tied PCC shoulder (measured by FWD, in database)
W = Slab width, ft.(database)

Clusters

Stress = Tensile stress from load and thermal curling obtained from Salsilli (modification of Westergaard)

Stress / Flexural Strength of concrete slab

Miner's fatigue damage summation ratio

JOINT FAULTING VARIABLES AND CLUSTERS

Past research has shown that the development of joint faulting distress is in essence caused by repeated deflections from wheel loads at the transverse joint, particularly differential deflections across the joint. The differential deflection is defined as the deflection of the loaded side minus that of the unloaded side of a joint. The differential deflection is considered to be more closely related to faulting than load transfer since it represents an absolute difference in deflections as a wheel rolls across the joint, and thus, should correlate well with pumping and erosion beneath the joint. This differential deflection causes water to flow forward and backward beneath the joint at a high velocity which ultimately leads to erosion and a buildup of material under the approach joint causing faulting.

The major causes of high differential deflections (and high deflections in general) are as follows:

- Repeated moving heavy traffic loads across the joint (particularly near the corner).

- Greater than perfect (zero) differential deflection that results from several causes, including joint opening when slab contracts, no mechanical load transfer device, enlargement of dowel socket from high bearing stresses. The main causes of slab contraction include (1) drying shrinkage of the concrete and (2) temperature and moisture changes in the slab.

- Negative thermal and moisture gradients through the slab causing corners and edges to curl/warp upward creating voids between the slab and stabilized base where moisture can accumulate and then pump under deflection.

In addition to differential deflection, the erosion resistance of the base layer and also its permeability are other variables that are closely related to faulting. Also, the availability of free moisture beneath the slab and or treated base layer (sometimes erosion occurs beneath the treated base layer) is an important factor. Variables and clusters relating to these variables are presented.

In conceptual form, joint faulting is considered to be related to the following major variables:

FAULT = f (DIFFERENTIAL DEFLECTION, BASE ERODABILITY, MOISTURE AVAILABILITY, SLAB CURL/WARP, NO. LOAD APPLS.)

Where:

FAULT = Mean joint faulting, in

f = Functional relationship between faulting and independent variables, could be of several different forms (two different approaches will be considered: non-linear regression with proper functional form and incremental faulting damage)

DIF. DEF. = Differential deflection, difference between loaded side and unloaded side deflections as measured by the FWD, in

BASE EROD = An index of the erodability of the base course

NO. APPLS = Number of applications applied at a given load level and axle type

SLAB CURL = Upward curling of corner under mean nighttime temperature gradient.

Variables And Clusters For Deflections

Corner Deflections From Traffic Loads

The corner deflection is the largest deflection anywhere in the slab, and thus is the point at which the faulting mechanism is likely to be the strongest to develop. The deflection of a free corner is given by Westergaard's equation:

$$DEF = P \{ 1.1 - 0.88 (1.141\ a/l) \} / k\ l^2$$

Where:

DEF =	Free corner deflection under circular load tangent to the corner, in
P =	Applied wheel load, lbs.
k =	Effective k-value beneath slab, psi/in
a =	Load radius (calculated using 9,000 lb. load and 100 psi pressure), in
l =	Radius of relative stiffness, in
=	$[E h^3 / 12 k (1 - u^2)]^{0.25}$
h =	Slab thickness, in
E =	Slab modulus of elasticity, psi
u =	Poisson's ratio

Rearranging this equation gives a dimensionless cluster:

$$Def * k * l^2 / P = f(a / l)$$

The major factors include the wheel load P and the k support modulus. In addition to these factors, the corner deflection depends greatly on the following:

- load transfer of the transverse joint and longitudinal joint (100 percent load transfer decreases deflection by 50 percent and decreases differential deflection to 0)

- the amount of curl/warp of the slab at the corner
- loss of support at the corner increases the deflection greatly

The differential deflection across the joint is dependent on the transverse joint load transfer. A finite element program such as ILLISLAB or JSLAB can be used to show the effect of load transfer, curling and loss of support on corner deflection and differential deflection. A search is underway for a closed form solution that considers these factors directly.

Faulting Of Non-Doweled Joints

The differential deflection of non-doweled joints begins to increase with traffic loadings soon after opening to traffic (as load transfer decreases). It is highly dependent on the aggregate interlock of the joint, which in turn depends on maximum aggregate size (to produce large unevenness through the joint), the hardness of the aggregate to resist breakdown under repeated shearing from loads, and the width of the joint.

Differential deflection also depends greatly upon the opening of the joint. Joint opening results in a loss of joint load transfer and an increase in the dowel bearing stress. The mean joint opening is a function of the thermal coefficient of contraction of the concrete, the friction between the slab and base, the slab length and the temperature change or shrinkage of the slab. The mean expected joint opening is given as follows:

$$w = F * L (C * DT + e)$$

Where:
- w = Joint opening, in
- L = Joint spacing, in
- F = Friction factor between base and slab (empirical data gives 0.80 for granular base and 0.65 for treated base)
- DT = Temperature range (maximum July - minimum January), Degrees F
- C = Thermal coefficient of contraction of concrete (5 - $6*10^{-6}$ / degree F)
- e = Drying shrinkage coefficient of concrete over time (0.5 - 2.5 * 10^{-4} strain)

Dimensionless cluster = C * DT + e

The amount of faulting of a non-doweled joint also depends upon the amount of moisture that is available beneath the slab. The number of days having precipitation greater than 0.1 in a year is one index for this variable. The amount of joint sealing is not believed to have much effect on the amount of moisture beneath a slab.

Faulting Of Doweled Joints

Faulting of doweled joints can occur if the bearing stresses between the dowel and the concrete becomes too large and the concrete is worn away causing a gap at the top and bottom of the dowel. After the dowel loosens, the faulting mechanism would be identical to non-dowelled joints and described above.

Dowel bearing stress is calculated by the following model (8):

BSTRESS = A(pavement) * B(load)

Where:

BSTRESS = Dowel/concrete bearing stress, psi
A = $K (2 + B w) / (4 B^3 E_s I)$
B = $P * \%TL * f_d$

K = modulus of dowel support
B = $K d / (4 E_s I)^{0.25}$
d = dowel diameter
E_s = modulus of elasticity of dowel
I = Moment of inertia of dowel bar
w = Width of joint opening (C*DT*L)
C = Thermal coefficient of contraction of PCC
DT = Temperature range
TL = Joint load transfer
L = Joint spacing
f_d = Distribution factor indicating how much of the transferred load acts on critical dowel bar
P = Applied wheel load

Rearranging this equation gives a dimensionless cluster:

$$BSTRESS * (1/B^2) / P = f \{ (2 + B w) / B d \}$$

The major factor that affects the bearing stress is dowel diameter and spacing. The larger the diameter and closer the spacing, the lower the bearing stress. Under heavy repeated loadings, small diameter dowels will loosen very rapidly to the point that the joint behaves like a non-doweled joint and faults significantly.

Variables And Clusters For Faulting Model

There are two different approaches to the development of faulting models. One approach is to use non-linear regression techniques to fit a model that fits the functional

form and boundary conditions. The other one is to develop an incremental faulting damage model, similar to that for cracking, that considers various increments of time and sums faulting over each increment. Either approach requires the identification of key variables and clusters.

An example of the clusters that should be included in a non-linear mechanistic-empirical faulting model is illustrated below. This will be a non-linear model with each term likely having coefficients and exponents.

$$FAULT = N^{c1} \{ a/l,\ LT,\ (2+B\ w)/(B\ d),\ C*DT+e,\ L/l,\ BASE_e,\ PRECIP,\ SUBDRAIN \}$$

Based on this expression, joint faulting is a function of traffic loadings (N), (c1 is a regression constant that will be less than 1.0 to provide for the proper functional form of faulting with load applications), corner deflection (a/l), load transfer (LT) which controls differential deflection), dowel/concrete bearing stress for doweled joints ((2+B w)/(B d)), joint opening (C*DT+e), base erosion ($BASE_e$ to be derived), precipitation (PRECIP) and subdrainage (SUBDRAIN). Further conceptual work is needed to develop a more fundamental approach to combining particularly base erosion, precipitation and subdrainage into cluster variables.

JOINT FAULTING SUMMARY

Variables

The following variables are needed to develop the M-E models for joint faulting. Where each will be obtained is given in parentheses.

- P = Applied wheel load (9,000 lbs., or 18-kip axle load)
- k = Effective k-value beneath slab (from backcalculation, estimate seasonal variation)
- a = Load radius (calculated using 9,000 lb. load and 100 psi pressure)
- h = Slab thickness (database)
- E = Slab modulus of elasticity (backcalculation, backcast over time)
- u = Poisson's ratio (0.15 assumed)
- L = Joint spacing (database)
- N = Number of 18-kip ESALs accumulated in traffic lane (database)
- G = Slab hourly thermal gradients over a year time period (computed using CMS program and data from climatic database)
- Lts= Load transfer of longitudinal joint if tied PCC shoulder (measured by FWD, in database)
- K = modulus of dowel support (assume 1,500,000 psi/in)
- d = dowel diameter (database)

E_s = modulus of elasticity of dowel (assumed 29 million psi)
I = moment of inertia of dowel bar (calculated)
w = width of joint opening (calculated)
TL = joint load transfer
f_d = distribution factor indicating how much of the transferred load acts on critical dowel bar
F = friction factor between base and slab (empirical data gives 0.85 for granular base and 0.8 for treated base)
DT = temperature range (maximum July - minimum January), Degrees F
C = thermal coefficient of contraction of concrete (5 - $6*10^{-6}$ / degree F)(assumed based upon coarse aggregate type)
e = drying shrinkage coefficient of concrete over time (0.5 - 2.5 * 10^{-4} strain)

Clusters

Corner Deflection	=	Westergaard corner model, modified to consider joint load transfer
Differential deflection	=	Difference between loaded and unloaded side of joint, determined from above modified model
Joint deflection load transfer	=	Unloaded side deflection divided by loaded side deflection
Dowel/concrete bearing stress	=	Calculated from modified Westergaard's equation with various assumptions
Slab corner curling	=	Equation for uplift of corner from negative curling gradient (from German research)

SUMMARY

The variables and their arrangement in a predictive model is very important. This memorandum identifies the mechanistic variables and clusters of variables that are believed to be related to selected concrete pavement distress types. This approach builds upon past work with regard to the development of theoretical mechanisms that cause distress in concrete pavements and in the development of M-E prediction models. The concepts included in this memo will be useful in the development of the M-E models during the initial analysis of the LTPP P020 data.

ACKNOWLEDGEMENT

This memo contains some ideas and concepts on dimensional analysis from Prof. A. M. Ioannides of the University of Illinois.

REFERENCES

1. Bridgman, P.W. (1931), "Dimensional Analysis," Second Edition, Yale University Press, New Haven, CT.

2. Langhaar, H.L (1951), "Dimensional Analysis and Theory of Models," John Wiley and Sons, Inc. New York, NY.

3. Darter, M.I. (1980), "Requirements for Reliable Predictive Pavement Models," Transportation Research Record 766, Transportation Research Board, National Research Council, Washington, D.C., pp. 25-31.

4. Ioannides, A.M. (1988). "The Problem of a Slab on an Elastic Solid Foundation in the Light of the Finite Element Method," Proceedings, 6th International Conference on Numerical Methods in Geomechanics, Paper No. 408, April 11-15, Innsbruck, Austria, pp. 1059-1064.

5. Ioannides, A.M., and Salsilli-Murua, R. (1989), "Temperature Curling in Rigid Pavements: An Application of Dimensional Analysis," Transportation Research Record 1227, Transportation Research Board, National Research Council, Washington, D.C., pp. 1-11.

6. Ioannides, A.M., Barenberg, E.J., and Lary, J.A. (1989), "Interpretation of Falling Weight Deflectometer Results Using Principles of Dimensional Analysis," Proceedings, Fourth International Conference on Concrete Pavement Design and Rehabilitation, Purdue University, April 18-20, 1989, W. Lafayette, IN., pp. 231-247.

7. Darter, M.I. (1977), "Design of Zero-Maintenance Plain Jointed Concrete Pavement: Vol. I - Development of Design Procedures," Federal Highway Administration, Report No. FHWA-RD-77-111, Washington, D.C., June.

8. Ioannides, A.M., Lee, Y.H., and Darter, M.I., "Control of Faulting Through Joint Load Transfer Design," Transportation Research Record No. 1286, Transportation Research Board, National Research Council, Washington D.C., 1990

9. SALSILLI R.A. Calibrated mechanistic design procedure for jointed plain concrete pavements. Ph.D. thesis, Un. of Illinois, Urbana, IL, 1991.

10. WESTERGAARD H.M. New formulas for stresses in concrete pavements of airfields. Trans. ASCE, vol. 113, 1948, 425-439.

11. Smith, K.D., A.L. Mueller, M. I. Darter, and D. G. Peshkin, "Performance of Jointed Concrete Pavements, Volume II–Evaluation and Modification of Concrete Pavement Design and Analysis Models," FHWA-RD-89-137, 1990.

12. Miner, M. A., "Cumulative Damage In Fatigue," Transactions, ASME, Vol. 67,1945, A159-A164.

13. Bradbury, R. D., "Reinforced Concrete Pavements," Wire Reinforcement Institute, Washington, D.C., 1938.

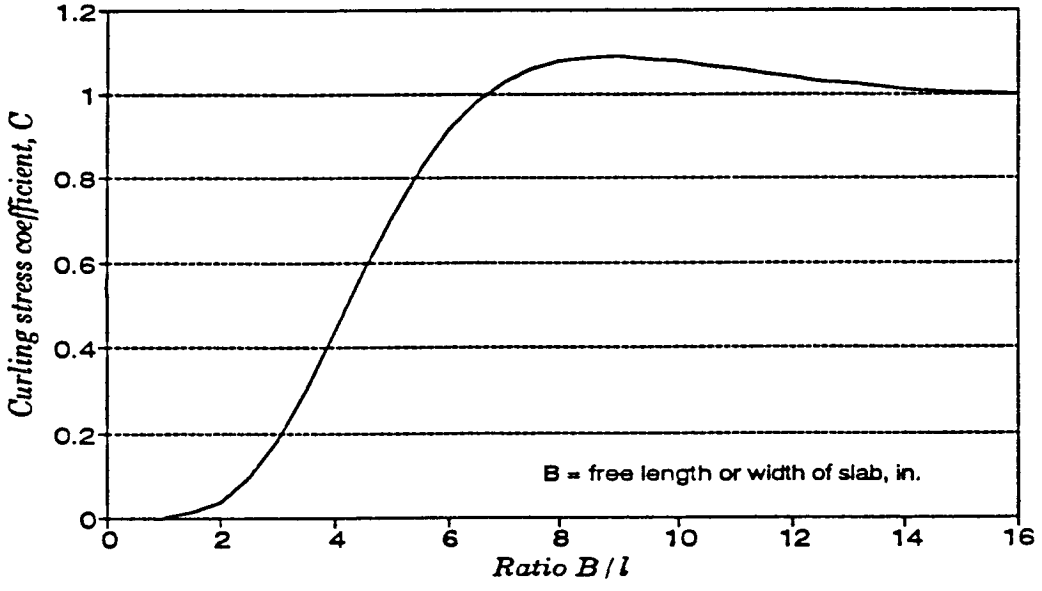

Figure 1. Variation in the differential temperature stress coefficient C with B/*l* (60).

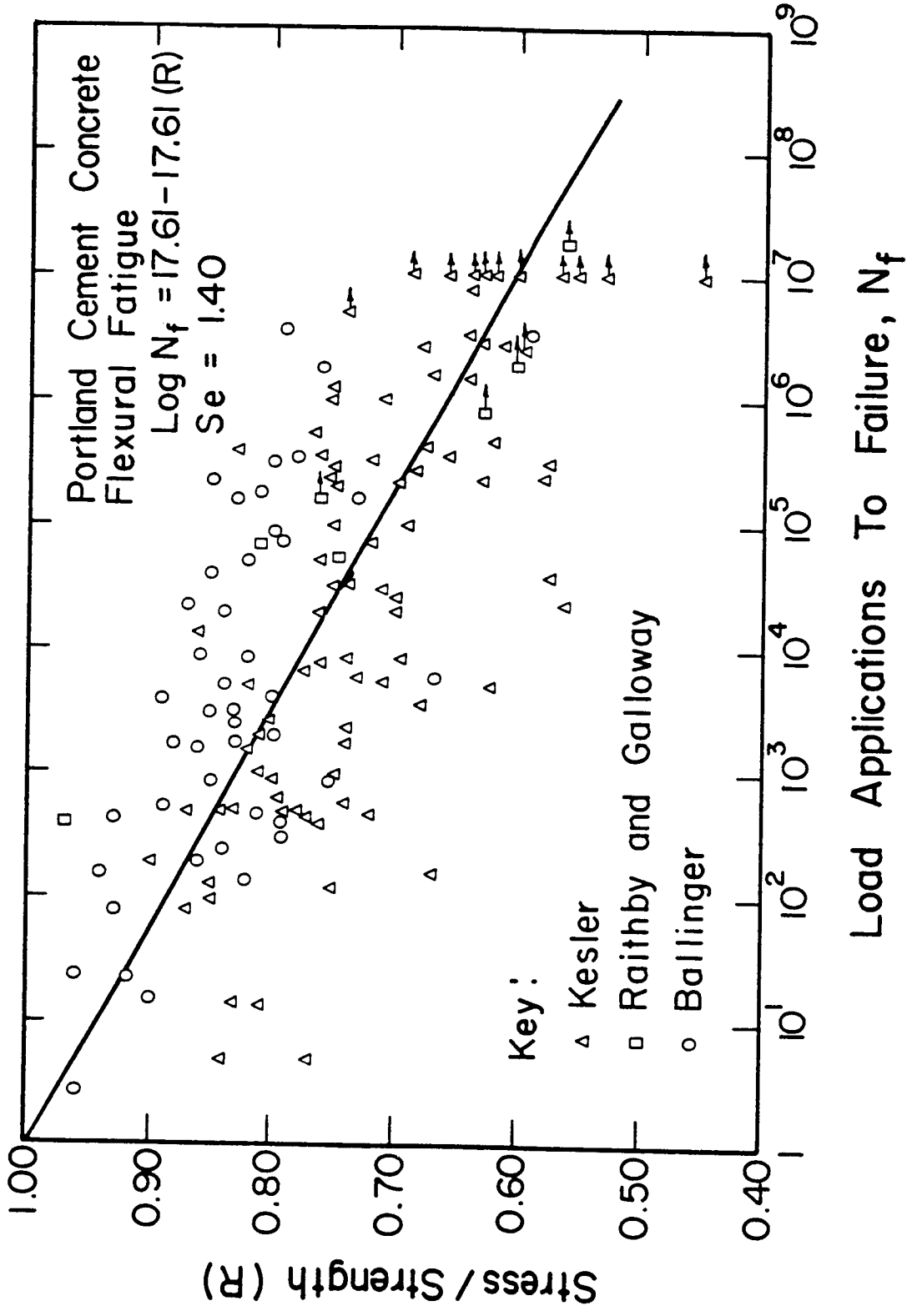

Figure 2. Summary of PCC Flexural Fatigue Data.

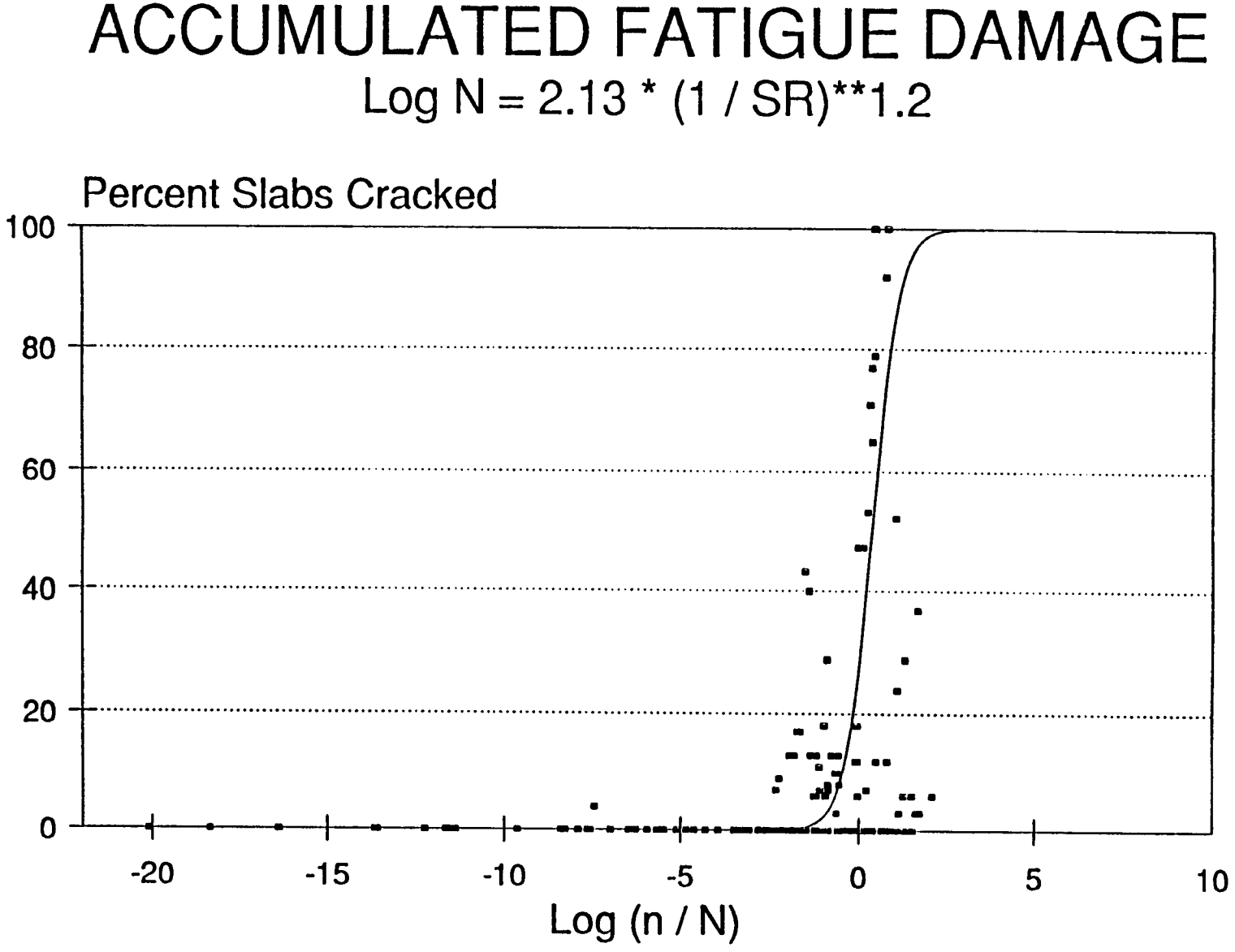

Figure 3. Percent slabs cracked versus accumulated fatigue damage.

Table 1. Governing Dimensionless Parameters for Concrete Pavements.

BRIEF DESCRIPTION	DIMENSIONLESS VARIABLE	REFERENCES
Load Size Ratio	(a/l)	[20]
Slab Size Ratio	(L/l)	[28; 24]
Normalized Load Placement Distance	(D/l)	[41]
Nondimensional Deflection	$(\delta kl^2/P)$ or $(\delta D^*/Pl^2)$	[22; 20]
Nondimensional Subgrade Stress	(ql^2/P)	[54; 20]
Nondimensional Bending Stress	$(\sigma h^2/P)$	[28; 20]
Tire-print Spacing Ratio	(S/a)	[25]
Linear Thermal Differential Product	$\alpha \Delta T$	[7]
Nondim. Joint Stiffness (undoweled joint)	(AGG/kl)	[55]
Nondim. Joint Stiffness (doweled joint)	(D'/skl)	[56]
Modular Ratio for Base Layer Evaluation	(E_c/E_b)	[43]

SYMBOLS USED:
a: load radius; l: radius of relative stiffness; L: slab length; D: load placement distance from slab edge; δ: deflection; k: subgrade modulus; P: total applied load; D^*:slab flexural stiffness; q: subgrade stress; σ: slab bending stress; S: tire spacing; α: coefficient of thermal expansion; ΔT: linear temperature differential; AGG: aggregate interlock factor; D': spring-in-series joint stiffness; s: dowel spacing; E_c:slab modulus; E_b:base layer modulus.

Table 2. Proposed Formulae (After Salsilli [45]).

Westergaard (1948) Edge Stress Equation:

$$\sigma_{West}=\frac{3(1+\mu)P}{\pi(3+\mu)h^2}\left[\ln\frac{Eh^3}{100ka^4}+1.84-\frac{4\mu}{3}+\frac{1-\mu}{2}+1.18(1+2\mu)(a/l)\right]$$

Alternate Formula for $(a/l)>0.5$:

$$\frac{\sigma_{corr}}{\sigma_{West}}=1-0.0621(a/l)^2+0.131(a/l)^3$$

Equivalent Radius for Duals, Spacing S (Perpendicular to Edge):
N = 20; $R^2=1$; COV = 1.2%. Limits: $0<(S/a)\leq 20$; $0.05\leq(a/l)\leq 0.5$

$$\frac{a_{eq}}{a}=0.909+0.339485(S/a)+0.103946(a/l)-0.017881(S/a)^2$$
$$-0.045229(S/a)^2(a/l)+0.000436(S/a)^3$$
$$-0.301805(S/a)(a/l)^3+0.034664(S/a)^2(a/l)^2+0.001(S/a)^3(a/l)$$

Equivalent Radius for Tandems, Spacing t (Parallel to Edge):
N = 16; $R^2=0.997$; COV = 2.1%. Limits: $4\leq(t/a)\leq 16$; $0.05\leq(a/l)\leq 0.3$

$$\frac{a_{eq}}{a}=2.199479+0.74761\ \ln(t/a)\ \ln(a/l)+0.548071\ \ln^2(t/a)$$
$$-0.486597\ \ln^2(t/a)*\ln(a/l)-0.29507\ \ln^3(t/a)-0.028116\ \ln^3(a/l)$$

Effect of Axle Width D (Perpendicular to Edge):
N = 28; $R^2=0.995$; COV = 6.9%. Limits: $0.13\leq(D/l)\leq 3$; $0.05\leq(a/l)\leq 0.3$

$$\frac{\sigma_D}{\sigma_{West}}=-0.15743211+0.26935303(a/l)+0.357644(l/D)$$
$$-0.0589073(l/D)^2+0.003486(l/D)^3$$

Effect of Slab Size, Length L (Parallel to Edge):
N = 12; $R^2=0.996$; COV = 0.29%. Limits: $3\leq(L/l)\leq 5$; $0.05\leq(a/l)\leq 0.3$

$$\frac{\sigma_L}{\sigma_{West}}=0.582282-0.533078(a/l)+0.181706(L/l)-0.019824(L/l)^2$$
$$+0.109051(a/l)(L/l)$$

Effect of Load Transfer Efficiency, Aggregate Interlock Factor AGG:
N = 16; $R^2=0.988$; COV = 2.45%. Limits: $5\leq(AGG/kl)$; $0.05\leq(a/l)\leq 0.3$

$$\frac{\sigma_{AGG}}{\sigma_{West}}=0.99864-0.51237(a/l)-0.0762\ \ln(AGG/kl)$$
$$+0.00315\ \ln^2(AGG/kl)+0.015936(a/l)^2\ \ln^2(AGG/kl)$$

Alternate Formula Used for $(a/l)>5$:

$$\frac{\sigma_{AGG}}{\sigma_{West}}=1.04284-0.84692(a/l)-0.09299\ \ln(AGG/kl)$$
$$+0.06837(a/l)\ \ln(AGG/kl)+0.63417(a/l)^2$$
$$+0.0042\ \ln^2(AGG/kl)-0.000629(a/l)\ \ln(AGG/kl)^3$$

Appendix D

Technical Memorandum by Dr. Olga J. Pendleton, April 27, 1992, "Statistical Methodology for LTPP Data Analysis"

TECHNICAL MEMORANDUM

DATE: April 27,1992

AUTHOR: Olga J. Pendleton

SUBJECT: Statistical Methodology for LTPP Data Analysis

The statistical methodology recommended for developing pavement distress models for the LTPP data analysis encompasses a wide variety of statistical tools and software. The discussion which follows are the methods presented in a tutorial given at Texas A&M University in November, 1991 to prospective LTPP data analysts.

The data analysis procedures will follow a systematic sequence of steps, as depicted in the flow chart of Figure 1. These steps will further be explained in the sections which follow.

The first essential step is the identification of potential explanatory variables to be used in the predictive equations for pavement distress. Statistically, these explanatory variables are referred to as "independent" variables, although, in reality, there is a great deal of dependency known to exist both between these variables and the pavement distress variables (dependent variables) and among the explanatory variables, themselves. The explanatory or independent variables are generically referred to as "x's" and the dependent variables, "y's". Some of the explanatory variables may actually be clusters representing a numbers of individual pavement characteristics or properties.

After identifying both the dependent and independent variables and their relationships, the second step is to examine the observed variables (the data) for potential distributional problems. That is, statistically, certain assumptions are required in order that the statistical method produce valid and reliable results (conclusions). Sometimes these assumptions are valid for the bulk of the data but appear to be invalid because of a few "unusual" data elements. Often these unusual data elements can be tracked down and found to be erroneous, in which case they can be deleted or corrected (transcription or measurement errors). Other times they may lead to the identification of another explanatory variable that was inadvertently omitted from the model definition. In any case, it is essential that statistical procedures be used to identify such data anomalies.

The second flow chart procedure of Figure 1 refers to procedures which will identify these 'unusual' data points or other problems for each variable separately (univariately). However, a data point may be within acceptable limits for two variables separately yet, the pair of values, be "unusual". To detect these types of "paired" anomalies, bivariate procedures are required (box 3 of the flow chart of Figure 1).

The final step in the analysis which includes the development of distress models and sensitivity analyses, is termed, collectively, multivariate analyses. There are several analyses involved under this umbrella with the ultimate objective being the development of pavement distress models along with ranges of sensitivity of the parameters to provide the initial step for long range pavement distress modeling and prediction.

1. **Identification of pavement distress model variables and their interrelationships**

Both dependent (pavement distress) and independent (explanatory) variables must be considered in this step. In order to apply the statistical methodology of least squares regression analysis, certain assumptions must be met.

Regarding the prediction variables, the assumption of independent, normally distributed random variables is essential. For example, distress variables such as rutting, transverse and alligator cracking, etc. must follow a normal probability distribution. That is, the degree of distress among pavements must evenly distribute itself about some mean value. This assumption is obviously questionable when combining pavements with some distress with a large number of pavements with no distress. The assumption is more tenable for degree of distress <u>given</u> some distress has been measured. Measured is a key word here as some pavements with no distress recorded or "measured" may, in fact, be distressed only not to the extent that it can be measured. This issue will be further addressed in the analysis procedures to be presented.

In order to satisfy the normal distribution assumptions for pavement distress, a two-stage model building process is proposed. The first step is to identify those explanatory variables which best predict whether or no a pavement will have measurable distress by finding the best model that discriminates between distressed and non-distressed pavements. The second step is to use only the data from those pavements that have distress and determine which explanatory variables best predict the <u>degree</u> of distress. For this stage, transformations of the distress are recommended as follows:

alligator and transverse cracking - transform to % area cracked by severity levels and take natural logs

rutting - convert to a ratio of rut depth relative to a threshold value of .5 and take natural logs

Initially, the second stage models may not be too informative as for some types of distress, there is very little data, i.e. very few pavements that have any measurable distress. As more time elapses and more of the non-distressed pavements show distress, these models may be more meaningful. Also, as more data is collected, more sophisticated statistical methods may be used such as modeling the time to distress and using censored procedures

for pavements for which we do not know time of distress.

Independent variables pose a real challenge. Although these variables are not required to follow any particular probability distribution, There are many known and hidden interrelationships among these variables which can cause serious problems (collinearity) in least squares model building. The extent to which these interrelationships or correlations can be avoided will enhance the degree of reliability and predictability of the models. Hence, if known relationships exist based on sound engineering principals, these should be incorporated in the basic model structure. These known relationships will be referred to as "clusters".

An example of a potential "cluster" is the deflection related variable DELTA:

$$\Delta = \frac{9000N}{ES\left(\left(\frac{E1}{ES}\right)^{\frac{1}{3}H1} + \left(\frac{E2}{ES}\right)^{\frac{1}{3}H2}\right)}$$

If this relationship among asphalt stiffness and thickness and cumulative KESALs is , in fact, sound, then it makes far more sense to use the single explanatory variable DELTA as a candidate independent variable than the six separate measurements of stiffness, thickness, and KESALs. That is not to say that only Delta should be used in the model, it is just a single candidate representing six candidates. Other independent variables and other clusters will also be candidate independent variables to form a selection pool. The variable selection process will enable us to determine which of these variables and clusters are most significant in predicting pavement distress. An added feature of using the cluster approach, in addition to simplification of the model, is that it reduces the correlation (collinearity) among the independent variables. That is, the variables that go into the definition of DELTA are likely to be correlated among themselves. Hence, using the six measurements separately would introduce a degree of collinearity that could be avoided if only DELTA were used. We will see later that this collinearity can greatly distort a model's outcome or predictive abilities.

Another consideration in identifying potential explanatory variables is how to code them. For example, it is important that qualitative variables (descriptive variables such as region, wet/dry, etc.) be coded as indicator variables as opposed to quantitative variables (variables that have some magnitude such as % asphalt) whose values can be entered directly into the model. An example of this is region code. It would be incorrect to enter region code as a single explanatory variable with values 1,2,3 or 4, because this implies some ordering and magnitude to the region code number, i.e. region 4 is "4 times greater" than region 1. The proper coding of such a variable would be to define three explanatory variables to define region (always one less than the number of categories of the qualitative variable). For region this could be done by defining X1, X2, and X3 as:

X1=1 if region=1;else X1=0

X2=1 if region=2;else X2=0

X3=1 if region=3:else X3=0

Region 4 is implicitly defined as X1=X2=X3=0. Now, by putting these variables into the model separately the following kinds of questions can be addressed:

1. Is there a significant amount of cracking in region 4? (This will be the significance test associated with the intercept term.)

2. Is the degree of cracking in region 1 equal to the degree of cracking in region 4?

3. Is the degree of cracking in region 2 equal to the degree of cracking in region 4?

4. Is the degree of cracking in region 3 equal to the degree of cracking in region 4?

Other considerations in defining explanatory variables are transformations or the additions of quadratic terms and interactions. Sometimes, the omission of these terms or need for transformation becomes apparent in the model building process from the examination of residual plots. In general, interaction terms should always be included initially, especially interaction terms involving a quantitative variable and a qualitative one, unless there is strong reason to believe that such an interaction cannot occur. For example, if region code and % asphalt were both in a model, the interaction terms (i.e. the product of the x's) are measuring the slope between the degree of distress and % asphalt for each region. Omitting the interaction terms would be equivalent to forcing a constraint on the model which says that this slope must be equal for all regions and equal to the slope for region 4. This may, indeed, be the fact. However, by including the interaction terms first, one can address the question of equality of slopes and if they are in fact equal, <u>then</u> delete them from the model.

2. Examining both distress variables and explanatory variables independently

The statistical term for examining variables one at a time is called univariate analyses. The objective of these analyses are:

1. To examine the distributions of each variable

2. To identify gaps in the data

3. To identify unusual observations or measurements

4. To identify potential functional forms

The SAS procedures for doing these analyses are Proc Univariate and Proc Freq. Proc Univariate is for continuous variables, i.e. KESALs/yr, degree of rutting, etc. This procedure will produce descriptive statistics about the distribution of the variable such as means, variances, quantiles, max and mins, mode, median, skewness, kurtosis, etc. In addition, with the proper options, this procedure will produce plots of the distributions and box plots. Box plots are graphical means of identifying observations that are not within the bulk of the data. Proc Freq can produce two-dimensional frequency tables. This procedure is generally used with categorical-type data such as region, wet/dry, etc. These tables can assist in the identification of data gaps.

All candidate variables and clusters should be screened using this procedure. In addition, the new distress variables should be created to identify pavements with and without distress. Then, the univariate procedure can be used with the BY statement to examine the distribution of a continuous variable or cluster, like DELTA, for pavements with and without a particular distress.

3. Analysis of paired relationships among variables.

The analysis of relationships between two variables is termed bivariate analyses. The purpose of bivariate analyses are:

1. To identify correlation between two variables

2. To identify observations that are unusual in both factors simultaneously

3. To identify data gaps in both variables simultaneously

4. To identify potential functional forms

5. To spot data "clusters"

The SAS procedures for doing these analyses are Proc Plot, Proc Corr, and Proc Freq. Proc Plot will provide scatter plots and a visual way of identifying data gaps, clusters, and relationships. Proc Corr will provide

statistical verification of any visual linear relationships in the form of the correlation coefficient. Proc Plot is primarily for continuous variables while Proc Freq attempts to do the same thing for categorized variables. The Chi-Square statistic and other measures of association can be used to statistically verify relationships among categorized variables.

Again, these relationships should be examined not only on the collective data but for distressed pavements separate from non-distressed ones.

4. Identifying relationships among many variables - modeling

The statistical analyses of more than two variables is termed multivariate analyses. The purpose of these analyses are to:

1. Identify relationships among groups of variables

2. Build pavement deformation models

The SAS procedures for conducting these analyses are Proc Reg and an in-house SAS routine for conducting a Principal Component analysis. The Proc Reg procedure will be used for two purposes:

1. To identify those explanatory variables and clusters which best differentiate between pavements that do and do not have distress

2. To identify those explanatory variables and clusters which best predict the degree of distress

The Principal component analysis will provide a method for identifying unusual observations and collinearities (associations) in a multivariate way. In so doing, it may be possible to identify observations that are masking a problem, i.e. there may be a serious collinearity that is being hidden by a few unusual observations or these unusual observations may be causing an artificial collinearity that really isn't a problem.

BASIC STRATEGY

The basic steps in performing the analyses and building the statistical models for describing pavement distress will be outlined here. There are five basic steps which will enable us to address the following questions:

1. How do we "describe" distressed and non-distressed pavements in terms of potential physical and environmental factors that might relate to distress?

EXAMPLE: What is the average age of pavements that do not have any measurable degree of alligator cracking and what is the average age for pavements that do have some alligator cracking?

2. What is the relationship among potential explanatory variables that might relate to distress?

EXAMPLE: Are AADT and asphalt thickness correlated or is asphalt thickness correlated to some function of other explanatory variables? Will this relationship cause problems in the modeling of distress or determining the sensitivity of the variables in the model?

3. What variables determine the degree or extent of distress?

EXAMPLE: What explanatory variables and/or what functional form of these variables significantly predict the amount of rutting in a pavement?

4. How do distressed and non-distressed pavements compare?

EXAMPLE: Do pavements with transverse cracking have the same traffic load as pavements with no measurable transverse cracking?

5. Which variables significantly determine non-distressed pavements from distressed pavements?

EXAMPLE: Is the percent of voids a significant factor in identifying pavements with some alligator cracking?

The statistical steps for answering each of these questions, respectively, are presented below along with the statistical name for the methods to be used.

1. Examine descriptive statistics of potential explanatory variables and clusters for each type of distress for:

All pavement sections
Distressed sections only
Non-distressed sections only

Statistical method: Univariate analyses

2. For any potential explanatory variables and clusters that are candidates for predictive models, examine their inter-relationships. These relationships can occur in three basic ways:

1. Among pairs of variables (Pearson's correlation)
2. One variable may be correlated with all other variables (Multiple correlation coefficient)
3. Some subgroup of variables may be correlated (eigenvector analysis)

These relationships should be examined for each type of distress for

All pavement sections
Distressed sections only
Non-distressed sections only

Statistical methods: Bivariate analyses
Multiple regression modeling
Principal component (eigen) analyses

3. Build models (select important variables, build prediction equations, test sensitivity of the final equations)

These analyses should be performed for each type of distress for

All pavement sections
Distressed sections only
Non-distressed sections only

Statistical methods: Regression analysis
Diagnostic methods
Sensitivity analysis

4. Compare descriptive statistics and distributions of explanatory variables and clusters for:

All pavement sections
Distressed sections only
Non-distressed sections only

5. Determine which variables best discriminate between distressed and non-distressed pavements.

Statistical method: Discriminant analysis

A very important question that ultimately needs to be addressed is:

Which variables best predict time to distress or time to failure?

In order to answer this question, pavements sections need to be monitored over time. At this point in our study, we will only have, at most, three points in time and for many sections, only one point in time (i.e. observed distresses from distress surveys over a period of two years). This is not sufficient data to allow us to address the above question. Eventually there will be sufficient data as determined by the number of pavements that show distress. That is, if within five years we can expect to observe that 50% of the pavements which currently have no distress as exhibiting some distress, then a five year period should be sufficient to allow for modeling the time to distress. Time to failure will be much more difficult to model. This will require a clear definition of what constitutes failure and will probably require a much longer observation period to observe enough failed pavements.

At any rate, when sufficient data has been obtained, other problems will need to be addressed, namely censoring. Censored data is defined as data for which only partial information is available. In this application, our censored data will be those pavements which have already shown some degree of distress. The reason for this is that the key variable being modeled, namely time of distress, is not known for the pavements we have already found distress on. We know that at the time the study began, some degree of distress was observed. These sections still provide valuable information for the model but must be handled differently from those pavements for which we know the time of distress. Had we been able to observe that time, it would have been to the left (less than) of the time we observed the distress. This is known as left censoring. A second type of censoring is known as right-censoring. This occurs if the time to distress could not be observed because the pavement section had to be dropped from the study, for example, had to be resurfaced. The observed time to distress can never be realized and all we know is that at the time the section went off-study, it had not failed. The true time to failure is somewhere to the right (greater than the observed time) and hence the

observed time must be right censored. The statistical method to build these models of time to distress are Cox regression and survival analysis.

Since we do have some pavements for which we have multiple points in time, these will be handled by our analyses as follows. Preliminary models will be built based on the initial distress surveys. These models will then be re-run or updated for all sections after the second distress surveys. That is, the model that discriminates between pavements that do and do not show distress will now have a shift of data from the group that did not show distress to the group that did. The effect of these sections, i.e., their explanatory variables, on the resulting discrimination model can then be assessed. When a third survey is made, another model update will be performed. Now even more sections will shift from the non-distressed group to the distressed groups. This type of sequential modeling should be performed throughout the time period that pavement sections will be monitored. The models will be revised as more information on distress is made available.

DETAIL ON STATISTICAL PROCEDURES

1. Univariate analyses

Univariate analyses consist of statistical methods for describing the distribution of continuous random variables. Examples of continuous variables for this study are cumulative KESALs, age, AADT, % trucks, etc. These distributions should be examined for all sections as well as for distressed and non-distressed sections separately. A sample of the Proc Univariate output from SAS for one of the potential cluster variables, DELTA, is shown in Table 1. Figure 2 shows continued output from Proc Univariate depicting the frequency distribution, box plot, and Normal Probability plot. From Table 1, descriptive statistics such as number of sections (190), mean delta (671.5),standard deviation (199.5053), etc. can be found. Figure 2 shows the distribution, which is somewhat skewed to the left. The box plot can be useful in identifying outliers, the * and 0's and the mean and standard deviation of the distribution (dashed lines). The SAS statements for generating this output are:

```
PROC UNIVARIATE NORMAL PLOT;
VAR X1 X2 X3 X4 ETC.;
```

To do this for each level of another variable, say Y1 where Y1 is 0 for pavements with no distress and Y1=1 for pavements with distress, the BY option can be used if the data is sorted first, e.g.

```
PROC SORT;BY Y1;
PROC UNIVARIATE NORMAL PLOT;BY Y1;
VAR X1 X2 X3 X4 ETC.
```

2. Bivariate analyses

Correlation

The simple linear relationship between pairs of variables can be measured and statistically tested for significance using the Pearson's Correlation Coefficient. This is a value between -1 and 1 where -1 denotes a strong negative relationship, +1 denotes a strong positive relationship, and 0 denotes no relationship.

Table 2 gives an example of the output from SAS's Proc Corr which estimates the correlation coefficient. The first number in the set is the estimate of the correlation coefficient, i.e., the correlation between DELTA and the log of alligator cracking (LD1) is .19577. The second number is the p-value or the level of significance at which you would reject the hypothesis of no significant correlation. For the DELTA and LD1 correlation, this value is .3088. If this value is less than .05, it would be concluded that the correlation is significant. In this example, the correlation between DELTA and LD1 is not significant. The third number is the number of pairs on which this correlation was based, namely, 29 pavement section DELTAs and LD1s.

Frequency Tables

Classification variables such as wet/dry, region, etc. should be examined in pairs as to the distribution of sites by these variables. The statistic for measuring the association among these classification variables is Pearson's Chi-square. The SAS procedure to do this analysis is Proc Freq, and the required statements are:

```
PROC FREQ;
TABLES X1 X2 X3/cellchi2 all;
```

Table 3 gives a sample output from this procedure for examining the distribution of sites that did and did not have alligator cracking by wet or dry region. There are four numbers in the table. The first is the number of sites in that cell, e.g. 94 sections in wet regions did not have alligator cracking. The second number is the proportion of sections in that cell relative to the total number of sections, e.g. 49.74% of the sections (94/189) had no alligator cracking and were in the wet region. The third number is the row percent, e.g. 59.49 % of the sites with no alligator cracking were in the wet region (94/158). The last number is the column percent, e.g., 82.46% (94/114) of the sections in the wet region had no alligator cracks. The marginal proportions (i.e. under headings of Total) tell how the data is distributed for one variable ignoring the other, e.g., 83.60% (158/189) in this data set had no measurable amount of alligator cracking. These numbers can be useful in getting a feel for data gaps which ultimately will dictate the limitations of the statistical modeling procedures.

Scatter Plots

Scatter plots of variable pairs can be very informative and essential to identifying data gaps, model distributional requirements, etc. These plots should be examined for relevant explanatory variables and clusters. The SAS procedure for doing this is Proc Plot, and the required statements are:

```
PROC PLOT:
PLOT (X1 X2 X3)*(DELTA X4);
```

This SAS statement will produce 6 plots, namely, X1 vs DELTA, X2 vs DELTA, X3 vs DELTA, X1 vs X4, X2 vs X4, and X3 vs X4. There are obviously many superior graphic programs other than SAS and any of these could be used in place of Proc Plot if desired. Figure 3 is an example of a scatter plot of percent trucks vs KESAL/year for all sections that had some alligator cracking. From this plot we see a potential outlier section that has an unusually high value for KESAL/year.

3. Multivariate analyses

Regression analysis

Ordinary least squares regression models attempt to explain some dependent variable, y, in terms of many independent (explanatory variables), x's. The SAS procedure for doing this is called Proc Reg.

```
PROC REG;
MODEL Y=X1 X2 X3 X4 X5/P R INFLUENCE COLLINOINT VIF;
OUTPUT OUT=NEW PRED=PRED RESID=RESID;
```

These SAS statements will find the estimates for the model coefficients that will provide the best (least squares) fit to the data. The model corresponding to the above SAS statements is:

$$y=\beta_0+\beta_1 x_{1i}+\beta_2 x_{2i}+\beta_3 x_{3i}+\beta_4 x_{4i}+\beta_5 x_{5i}$$

The statements following the / in the model statement request diagnostics for influential observations and collinearity. The output statement creates a file called "NEW" which will contain predicted values and residuals. This file can then be used in plot statements to plot the data:

```
PROC PLOT DATA=NEW;PLOT (Y PRED)/OVERLAY;
PROC PLOT DATA=NEW;PLOT RESID * (X1 X2 X3 X4 X5);
```

In the first plot statement, one plot will result with both the observed and predicted values on the same plot (OVERLAY option). In the second plot statement, 5 plots of the residuals vs each x value will result. These plots are very useful in identifying unusual points or in identifying possible necessary transformations and relationships (logs, quadratic terms, etc.)

Table 4 presents the SAS Proc Reg output for modeling the degree of alligator cracking (i.e. no sections with zero cracking are included) as a function of 12 explanatory variables. The analysis of variance table provides information on the model's overall fit. In this example, this model does not provide a significant explanation for the degree of alligator distress (Prob>F=.3271, this value would have to be less than .05 for the model to be significant). There were 20 observations in this data set, DF for C Total + 1). The Root MSE can be used to compute the 95% prediction interval at the point where it is narrowest (at the mean of each x) as follows:

$$\bar{y} \pm 1.96\sqrt{MSE(1+\frac{1}{n})}$$

Upper 95% Prediction interval:

$$803.4 + 1.96(808.3943)(1.0246) = 2426.83$$

Lower 95% prediction interval:

$$803.4 - 1623.43 = -820.03$$

This interval is interpreted as follows: We could expect, with 95% accuracy that the predicted total amount of alligator cracking would be between -820.03 and 2426.83. Obviously, these are ridiculous numbers. This is because this model did not provide a significant fit to the data in the first place and the amount of error in this model (MSE) is extremely large. In practice, one would not even compute this prediction interval and would abandon this model in search of another. The computation is presented here for purely illustrative purposes.

Both R^2 and adjusted R^2 are provided on this output. These both measure the percent of the total variation in alligator cracking that is explained by the model. The adjusted R^2 adjusts for the degrees of freedom in the model and is a more accurate estimate. For example, the unadjusted R^2 of .7102 looks deceptively good in view of the fact that we know this is not a good model. However, the unadjusted R^2 is only large because of the larger number of variables in the model (12) relative to the few observations (20). The adjusted R^2 of .2133 is more realistic and adjusts for this fact.

The model equation can be obtained from the column Parameter Estimate. The test of significance for each model variable is shown along with its p-value (Prob > |T|). Any values less than .05 correspond to model variables which are statistically significant. No model variables are significant in this example.

The column labeled Variance Inflation measures the amount of collinearity in the model. If any of these numbers exceed 10, it means that there is collinearity. Model variables with a variance inflation factor greater than 10 are variables which, when regressed on all the other X-variables would have an R^2 greater than .9. For example, X1 has a variance inflation factor of 19.724. This means that X1 is highly correlated with all other X variables.

Table 5 is the second page of output from PROC REG and contains additional information on the collinearity among the explanatory variables. The variance inflation factor merely identifies relationships between a given X-variable and all other X-variables. The collinearity diagnostics can find relationships among subgroups of explanatory variables. The SAS Proc option COLLINOINT produces this output. It is important to adjust for the intercept, hence the option COLLINOINT rather than COLLIN.

To identify the source of the collinearity, find values under the column heading Eigenvalue that are close to zero. These are ordered largest to smallest. For this example there are two such eigenvalues, the 11th and 12th with values of .05756 and .02086, respectively. The next step is to check the numbers in the columns labeled Var Prop X1, Var Prop X2, etc. Any large numbers in these columns reflect the weight of each X-variable in the association. Basically, these relationships can be defined as:

$$k_1x_1+k_2x_2+\ldots+k_{12}x_{12}=0$$

where the k_i's are the Var Prop values and the zero is the assumed value of the small eigenvalue. For this example, then, the relationship for the 12th (smallest) eigenvalue is:

$$0.9363x_1+0.5786x_2+0.133x_3+0.007x_4+0.8152x_5+0.1891x_6$$
$$+0.4884x_7+0.7187x_8+0.6318x_9+0.6327x_{10}+$$
$$0.1743x_{11}+0.0008x_{12}=0$$

This means that the major contributors to this relationship are x_1, x_2, x_5, x_8, x_9, x_{10}, and x_{12}. Note that the second smallest eigenvalue identifies variables x_{11} and x_{12} as being correlated. These variables happen to be % trucks and KESALs/yr, a logical relationship.

If these relationships can be identified, they may lead to the formation of additional clusters or, as in the case of % trucks and KESALs/yr, the exclusion of one variable in favor of another. In other words, if single variables or variables in clusters are contributing the same amount of information to the model, it is not necessary to include both or to include the cluster variables independently.

Table 6 yields the diagnostics for identifying outliers or influential observations. The model used to generate this table was based on only on x- variable, the log of DELTA, and the y-variable was the log of the % area with alligator cracking for those 20 pavement sections that had some measurable amount of alligator cracks. Only 19 pavements had all the values necessary to compute DELTA, hence the total number of observations for this model is 19.

Many of the diagnostics listed in Table 6 yield the same information. Four basic diagnostics and their criteria for identifying an unusual observation will be described here.

1. RSTUDENT > 1.96 - This diagnostic indicates a large deviation from the fitted model with respect to the dependent or y- variable.

2. HAT DIAG > 2p/n - where p is the number of independent variables in the model plus 1 and n is the number of observations. This diagnostic identifies observations that are having a significant influence on the prediction of the dependent variable.

3. Cook's D > $F_{.05,p,(n-p)}$ - where F is the F-statistic at the 5% level of significance for p and (n-p) degrees of freedom (n is the total number of observations in the model. This diagnostic identifies observations that significantly changes one or more of the model coefficient, i.e., it measures the sensitivity of the coefficients to the observation or that site's distress.

4. DFBETAS > 2/$\sqrt{n}$ - This measures the influence of each observation on each independents variable (see Table 7). That is, whereas Cook's D measures the influence on all model coefficients collectively, the DFBETA for each x-variable measures the sensitivity of the coefficient for that variable to the observed distress for each pavement section.

From Table 6 for this example we see that the RSTUDENT diagnostic identifies observation # 2 (2.0944) and # 7 (-2.4613) as outliers on the distress variable. The Hat Diag would have to exceed .2105, (2(2/19)) and hence identifies observation # 9 (.2089). Cook's D would have to exceed the F value at the 5% level of significance for 2 and 17 degrees of freedom which is 3.68. No observations are flagged by this criteria. The last criteria, DFBETAS, appear in Table 7. The DFBETAS are listed for the intercept and the single x-variable, LDELTA. These values would have to exceed .4588 (2/√19) in order for an observation to significantly influence the sensitivity of these coefficients. Observations # 7 and 20 exceed this value for both the intercept (.6786,-.9517), and LDELTA (.7537,.6841). These diagnostics seem to indicate that three observations are influential, in some sense, namely, 2, 7, and 20. A plot of the dependent variable vs LDELTA is shown in Figure 4 with the three suspect observations identified.

Variable Selection

In order to obtain the model that best describes the data with the fewest parameters, variable selection is of interest. In fact, it is possible to actually obtain a worse model by including too many variables. Whereas R^2 will always increase as the number of variables increase, the predictive error of the model may be optimal (minimal) at some subset of the variables and then increase as variables are added. Hence, a 5-variable model may actually yield a better prediction (as reflected in the mean squared error, MSE) than a 20 variable model even though the 20-variable model will have a superficially larger R^2. Figure 5 depicts this.

The RSQUARE option of Proc Reg will examine all possible subsets and present the results to be used in selecting the best subset. This procedure is superior to any other stepwise selection methods because the stepwise methods are sensitive to collinearities in the model variables and might not produce the best model in the presence of this collinearity. These methods are outdated and should never be used. Their computational advantage (i.e. not having to examine all possible subsets) is no longer a factor in this day of high-speed computing. The criteria for choosing the best model is minimum C_p. C_p is a function of the model mean squared error (MSE) which adjusts for the number of model parameters relative to the number of observations similar to adjusted R^2.

A sample output from Proc Reg with the RSQUARE option are given in Table 8. The SAS statements used to generate this output are:

```
PROC REG;
MODEL Y = X1 X2 X3 ... X12/P R CP SELECT=RSQUARE;
```

In Table 8 all 1-variable, 2-variable, 3- variable, etc. models are listed in descending order of C_p. That is, for the 1-variable models, the one with X4 had the smallest C_p of all other 1-variable models, 4.75999. Examining the first entries in any variable size category shows that the minimum C_p for any given subset size group decreases as the number of variables increase up to the 6-variable case, i.e. 4.75999 > 3.48571 > 3.2744 > 2.24925 < 3.2489. That is, the best 5-variable model has a smaller prediction error than the best 6-variable model.

The variables that form the best 5-variable model are X2, X4, X6, X10LOG, and X12. In order to obtain these model coefficients and diagnostics, Proc Reg would need to be re-run specifying only these variables in the model statement.

Eigenanalysis

Eigenanalysis (Principal Component Analysis) is a multivariate procedure which enables examining the data for both influential observations and collinearity simultaneously. It is possible for the collinearity diagnostics from Proc Reg to indicate a significant collinearity problem which is really only being caused by a few observations. Conversely, the diagnostics may show no problem when a serious collinearity exists but is being masked by a few observations. This is known as the masking problem.

There is no SAS procedure for doing this analysis. However, several SAS procedures can be combined to produce this analysis. Proc Factor of SAS, with the no rotation option, produces principal component factors. If these factors are multiplied by $(\delta_i/n)^{1/2}$, where δ_i is the eigenvalue, the resulting principal component factor becomes the eigenvector for that eigenvalue. Plots of pairs of eigenvectors that correspond to small eigenvalues provide a visual means of identifying potential masking problems.

The SAS statements to do this are:

```
PROC FACTOR SIMPLE CORR MINEIGEN=0 EV
     NFACTORS=12 OUT=SCORES1;
VAR X1-X12;

DATA NEW;SET SCORES1; K10=SQRT(.155415/19);
     K11=SQRT(.057561/19);K12=SQRT(.020860/19);
     FACT10=K10*FACTOR10;FACT11=K11*FACTOR11;
     FACT12=K12*FACTOR12;

PROC PLOT DATA=NEW;
PLOT FACT10*FACT11 FACT10*FACT12 FACT11*FACT12;
```

These statements were written for a 12-variable model with 19 observations. The eigenvalues were obtained from the previous Proc Reg run of this model with the VIF option or from the output of Proc Factor. The three factors corresponding to the three smallest eigenvalues were chosen. In other situations, more factors may be necessary depending on the number of small eigenvalues that occur. Table 9 is a sample output from the Proc Factor procedure which contains the eigenvectors and eigenvalues as defined in the Proc Reg output earlier. Figure 6 shows a sample plot revealing a single observation that appears to be masking a collinearity. Collinearity is present when the shape of the ellipse drawn around the data is elongated. The more the ellipse resembles a circle, the less the degree of collinearity. The major axes of the ellipse drawn around the data are the reciprocals of the square root of the eigenvalues. Hence the smaller the eigenvalue, the greater the length of the major axis and the more elongated the ellipse. In Figure 6, if we were to draw an ellipse about the data excluding the observation in the lower left corner, that ellipse would be elongated, signifying a collinearity. By including the observation, the ellipse is more circular, indicating no collinearity.

Discriminant analysis

The purpose of discriminant analysis is to identify which variables are significant in classifying data into groups. For this application, we want to use discriminant analysis to address the question:

> Which explanatory variables and clusters discriminate between those pavements with no measurable distress and those with measurable distress?

A discriminant analysis with only two categories to choose from, e.g. distress and no distress, can be performed using a multiple regression procedure, if the y-variable is defined in a certain way. The advantage of doing this as opposed to using a standard discriminant analysis program is the availability of the diagnostics for collinearity, influential observations, etc. which are generally not available with discriminant analysis programs.

The key is to code the y-variable as follows:

$y=-n_2/n$ for pavements <u>without</u> distress

$y=n_1/n$ for pavements <u>with</u> distress

where n_1 = the number of pavements without distress, n_2 is the number of pavements with distress and n is the total number of pavements. Note: these numbers are not backwards; i.e., for pavements <u>without</u> distress y is the negative proportion of distressed pavements and for pavements <u>with</u> distress

y is the proportion of non-distressed pavements.

As an example, this procedure was done for data with 31 pavement sections with alligator cracking and 158 pavements without, using 13 explanatory variables and clusters. The y-variable was coded as:

y=-31/189=-.164 for pavements with no distress

y=158/189=.836 for pavements with distress

Table 10 is the output from running the Proc Reg procedure using this coded y-variable as the dependent variable in the model. The significant model F-value (Prob>F=.0114) indicates that this model significantly discriminates between pavements with and without alligator cracking. The R^2 statistics for this model are meaningless. The variables which were significant according to the Prob > |T| statistics are H2 E5, and X6. The Variance Inflation factor for LDELTA indicates that LDELTA is highly correlated with the other model variables. This is not surprising since DELTA is a cluster of many of the other variables in the model.

In order to determine how well the model classifies pavements, the Proc Freq procedure can be used to classify pavements according to predicted distress, yes or no, and actual distress, yes or no.

TABLES

Table 1. Univariate Output for Variable E_1

Moments			
N	190	Sum Wgts	190
Mean	671.5053	Sum	127586
Std Dev	199.2837	Variance	39713.99
Skewness	0.755811	Kurtosis	1.073465
USS	93180614	CSS	7505943
CV	29.67716	Std. Mean	14.45756
T:Mean = 0	46.44666	Prob > |T|	0.0001
Sgn Rank	9072.5	Prob > |S|	0.0001
Num = 0	190		
W:Normal	0.959326	Prob < W	0.0003

Quantiles (Def = 5)			
100% Max	1490	99%	1310
75% Q3	774	95%	1007
50% Med	638	90%	960
25% Q1	546	10%	448.5
0% Min	292	5%	370
Range	1198	1%	310
Q3 - Q1	228		
Mode	851		

Extremes			
Lowest	Obs	Highest	Obs
292(	148)	1048(	42)
310(	130)	1168(	41)
314(	142)	1187(	18)
330(	134)	1310(	43)
336(	78)	1490(	83)

Variable = E1

Table 2. Correlation Analysis for Alligator Cracking Less than 0

	LFZ	LFF	LD1	LD2	LD3
DELTA	0.13607	-0.61042	0.19577	-0.11679	0.41401
	0.4815	0.0004	0.3088	0.5463	0.0256
	29	29	29	29	29
LDELTA	-0.17308	-0.55805	0.23408	0.12977	0.45891
	0.3693	0.0017	0.2216	0.5023	0.0123
	29	29	29	29	29
F1	0.56055	0.36576	-0.16305	-0.17999	-0.13817
	0.0010	0.0430	0.3808	0.3326	0.4585
	31	31	31	31	31
F2	0.88019	-0.54211	0.04023	-0.20509	0.29773
	0.0001	0.0016	0.3299	0.2684	0.1038
	31	31	31	31	31
LF1	0.59661	0.34642	-0.19208	-0.16658	-0.11545
	0.0004	0.0563	0.3006	0.3704	0.5363
	31	31	31	31	31
LF2	1.00000	-054617	-0.04162	-0.34030	0.31880
	0.0	0.0015	0.8241	0.0610	0.0805
	31	31	31	31	31
LFF	-0.54617	1.00000	-0.15184	0.22390	-0.49315
	0.0015	0.0	0.4148	0.2260	0.0048
	31	31	31	31	31
LD1	-0.04162	-0.15184	1.00000	0.20490	0.48697
	0.8241	0.4148	0.0	0.2588	0.0055
	31	31	31	31	31
LD2	-0.34030	0.22390	0.20490	1.00000	-0.08048
	0.0610	0.2260	0.2688	0.0	0.6669
	31	31	31	31	31
LD3	0.31880	-0.49315	0.48697	-0.08048	1.00000
	0.0805	0.0048	0.0055	0.6669	0.0
	31	31	31	31	31

Pearson Correlation Coefficients/Prob > |R| under Ho: Rho = 0 /number of observations

Table 3. Frequency Table of Alligator Cracking versus Rainfall

Table of Y1I by Z2			
Y1I	**Z2**		
Frequency Percent Row Pct Col Pct	Wet 1	Dry 3	Total
0	94 49.74 59.49 82.46	64 33.86 40.51 85.33	158 83.60
1 Alligator	20 10.58 64.52 17.54	11 5.82 35.48 14.67	31 16.40
Total	114 60.32	75 39.68	189 100.00

Frequency Missing = 1

Table 4. Analysis of Variance from Regression for Alligator Cracking

Model: MODEL1 Dependent variable: Y1

Source	DF	Sum of Squares	Mean Square	F Value	Prob > F
Model	12	11208369.228	934030.76897	1.429	0.3271
Error	7	4574509.5723	653501.36747		
C Total	19	15782878.800			

Root MSE	808.39431	**R-square**	0.7102
Dep Mean	803.40000	**Adj R-sq**	0.2133
C.V.	100.62165		

Variable	DF	Parameter Estimate	Standard Error	T for H0: Parameter = 0	Prob > |T|
INTERCEP	1	3155.782427	10833.738236	0.291	0.7793
X1	1	23.799726	150.99011294	0.158	0.8792
X2	1	156.811760	118.57122389	1.323	0.2276
X3	1	-16.959703	21.59474780	-0.785	0.4580
X4	1	-594.106341	302.91171376	-1.961	0.0906
X5	1	-44.095722	225.20587319	-0.196	0.8503
X6	1	-1035.284160	545.5885509	-1.898	0.0996
X7	1	-239.820747	241.25263131	-0.994	0.3533
X8LOG	1	-56.769891	952.37371728	-0.060	0.9541
X9	1	-56.978781	97.30548221	-0.586	0.5765
X10LOG	1	667.512166	641.79166028	1.040	0.3329
X11	1	-14.995743	58.52547572	-0.256	0.8051
X12	1	-1.315447	2.09458646	-0.628	0.5499

Variable	DF	Variance Inflation	
INTERCEP	1	0.00000000	
X1	1	19.7240959	Base + Subbase Thickness
X2	1	6.96501220	
X3	1	1.84106651	
X4	1	2.36954343	
X5	1	11.10971094	% Asphalt
X6	1	2.79560614	
X7	1	6.47751189	
X8LOG	1	4.63584514	
X9	1	5.08479402	
X10LOG	1	7.38128762	
X11	1	7.01716524	
X12	1	9.13532406	

Table 5. Eigenanalysis for Parameters Used in the Model of Alligator Cracking

No.	Eigenvalue	Cond. no.	X1	X2	X3	X4	X5	X6	X7	X8LOG	X9	X10LOG	X11	X12
1	3.49531	1.00000	0.0006	0.0004	0.0196	0.000	0.0030	0.0002	0.0042	0.005	0.0031	0.0059	0.0074	0.0066
2	2.57099	1.16598	0.0056	0.0118	0.0029	0.0134	0.0038	0.0143	0.0069	0.004	0.0019	0.0007	0.0000	0.0018
3	1.47762	1.53802	0.0004	0.0153	0.0137	0.0470	0.0073	0.0050	0.0112	0.0106	0.0399	0.0002	0.0007	0.0000
4	1.35073	1.60864	0.0000	0.0010	0.0027	0.0329	0.0010	0.0287	0.0029	0.0840	0.0082	0.0102	0.0025	0.0018
5	1.02277	1.84865	0.0009	0.0135	0.0320	0.1232	0.0000	0.1505	0.0014	0.0010	0.0001	0.0041	0.0047	0.0019
6	0.64804	2.32242	0.0001	0.0019	0.0483	0.0005	0.0009	0.0624	0.0077	0.0262	0.0275	0.0412	0.0825	0.0066
7	0.55466	2.51032	0.0026	0.0049	0.5574	0.0395	0.0000	0.0018	0.0194	0.0025	0.0744	0.0048	0.0006	0.0040
8	0.37784	3.04150	0.0120	0.0003	0.1700	0.0147	0.0013	0.0002	0.0507	0.1171	0.0411	0.1083	0.0192	0.0032
9	0.26820	3.61007	0.0128	0.0095	0.0082	0.3546	0.1216	0.0898	0.0443	0.0122	0.0013	0.0007	0.0031	0.0629
10	0.15541	4.74239	0.0203	0.3543	0.0040	0.0336	0.0446	0.2481	0.2254	0.0048	0.1317	0.0011	0.0114	0.0054
11	0.05756	7.79256	0.0083	0.0085	0.0082	0.3400	0.0012	0.2099	0.1374	0.0220	0.0391	0.1901	0.6935	0.9051
12	0.02086	12.94449	0.9363	0.5786	0.1330	0.0007	0.8152	0.1891	0.4884	0.7187	0.6318	0.6327	0.1743	0.0008

Variety Properties
X1 = Base + Subbase Thickness
X2 = Stiffness
X5, X6 = Asphalt Thickness
X7 = Voids
X8LOG = Viscosity
X9 = Age
X10LOG = AADT
X11 = % Truck
X12 = kESALs/year

Table 6. Analysis of Influential Observations

Obs	Dep Var LD1	Predict Value	Std Err Predict	Residual	Std Err Residual	Student Residual
1	2.8651	2.9904	0.451	-0.1253	1.345	-0.093
2	6.2097	3.5775	0.343	2.6322	1.376	1.913
3	4.3239	3.2788	0.389	1.0451	1.364	0.766
4	2.3128	3.8542	0.326	-1.5414	1.380	-1.117
5	3.5294	3.1987	0.404	0.3306	1.359	0.243
6	5.1151	5.2688	0.581	-0.1537	1.294	-0.119
7	2.5326	5.3147	0.595	-2.7821	1.288	-2.161
8	5.5185	4.6673	0.424	0.8512	1.353	0.629
9	6.0572	5.4948	0.648	0.5624	1.261	0.446
10	6.0076	5.0304	0.515	0.9772	1.322	0.739
11	0.9765	.	.	.	.	.
12	2.8651	4.1017	0.334	-1.2366	1.378	-0.897
13	5.8052	4.2990	0.356	1.5062	1.373	1.097
14	3.7466	3.3909	0.369	0.3557	1.370	0.260
15	2.8651	3.5401	0.347	-0.6750	1.375	-0.491
16	2.8651	3.1756	0.409	-0.3105	1.358	-0.229
17	2.0733	2.8343	0.491	-0.7610	1.331	-0.572
18	2.8556	4.3090	0.357	-1.4534	1.373	-1.059
19	5.8052	3.6208	0.338	2.1844	1.377	1.586
20	0.5080	1.9140	0.761	-1.4059	1.197	-1.175

Obs	-2-1-0 1 2	Cook's D	Rstudent	Hat Diag H		Cov Ratio	Dffits
1	| |	0.000	-0.0904	0.1013		1.2549	-0.0304
2	| ***	0.114	2.0944	0.0584		0.7385	0.5218
3	| *	0.024	0.7565	0.0750		1.1377	0.2155
4	** |	0.035	-1.1253	0.0527		1.0233	-0.2654
5	| |	0.003	0.2364	0.0813		1.2203	0.0703
6	| |	0.001	-0.1153	0.1681		1.3547	-0.0518
7	**** |	0.498	-2.4613	0.1759	✓	0.7207	-1.1369
8	| *	0.019	0.6174	0.0894		1.1828	0.1935
9	| |	0.026	0.4350	0.2089		1.3939	0.2236
10	| *	0.041	0.7291	0.1317	✓	1.2178	0.2839
11							
12	* |	0.024	-0.8916	0.0554		1.0847	-0.2160
13	| **	0.040	1.1041	0.0629		1.0401	0.2860
14	| |	0.002	0.2525	0.0675		1.2011	0.0679
15	| |	0.008	-0.4796	0.0599		1.1671	-0.1211
16	| |	0.002	-0.2222	0.0833		1.2239	-0.0670
17	* |	0.022	-0.5602	0.1197	✓	1.2336	-0.2066
18	** |	0.038	-1.0629	0.0634		1.0516	-0.2765
19	| ***	0.076	1.6668	0.0569		0.8690	0.4095
20	** |	0.279	-1.1892	0.2882		1.3389	-0.7567

$F_{2,17} \approx 3.65$ $\qquad \frac{2p}{n} = \frac{2(2)}{19} = .1053$

Table 7. Analysis of Influential Observations using DFBETAS

Obs	INTERCEP Dfbetas	LDELTA Dfbetas
1	-0.0273	0.0210
2	0.3253	-0.1645
3	0.1728	-0.1177
4	-0.1004	0.0094
5	0.0587	-0.0418
6	0.0303	-0.430
7	0.6786	-0.9517
8	-0.0652	0.1241
9	-0.1428	0.1934
10	-0.1445	0.2199
11	.	.
12	-0.0273	-0.0483
13	-0.0180	0.1154
14	0.0507	-0.0319
15	-0.0788	0.0423
16	-0.0565	0.0406
17	-0.1924	0.1546
18	0.0199	-0.1139
19	0.2415	-0.1126
20	-0.7537	0.6841

Sum of Residuals: -2.08722E -14
Sum of Squared Residuals: 34.1970
Predicted Residual SS. (Press): 43.4585

Table 8. Model Selection Using R^2 and Mean Square Error.

Number in Model	R^2	C(p)	Variables in Model
1	0.14041767	4.75999	X4
	0.10471620	5.62223	X6
	0.05915383	6.72262	X10LOG
	0.03164997	7.38687	X2
	0.02912569	7.44783	X11
	0.02615253	7.51964	X8LOG
	0.02039141	7.65878	X1
	0.01154603	7.87240	X3
	0.00632104	7.99859	X7
	0.00475496	8.03642	X5
	0.00359339	8.06447	X12
	0.00108421	8.12507	X9
2	0.27599174	3.48571	X4 X6
	0.21300391	5.00694	X2 X4
	0.20452211	5.21179	X1 X4
	0.20420051	5.21956	X4 X11
	0.19622190	5.41225	X4 X10LOG
	0.16616485	6.13817	X6 X10LOG
	0.15696922	6.36025	X10LOG X12
	0.15622501	6.37823	X4 X8LOG
	0.15020104	6.52371	X5 X6
	0.14835465	6.56830	X4 X5
	0.14827520	6.57022	X3 X4
	0.14760360	6.58644	X10LOG X11
3	0.36755082	3.27444	X6 X10LOG X12
	0.34862110	3.73162	X2 X4 X6
	0.34553724	3.80610	X4 X10LOG X11
	0.34049162	3.92796	X4 X6 X11
	0.33396977	4.08547	X4 X6 X10LOG
	0.32860169	4.21511	X5 X6 X10LOG
	0.30323452	4.82776	X4 X6 X8LOG
	0.29352491	5.06226	X4 X6 X12
	0.29116969	5.11914	X4 X5 X11
	0.28816534	5.19170	X4 X11 X12
	0.28783026	5.19979	X3 X4 X6
	0.28692347	5.22169	X1 X4 X6
4	0.52049374	1.58068	X4 X6 X10LOG X12
	0.48614949	2.41014	X4 X6 X10LOG X11
	0.42566819	3.87083	X5 X6 X10LOG X12
	0.40708906	4.31954	X2 X4 X6 X11
	0.40245724	4.43141	X1 X4 X10LOG X11
	0.39998337	4.49116	X3 X6 X10LOG X12
	0.39995091	4.49194	X3 X4 X6 X10LOG
	0.39593012	4.58905	X2 X4 X6 X7
	0.39320081	4.65496	X2 X4 X6 X10LOG
	0.39083765	4.71204	X4 X5 X6 X10LOG
	0.38777065	4.78611	X6 X10LOG X11 X12
	0.38740672	4.79490	X2 X4 X10LOG X11

5	0.57562240	2.24925	X2 X4 X6 X10LOG X12
	0.54616070	2.96079	X3 X4 X6 X10LOG X12
	0.53684093	3.18587	X2 X4 X6 X7 X11
	0.53609602	3.20386	X1 X4 X6 X10LOG X12
	0.52805927	3.39796	X4 X6 X9 X10LOG X12
	0.52767380	3.40727	X2 X4 X6 X10LOG X11
	0.52606658	3.44609	X4 X6 X8LOG X10LOG X12
	0.52341923	3.51002	X4 X5 X6 X10LOG X12
	0.52187538	3.54731	X4 X6 X10LOG X11 X12
	0.52112358	3.56547	X4 X6 X7 X10LOG X12
	0.50999945	3.83413	X3 X4 X6 X10LOG X11
	0.49326628	4.23826	X4 X6 X9 X10LOG X11
6	0.61704154	3.24893	X2 X4 X6 X7 X10LOG X12
	0.60772018	3.47405	X2 X3 X4 X6 X10LOG X12
	0.59805021	3.70759	X2 X4 X6 X7 X10LOG X11
	0.58875144	3.93217	X1 X2 X4 X6 X10LOG X12
	0.58546208	4.01161	X2 X4 X6 X9 X10LOG X12
	0.58074607	4.12551	X2 X4 X6 X8LOG X10LOG X12
	0.57992858	4.14525	X2 X4 X6 X7 X9 X11
	0.57597854	4.24065	X2 X4 X5 X6 X10LOG X12
	0.57563081	4.24905	X2 X4 X6 X10LOG X11 X12
	0.56398300	4.53036	X2 X4 X6 X7 X8LOG X11
	0.55895326	4.65183	X2 X3 X4 X6 X10LOG X11
	0.55836548	4.66603	X1 X3 X4 X6 X10LOG X12
7	0.66337120	4.13001	X2 X3 X4 X6 X7 X10LOG X12
	0.65748577	4.27215	X2 X4 X6 X7 X9 X10LOG X12
	0.64744027	4.51476	X2 X4 X6 X7 X9 X10LOG X11
	0.64130235	4.66300	X2 X3 X4 X6 X7 X10LOG X11
	0.63648918	4.77924	X1 X2 X3 X4 X6 X10LOG X12

N = 20 Regression models for dependent variable Y1

Table 9. Eigenanalysis Using Proc Factor

	1	2	3	4	5	6	7	8	9	10	11	12
Eigenvalue	3.495310	2.570989	1.477624	1.350735	1.022768	0.648041	0.554659	0.377841	0.268198	0.155415	0.057561	0.020860
Difference	0.924321	1.093365	0.126890	0.327966	0.374727	0.093382	0.176818	0.109643	0.112783	0.097854	0.036701	.
Proportion	0.2913	0.2142	0.1231	0.1126	0.0852	0.0540	0.0462	0.0315	0.0223	0.0130	0.0048	0.0017
Cumulative	0.2913	0.5055	0.6287	0.7412	0.8265	0.8805	0.9267	0.9582	0.9805	0.9935	0.9983	1.0000

Initial Factor Method: Principal Components. Prior Community Estimates: ONE. Eignevalues of the Correlation Matrix: Total = 12 Average = 1
12 factors will be retained by the NFACTOR criterion

Eigenvectors

	1	2	3	4	5	6
X1	0.20340	-0.53423	-0.10553	0.00625	0.13370	0.02981
X2	-0.09560	0.45902	0.39693	0.09658	0.30973	0.09301
X3	0.35474	0.11708	0.19329	-0.08175	0.24530	-0.23996
X4	-0.01295	0.28526	-0.40587	-0.32436	0.54646	0.02700
X5	0.34139	0.32756	-0.34567	-0.12286	-0.01737	0.08122
X6	-0.04658	-0.32015	0.14338	0.32942	0.65596	0.33618
X7	-0.31018	0.33847	0.32795	0.15901	-0.09539	0.18026
X8LOG	-0.08741	0.06907	-0.26901	0.72544	-0.06847	-0.28036
X9	0.23565	-0.15656	0.54751	-0.23697	-0.02319	-0.30091
X10LOG	0.39116	0.11416	0.04630	0.31863	0.17556	-0.44368
X11	0.42742	-0.00641	0.08494	0.15472	-0.18363	0.61250
X12	0.45792	0.20522	0.01103	0.14819	-0.13395	0.19720

Table 10. Analysis of Variance for Discriminant Analysis

Source	DF	Sum of Squares	Mean Square	F Value	Prob > F
Model	12	4.19597	0.34966	2.979	0.0013
Error	106	12.44268	0.11738		
C Total	118	16.63866			

Root MSE	0.34261	R-square	0.2522
Dep Mean	0.00405	Adj R^2	0.1675
C.V.	8465.38180		

Model: MODEL1 Dependent Variable: Y1IP

Parameter Estimates

Variable	DF	Parameter Estimate	Standard Error	T for H0: Parameter = 0	Prob > |T|	Variance Inflation
INTERCEP	1	1.518747	0.71037038	2.138	0.0348	0.00000000
X1	1	-0.008313	0.00339118	-2.451	0.0159 ✓	1.28473359
X2	1	-0.004231	0.00623298	-0.679	0.4987	1.32650530
X3	1	-0.004648	0.00195803	-2.374	0.0194 ✓	1.20829616
X4	1	-0.030028	0.03680241	-0.816	0.4164	1.19155741
X5	1	-0.047232	0.01433407	-3.295	0.0013 ✓	1.65481066
X6	1	-0.131173	0.05091416	-2.576	0.0114 ✓	1.36065513
X7	1	-0.015705	0.01548284	-1.014	0.3127	1.17135716
X8LOG	1	-0.048839	0.06995496	-0.698	0.4866	1.19218210
X9	1	0.015770	0.00654470	2.410	0.0177 ✓	1.22658903
X10LOG	1	0.056736	0.06203130	0.915	0.3625	3.30498192
X11	1	-0.002767	0.00497717	-0.556	0.5794	2.33804892
X12	1	0.000469	0.00038445	1.221	0.2248	3.04153336

T = Tests:
X1 = base + subgrade thickness
X3 = Subgrade stiff
X5 = asphalt thickness
X6 = % asphalt
X9 = age
Subset selection: adds X10 = AADT

FIGURES

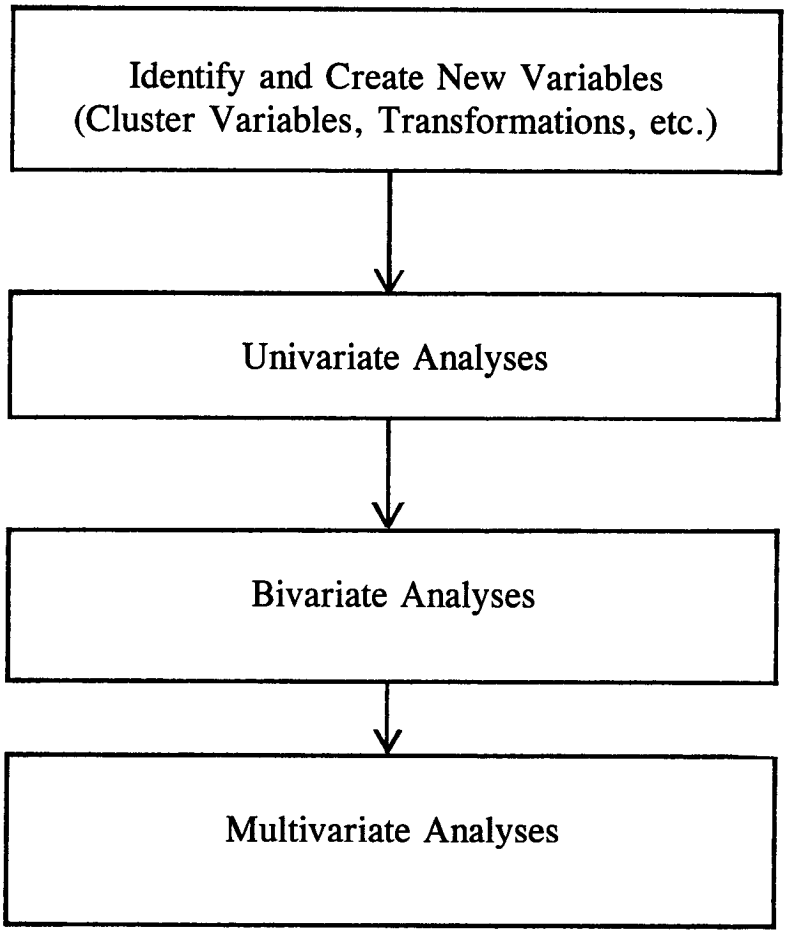

Figure 1. Flow chart for P-020 LTPP Analyses

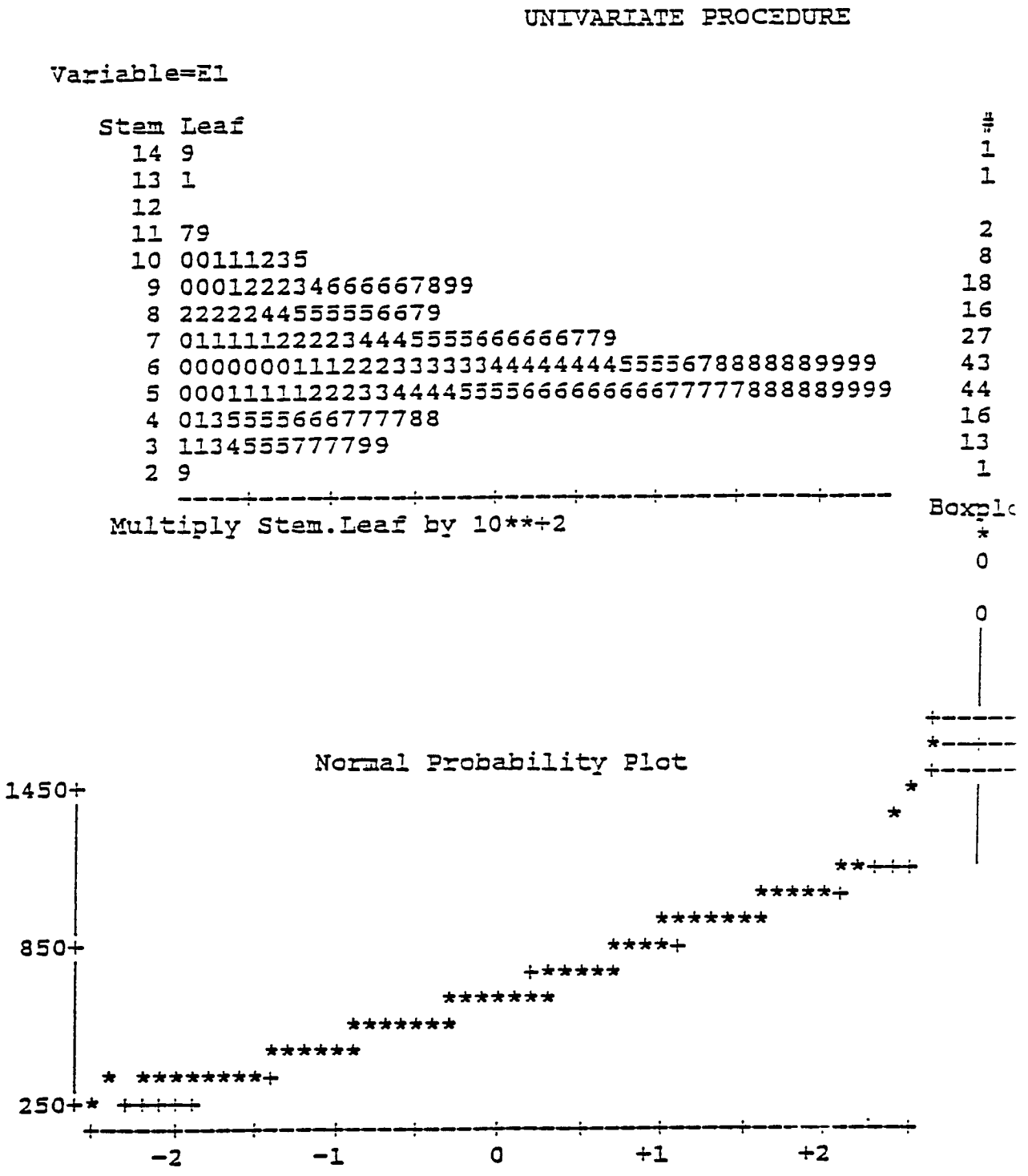

Figure 2. Frequency Plots for Variable E_1

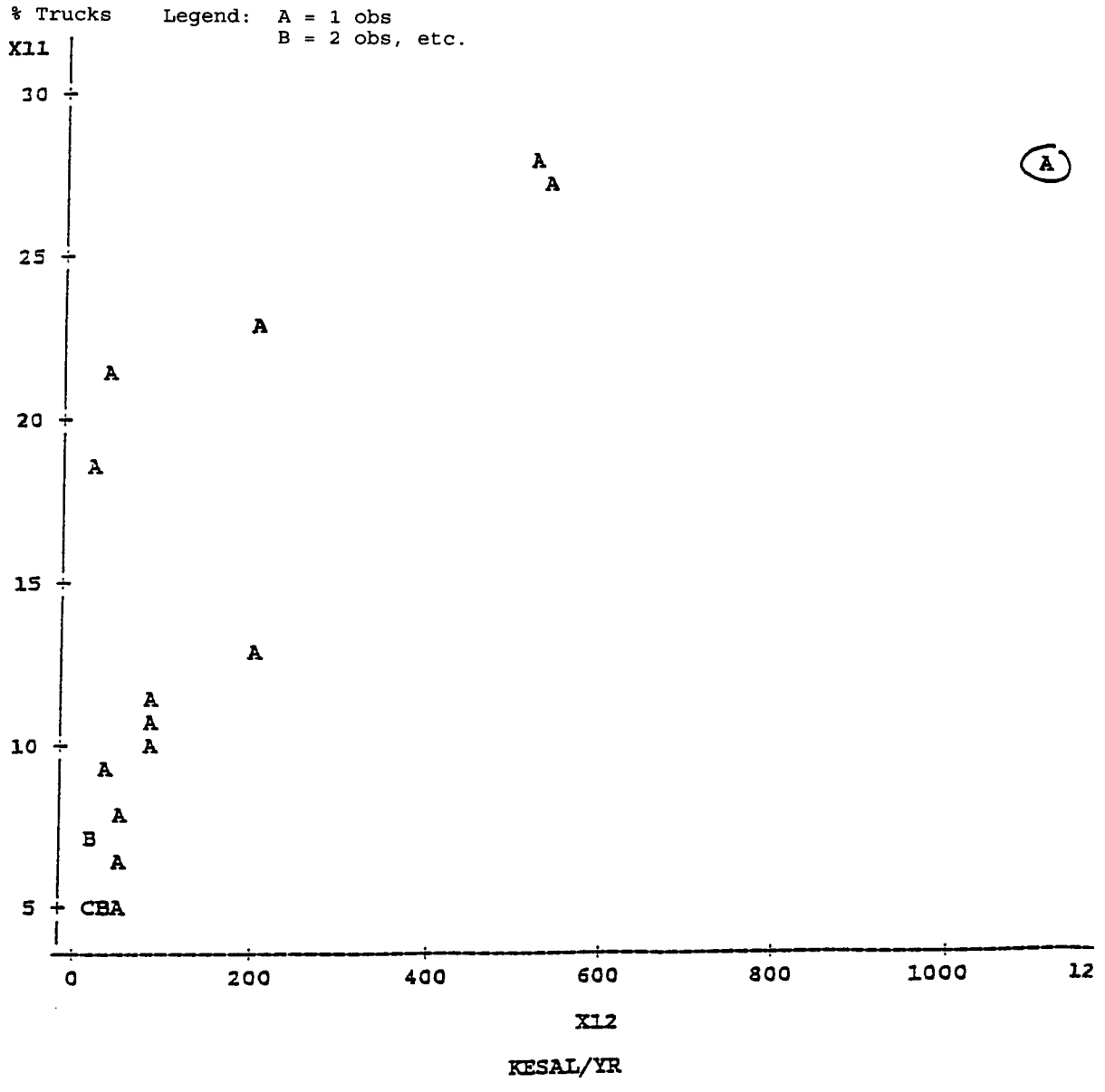

Figure 3. Scatter Plot Percentable of Trucks versus kESALs per Year for Alligator Cracking Less than 0

Plot of LD1*LDELTA. Legend: A = 1 observation, B=2, etc.
Note: One observation had missing values

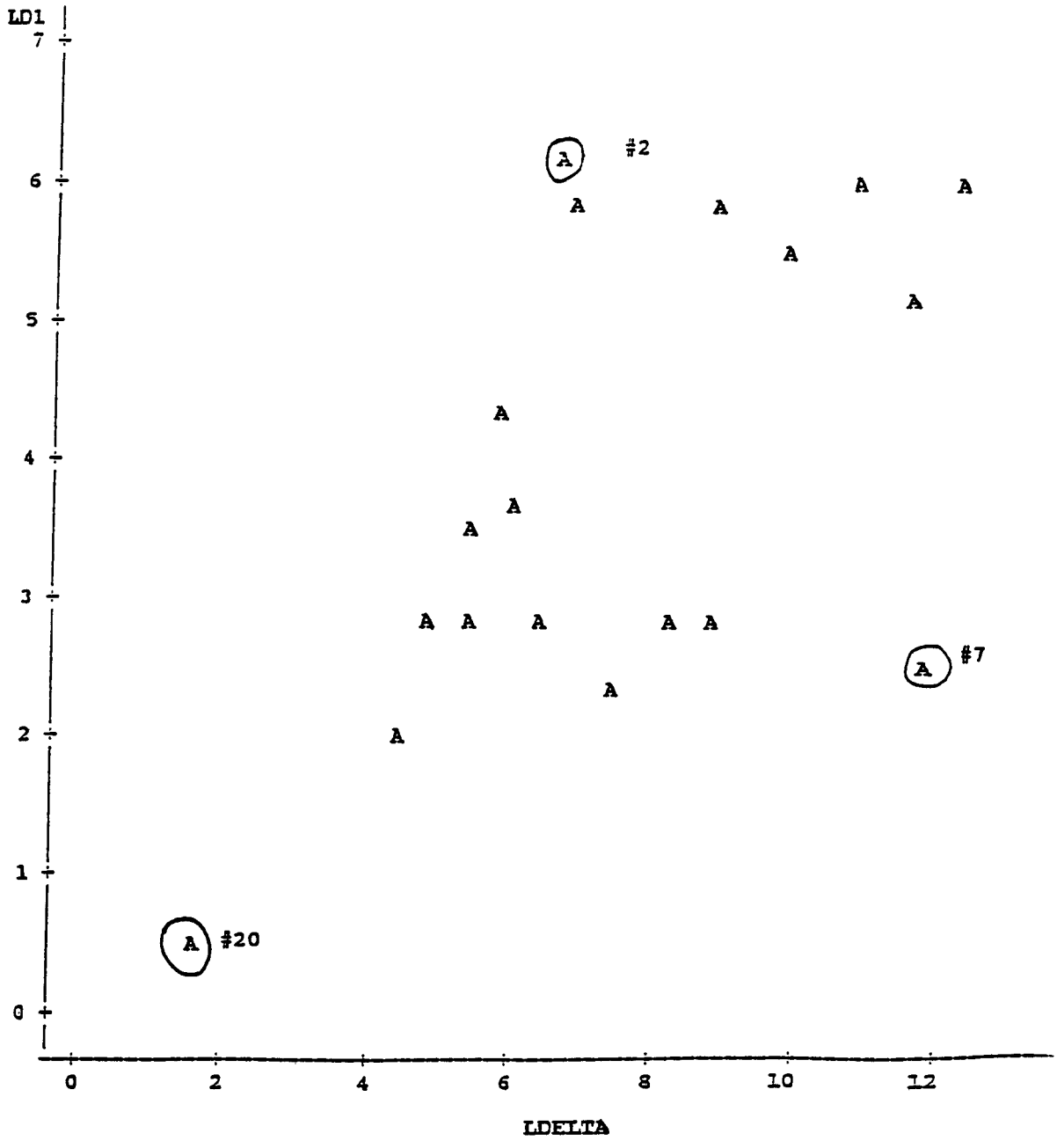

Figure 4. Plot of Influential Observations

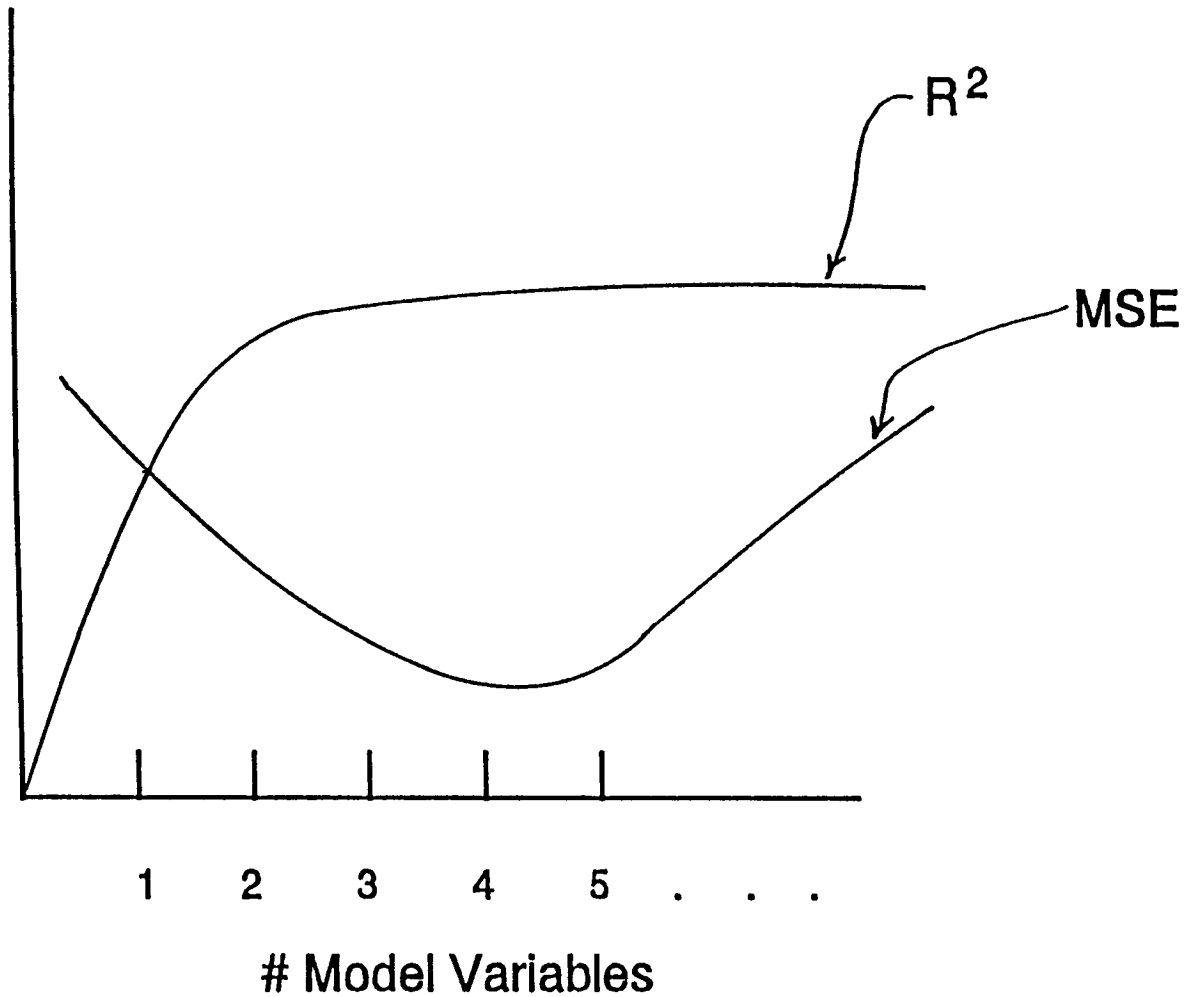

Figure 5. Relation of F^2 and Mean Square Error to the Number of Variables Used.

Plot of FACTOR10*FACTOR12. Legend: A = 1 observation, B=2, etc.
Note: Seven observations had missing values

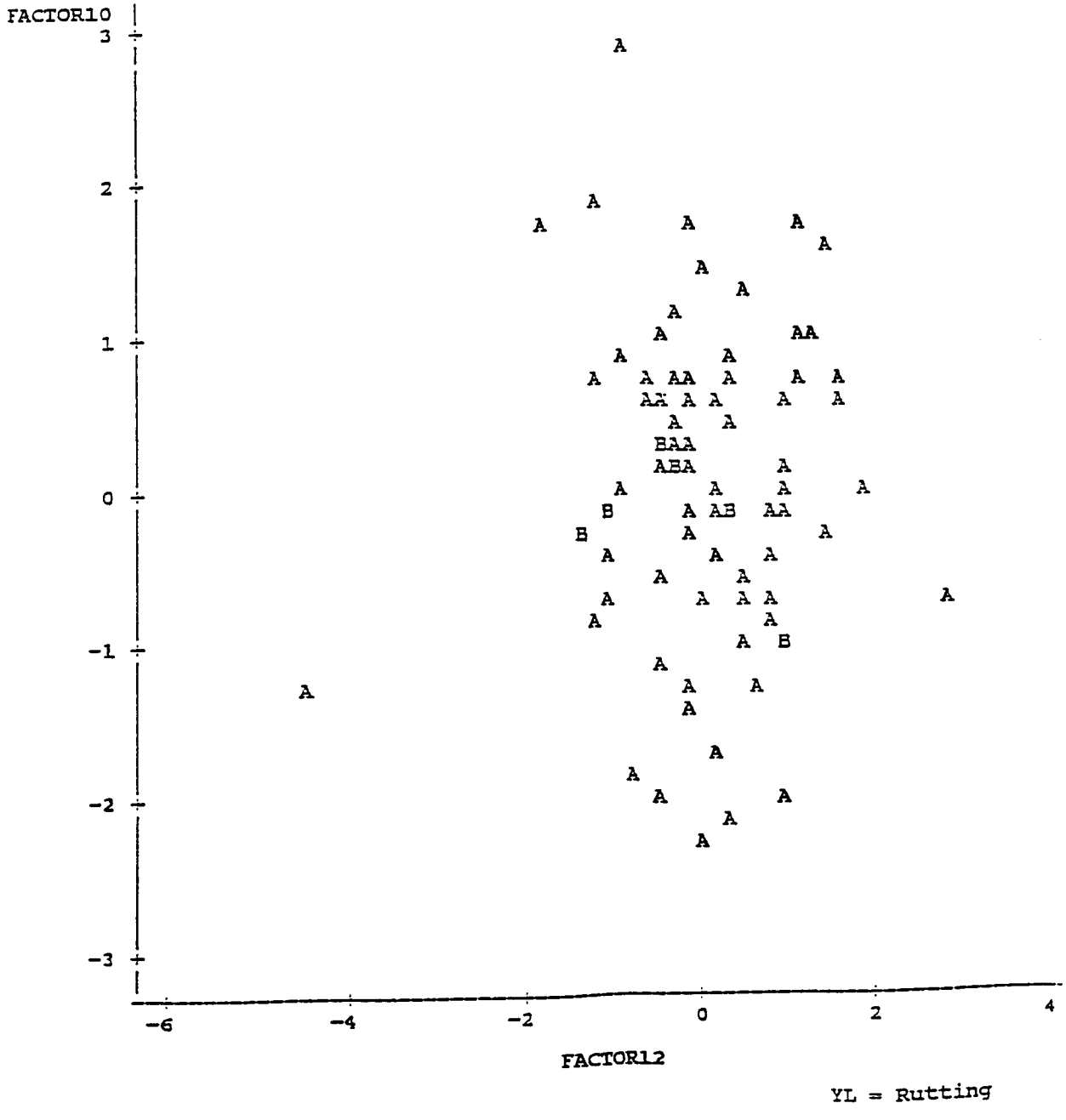

Figure 6. Scatter Plot of Eigenanalysis